

MCR-68-119

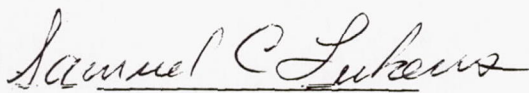
STERILIZABLE LIQUID PROPULSION SYSTEM  
FINAL REPORT  
PART I

August 1968

Authors

F. Brady  
D. DiStefano

Approved



Samuel C. Lukens  
Program Manager

JPL Contract 951709

This work was performed for the Jet Propulsion Laboratory,  
California Institute of Technology, as sponsored by the National  
Aeronautics and Space Administration under Contract NAS7-100.

MARTIN MARIETTA CORPORATION  
P. O. Box 179  
Denver, Colorado

NOTICE

This report was prepared as an account of Government-sponsored work. Neither the United States, nor the National Aeronautics and Space Administration (NASA), nor any person acting on behalf of NASA:

- a. Makes warranty or representation, expressed or implied, with respect to the accuracy, completeness, or usefulness of the information contained in this report, or that the use of any information, apparatus, method, or process disclosed in this report may not infringe privately-owned rights; or
- b. Assumes any liabilities with respect to the use of, or for damages resulting from the use of any information, apparatus, method, or process disclosed in this report.

As used above, "person acting on behalf of NASA" includes any employee or contractor of NASA, or employee of such contractor, to the extent that such employees or contractor of NASA, or employee of such contractor prepares, disseminates, or provides access to, any information pursuant to his employment with such contractor.

Requests for copies of this report should be referred to:

National Aeronautics and Space Administration  
Office of Scientific and Technical Information  
Washington 25, D. C.

Attention: AFSS-A



68-407

JPL Contract 951709

# STERILIZABLE LIQUID PROPULSION SYSTEM

## FINAL REPORT

### (PART I)

#### Authors

H. Frank Brady

Dominic DiStefano

AUGUST 1968

MARTIN MARIETTA CORPORATION  
P.O. Box 179  
Denver, Colorado 80201

FOREWORD

This report is submitted in accordance with paragraph (a)(1) (v)(F) of Article 1 and paragraph (b)(6) of Article 2 of JPL Contract 951709. This is Part I of two parts.

CONTENTS

	<u>Page</u>
Foreword . . . . .	ii
Contents . . . . .	iii thru x
I. Introduction . . . . .	I-1
II. Program Plan . . . . .	II-1 thru II-4
III. System Design . . . . .	III-1
A. Propellant Selection . . . . .	III-2
B. Engine Selection . . . . .	III-5
C. Propulsion Module Design . . . . .	III-11
D. Component Selection . . . . .	III-16
E. Components and System Test Plan . . . . .	III-30
F. Flight System Design . . . . .	III-34 thru III-36
IV. Material Evaluation . . . . .	IV-1
A. Literature Review . . . . .	IV-1
B. Development of Test Technique . . . . .	IV-6
C. Test Fixture Design and Fabrication . . . . .	IV-14
D. Materials Testing . . . . .	IV-15 thru IV-48
V. Component Development and Test . . . . .	V-1
A. Component Procurement and Acceptance . . . . .	V-1
B. Test Fixture Design and Fabrication . . . . .	V-14
C. Test Method . . . . .	V-22
D. Component Sterilization . . . . .	V-24
E. Component Disassembly, Inspection, and Performance . . . . .	V-37
F. Reliability Evaluation . . . . .	V-63 and V-64

VI.	System Assembly and Test . . . . .	VI-1
	A. System Fabrication and Assembly . . . . .	VI-1
	B. System Test Fixtures . . . . .	VI-3
	C. Test Method . . . . .	VI-7
	D. Decontamination and Sterilization . . . . .	VI-7
	E. System Test Firing . . . . .	VI-18
	F. Disassembly and Examination . . . . .	VI-23 thru VI-30
VII.	Conclusions . . . . .	VII-1
	A. System . . . . .	VII-1
	B. Components . . . . .	VII-1
	C. Piece Parts and Materials . . . . .	VII-2
	D. Facilities . . . . .	VII-3
VIII.	Recommendations . . . . .	VIII-1
	A. System . . . . .	VIII-1
	B. Components . . . . .	VIII-1
	C. Piece Parts and Materials . . . . .	VIII-2
	D. Facilities and Processes . . . . .	VIII-2 and VIII-3
IX.	New Technology . . . . .	IX-1 and IX-2
X.	References and Bibliography . . . . .	X-1
	A. References . . . . .	X-1
	B. Bibliography . . . . .	X-2 and X-3



Appendix A -- Calculation of Flow Annulus . . . . .	A-1 and A-2
Appendix B -- Sterilizable Liquid Propulsion System Component Design Analysis . . . . .	B-1 thru B-14
Appendix C -- Pressurant Side Tank Outlet Volume Calculation . . . . .	C-1
Appendix D -- Propellant Loading, Level, and Ullage Calculation . . . . .	D-1 thru D-5

Figure

II-1	Program Plan . . . . .	II-2
II-2	Program Organization . . . . .	II-4
III-1	Marquardt R-4D Rocket Engine . . . . .	III-10
III-2	System Configurations . . . . .	III-12
III-3	System Structural Truss and Assembly Fixture . .	III-14
III-4	System Schematic . . . . .	III-15
III-5	Proposed Welded Configuration of Screen Trap . .	III-20
III-6	Screen Trap Riveted Configuration . . . . .	III-21
III-7	Teflon Diaphragm . . . . .	III-29
III-8	Program Test Flow Chart . . . . .	III-32
III-9	Heat Sterilization Cycle . . . . .	III-33
III-10	ETO Decontamination Cycle . . . . .	III-33
IV-1	Material Test Program . . . . .	IV-7
IV-2	NASA-Langley Test Specimen Configurations . . .	IV-9
IV-3	Specimen Test Tubes and Holding Rack . . . . .	IV-11
IV-4	Oxidizer Test Fixtures . . . . .	IV-11
IV-5	Fuel Test Fixtures . . . . .	IV-11
IV-6	Long-Term Storage Tanks . . . . .	IV-12
IV-7	Compatibility Screening Test Fixture . . . . .	IV-15
IV-8	Oxidizer Test Maraging Steel Specimen . . . . .	IV-23
IV-9	Oxidizer Test Specimens . . . . .	IV-23
IV-10	Oxidizer Test Specimens . . . . .	IV-24
IV-11	Oxidizer Test Specimens . . . . .	IV-24
IV-12	Oxidizer Test Specimen Rack . . . . .	IV-25
IV-13	Titanium (6Al-4V) after Exposure to $N_2O_4$ for 600 hr (200X) . . . . .	IV-25
IV-14	Etched Titanium Foil after Exposure to $N_2O_4$ for 600 hr at 275°F . . . . .	IV-26
IV-15	Aluminum (6061-T6) after Exposure to $N_2O_4$ for 600 hr at 275°F (200X) . . . . .	IV-27
IV-16	Aluminum Screens (5056) after Exposure to $N_2O_4$ at 275°F . . . . .	IV-27

IV-17	Stainless Steel (Type 347) after Exposure to $N_2O_4$ for 600 hr at 275°F . . . . .	IV-29
IV-18	Steel (Maraging) after Exposure to $N_2O_4$ for 600 hr at 275°F . . . . .	IV-30
IV-19	Materials after Exposure to $N_2O_4$ for 600 hr at 275°F (200X) . . . . .	IV-31
IV-20	Bimetallic Couples, Titanium 6Al-4V and 6061-T6 Aluminum after Exposure to $N_2O_4$ for 600 hours at 275°F . . . . .	IV-32
IV-21	Pure Nickel Screen after Exposure to $N_2O_4$ for 600 hr at 275°F . . . . .	IV-33
IV-22	Face of Stressed Titanium Specimen . . . . .	IV-34
IV-23	Edge of Stressed Titanium Specimen . . . . .	IV-34
IV-24	Copper Tube Fittings from ETO Test . . . . .	IV-40
IV-25	Transition Joint, Titanium 6Al-4V and 6061-T6 Aluminum Alloy . . . . .	IV-41
IV-26	Titanium 6Al-4V Alloy Exposed to ETO/Freon 12 . . . . .	IV-43
IV-27	Monomethylhydrazine Vapor Pressure Test Fixture . . . . .	IV-46
IV-28	Monomethylhydrazine Vapor Pressure . . . . .	IV-48
V-1	Oxidizer Tank, Seal Joint Design . . . . .	V-3
V-2	Oxidizer Tank, Improved Seal Joint Design . . . . .	V-4
V-3	Fuel Tank Screen Trap Assembly . . . . .	V-7
V-4	Test Fixture Schematic, Regulator Valve Functional Test . . . . .	V-15
V-5	Functional Test Setup, Regulator . . . . .	V-16
V-6	Regulator Holding Fixture . . . . .	V-16
V-7	Sterilization and Decontamination Test Fixture . . . . .	V-17
V-8	Sterilization Chamber, Shroud and Dome Removed . . . . .	V-18
V-9	Sterilization Chamber, Internal View . . . . .	V-18
V-10	Sterilization Chamber Qualification Distribution Thermocouple Array . . . . .	V-19
V-11	Component Installation in Sterilization Chamber . . . . .	V-25
V-12	Oxidizer Tank Leak Measurement Schematic . . . . .	V-38

V-13	Determination of Leak Point during Drain . . . . .	V-39
V-14	Diaphragm Apex Patch . . . . .	V-41
V-15	Diaphragm Apex Patch . . . . .	V-41
V-16	Oxidizer Tank Diaphragm . . . . .	V-42
V-17	Oxidizer Tank Diaphragm Seal Area . . . . .	V-43
V-18	Oxidizer Tank Diaphragm Configurations and Pro- pellant Heights during Sterilization . . . . .	V-47
V-19	Fuel Tank Screen Trap Assembly . . . . .	V-52
V-20	Fuel Tank Screen Trap Leakage Points . . . . .	V-52
V-21	Regulator Internal Filter . . . . .	V-54
V-22	Regulator Poppet Ball . . . . .	V-54
V-23	Solenoid Valve Coil . . . . .	V-56
V-24	Component Test Filter Disassembly . . . . .	V-57
V-25	Hand Valve Disassembly . . . . .	V-58
V-26	Hand Valve Poppet . . . . .	V-59
V-27	Hand Valve Stem Seal Chevrons . . . . .	V-59
V-28	Hand Valve Stem Cap Seal Configurations . . . . .	V-60
VI-1	Assembled Propulsion Module . . . . .	VI-2
VI-2	Schematic of Regulator Functional Test . . . . .	VI-4
VI-3	Firing Test Schematic . . . . .	VI-6
VI-4	Decontamination and Sterilization Chamber Schematic . . . . .	VI-9
VI-5	ETO Cycle No. 1 Test History . . . . .	VI-11
VI-6	ETO Cycle No. 2 Test History . . . . .	VI-12
VI-7	Dry Heat Sterilization, Cycle 1 . . . . .	VI-16
VI-8	Dry Heat Sterilization, Cycle 6 . . . . .	VI-17
VI-9	Engine Performance . . . . .	VI-22
VI-10	Hand Valve Stem Cap Seal . . . . .	VI-25
VI-11	Ordnance Valve Flange and Gasket . . . . .	VI-25
VI-12	Oxidizer Fill and Drain Tube . . . . .	VI-27
VI-13	Oxidizer Fill and Drain Tube Crack, External View . . . . .	VI-27



VI-14	Oxidizer Fill and Drain Tube Crack, Internal View . . . . .	VI-27
VI-15	Module Oxidizer Tank Diaphragm Failure, Side View . . . . .	VI-28
VI-16	Module Oxidizer Tank Diaphragm Failure, Top View . . . . .	VI-28
VI-17	Diaphragm Apex Doubler . . . . .	VI-28
VI-18	Module Oxidizer Inlet Hemisphere . . . . .	VI-30
VI-19	Module Oxidizer Tank Gas Inlet Fitting . . . . .	VI-30

### Table

III-1	Oxidizer Selection Data . . . . .	III-2
III-2	Fuel Selection Data . . . . .	III-4
III-3	Propellant Combination Comparison . . . . .	III-5
III-4	Engines Considered . . . . .	III-6
III-5	Engine/Propellant Consideration . . . . .	III-7
III-6	Final Engine Selection . . . . .	III-9
III-7	Propellant Weight Statement . . . . .	III-17
III-8	Component Selection Sheet . . . . .	III-27
IV-1	Compatibility of Materials Literature Review . .	IV-3
IV-2	Ethylene Oxide and Thermal Compatibility of Metals during Decontamination and Sterilization Cycles . . . . .	IV-4
IV-3	Summary of Typical Nonmetals Compatible with Decontamination and Sterilization Cycles . . . .	IV-5
IV-4	Prescreening Tests, N <sub>2</sub> O <sub>4</sub> Compatibility with Metals . . . . .	IV-18
IV-5	Prescreening Tests, N <sub>2</sub> O <sub>4</sub> Compatibility with Non-metals . . . . .	IV-19
IV-6	Prescreening Tests, MMH Compatibility with Non-metals . . . . .	IV-20
IV-7	Properties of Adhesives after Exposure to 275°F . . . . .	IV-35
IV-8	Properties of Plastic and Rubber Sheet and Film after Exposure at 275°F . . . . .	IV-36

IV-9	Properties of Potting, Encapsulating, and Sealing Resins after Exposure at 275°F . . . . .	IV-37
IV-10	Testing of Coatings and Finishes after 600 hr Exposure at 275°F . . . . .	IV-38
V-1	Component Functional Test Schedule . . . . .	V-23
V-2	Performance Data, Propellant Tanks . . . . .	V-30
V-3	Performance Data, Pressure Regulator . . . . .	V-31
V-4	Performance Data, Solenoid Valve . . . . .	V-32
V-5	Performance Data, Filter . . . . .	V-33
V-6	Performance Data, Hand Shutoff Valve . . . . .	V-34
V-7	Performance Data, Ordnance Valve . . . . .	V-35
V-8	Performance Data, Thrust Chamber Valves . . . . .	V-36
V-9	Diaphragm Positions . . . . .	V-46
V-10	Volume due to Permeation and Leakage as a Function of Diaphragm Position . . . . .	V-48
V-11	MMH Gas Chromatograph Analysis Results . . . . .	V-49
V-12	Sterilizable Liquid Propulsion System Reliability Estimate . . . . .	V-64
VI-1	Performance of Propulsion Module Components before and after Decontamination and Sterilization . . . . .	VI-19
VI-2	Propulsion Module Firing Test Quick-Look Data . . . . .	VI-21

## I. INTRODUCTION

This is the program final report submitted in accordance with JPL Contract 951709. The report covers the period from October 5, 1966 thru March 31, 1968.

The program involved the exposure of an assembled and fueled bipropellant liquid propulsion system to the ethylene oxide (ETO) and heat sterilization requirements specified by JPL Specification VOL-50503-ETS. After exposure the system was fired for 280 sec.

The program plan included a design and component selection phase during which the propulsion system design was evolved. A second phase involved the procurement of components for both a component test series and for assembly into the complete system. The third phase of the program, carried on in parallel with the design phase, was a materials investigation. The fourth phase of the program involved the assembly and test of the complete propulsion system.

The components underwent 12 heat sterilization cycles along with functional tests to measure degradation. Corrections or modifications were made as required to allow system testing.

The module was assembled and exposed to six heat sterilization cycles with propellants loaded. After a poststerilization checkout of some of the critical components, the system was successfully fired for 280 sec.

This report was prepared by the Denver Division of the Martin Marietta Corporation under Jet Propulsion Laboratory Subcontract 951709, dated October 5, 1966. The JPL technical monitor for the contract was Mr. Merle E. Guenther. The Program Manager at Martin Marietta was Mr. Samuel C. Lukens.

The following personnel at Martin Marietta were major contributors to the program effort:

- H. F. Brady, Technical Lead and Design
- C. Caudill, Materials Engineering
- C. Holt, Materials Test
- J. B. Keough, Systems Test



## II. PROGRAM PLAN

To implement the program in an orderly and timely fashion, the overall plan shown in Fig. II-1 was formulated. The program consisted of four technical tasks that provided for system analysis and design, a materials compatibility experimental test program, and a components test activity followed by a system assembly and test activity. A fifth task provided for reporting, planning, and documentation.

In Task I the work was directed toward system design. Propellants and engine were selected and the system was sized after a survey of available components. The results of the materials investigation was coordinated into this system design activity.

The object of Task II was to establish the effects of sterilization at the component level so the necessary corrective action could be taken and incorporated into the system. To accomplish Task II, the components were procured and exposed to two complete dry heat exposures, each consisting of six dry heat cycles at 135°C. Performance degradation was established by comparing baseline performance tests with additional performance tests at the midpoint and completion of all exposures. Each unit was then examined in detail and evaluated to formulate the results and necessary corrective action.

Task III supported the design activity. A literature search was initiated to screen materials, both metals and nonmetals, that would be suitable for use in the environments of propellants, ethylene oxide, and dry heat sterilization. This activity was then followed by a prescreening metals test; a 600-hr screening test of candidate materials of construction; a 600-hr test of candidate nonmetals that included adhesives, coatings, lubricants, potting compounds and plastics; and finally, a long-term storage test of materials of construction of each propellant tank.

In the long-term storage activity all the materials in combination that constituted the propellant tanks and expulsion devices were assembled into a subscale tank, loaded with the appropriate propellant, exposed to the dry heat sterilization, and then stored at ambient conditions for up to a year.



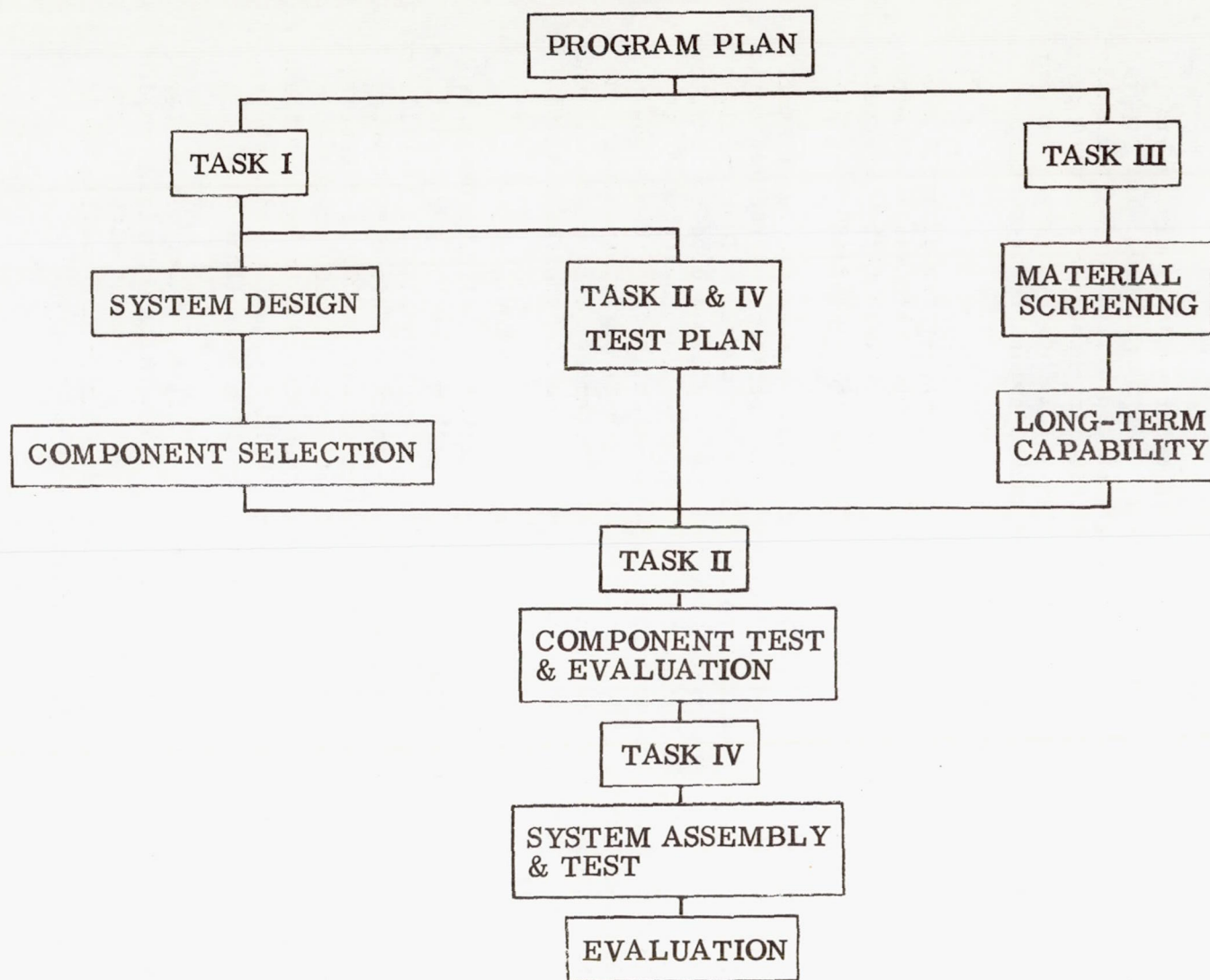


Fig. II-1 Program Plan

The complete module was assembled, loaded, exposed, and test fired in Task IV. The exposure of the assembled and loaded module consisted of both the decontamination environment of ethylene oxide and Freon 12 at 50°C followed by six cycles of dry heat sterilization at 135°C. After the environmental exposure, the module was transferred to the test firing cell, given appropriate firing readiness checks and then test fired for 280 sec. The performance and degradation were then compared to the assembly checkout levels and engine baseline tests performed at the engine manufacturer's facility.

Management of the program was implemented by a project organization shown in Fig. II-2. It was characterized by the direct design and engineering organization shown at the first level supported by manufacturing, quality, and safety shown on the second level.

Program management was aided and advised by two committees made up of recognized leaders in the particular areas of interest.

The equipment selection committee membership included technical experts with extensive experience. The function of this committee was to meet once or twice as necessary to review the system design and the selection of the components. Thus additional experience was used in the component selection process.

The Technical Advisory Group membership included individuals of demonstrated excellence in systems and project management. The group met quarterly for a technical and management review of the program. In this way corporate management could focus on the program and direct the resources of the corporation in support of the project, if necessary. Furthermore, the committee advised project members of activities in other programs that were relevant.

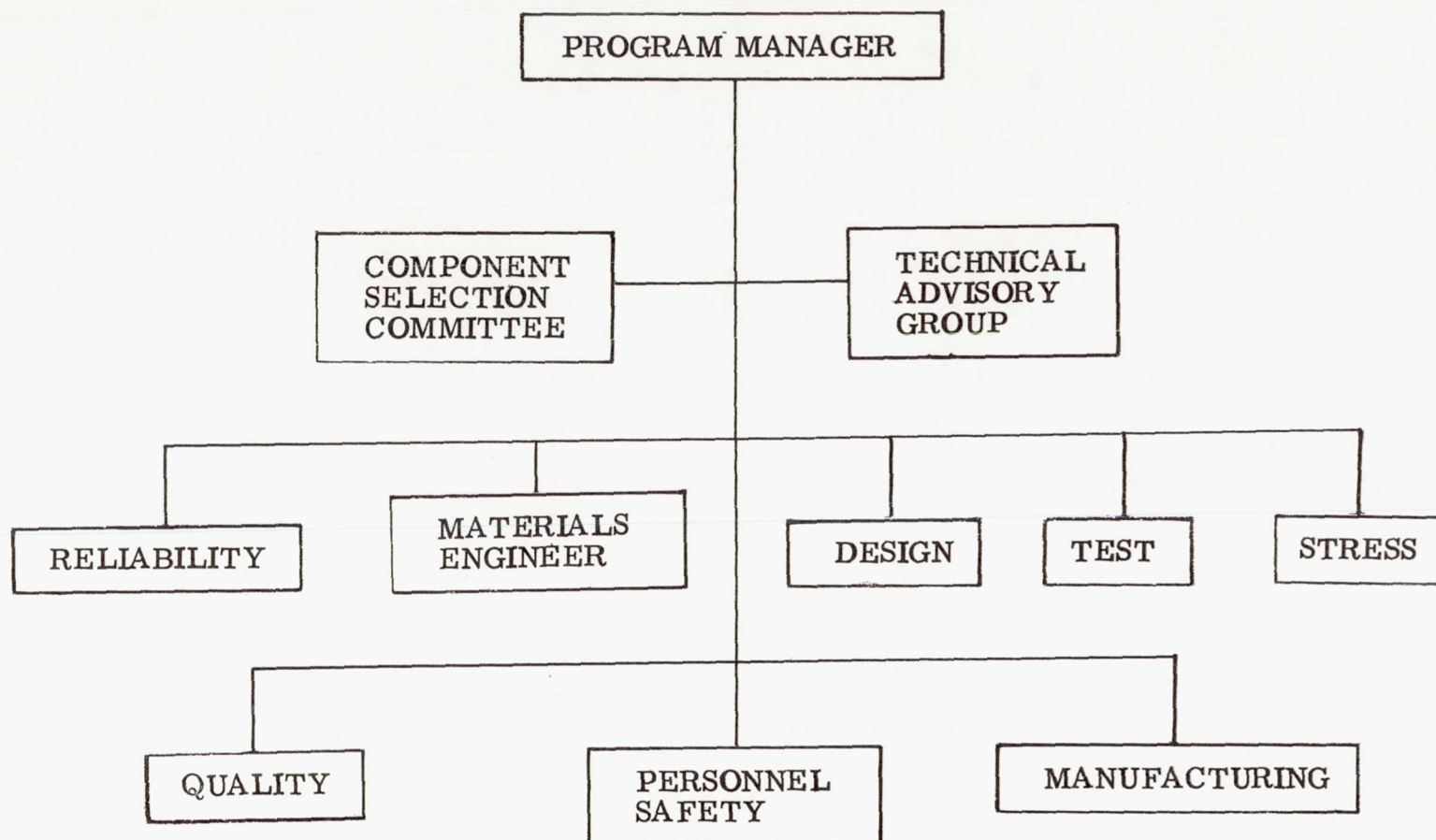


Fig. II-2 Program Organization



### III. SYSTEM DESIGN

The first major step to be completed in the program was the design of the complete propulsion system. To properly accomplish this task, program ground rules were established and a system design criteria document was developed. In addition, a parallel effort was initiated to study the effects of the sterilization and decontamination environments on system materials of construction.

Many of the program ground rules were specified in the statement of work, providing guidelines for system size and operating requirements. Additional ground rules were set up as required to establish the scope of program effort. The major ground rules used are as follows:

- 1) Propellants - Hydrazine-derivative fuels, or blends, and nitrogen oxide-derivative oxidizers, or blends, including nitric acid;
- 2) Thrust Level - Approximately 100 lb<sub>f</sub> (throttling capability over 3 to 1 range or greater was desired but was not considered a requirement);
- 3) Specific Impulse - A minimum of 275 lb<sub>f</sub>-sec/lb<sub>m</sub> at maximum engine thrust under vacuum conditions with an expansion ratio of 40;
- 4) Injector Head Pressure - Not to exceed 500 psi;
- 5) Feed System - Gas regulated, pressure fed, with positive expulsion assured;
- 6) Operating Duration - Minimum of 300 sec;
- 7) Exposure to the sterilization environment defined by JPL Specification Vol-50503-ETS. The requirement included exposure of the propulsion system to both ethylene oxide mixed with Freon and to dry heat.

The design criteria document provided complete definition of the system and its operating and test requirements. As the design phase progressed the criteria were updated as necessary.

Several preliminary steps were necessary to allow the design layout of the system to proceed. Selection of propellants was required so that an engine could be selected. With the engine selected, the feed system could be sized and component configurations established.



## A. PROPELLANT SELECTION

Based upon one of the program ground rules, the propellants to be selected were limited to hydrazine-derivative fuel or blends and nitrogen-oxide-derivative oxidizers or blends including nitric acid. Four candidate fuels and three candidate oxidizers were considered. The candidate fuels were hydrazine ( $N_2H_4$ ), monomethylhydrazine (MMH), unsymmetrical dimethylhydrazine (UDMH), and Aerozine 50 (A-50). Oxidizers considered included nitrogen tetroxide ( $N_2O_4$ ), mixed oxides of nitrogen (MON), and inhibited red fuming nitric acid (IRFNA). The major considerations used for propellant selection were:

- 1) Vapor pressure at elevated temperature;
- 2) Stability at elevated temperature;
- 3) Material compatibility at elevated temperature;
- 4) Engine test experience, including demonstration of performance.

1. Oxidizer Selection

A summary of the selection factors for an oxidizer is presented in Table III-1.

Table III-1 Oxidizer Selection Data

Propellant	Vapor Pressure (psi @ 275°F)	Thermal Stability	High Temperature Compatibility	$I_{sp}$ Performance Demonstrated (sec)	Production Systems using This Propellant	Engine Test Experience
$N_2O_4$	800	Decomposition only slight @ 275°F	Materials available	>290	Many sys- tems	Greatest
IRFNA	125	Equilibrium pressure 300 to 400 psi @ 275°F	Questionable	>275	Drone sys- tems	Minimum
MON	>800	Decomposition only slight @ 275°F	Materials available for ambient temperature use	>290	More than one	Adequate

The MON mixture was eliminated primarily because of a very high vapor pressure. Use of this oxidizer would cause a severe penalty in tankage weight for a system that would be sterilized with propellants loaded. An additional factor that led to elimination of MON was the complete lack of high temperature compatibility data.

A summary of existing high temperature compatibility data indicated  $N_2O_4$  would be a better choice than IRFNA. In addition, in combination with the fuels considered,  $N_2O_4$  provides higher performance than IRFNA. As indicated in Table III-1, IRFNA was superior in the area of vapor pressure, being less than 1/6 that of  $N_2O_4$ .

With all factors considered  $N_2O_4$  was selected as the oxidizer for the program. It was felt that the high temperature compatibility and performance of  $N_2O_4$  overshadowed the vapor pressure advantage of IRFNA.

## 2. Fuel Selection

Since there was little variation in vapor pressures and high temperature compatibility properties for the three candidate fuels considered, the main criteria for the selection were thermal stability of the fuel, performance with the selected oxidizer, and engine availability. On the basis of specific impulse and system weight, neat hydrazine is clearly superior to either of the fuel candidates from a pure theoretical standpoint; however, from the standpoint of thermal stability, it is less desirable than either A-50 or MMH, and was therefore eliminated. The very limited decomposition rate data available for MMH (at ambient, 160°F and 400°F) are similar to rates observed for pure hydrazine (Ref 1). Certain impurities, particularly oxygen, can increase the sensitivity to thermal decomposition markedly. For example, MMH that has been exposed to air sufficiently to cause a slight yellowish discoloration will show increased thermal instability.

The low sensitivity of UDMH to catalytic decomposition is well documented, and the decreased sensitivity of the mixture with hydrazine (A-50), has been demonstrated in the successful use of this fuel in regeneratively cooled upper stage engines. UDMH was eliminated even though it exhibits superior thermal properties because of its low performance capability. Stability testing of the candidate fuels is well documented for normal storability limits below 160°F in both open and closed vessels; however, all will decompose rapidly at elevated temperatures.



Bomb test data reported by Rocketdyne (Ref 2) reveal the approximate temperatures at the onset of rapid decomposition for the fuels are 480°F for  $N_2H_4$ , 640°F for MMH, and 720°F for UDMH. Between the normal storage temperature and rapid decomposition temperature of the fuels, very little experimental work indicating decomposition rates has been performed. Consequently, the actual relative stability rating for the hydrazine fuels in the range of interest at 285°F, can only be speculated. A recent Martin Marietta attempt to correlate these data (Ref 3) indicated that the decomposition rates of the candidate fuels are of the same magnitude at ambient temperatures. General opinion of various sources in the industry indicate that the stability rating in declining order is as follows: UDMH, MMH, A-50, and  $N_2H_4$ . There is some disagreement as to the comparative stability of MMH and A-50. The most desirable engine operating characteristics favor MMH.

A summary of the factors considered for fuel selection is presented in Table III-2.

Table III-2 Fuel Selection Data

Propellant	Vapor Pressure (psia @ 275°F)	Thermal Stability	High Temperature Compatibility	$I_{sp}$ Performance Deconstructed (sec)	Engine Test Experience
$N_2H_4$	25	Good in absence of catalytic materials	Materials available	>290	Minimum
MMH	63	Good, some sensi- tivity to catalysts	Materials available	>290	Maximum
A-50	75	Very good	Materials available	>290	Sufficient

Note: Based on the above data the selected fuel could be either MMH or A-50. Additional considerations are:

- 1) Less ignition spike occurs with MMH;
- 2) MMH burns cooler;
- 3) MMH better film coolant;
- 4) More engine test experience with MMH on candidate engines;
- 5) A-50 performance in slightly greater than MMH.



As a final verification of the individual selections of oxidizer and fuel, a check was made of the particular propellant combination. Table III-3 compares some of the commonly used combinations with MMH/N<sub>2</sub>O<sub>4</sub>.

Table III-3 Propellant Combination Comparison

Propellant Combination	State-of-Art Rating*	Theoretical Vacuum Performance Equilibrium P <sub>c</sub> = 150 psia, ε = 40	
		I <sub>sp</sub> (sec)	Oxidizer/Fuel Ratio
N <sub>2</sub> O <sub>4</sub> /N <sub>2</sub> H <sub>4</sub>	3	340.7	1.53
IRFNA/N <sub>2</sub> H <sub>4</sub>	3	325.7	1.6
N <sub>2</sub> O <sub>4</sub> /MMH	1	337.7	2.2
IRFNA/MMH	2	320.9	2.4
N <sub>2</sub> O <sub>4</sub> /A-50	1	338.1	2.0
*Low number indicated highest rating.			

On the basis of all the above information MMH was chosen as the fuel for this system.

## B. ENGINE SELECTION

The propellant and engine selection activities were carried on simultaneously because of the interdependence of functions. Engine selection was accomplished in four phases. The factors considered in each phase are listed as follows:

Phase I - Engine propellant considerations were:

- 1) Propellant test experience;
- 2) Production system experience;
- 3) Demonstrated performance.

Phase II - Engine program restraints were:

- 1) Engine availability;
- 2) Engine cost;
- 3) Engine predelivery characterization.

Phase III - Preliminary engine screening considerations were:

- 1) Selected propellant test experience;
- 2) Minimum performance capability demonstrated ( $-3\sigma$ );
- 3) Duration capability;
- 4) Materials of construction.

Phase IV - Final engine screening considerations were:

- 1) 12% ETO - 88% Freon decontamination compatibility;
- 2) 280°F extended temperature exposure capability;
- 3) Engine rework required to meet system requirements.

During the first phase of engine selection, a list of small possible candidate engines was compiled. The list also included engines still in a development of R&D status to provide as much test experience as possible. Table III-4 presents the total list of engines from which test data were obtained.

Table III-4 Engines Considered

1.	Rocketdyne - Gemini 23 lb <sub>f</sub> , 79 lb <sub>f</sub> , 94.5 lb <sub>f</sub> - ablative
2.	Rocketdyne - Transtage 25 lb <sub>f</sub> , 45 lb <sub>f</sub> - ablative
3.	Rocketdyne - Apollo 91 lb <sub>f</sub> - ablative
4.	Rocketdyne - Beryllium 100 lb <sub>f</sub> - heat sink
5.	Marquardt - Apollo 100 lb <sub>f</sub> - radiation
6.	Thiokol (RMD) - Surveyor 104 lb <sub>f</sub> - regenerative
7.	Thiokol (RMD) - Apollo, C-1 100 lb <sub>f</sub> - regenerative
8.	TRW Systems - Surveyor backup MIRA-150A - ablative (radiation alternative)
9.	TRW Systems - URSA-100R 100 lb <sub>f</sub> - radiation
10.	Bell Aerosystems - Agena second propulsion 16 lb <sub>f</sub> , 200 lb <sub>f</sub> - radiation
11.	Bell Aerosystems - NASA Program Model 8414 100 lb <sub>f</sub> - radiation
12.	Bell Aerosystems - NASA Program Model 8374 100 lb <sub>f</sub> - adiabatic wall
13.	IR&D and/or exploratory testing



A compilation of the data obtained for the listed engines with respect to propellant combination versus experience and demonstrated performance is presented in Table III-5.

Table III-5 Engine/Propellant Considerations

Propellant Combinations	Production System Usage	Substantial Test Experience	Limited Test Experience	Demonstrated Performance, $I_{sp}$ (sec)
NTO/MMH	1, 3*	4, 5, 7, 8, 9, 12	6	298
NTO/UDMH			13	260
NTO/N <sub>2</sub> H <sub>4</sub>			13	--
NTO/A-50	2, 5	7, 8, 9, 11	4	298
IRFNA/UDMH			13	270
MON/MMH		8	6	298
MON/MMH Hydrate	6			287
MON/UDMH	10			260
*Numbers refer to engines listed in Table III-4.				

As a result of the investigations under the first phase of engine selection, the following 100 lb<sub>f</sub> engines were carried to the second phase of selection:

- 1) Rocketdyne - Beryllium - heat sink;
- 2) Marquardt - Model R-4D - radiation;
- 3) Thiokol, RMD - Model C-1 - regenerative;
- 4) TRW Systems - MIRA-150R - radiation;
- 5) Bell Aerosystems - Model 8414 - radiation;
- 6) Bell Aerosystems - Model 8374 - adiabatic wall.

From the list of Table III-4, engines 1, 6, 8, and 12 were eliminated at the end of the first phase of selection. Engines 1 and 8 with ablative nozzles were eliminated because of uncertainty of compatibility with the ETO decontaminate. In addition there was considerable doubt that the engines could meet the required 300-sec firing duration. Engine 6 was eliminated because of very limited test experience with the selected propellants.



Engine manufacturers were contacted to determine engine availability, detailed performance data, and engine test histories.

As a result of these inquiries three remaining engines were evaluated as to ETO and thermal compatibility. All are compatible with the defined sterilization system requirements. The final selection of the engine was based on previous test experience with the selected propellants, system adaptability, component simplicity, reliability, and development status.

The engine selection criteria for final screening between the Marquardt R-4D and Reaction Motor Division (RMD) C-1 engines are presented in Table III-6.

The Marquardt engine was selected based on test experience of the fixed R-4D design and the RMD C-1 engine was chosen as an alternate, if required.

The R-4D rocket engine, Fig. III-1, will provide a 275-sec ( $-3\sigma$ ) minimum vacuum specific impulse at 100 lb<sub>f</sub> thrust using N<sub>2</sub>O<sub>4</sub> and MMH propellants at an oxidizer-to-fuel ratio of 1.6 and a nozzle expansion ratio of 40:1, as required.

Before delivery of the engine to Martin Marietta, the engine contractor performed a hot fire characterization. This was accomplished by exposing the engine to a standard acceptance test procedure during which three 5-sec steady-state firing runs were made. The acceptance test firings were altitude firings using a full bell with an area ratio of 40:1. Results of the firing runs are presented as follows:

Mean $O/F_s$	1.600
$\Delta O/F_s$	0.006
Mean $F_{vac_s}$	99.6 lb
$\Delta F_{vac_s}$	0.4 lb
Mean $l_{sp_{vac_s}}$	286.7 sec
$\Delta I_{sp_{vac_s}}$	1.7 sec

Table III-6 Final Engine Selection

Test Experience	Reliability	Engines Qualification Status	Complexity	12% ETO 88% Freon 12 Compatibility (@ 50°C (122°F))	Physical Property Heat Cycle Compatibility Extended Duration (@ 135°C (275°F))	Compatibility of Dissimilar Material Ther- mal Expansion	System Design Suitability	High Temperature Component Exposure	Satisfies Program Performance Requirements
<u>Marquardt R-4D</u> No. of Altitude Tests: 633 No. of Altitude Starts: 1,141,000 Accumulated Burn Duration: 489,400 sec Total Valve Cycles: 5,812,800  <u>NTO/A-50</u> Maximum Duration, One Engine: 13,000 sec No. of Starts: 103,000 Maximum Steady-State Duration: 2100 sec  <u>NTO/MMH</u> <u>Three Qualification Engines</u> No. of Altitude Starts: 26,864 Accumulated Burn Duration: 2136 sec <u>Two Development Engines</u> No. of Altitude Starts: 5000 Accumulated Burn Duration: 2000 sec Maximum Steady-State Duration: 1020 sec  Rating: 10	<u>Engine</u> NAA: 5518 Cycles 0.995 @ 50% Con- fidence 0.983 @ 90% Con- fidence  <u>Valve</u> 0.996 @ 50% Con- fidence The reliability is the same for A-50 and MMH since pro- pellant change af- fects only per- formance	Developed and qualified for SM, LEM, and Lunar Orbiter with NTO/A-50. Supplemental qualification completed for NTO/MMH for use on SM. 445 en- gines delivered with 208 remain- ing to be de- livered.	<u>Moderate</u>  <u>Valves</u> Individual fuel and oxidizer solenoid valves.  <u>Injector</u> Shrunk fit in- jector assembly, small injector orifice holes susceptible to clogging and distortion. 8 sets, multi- triplet type with one set preignition.	Compatible	Compatible	Compatible	Supply pres- sure: 180 psi. Exist- ing thrust mount and chamber pressure pickup adequate.	Four solenoid valves; two fuel, two oxi- dizer subjected to 250°F nonoperat- ing temper- ature and functionally evaluated. No degrada- tion in function evidenced.	Satisfactory          10 Rating 97
<u>RMD C-1</u>  <u>NTO/A-50 and NTO/MMH</u> No. of Tests: 4092 No. of Starts: 431,000 Accumulated Burn Duration: 148,000 sec (60% of above tests with NTO/MMH)  <u>NTO/MMH</u> Maximum Duration for One Engine: 12,706 sec No. of Starts: 9920 Maximum Steady-State Duration: 1400 sec  Rating: 8	<u>Engine</u> Required to demon- strate 69 success- ful engine firings. Most severe duty cycle: 28 engines, 20 environmental engines. Test to failure: 25 of 48 engines total. 0.99 @ 50% Con- fidence.	Developed and to be qualified by 15 July 1967, as backup for SM, LEM, S-IVB, and AAP. Uses both NTO/A-50 and NTO/ MMH. Over 100 engines in program; some already delivered.	<u>Minimum</u>  <u>Valve</u> Single integrated torque motor op- erated bipropel- lant valve.  <u>Injector</u> All welded in- jector assembly moderate injector orifice holes. 4 sets, vortex type.	Compatible	Compatible	Compatible	Supply pressure: 179-191 psi. Existing thrust mount and chamber pressure pickup adequate.	Valve func- tionally tested with average coil temp at 500°F with- out detri- mental effects.	Satisfactory          10 Rating 94

MCR-68-119





Fig. III-1 Marquardt R-4D Rocket Engine

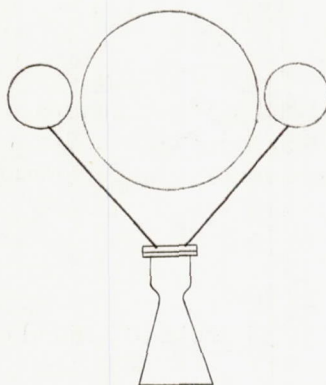


Data were also provided on the injector head and valve assemblies. Flow pressure drop and response under water flow calibration were measured to provide a baseline for component degradation during sterilization.

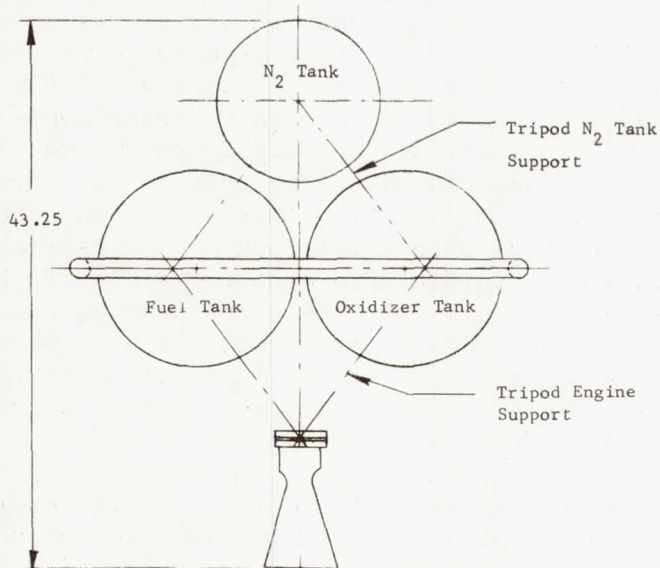
### C. PROPULSION MODULE DESIGN

During the same period of time and in parallel with the propellant and engine selections, an effort was underway to lay out the propulsion module. A system schematic was drawn up and a component arrangement layout was started. Early configurations considered included the tank layout arrangements shown in Fig. III-2. The bipropellant tank configuration was eliminated because of the limitations placed on the type of positive expulsion devices that could be used with this tank. In general this type of tank is suited for metallic convoluted hemispherical diaphragms. Propellants are contained in opposite sides of the sphere with double diaphragms between. The pressurant gas is then introduced between the diaphragms to effect expulsion. One intent of the program was to try at least two types of devices such as diaphragms and surface tension systems so this approach was dropped from further consideration.

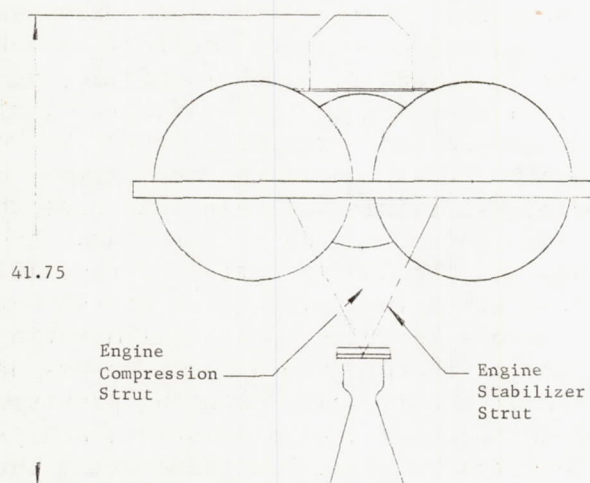
Another problem encountered involved the choice of propellant and pressurant tank arrangement. Since the system to be designed was not intended to be an exact simulation of a flight system, control of the center of gravity was not considered to be of paramount importance. On the other hand, the system was designed to meet the environmental criteria defined in JPL Spec 30250B with Amendments 1, 2, and 3, which specified, as an example, an acceleration load of  $\pm 14$  g in three axes for 5 minutes. Under this magnitude of loading structural integrity became a major consideration. For this reason the arrangement of tanks shown by Fig. III-2(b) was eliminated. In this case the support of the pressurant tank from the major structural truss became quite complex and heavy. The configuration of Fig. III-2(c), however, placed all three tanks in a plane with the structural truss and made mounting simple assuming equatorial mounting provisions on the tanks. Late in the program a decision was made to use propellant tanks having only polar mounting provisions. Rather than doing a complete redesign including stress analysis, the tanks were mounted off the existing box frame using curved tubular supports.



(a) Bipropellant Tank Configuration



(b) Pyramid Tank Configuration



(c) Planar Configuration

Fig. III-2 System Configurations



The module structural truss assembly is shown in Fig. III-3 mounted on its fabrication fixture.

The primary structural member was made up of a box section of carbon steel on which the tank supports and the engine supports were mounted. In general, no attempt was made to use high strength-to-weight ratio structural materials since the module was not intended to be a structural test model. Material investigations provided results sufficient to answer questions concerning the sterilizability of structural materials (see Chapter IV). In the case of the carbon steel parts a zinc chromate coating was applied to avoid contact of iron oxide with the ETO vapor. Metal oxides generally act as a catalyst to decompose ETO that would degrade the decontamination atmosphere. The system schematic evolved during the design phase is shown in its final form in Fig. III-4. Since the system was to be exposed to severe environments (heat sterilization) while loaded with propellants, design for minimum leakage was emphasized. Three portions of the system were designed to be hermetically sealed: the oxidizer and fuel storage systems, and the pressurant gas storage system. Welded joints were used wherever possible to limit external leakage and normally open/normally closed ordnance-operated valves were used to limit internal leakage. Bimetallic transition joints were used to join portions of the systems where material changes were required. For example, the propellant tanks were of titanium alloy and the hand valves were of aluminum alloy. A titanium/aluminum joint was used in the line between the components. The only joints in the hermetically sealed areas that were not a weld joint or a transition joint were the ordnance valve flange joint and AN fittings in the propellant fill line. The ordnance valve joint incorporates a soft aluminum gasket clamped between serrated flange surfaces and is a low leakage type joint. On the external side of the fill and drain and vent valves, the line was capped using a soft aluminum seal under an AN flared tube cap. The remainder of the systems were subject to leakage only after ordnance valve opening and during module firing so that standard AN and MS joints were used allowing more rapid assembly and disassembly.

A drawing system was established to provide for logical fabrication and final assembly of the system. In addition to defining the steps of fabrication and assembly, all in-process inspection and test steps were included in the drawing notes. For example, the steps of proof pressure test and leak check of the various portions of the system were defined in a sequence that would allow for repair before complete assembly. Since the liquid systems were generally hermetically sealed by weld joints, the repair of a leak late in the assembly process could result in considerable disassembly for repair.



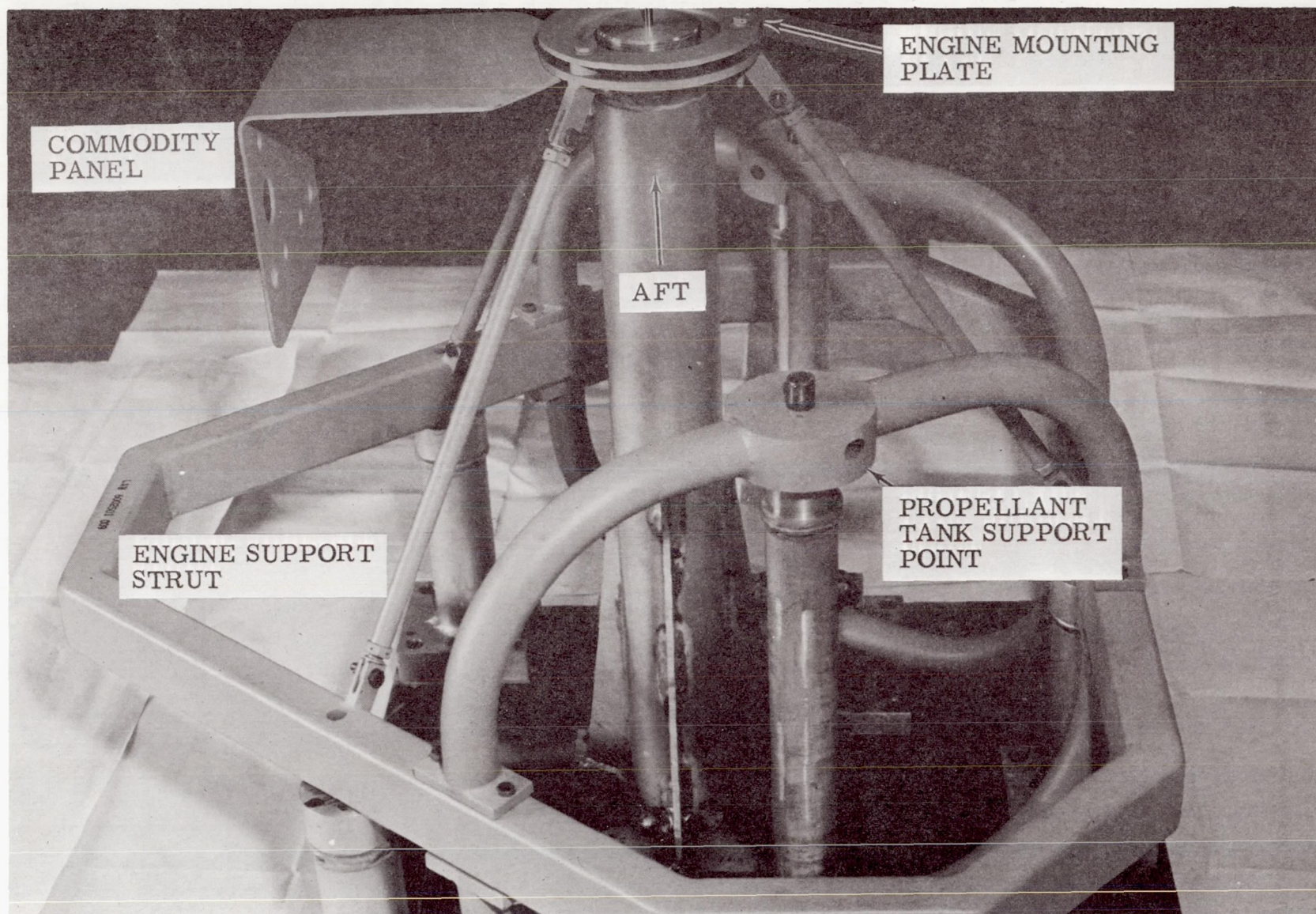


Fig. III-3 System Structural Truss and Assembly Fixture

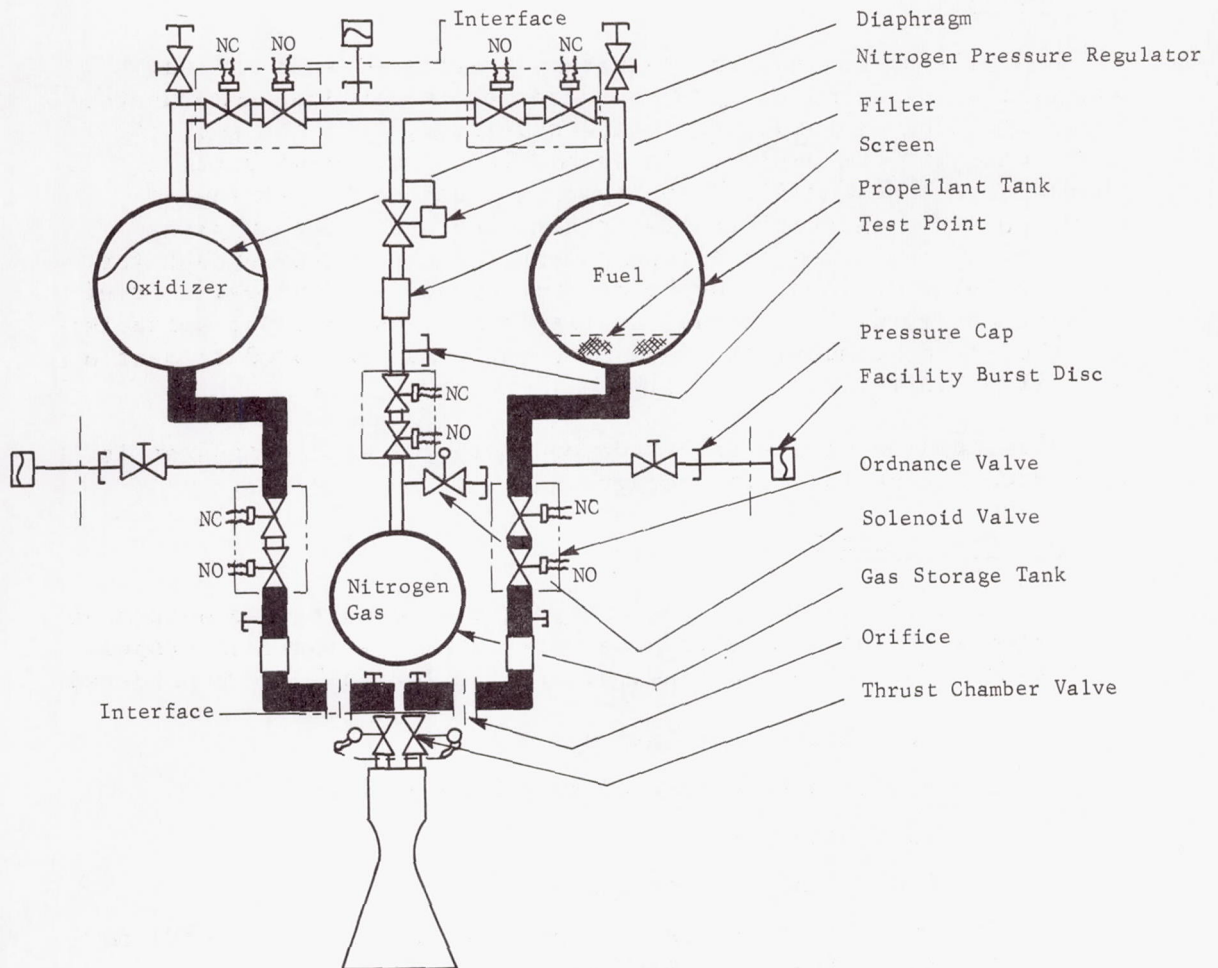


Fig. III-4 System Schematic



## D. COMPONENT SELECTION

### 1. Analysis

Analysis of the systems requirement dictated some minimal and maximal performance parameters for the individual components. Investigations were made to locate qualified, "off the shelf," components for the system. It was desired that these units should have been qualified for systems equal to the stringent requirements of a sterilizable system. Requests for supplier proposals were issued on all components of the system except for the expulsion devices. In the case of expulsion devices, a brief initial survey disclosed that available designs were not suitable; and therefore, components would have to be manufactured to meet a specific requirement.

A discussion of the selection or design of each component is presented in the following paragraphs.

#### a. Propellant Tanks

An initial tank sizing analysis was conducted to determine the volumes and minimum allowable wall thickness for each propellant tank. The following tank volume calculations were considered:

- 1) Propellant mass loaded;
- 2) Approximate volume of expulsion device;
- 3) 5% ullage volume;
- 4) Propellant decomposition;
- 5) Propellant expansion from room temperature (70°F) to sterilization temperatures (285°F).

A 10°F margin was applied to the sterilization temperature for the design point.

The calculations resulted in 15 in. and 16.25 in. inside diameter spheres for fuel and oxidizer tanks, respectively. The minimum wall thickness calculations considered safety factors of 2.0 and 2.50 for yield and ultimate, respectively. Considering worst conditions of tank pressure and temperature, the oxidizer tank minimum wall thickness required 0.292 in. for a maximum pressure of 942 psia experienced during sterilization. A fuel tank minimum allowable wall thickness of 0.0596 in. was required for the tank operating pressure of 250 psia. Both tanks were initially designed using 321 stainless steel as the material.



Following later investigations in material compatibility and the disclosure of iron adduct deposit with the stainless steels in contact with  $N_2O_4$ , titanium was selected for both tanks due to its compatibility, high strength-to-weight ratio, and also its availability. Aluminum tanks, while compatible with the fuel, were heavy and not in production by any supplier.

Several other studies were conducted to determine the amount of propellant mass loaded. The final figures based on 70°F propellant and a 1.60 mixture ratio are given in Table III-7.

Table III-7 Propellant Weight Statement

Item	Oxidizer (lb)	Fuel (lb)	Total (lb)
Total Usable	69.55	43.45	113.00
Unusable			
Propellant Decomposition	0.35	1.74	2.09
Propellant Sample	0.20	0.12	0.32
Trapped in Feed System	10.90	0.06	10.96
Loading Uncertainty	0.50	0.50	1.00
Fuel Bias	--	1.30	1.30
Maximum Outage	1.39	0.87	2.26
Burning Time Margin (7.46 sec minimum)	1.63	3.89	5.52
Nominal Propellant Loaded	84.52	51.93	136.45

b. Zero-g Expulsion Devices

These devices must be capable of withstanding the sterilization temperature while in contact with propellants with low or no permeability of propellant vapor. Elastomers, in general, were either permeable, not compatible with the propellants, or cured at a temperature less than the sterilization temperature. Metals, on the other hand, were not permeable, and not affected by the temperature; however they were not compatible with the propellants under the usage conditions. Some of the possible candidates that were initially considered were:

Stainless steel and/or aluminum bladder;  
 Concentric convoluted aluminum diaphragm;  
 Teflon (TFE, FEP laminates) diaphragm;  
 Stainless steel bellows.

Each of the above configurations were investigated for advantages and disadvantages with respect to the environmental and functional conditions.

Metallic diaphragms can apparently stand several complete reversals and would be impermeable because of all-metal construction. However, this system requires a tank of the same material, to effect a welded joint, and as material tests proved later, stainless steel and/or aluminum would be usable only in the fuel system.

A concentric convoluted aluminum diaphragm would also be impermeable to propellants, but would be limited to one complete expulsion cycle and would be limited to the fuel system because of material compatibility with  $N_2O_4$ .

A diaphragm made of Teflon laminates, TFE, and FEP, would withstand the sterilization temperatures (TFE and FEP are good for 500°F and 400°F, respectively), but would probably swell and allow propellant permeation.

A stainless steel bellows would withstand sterilization temperatures and cycling without difficulty but would be limited to use in the fuel system.

In addition to the bladder-diaphragm-bellows-type expulsion used in one propellant tank, a screen-type expulsion system was considered for incorporation in the other propellant tank. The capillary screen concept would withstand the sterilization cycle without difficulty except for possible compatibility problems between the screen material and the propellant.

Initially, consideration was given to the use of a screen trap for the oxidizer tank. As the materials compatibility testing progressed, it became evident that stainless steel, nickel, and aluminum screens were not compatible with  $N_2O_4$  at 275°F. No other screen material of the proper mesh size was available so a diaphragm or bladder expulsion device was necessary for the oxidizer tank.

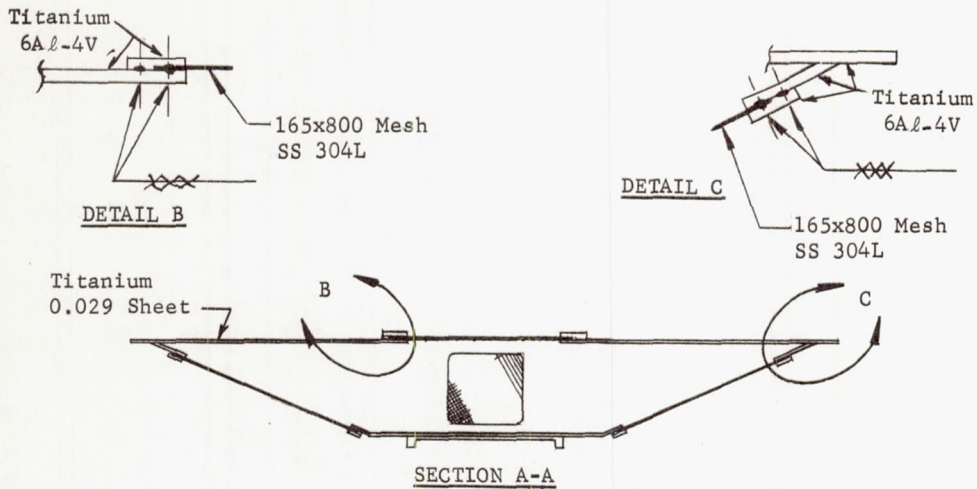
Results of the 600-hr screening test of materials in  $N_2O_4$  at 275°F indicated Teflon was compatible. On this basis it was decided to use a Teflon laminate diaphragm in the oxidizer tank and a screen trap in the fuel tank.



Since the tank material was titanium, an attempt was made to find a supplier of titanium woven screen in the mesh size necessary to support at least 2 in. of MMH. Screen of this mesh is beyond the current state of the art in both wire drawing and weaving. The material becomes highly susceptible to corrosion in small diameters and is quite brittle, making weaving extremely difficult. Further investigation revealed etched titanium foil was available in proper mesh sizes although the material thickness was a problem. The supplier could etch hole diameters no smaller than the material gage. Material 0.001 in. thick etched to the required mesh size was exposed to fuel (MMH) at elevated temperature (275°F) with no material degradation or fuel decomposition. Welding of this etched foil into a trap assembly, however, required a welding development program. One alternative solution was available: use titanium sheet to build up a frame assembly and attach stainless steel screen window assemblies using a crimping, riveting, or bolting technique. A seam welding technique was developed to form a joint, as shown in Fig. III-5. The stainless steel screen was sandwiched between sheets of titanium. A seam weld was made outside the screen to fuse titanium to titanium and a second seam was made through the screen. This latter weld did not provide complete fusion of the two metals; however, it did provide a good mechanical bond and sealed the joint against fuel leakage around the edge of the screen. Seam weld samples as previously described were prepared. Although the weld was possible and proved to be adequate from a structural attachment standpoint, fuel compatibility was a problem. Weld samples were passivated in a mixture of water and MMH. After all gas generation had stopped, the samples were exposed to pure MMH at elevated temperature. Some samples caused no propellant decomposition while others of similar construction did cause decomposition.

On the basis of the erratic results obtained from the weld samples, additional samples using a riveted sandwich were tried. Best results from a leakage standpoint were obtained using aluminum alloy rivets; however, joints were fabricated using monel rivets because fuel tank passivation was best accomplished using a water-MMH mixture and this mixture will attack aluminum rivets. The screen trap in its final configuration is shown in Fig. III-6.





Note: Dimensions in inches.

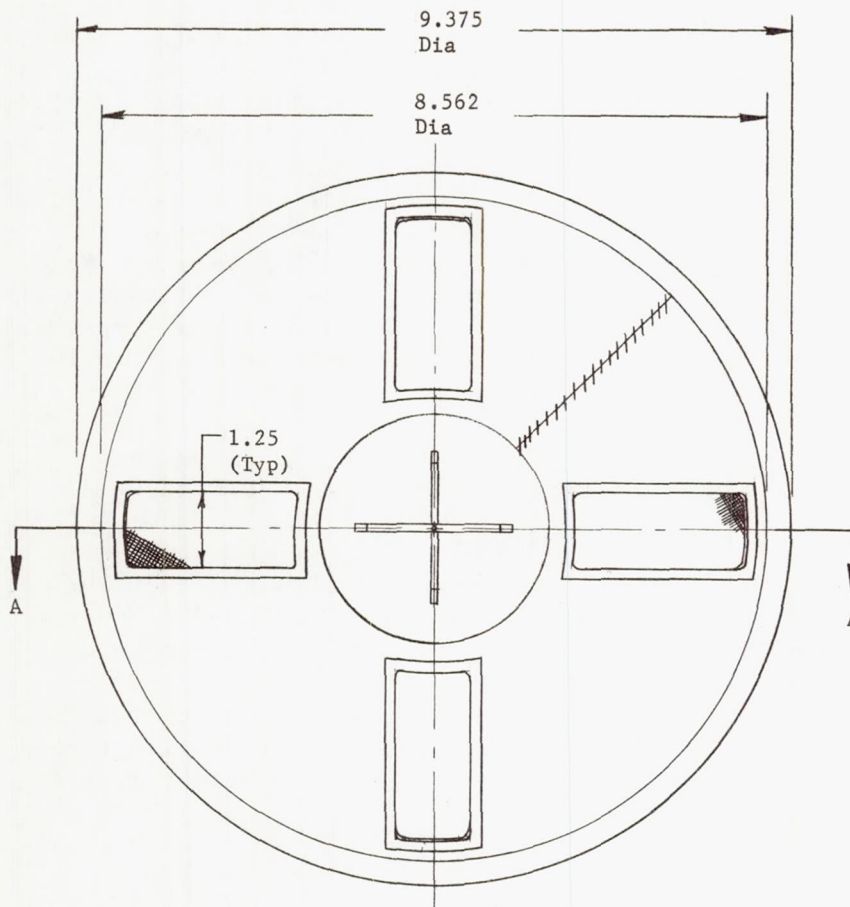


Fig. III-5 Proposed Welded Configuration of Screen Trap

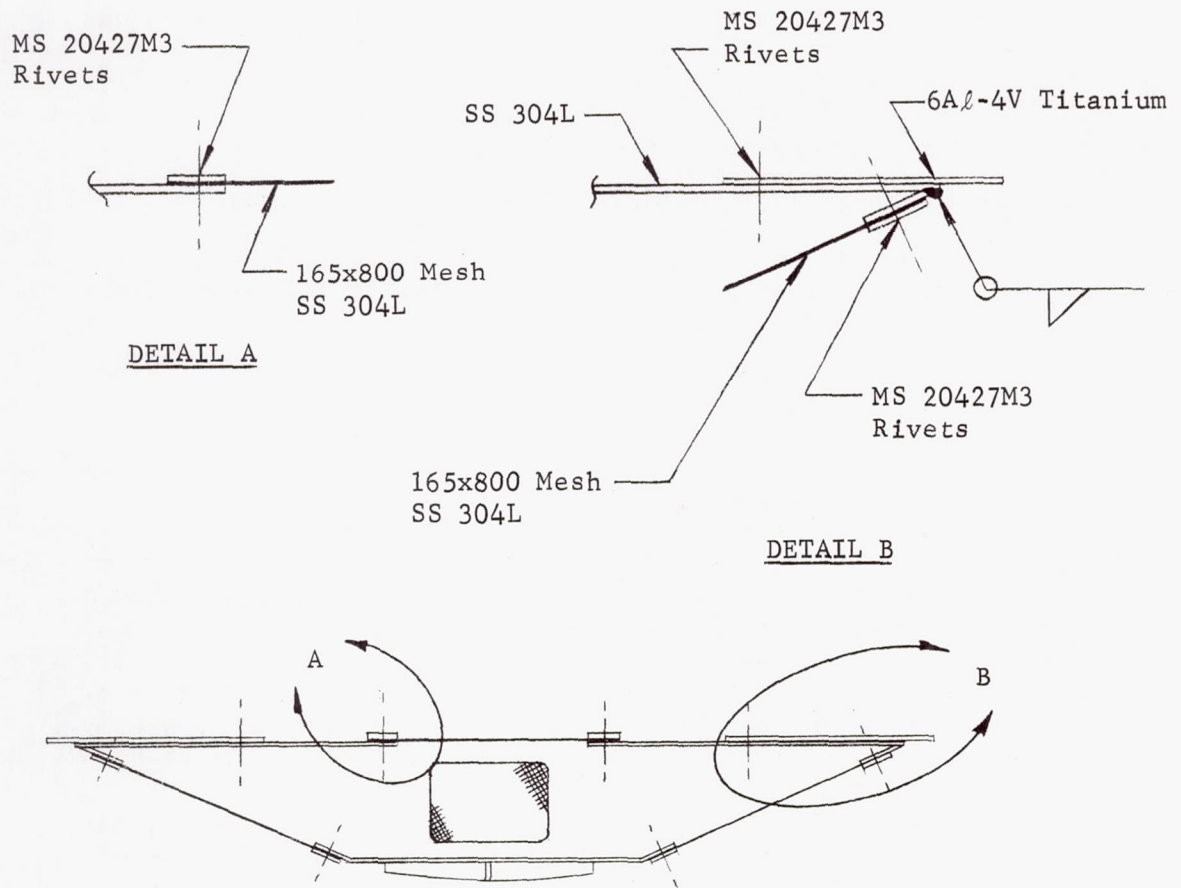


Fig. III-6 Screen Trap Riveted Configuration

c. Pressurant Gas Sphere

This analysis was conducted to determine the amount of nitrogen required for pressurization and to determine if the size of the selected container at the selected loaded conditions was adequate for the pressurization of the propellant tanks. The loaded condition was selected to be ambient temperature (70°F) and a pressure of  $1550 \pm 50$  psia. The primary factors considered in selecting the loaded sphere pressure were:

Sphere design pressures at 70°F;

Required ordnance valve safety factors of 1.5 and 2.5 and an ordnance valve proof pressure of 5400 psia and burst pressure of 8000 psia at 70°F;

A margin to verify the proof and burst pressures up to a temperature of 285°F was considered.

A propellant tank pressurization and thermodynamics computer program (Martin Marietta Program ODO41) was used to perform the pressurant storage analysis. This computer program was used to simulate the expected test firing. The simulated test firing consisted of a 100-sec prepressurization period followed by a 300-sec burn (propellant outflow) period. The pressurization time of a 100 sec was approximately the time required for prepressurization at the regulator design nitrogen flow rate of 0.015 lb/sec. The burn time of 300-sec was the design objective. Because of a computer program limitation, the pressurization and propellant storage system was simulated by a nitrogen sphere supplying nitrogen to one propellant tank instead of two tanks. The volume of the single tank was equal to the total volume of both fuel and oxidizer tanks. Two runs were made -- one run using oxidizer (NTO) and the other run using fuel (MMH). The computer program calculated the pressure and temperature in both the nitrogen container and the propellant tank. It also calculated the nitrogen mass in the storage container and the nitrogen and propellant masses in the propellant tank as a function of time.

As a part of the pressurant storage analysis, the possibility of freezing oxidizer (NTO) during module propellant expulsion was investigated. During pressurant sphere blowdown, the temperature of the nitrogen entering the tank could possibly drop below the oxidizer freezing temperature, and therefore, could result in some NTO freezing.



The pressurization and propellant expulsion of the oxidizer tank was simulated using the same computer program that was used for the pressurant storage analysis. The results of this investigation indicated that while the nitrogen entering temperature dropped approximately to the freezing temperature of the oxidizer ( $472^{\circ}\text{R}$ ), the oxidizer temperature only dropped  $2^{\circ}\text{R}$  from its initial temperature of  $530^{\circ}\text{R}$ . The main reason for this small drop in liquid temperature was due to the high heat capacity of not only the liquid but the propellant tank. Another, but less significant, factor that attributed to the small liquid temperature drop was the increase in ullage temperature during prepressurization. During prepressurization the ullage gases were compressed and the temperature increased. This warmed instead of cooled the liquid. This factor is less significant because even if the ullage temperature was allowed to cool down, the high heat capacities of both the liquid and tank are sufficient to keep the liquid from freezing.

After obtaining nitrogen and propellant mass flow rates, line sizing was completed with the selection of 1/4-in. gas lines and 1/2-in. propellant lines.

d. Gas Pressure Regulator

Preliminary investigation for a suitable regulator design first emphasized a proved off-the-shelf item that would require a minimum of changes to meet the desired design parameters. Vendors were asked to submit a history of accomplishment, and/or qualification, and a materials of construction list. Proposed materials were included in the material compatibility tests. During this period discussions were carried on with the various vendors to determine their proposed design philosophies, such as single stage versus multiple stage regulation. It was desired to achieve the simplest design possible to provide reliability. This had to be accomplished within the range of control parameters that were specified by the system analysis.

A more complete analysis of thermal, pressure, and compatibility effects could not be accomplished at this time because detail drawings were not available. This analysis was completed later in the program and is shown in Appendix A. The subjects covered include stress analysis, tolerance analysis over natural and induced temperature range, and a failure mode analysis. No attempt was made to make this a complete analysis in the sense of investigating each detail part; however, by inspection, those areas or details were selected that proposed the most critical or probable sources of failure.

e. Solenoid Valve

Investigation for a solenoid valve was confined to a direct acting, normally closed, two-way valve to be used as a fill-and-drain valve in the pressurant system. Reliability and a low order of external leakage were of prime importance. Since this type of valve is manufactured by many different vendors, an analysis of suitability resolved into selecting the valves that had the most experience in similar environments. Later in the program and after selection of a specific valve an analysis was performed and is shown in Appendix A.

Very early in this investigation it became apparent that soft seat valves using Teflon or similar materials on the main poppet would be vulnerable to deformation and cold flow during the heat cycling. Therefore, hard seat (metal to metal) valves were favored, but this was not made an absolute requisite if the vendor could justify his selection.

f. Filter

The filtration requirements for this system were initially based on the requirements used on similar systems on the Titan III program. This called for a nominal 10- $\mu$  filter. Later, when the engine requirements became known, this was upgraded to a nominal 5- $\mu$  filter.

Manufacturing firms were surveyed to determine design capabilities in small lightweight filter assemblies. Information initially received disclosed many designs with elastomeric seals and a limited number of all welded filter designs. While all welded filters were favored, they were not specifically required and final evaluation was based on the results of the material compatibility tests.

A more complete analysis was conducted at a later time after component selection. The results are shown in Appendix A.

g. Hand Valves

The design of the hand valves required for this system emphasized a very low order of external and internal leakage. Secondary parameters were flow and pressure drop. Initially the vendors all proposed stainless steel valves. When stainless steel incompatibility with oxidizer became known, all proposals were rejected and the vendors were asked to resubmit designs using aluminum or titanium. One supplier submitted a design in aluminum that duplicated an existing stainless steel design. It



was apparent that off-the-shelf proven designs would not be available and each design would have to be evaluated on its mechanical merits and its material compatibility. Further analysis could not be performed at this time because detail drawings were not available. However, the analysis was performed later and results are shown in Appendix A.

#### h. Ordnance Valves

This valve was supplied by JPL as government-furnished equipment. The structural design of the valve was compatible with the system operating pressure requirements. Since the valve and squib had been exposed to sterilization environment on another program without degradation, it was used in this system and no further search for a valve was made. This component is a combination of a normally open and normally closed valve in one housing.

#### i. Throttling Valve and Thrust Chamber Valves

The initial intent of this program was to provide an engine with throttling capability. When the selected engine did not have throttling valves, it was decided that a separate bipropellant throttling valve would be subjected to the component sterilization cycles. This valve was submitted as GFE and exposed, in contact with the propellants, to the heat sterilization cycles. It was then shipped to the JPL for test and analysis.

The thrust chamber valves -- one oxidizer and one fuel -- were component parts of the engine selected for this program. One of each of these valves was submitted by the engine manufacturer for inclusion in the component sterilization test.

## 2. Specifications

After the initial system studies established the required component parameters, specifications were written for each of the components and submitted to vendors. A short form specification was prepared that set forth the operating requirements, materials compatibility, and nonoperating temperature exposure. No vibration requirements were imposed. Acceptance testing was confined to operating parameters and leakage.



### 3. Selection

Criteria for the selection of each component were established and a weighted grading system was set up. These criteria were determined for each component on the basis of function with weighting performed on the basis of expected and/or required reliability.

The grading sheets were submitted to JPL for approval on 23 November 1966. A sample grading sheet is shown in Table III-8.

Components were first considered on the basis of technical qualifications, as indicated by the weighted grading, followed by a consideration of cost and delivery schedule. In the case of the hand shutoff valve, the Teflon diaphragm, and the screen trap expulsion device, only single proposals were available. Therefore, the only considerations in the latter selections were whether the component was operationally capable of doing the job. The screen trap was designed by Martin Marietta Corporation and it was ultimately decided to build it "in-house."

#### a. Propellant Tanks

The tank design selected, Pressure Systems Inc. 80011-1, was the same design used in the JPL Advanced Lightweight Pressurization System (ALPS) Generant Tank Program with a few minor design changes. The inlet and outlet ports were strengthened to accommodate mounting provisions. In addition, the forgings that were used for the fuel tanks allowed extra metal near the outlet port. This extra metal permitted machining of a ring to allow welding of the screen trap to the tank. The diaphragm material was Teflon rather than butyl or ethylene propylene compounds as used in the ALPS program.

In addition to the modifications listed above, the inlet shower head holes were drilled to a smaller diameter to prevent diaphragm extrusion at the high vapor pressure at sterilization temperatures.

Table III-8 Component Selection Sheet

Component Selection Criteria Gas Pressure Regulator						
1. Basic Design Analysis						
a) Insensitivity to thermal changes (-10 → +10)						
b) Protection of small orifices (-10 → +10)						
c) Complexity (0 → 5)						
d) Seat design (0 → 5)						
e) Structural capability (0 → 10)						
2. Materials of Construction - Compatibility (0 → 10)						
3. Leakage						
a) Internal (0 → 5)						
b) External (0 → 5)						
4. Performance						
a) Regulation pressure bandwidth (0 → 10)						
b) Overshoot on lockup (0 → 5)						
c) Overshoot on inlet "squib valve" initiation (0 → 5)						
d) Pressure band drift due to environmental changes (0 → 5)						
e) Allowable inlet pressure variation (0 → 10)						
5. Vendor						
a) Previous experience requiring minimum development (0 → 10)						
b) Delivery (one negative for each week past target date)						
6. Envelope and Weight (0 → 5)						
7. Qualification Status						
a) Degree of testing in compliance with JPL 30250B (0 → 20)						
b) Changes required (0 → 20)						
Total						

b. Expulsion Diaphragm

Final selection of a diaphragm for the oxidizer tanks involved the selection of a type of diaphragm rather than the selection of a supplier. Both metal and Teflon designs were considered. The Teflon design of Dilectrix was selected primarily because of its qualification status and cycle life capability. The Teflon diaphragm consisted of laminates of TFE (4 mils thick) and FEP (4 mils thick). It also incorporated a crown of FEP (0.030 to 0.035 in. thick) at the gas inlet area to prevent extruding of the Teflon through the barrier plate located in the inlet port (Fig. III-7).

c. Pressurant Tank

The Menasco tank, P/N 812500-501, was selected because it scored higher than the other supplier tanks, primarily in the area of test experience. Another Menasco design, P/N 785000-503, had been initially selected because it had better mounting provisions and lower cost. However, the material was titanium, 7Al-4Mo, which is extremely difficult to weld. A decision was made not to risk the welding problems. Only a single bottle fabricated from the 7Al-4Mo material existed. In addition, Menasco indicated that no additional bottles of this material would be made, therefore, loss of the bottle at any point in the program would require a change to another bottle configuration. No modifications to the selected tank were required.

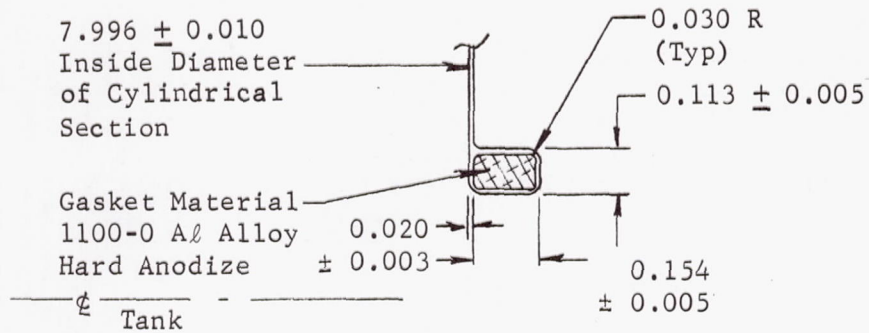
d. Gas Pressure Regulator

The selected design, Sterer Drawing 35570, was chosen in preference to Sterer Drawing 23010 because it is a proved, qualified design. It was basically the same design as that used on Mariner II (Sterer Drawing 18910). Material in the cap and ball reseating pin was changed from 2024-T4 Al to stainless steel. Other changes include the addition of a 10- $\mu$  filter on the inlet side, change of inlet and outlet ports, and change of pressure setting to conform to the present application.

e. Solenoid Valve

The chosen design was selected because it was basically the same as Sterer Drawing 31580, which was qualified for use on the biosatellite. Minor changes included the substitution of Kynar for a nylon threadlock. The threadlock was in a noncritical area and was backed up by a final wire lock. The solenoid potting compound was changed to one that was compatible with ethylene oxide and the ports were changed to conform to the present application.



DETAIL A

Note: All dimensions in inches.

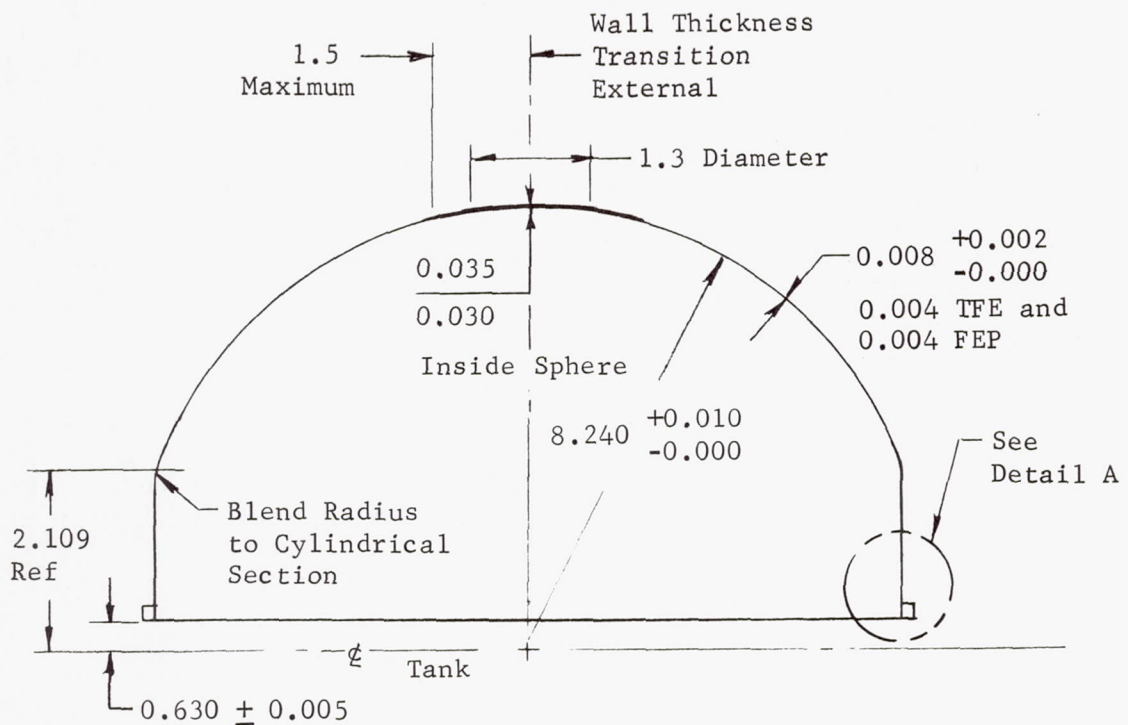


Fig. III-7 Teflon Diaphragm

This valve incorporates filters at both the inlet and outlet ports, thereby reducing the possibility of seat contamination during both the fill and drain operation. Since this valve must be closed during the thermal cycling, the all-metal seat precludes any degradation by cold flow that might be present in a soft seat design.

f. Filter

The Western filter and the second choice designs were rated equal on a technical basis with the Western filter selected on the basis of cost. All filter designs were of stainless steel, however, in this case this was not a problem since the filter assemblies were not in contact with propellants during the heat sterilization cycles.

g. Hand Shutoff Valve

Results of the 600-hr compatibility program indicated that iron or nickel bearing alloys could not be used in contact with oxidizer. In addition, aluminum was mildly incompatible with  $N_2O_4$  at 600 hr, but not at 300-hr exposure. Only titanium proved to be a completely compatible metal. All proposals originally received indicated use of steel hand valves. A second round of proposal requests indicated no titanium component designs and only a single aluminum design. Therefore, despite the partial incompatibility, the aluminum valve design by Vacco was selected. This decision was influenced by the fact that although corrosive action would occur on the aluminum, the propellant would not be degraded as would be the case with steels. Since both the customer-supplied aluminum ordnance valves and the selected hand valves were overdesigned structurally, the attack would not cause structural failure. If a flight system were to be built, titanium components should be used throughout that part of the system exposed to oxidizer ( $N_2O_4$ ) during heat sterilization.

E. COMPONENTS AND SYSTEM TEST PLAN

As a part of Task I -- the analysis and design of the propulsion system -- a comprehensive test plan, MCR-67-20, was prepared to initiate the support activity of the Test Department. The test plan included the step by step activity required for both Task II, Component Test and Evaluation, and Task IV, System Test

and Evaluation. In this way a uniform approach to the test support activities could be obtained. Figure III-8 presents the test requirements of Task II and IV. The dashed line and phantom areas show how support activities of design engineering contributed to the overall success of the test activity.

The tests in Task II were programed through a second series of test cycles to establish some degree of margin of the components. In this way initial information of the component reliability could be considered.

The requirement for test procedures was established by the test plan. The procedures provided step by step directions for performing each operation correctly and uniformly each time. They also provided for safety precautions, facility preparation, and instrumentation instructions.

By establishing a log book system with a checkoff procedure, each component was tested in accordance with the plan. In that way effective controls were maintained for comparison of performance degradation.

The provisions of JPL Specification VOL 50503-ETS were interpreted and implemented by the test plan. The heat sterilization test consisted of 12 cycles of exposure to the components and six cycles of exposure to the assembled module that followed the time-temperature profile shown in Fig. III-9. During the heat cycles the test atmosphere was gaseous nitrogen.

Sterilization requirements also dictated that the assembled module be qualified for exposure to the decontamination environment. This consists of six cycles of exposure to a mixture of 12% ethylene oxide and 88% Freon 12 over the time-temperature profile shown in Fig. III-10. To be effective, the concentration of the mixture is 600 mg/liter of gaseous atmosphere at a relative humidity of 50%. The remaining atmospheric constituent was gaseous nitrogen.

In addition to setting up the test requirements of the program the test plan set forth the schematic layout of all test fixtures for the components and of the complete module. This represented a major portion of the plan and presented a clear-cut outline for the test fixture design activity.

The instrumentation list for each component test and the complete module firing test was prepared that established the channel to be instrumented, the expected range and the accuracy required.



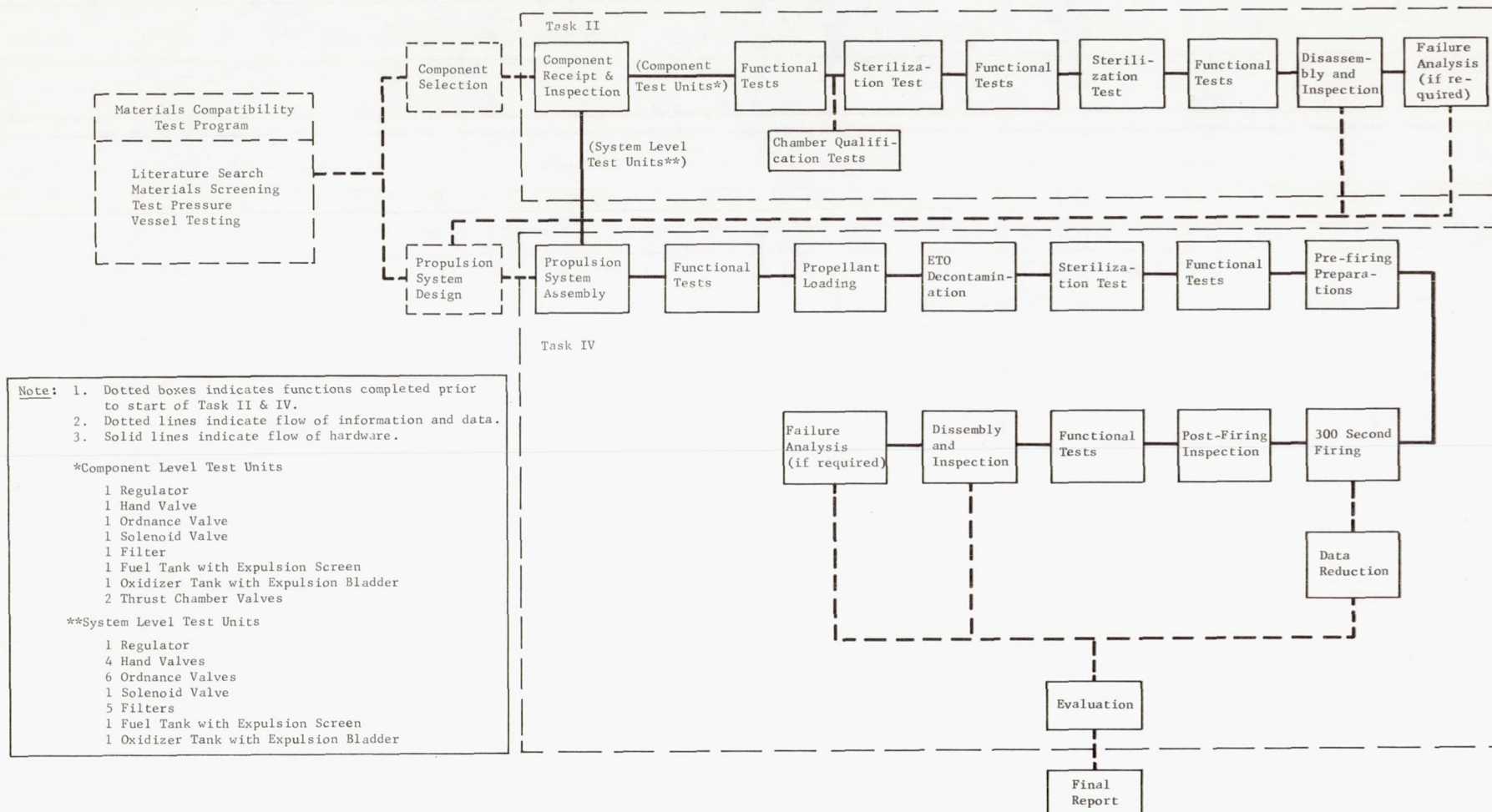


Fig. III-8 Program Test Flow Chart

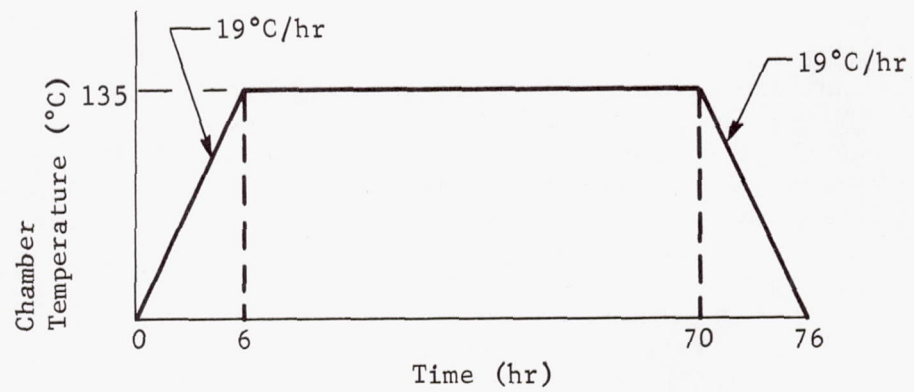


Fig. III-9 Heat Sterilization Cycle

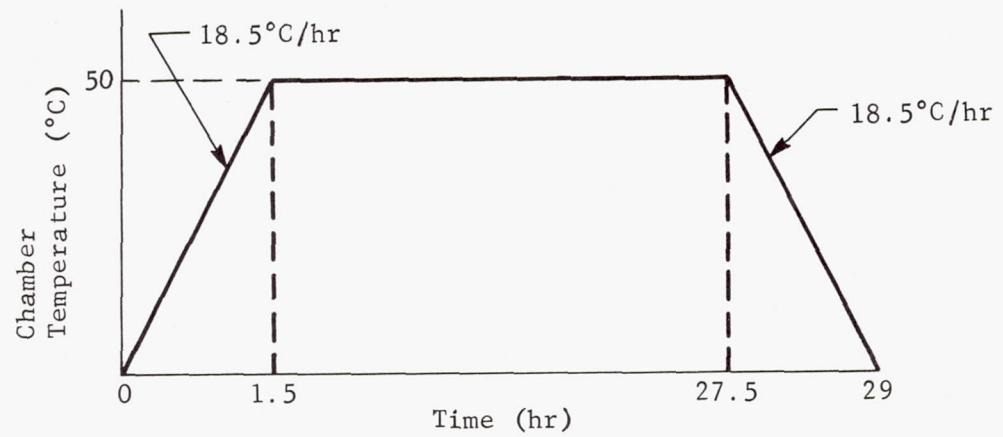


Fig. III-10 ETO Decontamination Cycle

## F. FLIGHT SYSTEM DESIGN

As indicated previously, no attempt was made to design and build a flight-qualified system. It would be well, however, to point out the differences between this system and a similar flight ready system. In general, the differences are those that would make the system more nearly meet a specific set of performance requirements in a reliable way. The specific system differences are as follows:

- 1) Structural design and fabrication materials would be of the greatest strength-to-weight ratio compatible with the required environments. This would probably result in the use of titanium alloys for a major portion of the structure;
- 2) System components would meet the specific performance required. Components selected for use in the program were necessarily of the off-the-shelf variety. An attempt was made to obtain units qualified on other programs which would meet the performance requirements of this program. Specifically, the following changes would be made -
  - a) Propellant Tanks - Each tank would be designed to meet its specific requirement. In this program both the fuel and oxidizer tanks were identical. The particular design selected nearly matched the oxidizer tank requirement of volume and maximum operating pressure but was considerably overdesigned for the fuel application,
  - b) Regulator - The regulator chosen for the module very nearly matched the performance requirement. Modifications were made in the end connections to make the regulator compatible with the external leakage criteria so that this component, which had been adequately qualified on another program, would require no change if a flight system were built,
  - c) Hand Valve - Much difficulty was experienced in finding a hand valve meeting the leakage and compatibility requirements of the system. Neither steel nor aluminum alloys are compatible with oxidizer ( $N_2O_4$ ) at the sterilization temperature ( $275^\circ F$ ). Flight system design would require a



valve of titanium using a titanium bellows stem seal and a hard seat and poppet. The valve used was of aluminum alloy and used a chevron stem seal packing of Teflon. Although adequate performance was obtained, the poppet and seat were oxidized after testing and the stem seal packing leaked as a result of extrusion of the Teflon packing,

- d) Ordnance Valve - Again the use of a titanium valve would assure compatibility with the oxidizer. In addition, a problem was experienced with the flange gasket seal joint on the propellant side of the valve. For the core of a flight system, welded tube joints would be used at both the inlet and outlet connections. The valve used met all performance requirements because it was qualified for spacecraft use,
- e) Line Filters - No difficulty was experienced with the propellant line and gas system filters. The stainless steel construction is allowable in this case since the filter is not in contact with propellant at sterilization temperature. For a flight system the filters used would be sized to meet the specific flow rates expected to minimize weight,
- f) Solenoid Valve - It is not clear that a solenoid valve would be required in a spacecraft system. In general, this function could be performed by normally open/normally closed ordnance valves unless a large number of actuations were required. If such a valve were required, it would be constructed of compatible material and would feature a hermetically sealed solenoid coil using high temperature insulation on the coil windings,
- g) Engine, Thrust Chamber Valves and Throttling Valve - These components are normally designed for a specific mission. Their construction would be of materials compatible with heat (275°F) and external ethylene oxide exposure,

- h) Expulsion Devices - Two types of expulsion devices were used for the module. Either type would be capable of spacecraft use. If a single-burn system were designed, the screen trap device would be adequate and reliable. In fact, a screen trap device of titanium or tantalum would be designed for the oxidizer tank since it is inherently more reliable than a diaphragm or bladder;
- 3) Design the system to provide additional reliability. This would include the addition of such redundant components as regulators and ordnance valves;
- 4) Control of component and system design, fabrication, and test would be greatly increased because larger and more detailed specifications are required to cover supplier operations. In addition, receiving inspection requirements would be increased along with specifications covering in-house processes and handling. The "product integrity" concept of engineering control would be used to a greater degree. This concept requires that a specific engineer be responsible for each component from the original supplier proposal evaluation through the usage on the space vehicle. In addition to being responsible, the engineer also carries the authority to revise or stop the program at any point that he feels the component is not being used properly.

#### IV. MATERIALS EVALUATION

##### A. LITERATURE SEARCH

Appropriate technical documents were surveyed to select materials for potential use in the design and fabrication of the sterilizable engine module. The purpose of the survey was to assure that only those materials showing the most promise would be evaluated, testing would be minimized, and that selected test methods would yield useful design data.

The following basic characteristics were considered in the survey:

- 1) Compatibility of the selected propellants -- monomethylhydrazine and nitrogen tetroxide -- when exposed to the dry heat sterilization temperature of 275°F;
- 2) The compatibility of materials of construction with the selected propellants at sterilization temperatures and for one year storage at room temperature;
- 3) Thermal properties of materials and propellants at the sterilization temperature;
- 4) Compatibility of materials with the decontamination agent of 12% ethylene oxide/88% Freon 12.

##### 1. Monomethylhydrazine (MMH)

Only a limited amount of data was available on the propellant at either room or elevated temperatures. Since the chemical properties of monomethylhydrazine and hydrazine are quite similar, and since hydrazine presents the more critical condition due to its greater reactivity, it was assumed that their compatibility characteristics were interchangeable. Furthermore, a review of the compatibility of selected materials revealed no discrepancies in the data.

Additional information was noted in the Olin Chemical Division Monomethylhydrazine Product Data (Ref 4). If long-term life is not a consideration, a material may be used although it would not normally be recommended for general applications. Olin also



indicates (Ref 5) that decomposition can be caused by contact with rust, molybdenum, and copper or its alloys, resulting in a spontaneous fire. When a film of MMH comes in contact with such metallic oxides as those of iron, copper, lead and manganese, it may cause the MMH to decompose often with sufficient temperature increase to cause spontaneous ignition.

## 2. Nitrogen Tetroxide ( $N_2O_4$ )

Numerous aerospace and research organizations have been active in testing compatibility of  $N_2O_4$  with various materials. The work done by Aerojet-General and Martin Marietta in support of Titan vehicle development greatly restricted the list of materials to be tested in this sterilization program. The literature search confirmed that in addition to the Martin Marietta Propellant Compatibility Report (Ref 6) there were data available covering the temperature range of 60 to 180°F, but very little data at the sterilization temperature of 275°F. Martin Marietta tests have shown that the degradation rate of materials at elevated temperatures is not linear, and that significant side effects may be experienced.

The literature also suggested that the formation of particulate matter in the presence of ferrous alloys would be cause for concern. If the ferrous alloys exhibited corrosion in the presence of  $N_2O_4$  at 275°F, significant quantities of  $Fe(NO_3)_3 \cdot N_2O_4$  would be formed. This substance is an insoluble nitrate formed in  $N_2O_4$ , contaminated with nitrosyl chloride (NOCl) in the presence of metallic iron.

## 3. Compatibility of Materials

A group of candidate materials of construction was developed so that our literature search could be confined to the most promising materials. All materials shown to be incompatible with  $N_2O_4$  or the UDMH/hydrazine blend during the Titan program were omitted from further consideration. Table IV-1 presents the data results for the more promising materials considered.

## 4. Thermal Properties of Materials

A study of the effects of the thermal property variation in the temperature range from 70 to 285°F was conducted. The effects of the thermal environment on the chemical and physical properties of the candidate materials have been compiled in Tables IV-2 and IV-3.

Table IV-1 Compatibility of Materials Literature Review

Material	N <sub>2</sub> O <sub>4</sub>	N <sub>2</sub> H <sub>4</sub> /MMH	Reference	Remarks
304L Stainless Steel	C*	C	7, 8, 9, 10, 11	Data limited to 160°F
321 Stainless Steel	C	C	7, 8, 9, 10, 11	Data limited to 160°F
17-4Ph (h1075) Stainless	C	C	9, 10, 11, 12	Data limited to: N <sub>2</sub> H <sub>4</sub> , 140°F N <sub>2</sub> H <sub>4</sub> , 100°F MMH, 160°F N <sub>2</sub> O <sub>4</sub> , to 200°F
Titanium 6Al-4V	C	C	8, 9, 10	
A-286 Steel	C	C	8, 9	Room temperature
Hastelloy Steel	C	†	8, 9, 13, 14	Up to 125°F
Maraging Steel	--	‡		No information found
Teflon	C	C	7, 8, 9	Up to 160°F
*C = Compatible. †Contradictory information found. ‡Maraging steel not recommended because oxides are easily formed that could cause the fuel to decompose.				



Table IV-2 Ethylene Oxide and Thermal Compatibility of Metals During Decontamination and Sterilization Cycles

Material	Coefficient of thermal expansion at 70 to 280°F in/in/ft	YTS at 70°F	YTS at 280°F	UTS at 70°F	UTS at 280°F	Ethylene Oxide Compatible	Remarks
304 st. stl, plate	$9.0 \text{ to } 9.4 \times 10^{-6}$	28 ksi	25 ksi	75 ksi	70 ksi	C	(1), (2)
321 st. stl., sht, plt, strip	$8.4 \times 10^{-6}$	30-35 ksi	*	85-90 ksi	*	C	
347 st., stl., sht, plt. strip	$9.2 \times 10^{-6}$	40 ksi max.	*	100 ksi max	*	C	
446 st. stl.	$5.6 \times 10^{-6}$	45 ksi	*	75 ksi	*	C	
17-4 ph st. stl.	$6.1 \times 10^{-6}$	170 ksi min	160 ksi min	190 ksi min	180 ksi min	C	
17-7 ph (th1050) sht. and plt.	$5.9 \times 10^{-6}$ approx	140 ksi min	130 ksi min	170 ksi min	165 ksi min	C	
Waspalloy	$6.7 \times 10^{-6}$ approx	56 ksi	55 ksi	80 ksi	76 ksi	C	
A-286, Sheet and plate	$8.9 \text{ to } 9.3 \times 10^{-6}$	95 ksi min	92 ksi min	140 ksi min	139 ksi min	C	1
L-605, bar and forgings	$6.8 \times 10^{-6}$ approx	45 ksi min	36 ksi min	125 ksi min	110 ksi min	C	Hot worked and stretched
AM-355, bar and forgings	$6.5 \times 10^{-6}$ approx	155 ksi min	*	170 ksi min	*	C	
Rene' 41	$6.5 \times 10^{-6}$ approx	100 to 130 ksi	*	170 ksi max	*	C	
Inconel X-750	$7.1 \text{ to } 7.6 \times 10^{-6}$	100 ksi min	99 ksi min	160 ksi min	159 ksi min	C	
Molybdenum, comm. pure	$2.8 \times 10^{-6}$ approx	79 ksi min	*	91.3 ksi min	*		Stress relieved
Molybdenum, comm. pure	$2.8 \times 10^{-6}$ approx	43.7 ksi min	*	58.2 ksi min	*		Recrystallized
Alnico IV	$11.3 \times 10^{-6}$	-	-	2.3 ksi	2.2 ksi	C	No yield strength listed
6061-T6 aluminum	$13.4 \times 10^{-6}$	35 ksi min	32 ksi min	42 ksi min	35 ksi min	C	Sheet and plate
Titanium, 6AL-4V	$5.3 \times 10^{-6}$	120 ksi min	*	130 ksi min	*	C	Annealed Sheet, plate, bar
Titanium, 6Al-4V	$5.3 \times 10^{-6}$	120 to 150 ksi	106 to 132 ksi	130 to 160 ksi	107 to 132 ksi	C	Heat treated bar & forging
Beryllium 12% Beo	$6.5 \times 10^{-6}$	50 ksi min	45 ksi min	70 ksi min	60 ksi min		Pressed block
Tantalum/10%w, sheet	$3.7 \times 10^{-6}$	82 ksi min	*	96 ksi min	*		
Columbium sheet	$4.0 \times 10^{-6}$ approx	-	-	80 to 100 ksi	65 to 80 ksi		Cold worked
Maraging steel	$5.6 \times 10^{-6}$	245 ksi min	*	255 ksi min	*	C	For N <sub>2</sub> O <sub>4</sub> use only
Hastelloy C, sheet	$6.5 \times 10^{-6}$	68 ksi	62 ksi	120 ksi	120 ksi	C	
Carpenter 20, sheet	$9.4 \times 10^{-6}$ *	50 ksi	*	90 ksi	*	C	Group "C"

\* Less than 5% reduction in tensile strength between 70°F and 280°F

\*\* Coefficient of expansion is between 68°F and 1200 °F



Table IV-3 Summary of Typical Nonmetals Compatible with Decontamination and Sterilization Cycles

Material Use	Trade Name	Basic Material	Applications
Adhesives	PD-454	Epoxy	General applications
	PD-458	Epoxy	General applications
	RTV-102	Silicone	One Component -100° to 320°F
	RTV-511	Silicone	General applications
	RTV-560	Silicone	General applications
	Eccobond 57c	Epoxy	Electrically conductive -70° to 350°F
	RTV-60	Silicone	General applications
	Eccobond 601	Epoxy	Thermally conductive
Coatings and Finishes	* D-4D paint	Silicone-alkyd	Thermal control coating
	* Vitavar PV-100	Silicone-alkyd	Thermal control coating
	* Wash primer	Penetrant primer	Penetrant primer
	* Zinc chromate primer	Zinc-chromate	Corrosion protection
	Silicone primer SS1101	Silicone	Primer for adhesive bonding
	* Lowe Brothers 17865	Glyceryl-pthalate	Heat resistant paint
	MSD-105	Zinc oxide-silicate	Thermo conductive coating
Tapes	* 3M-850	Metallized polyester	Sealing and joining mylar sheet
	Schjeldahl GT	Polyester	Heat sealable adhesive tape
	* 3M-56	Polyester	Harness bundle wrap
	* 3M-EE-3990	Copper foil tape	Electromagnetic harness shielding
	Silicone tapes DC-269	Silicone	Seal component against corrosive environment
	AM-FAB TV-20-60	Fluorocarbon	Insulation tape
Encapsulants	RTV-60	Silicone	Encapsulating
	LTV-602	Silicone	Potting and encapsulating
Insulating Material	Tissue Glass - 200a	Glass fiber-Cellulose	Thermal insulation
	Amfab 20-60	Fluorocarbon-glass	Thermal insulation
	*Epoxy glass S-30205, P-2	Epoxy-fiberglass	Circuit boards
	Thermofit RNF-100	Polyolefin	Thermal insulation
	Mylar (pre-shrunk 300°F)	Polyester	Electrical and moisture insulation
Lubricants and Greases	Grease G-300	Silicone	Bearing lubricant
	* Dry film	Molybdenum-disulfide	Lock assemblies
	Fabroid	Glassfibers-fluorocarbon	Bearing surfaces
	Grease MSD-104	Silver filled silicone	Joint filler
* Sterilizable in an inert atmosphere			
NOTE: Source - Ref 15			

In the metallic area, members of the ferrous, titanium, and other heat-resisting groups exhibit little change in the temperature range. Aluminum alloys may experience a slight loss in properties at the maximum temperature and those effected by long-term overaging will experience some degradation in elongation and tensile strengths and an increase in susceptibility to intergranular and stress corrosion.

In the nonmetals area, a review of data presented in reports from earlier studies was made. When using information of this type for some of the plastics, the formulation and cure cycle must be known. Compatibility properties can be significantly changed by variation in these items.

Table IV-2 lists the compatibility of a cross section of the materials studied.

#### 5. Candidate Materials Compatibility with 12% Ethylene Oxide/88% Freon

Results of the survey on compatibility of the candidate materials with the ethylene oxide decontamination fluid indicate that data are available on most material families. Those data have been compiled in Tables IV-1 and IV-2.

### B. DEVELOPMENT OF TEST TECHNIQUE

The materials test program included several distinct test activities in three broad categories: (1) tests of materials in contact with propellants in the sterilization temperature of 275°F; (2) test of materials in a dry heat environment in a nitrogen atmosphere; and (3) special purpose tests that included material compatibility with the ethylene oxide decontamination agent, and flammability tests of propellant with the decontamination agent to mention only two.

While the latter two categories were straightforward in test approach, we concerned ourselves with the materials testing in contact with propellants. To assure valid results in this area, a series of short-term prescreening tests were performed. This group of tests served to eliminate those materials showing degradation and to provide design and operations data for later screening tests and long-term storage tests. Figure IV-1 shows the overall materials test program in block form.

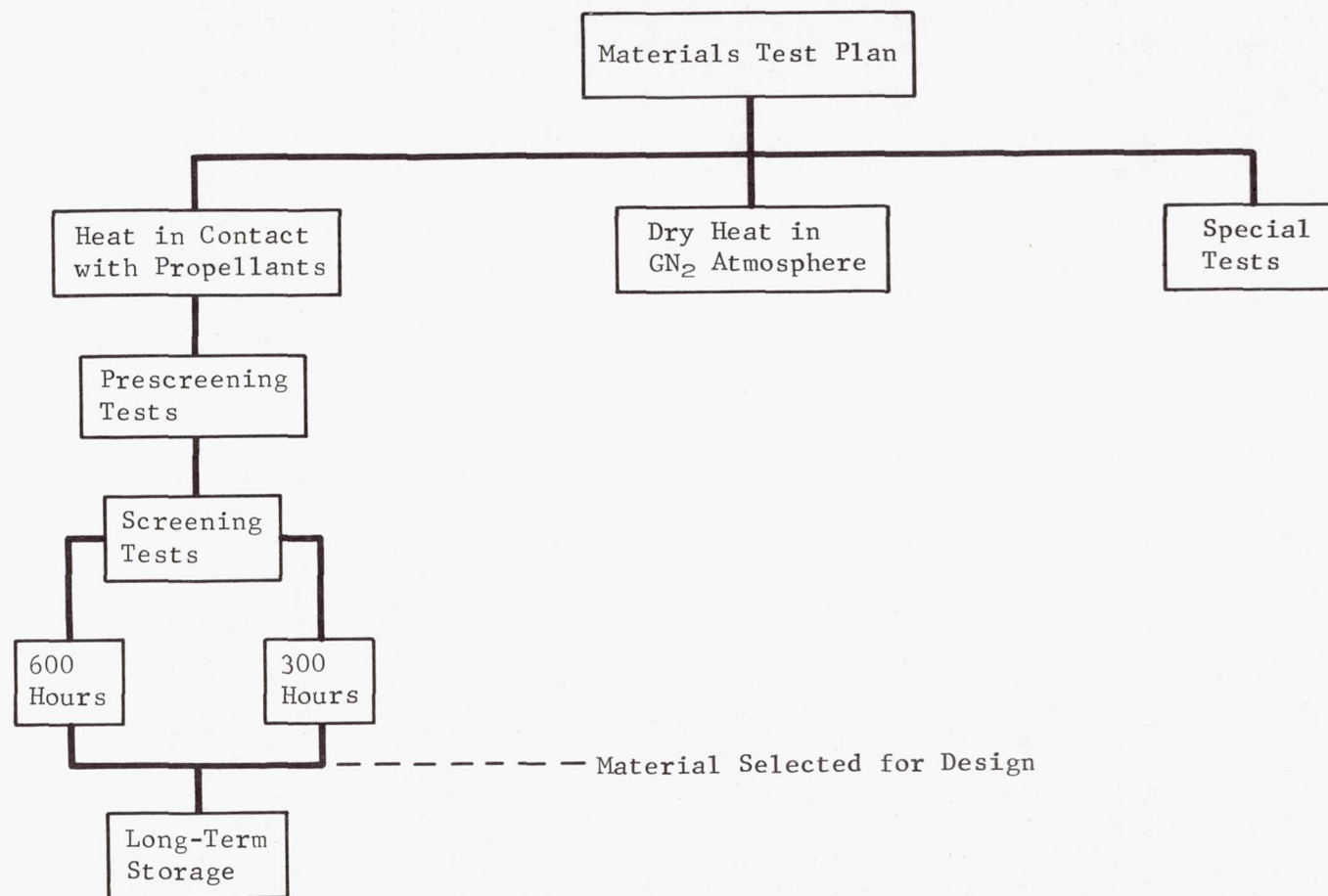


Fig. IV-1 Material Test Program



To implement the materials test program a Materials Evaluation Test Plan, MCR-66-63, was prepared and submitted to JPL. It described the tests to be run, the materials to be submitted for evaluation, and the test procedures. In addition, the equipment design, the safety precautions, and the instrumentation requirements were described. Detailed results are presented elsewhere in this report.

Instruction for the preparation of the material test specimens was presented. The necessary control ranges and instrumentation ranges and necessary accuracies were detailed. The test plan provided uniformity in test approach that led to reliable test results and evaluations.

#### 1. Material Prescreening Tests

So that timely information could be obtained from this series of tests simple test containers were employed. Hoke cylinders of 304 stainless steel were used for the oxidizer ( $N_2O_4$ ) tests, and 300 series stainless steel tube sections were used for the fuel (MMH) tests. The test durations were from 1 to 200 hr. Metal specimens conformed to the NASA Langley Research Center configuration shown in Fig. IV-2. Specimens were stressed to 50% and 75% of yield strength on the double beams, respectively. Standard processes were used for welding and cleaning equipment and specimens.

The high activity of the propellants obscured some of the results of the very early tests and made it necessary to continually reappraise the test techniques. During the course of the prescreening tests, it was determined that isolation of test specimens and meticulous care in the equipment cleaning contributed most to the later success of the screening, long-term, and special tests.

For later tests, specimens were contained in glass test tubes each containing some propellant so that cross talk between specimens and the propellant was isolated. Careful cleaning, passivation, and inspection techniques were used to reduce propellant reactions or decomposition to an absolute minimum.

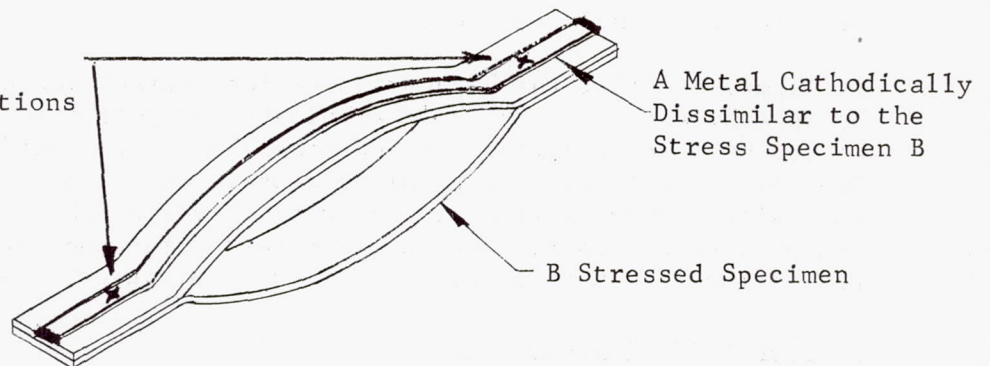


Note: Surface finish to be between 16 and 32 RMS.



(a) Double Beam Specimen

Spotweld or Rivet  
Depending upon  
Materials Combinations



(b) Dissimilar Metal Stress Specimen

Fig. IV-2 NASA-Langley Test Specimen Configurations



## 2. Screening Tests

To provide the necessary design data for materials selection, candidate materials for propellant storage tanks including those materials for expulsion devices were exposed to the propellants for 300 and 600 hr at 275°F. The shorter duration provided data for initial selection with a full 600-hr exposure providing final verification. The exposure duration was established to meet the requirements of the Voyager environmental sterilization specification for piece parts, VOL 50503 ETS, January 12, 1966. A continuous exposure of the planned duration was used rather than six cycles of 96 hr each. Since there were no moving parts involved, it was decided that continuous exposure to a full duration was justified as opposed to the cyclic exposure with attendant risk of refluxing the propellant out the glass tubes during the cooling cycles.

The specimens, all Langley specimens except Teflon and 1100-0 aluminum, were arranged in a rack inside a high pressure vessel described in the next section. Each specimen was in a glass test tube loosely stoppered to prevent contamination of the vial by vapors from the sacrificial propellant in the bottom of each high pressure vessel. Each specimen and vessel was thoroughly cleaned and passivated. The bombs were charged while maintained under a gaseous nitrogen blanket to avoid oxygen contamination. Slow heating and cooling rates were employed so that the propellants in the individual tubes would not reflux into the main reservoir of propellant. Figure IV-3 shows the overall arrangement of test tubes and holding rack.

Temperature of the high pressure fuel vessel was controlled by an ethylene glycol bath to eliminate any potential hot spots caused by a heating tape. A localized hot spot might initiate fuel decomposition. The oxidizer vessels were heated by heater tape since decomposition of the oxidizer was unlikely at the temperature of 275°F. The oxidizer test setup and the fuel test setup are shown in Fig. IV-4 and IV-5, respectively.

## 3. Long-Term Storage Tests

Subscale tanks containing the materials of construction, including expulsion devices, to be employed in the propulsion module were subjected to the temperature environment for evaluation after a one-year storage at ambient conditions. Three oxidizer tanks and three fuel tanks were exposed. One of each configuration was opened at four-month intervals, representing a full year's storage. A fourth was held as a control specimen.



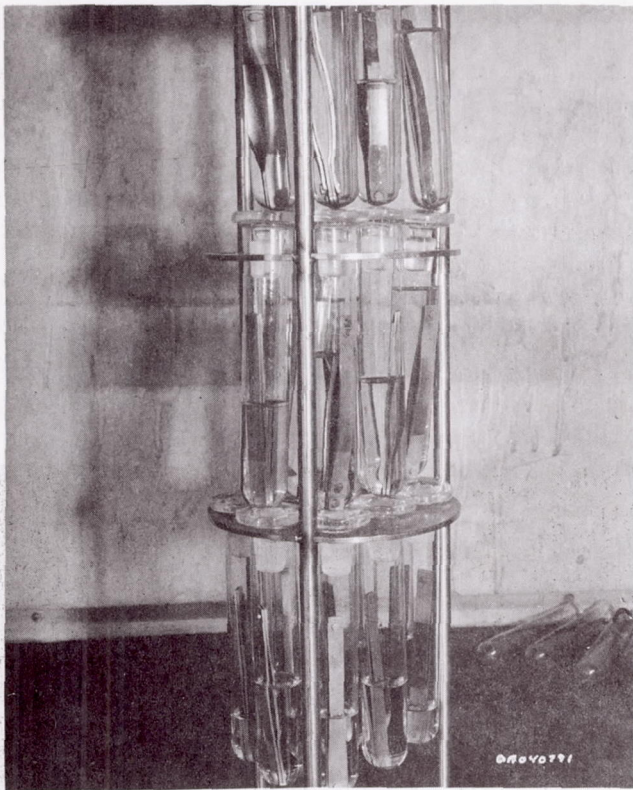


Fig. IV-3 Specimen Test Tubes and Holding Rack

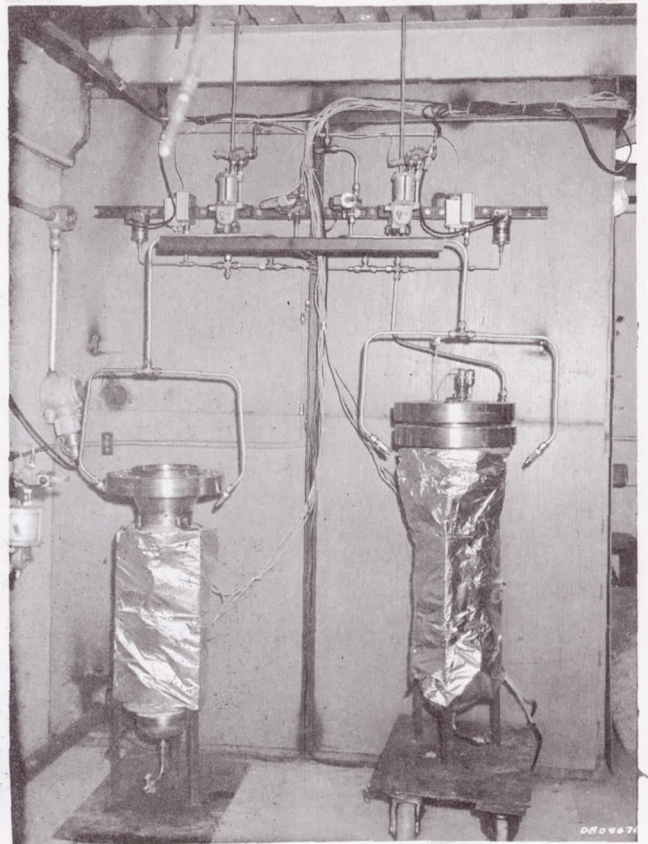


Fig. IV-4 Oxidizer Test Fixtures

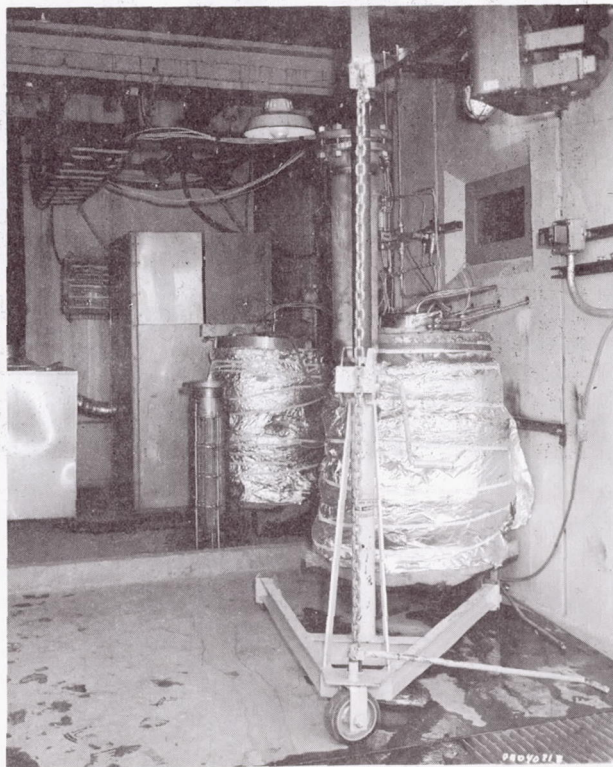


Fig. IV-5 Fuel Test Fixtures



Each subscale tank was fabricated from titanium 6Al-4V sheet stock since tubing of this material was not available. The fuel tank contained material representing the screen trap device. A screen sample of 165x800 mesh 304L stainless steel wire cloth was sandwiched by monel rivets between 0.050-in. 304L steel stock. One member of this sandwich was in turn riveted to a titanium 6Al-4V strip. The titanium in turn was welded to the wall of the vessel. To yeild additional information, a Langley specimen of titanium 6Al-4V having a weld in the stressed area was included in each vessel. All welds were made with commercially pure titanium rod material (Fig. IV-6).

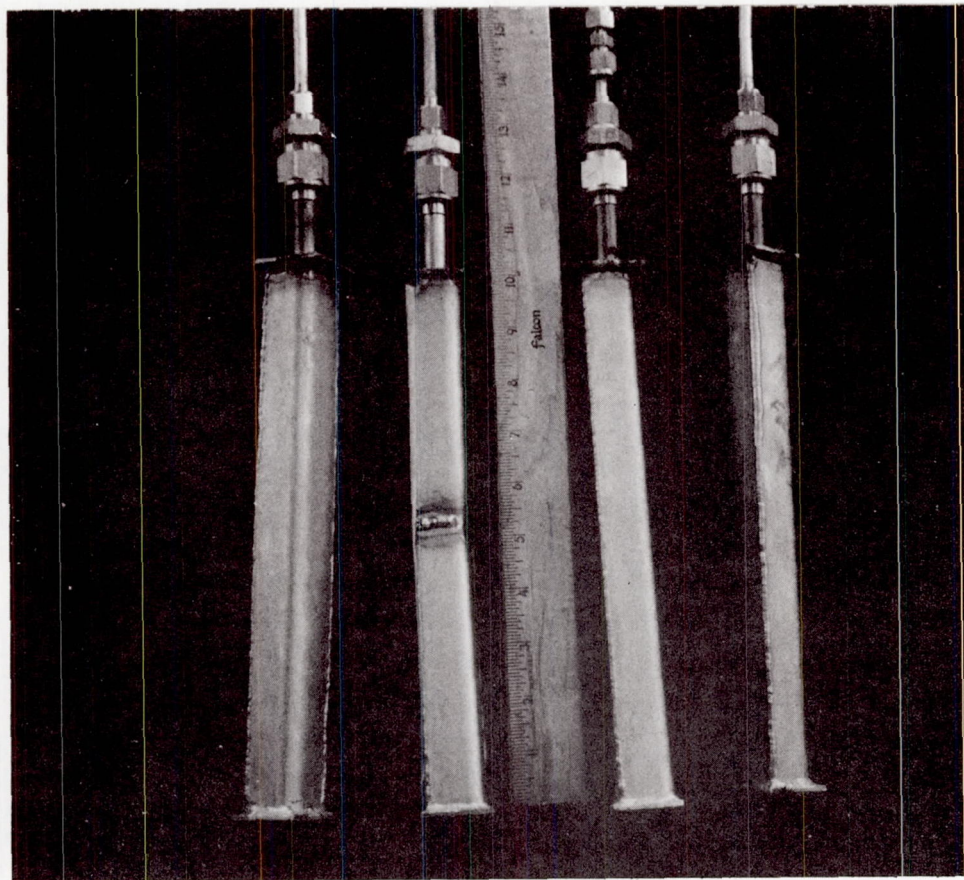


Fig. IV-6 Long-Term Storage Tanks

Each subscale oxidizer tank contained a sample of the Teflon laminate representing the expulsion bladder in those tanks. The Teflon strip was approximately 2x0.25 in. The thickness was made up of a laminate of 0.0075-in. TFE and 0.0075-in. FEP. The strips of Teflon were unstressed. Each tank also contained a welded titanium specimen similar to the fuel tanks.

#### 4. Ethylene Oxide Tests

Materials compatibility tests performed with the ethylene oxide decontamination agent were controlled in the following manner:

- 1) 12% ethylene oxide/88% Freon 12 was the decontamination agent;
- 2) The concentration was 600 mg/liter of atmosphere;
- 3) The remaining constituent was gaseous nitrogen;
- 4) The test temperature was 122°F;
- 5) Relative humidity, 45%  $\pm$  10;
- 6) Duration, 168 hr or as applicable.



### C. TEST FIXTURE DESIGN AND FABRICATION

The screening test pressure vessels were 6 in. in diameter by 24 in. long. One end was closed by a pipe dome and the other had a bolted flange. The specimens were mounted on a rack in three tiers, each tier containing nine glass specimen containers.

The oxidizer vessel was fabricated from schedule 80-304 stainless steel seamless pipe. The bolted flange and dome were 310 stainless steel with a rating of 900 psi. The vessels were hydrostatically tested to 1600 psi for a period of 5 minutes.

The fuel vessel was the same size as the oxidizer tank but it was 304 stainless steel throughout. The flange and dome were rated at 150 psi and the cylindrical pipe was schedule 40.

Figure IV-7 shows a typical schematic of the vessel installation. The oxidizer vessels were heated by electrical tape and located in a separate test cell. The fuel vessels were immersed in a barrel containing ethylene glycol for an even temperature bath. The fuel vessels were plumbed similar to the oxidizer tanks but located in a different test cell. Both tank configuration and associated equipment were cleaned according to Martin Marietta Drawing 327-902000 for liquid oxygen use.

Pressure and temperature measurements were made using Tabor transducer Model 176 and chromel/alumel thermocouples. Deadweight accuracies were  $\pm 0.001\%$  of full scale using Heise gage calibration equipment. Thermocouples were calibrated by selected temperature steps checked against a laboratory thermometer. Temperature control was maintained to within  $\pm 2^\circ\text{C}$  by a stepless power application to resistive heaters.

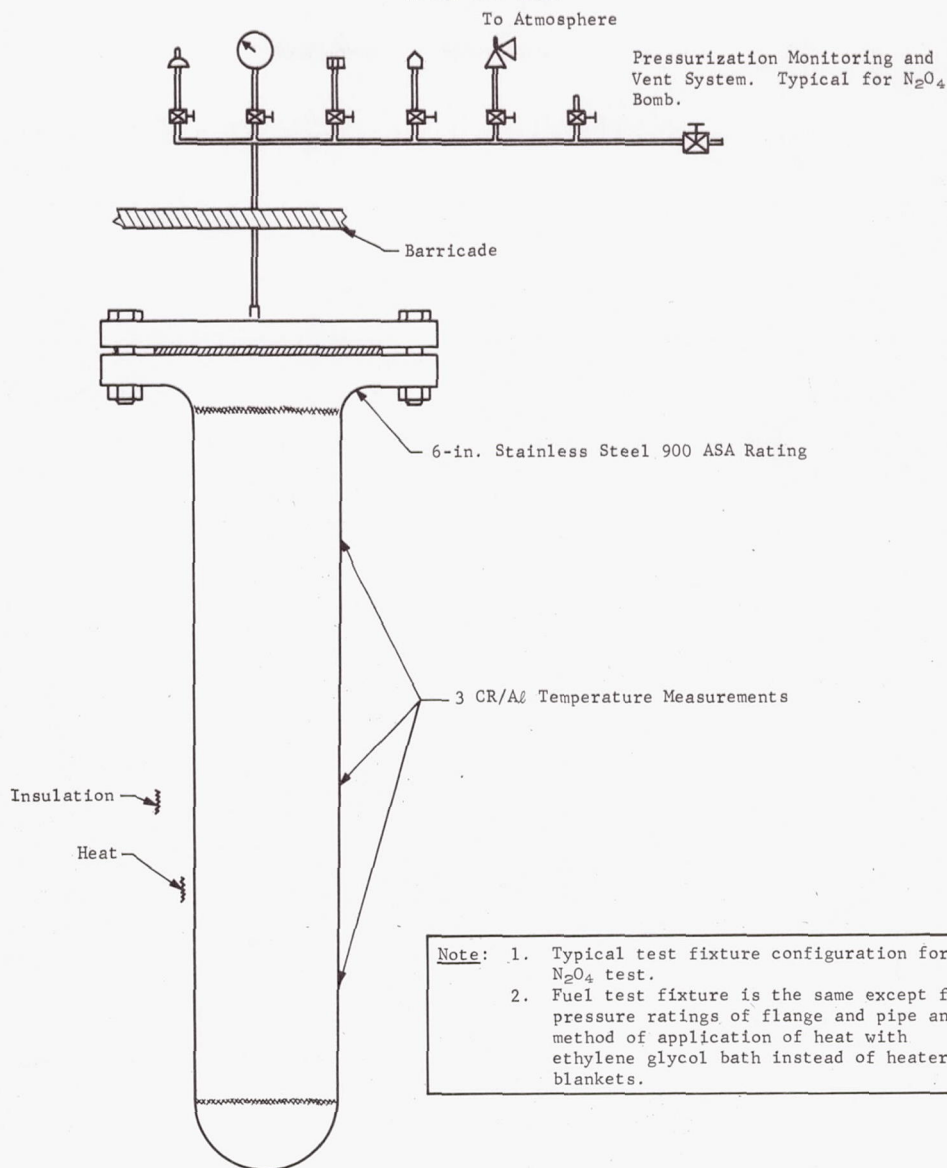


Fig. IV-7 Compatibility Screening Test Fixture

## D. MATERIALS TESTING

1. Material Testing with Propellantsa. Prescreening Tests

This series of short-term tests was performed to verify literature data and to assist in developing procedures for conducting the later screening tests. The tests consisted of exposing small material samples to each propellant in combination

with the dry heat sterilization temperature of 275°F for periods up to 120 hr. Sample containers were fabricated from 304 stainless steel Hoke cylinders or from 1-in. tubing sections of appropriate materials. The materials tested included:

6061-T6 Aluminum	FEP and TFE Teflon
1100-O Aluminum	B-591-8 Butyl Rubber, Packer
6A $\delta$ -4V Titanium	E515-8 Ethylene Propylene Rubber, Packer
321 Stainless Steel	AF-E-110 Carboxy Nitroso Rubber
Nickel	
Lead	S-9711 Silastic Compound

A number of important items of information was developed during this series of subscale tests. The formation of adducts of iron was a major problem. With only one exception, the phenomenon was found in all tests conducted on ferrous-based alloys in the presence of  $N_2O_4$ . In that instance a sample of 321 stainless steel was placed in an open glass vial containing  $N_2O_4$  and inserted into a 304 stainless steel Hoke cylinder, which also contained  $N_2O_4$  that did not, however, cover the vial. After the system was exposed to 275°F for 120 hr, a light residue was found on the walls of the Hoke cylinder, but none on the specimen. This phenomenon led to additional tests. These tests were conducted to ascertain whether the ferrous-based alloys would form the adducts in the absence of any other metal and any nonmetal.

Special containers were fabricated with appropriate welded end plates to assure a single constituent system rather than introducing unknowns from commercially available tube fittings. Both propellants were tested for 96 hr.

The results of these tests proved adducts of iron will be formed by any ferrous-based alloy when in contact with  $N_2O_4$  at 275°F. Rate of formation appears to be approximately linear and increases as the amount of alloying agents increases. Evidence indicates nickel and molybdenum as major causes of adduct formation. Conversely no residual contamination is formed when aluminum alloys or titanium alloys are exposed to the same environment.

Fuel did not react with any metal alloy except 316 stainless steel. This alloy was not considered for systems use but did form a part of the container used for screening tests. No attack was observed on the metal, however, decomposition of the fuel did occur. This was attributed to the presence of molybdenum in the alloy.



No nonmetals were tested that proved to be completely compatible with  $N_2O_4$  at 275°F. TFE and FEP Teflon specimens were slightly affected in tests up to 70 hr. Results were not clear since the first series of specimens was exposed in stainless steel Hoke cylinders, which resulted in oxidizer contamination. A second test of 69 hr at 275°F in a 6061-T6 aluminum container revealed similar effects on the Teflon materials, and a thin, white precipitate remained on the container walls and the Teflon specimens after the propellant was drained.

Elastomers including silastics, butyl rubber, ethylene propylene rubber, and nitroso rubber lost significant mechanical properties, blistered, ignited, or went into solution after short-term exposure to  $N_2O_4$  at 275°F.

Both nickel and lead sustained attack when exposed to  $N_2O_4$  at 275°F. This resulted in formation of nickel nitrate and lead nitrate, respectively. Sufficient attack occurred to eliminate both materials from further consideration.

All metals exposed to MMH fuel demonstrated compatibility. Teflon was the only nonmetal unaffected by exposure to the fuel at 275°F. Ethylene propylene rubber was the least effected of elastomeric rubbers when tested at 275°F for 24 hr.

Tables IV-4, IV-5, and IV-6 present the complete test history and results of the prescreening test series.

b. 300-hr Screening Test

This test was performed in the same manner as the full-scale 600-hr test except for duration. It was to provide advance information for materials selection and to indicate any basic error in the conception of the 600-hr test.

The results of the 300-hr test showed no attack on any materials exposed to the fuel. The following materials were all found to be compatible:

304 stainless steel	Carpenter 20 Cb
321 stainless steel	Hastelloy C
347 stainless steel	6Al-4V titanium alloy
17-7 stainless steel	1100-0 aluminum
17-4 stainless steel	2014-T6 aluminum
A286 aged	2219-T8 aluminum

Table IV-4 Prescreening Tests,  $N_2O_4$  Compatibility with Metals

Material Tested	Type Specimen and Container	Test Conditions	Results
6061-T6 Aluminum	Specimen placed in glass tube within Hoke cylinder.* Stressed specimen.†	195 hr at 275°F	Specimen unaffected. No residue in filtration of propellant inside glass container. Heavy residue in Hoke cylinder.
6Al-4V Titanium	Specimen placed in glass tube within Hoke cylinder. Stressed specimen.	195 hr at 275°F	Specimen unaffected. Crystals found on edge of specimen. No residue from filtration of propellant inside glass container.
Type 321 Stainless Steel	Specimen placed in glass tube within Hoke cylinder. Stressed specimen.	195 hr at 275°F	Light residue on Hoke Cylinder. Specimen unaffected. No residue from filtration of propellant inside glass container. Light residue in Hoke cylinder.
1100-0 Aluminum	Hoke cylinder, strip specimen.	195 hr at 275°F	Light residue in Hoke Cylinder. Specimen unaffected. No residue from filtration of propellant inside glass container. Light residue in Hoke cylinder.
Lead Shavings (chemically pure)	Specimen placed in glass tube in Hoke cylinder shavings.	88 hr at 275°F	Formed a lead nitrate coating on shavings. Observed lead nitrate crystals, small weight increase.
*Hoke cylinders, type 304 stainless steel. †Self-stressed specimen, NASA Langley type at 75% of yield strength.			

Table IV-5 Prescreening Tests,  $N_2O_4$  Compatibility with Nonmetals

Material Tested	Type Specimen and Container	Test Conditions	Results
Silicone Rubber S-9711	Strip specimen tested in glass test tube contained in 1x6 in. stainless steel tube.	2 hr at 275°F	Specimen dissolved completely.
Ethylene Propylene Rubber E-515-8	Strip specimens tested in same container concurrent with test No. 3. Specimens were 2 in. apart, separated by glass.	12 minutes at 275°F	Specimen burned.
Butyl Rubber B-591-8	Strip specimens tested in same container concurrent with test No. 2. Specimens were 2 in. apart, separated by glass.	12 minutes at 275°F	Specimen contained small surface blisters. Volume increased 10%.
TFE-FEP	ASTM standard tensile specimen stainless steel container.	18 hr at 240°F, 70 hr at 275°F, Total run 88 hr. Liquid propellant lost within first 48 hr. Remainder of test conducted in vapor phase.	TFE-ultimate tensile reduced by 7.3%, elongation reduced by 50%. FEP-ultimate tensile strength reduced 12%, no change in elongation. No other significant changes noted in either FEP or TFE.

MCR-68-119

IV-19



Table IV-6 Prescreening Tests, MMH Compatibility with Nonmetals

Material Tested	Type Specimen and Container	Test Conditions	Results
B591-8 Butyl Rubber	Strip, stainless steel container	24 hr at 275°F	Fuel discolored - Sample volume increased 10%. Hardness loss 10-12 Shore A.
E515-8 Ethylene Propylene Rubber	Strip, stainless steel container	24 hr at 275°F	Fuel discolored - Sample volume increased 7%. Hardness loss 5 Shore A.
B591-8 Butyl Rubber	ASTM tensile specimen, stainless steel container	48 hr at 275°F	Apparent fuel decomposition after 24 hr. Units contained to vent at 90 psig. Fuel discolored and had strong ammonia odor. B591-8 volume increased 20%. E515-8 volume increased 10%.
Teflon TFE-FEP Films	Film, stainless steel container	28 hr at 275°F	Specimens unaffected.
Teflon TFE-FEP	ASTM tensile specimen, stainless steel container	88 hr at 275°F	TFE - ultimate strength reduced 2.6%, elongation reduced approximately 10% from original value. FEP - ultimate strength reduced 7%, elongation reduced less than 10% from original value.

Figure IV-3 shows the fuel specimens after the 300-hr exposure. The specimens were unaffected and the propellant was a clear light straw color, unchanged from its original condition. Each specimen was isolated from the other by the stopper shown in each test tube.

Alloys found compatible with  $N_2O_4$  were:

1100-0 aluminum	Commercially pure titanium
2014-T6 aluminum	6Al-4V titanium
2219-T8 aluminum	Hastelloy C
6061-T6 aluminum	

Alloys found to be incompatible with  $N_2O_4$  were:

304 stainless steel	Nickel
321 stainless steel	A-286
347 stainless steel	Carpenter 20 Cb
17-4 stainless steel	Maraging steel
17-7 stainless steel	Lead

The formation of adducts of iron was found in all instances of exposure of ferrous-based alloys to the oxidizer. The ferrous materials were incompatible because of the formation of a material in the oxidizer that would be detrimental to the system operation. The adduct is identified because it:

- 1) Precipitates from the liquid propellant;
- 2) Does not transfer in the vapor phase;
- 3) Has a large volume when wet, but shrinks to less than 10% of original volume when dry;
- 4) Has the apparent viscosity of cold molasses with a high adhesive strength;
- 5) Is amorphous when dried of oxidizer.

The maraging steel was the only ferrous alloy which demonstrated structural failure. It was prestressed to 75% of yield. The specimen fractured in both the tested stressed area and in areas around the rivet. Significantly, this alloy contained the least amount of corrosion resistant metals, was the highest strength alloy tested, and formed the greatest amount of adduct (Fig. IV-8).



Figures IV-9, IV-10, IV-11 show the specimens after exposure to  $N_2O_4$  for 300 hr at 275°F. The small amounts of propellant remaining are due to distillation that occurred during rapid cooling of the bomb from 275°F to 40°F. Unaffected bright specimens are aluminum alloys. The titanium specimen (not shown) had a similar appearance, but the test tube was broken during removal from the test bomb. Rivet staining may be seen in several specimens. Ferrous-based alloys show a blackened effect (iron adduct). Iron adduct formation is most clearly seen on the bimetal specimen in Fig. IV-11 (aluminum interior specimen and 321 stainless outer specimen). Note fractured maraging steel specimen at extreme right.

Figure IV-12 shows the 304 stainless steel specimen rack after 300 hr in  $N_2O_4$  at 275°F. The rack was clean and bright before exposure. Deposits are iron adduct. The rack was made from stainless steel rather than aluminum alloy as specified in the test plan to provide uniformity of test bomb materials.

#### c. 600-hr Screening Test

##### 1) Metals Tested in Propellants

The materials tested in contact with propellants were not tested in the dry heat since all the materials are known to be capable of withstanding 275°F. Maraging steel was not tested in MMH because of the risk of oxidation that would react with MMH. All other materials discussed below were tested in MMH and none were attacked by the fuel. The reaction of each material to  $N_2O_4$  is presented in the following paragraphs.

Titanium 6Al-4V - There was no attack on this material as shown in Fig. IV-13. Figure IV-14 shows the condition of etched titanium foil before and after exposure indicating no attack.

Aluminum - Alloy designations 1100-0, 2014-T6, 2219-T87, and 6061-T6 were exposed to  $N_2O_4$ . All alloys were attacked by the propellant resulting (usually) in intergranular corrosion or in pitting. In all instances, a residual corrosion product was formed. This product varied from a white, granular deposit to a thick, viscous, semifluid. The products were amorphous. These results were not evident at 300 hr. Preliminary designs had to be reviewed to remove the aluminum usage except for limited application. Figure IV-15 shows the attack sustained by 6061-T6 that was typical of all the aluminum alloys tested. Figure IV-16 shows the condition of aluminum screens, indicating corrosion and pitting.



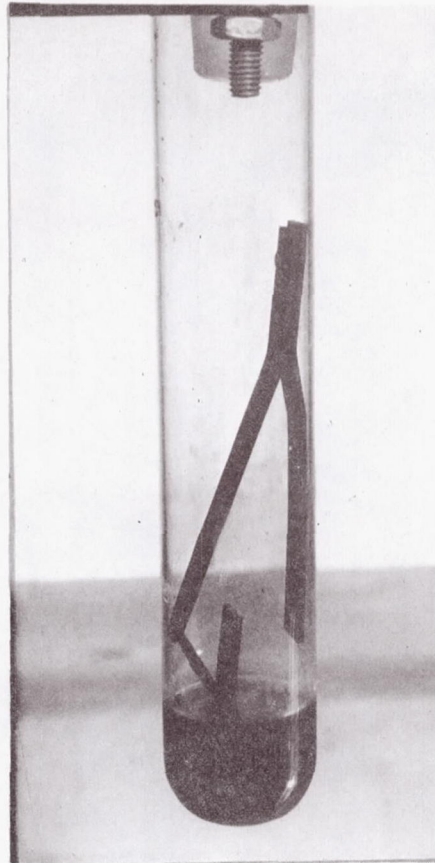


Fig. IV-8 Oxidizer Test Maraging Steel Specimen

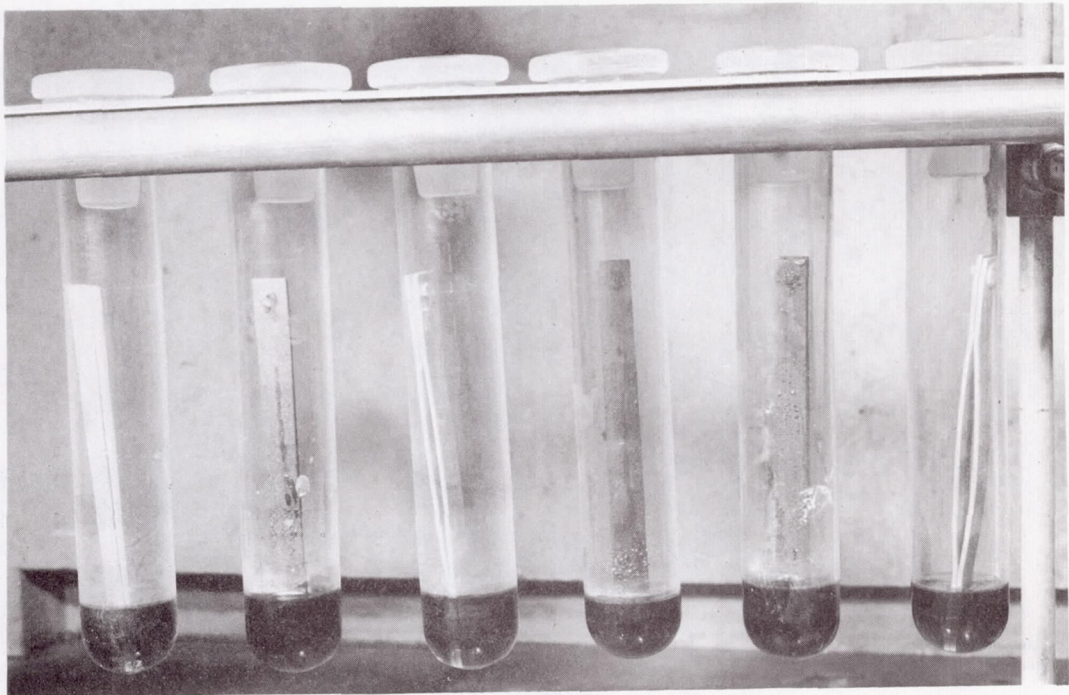


Fig. IV-9 Oxidizer Test Specimens

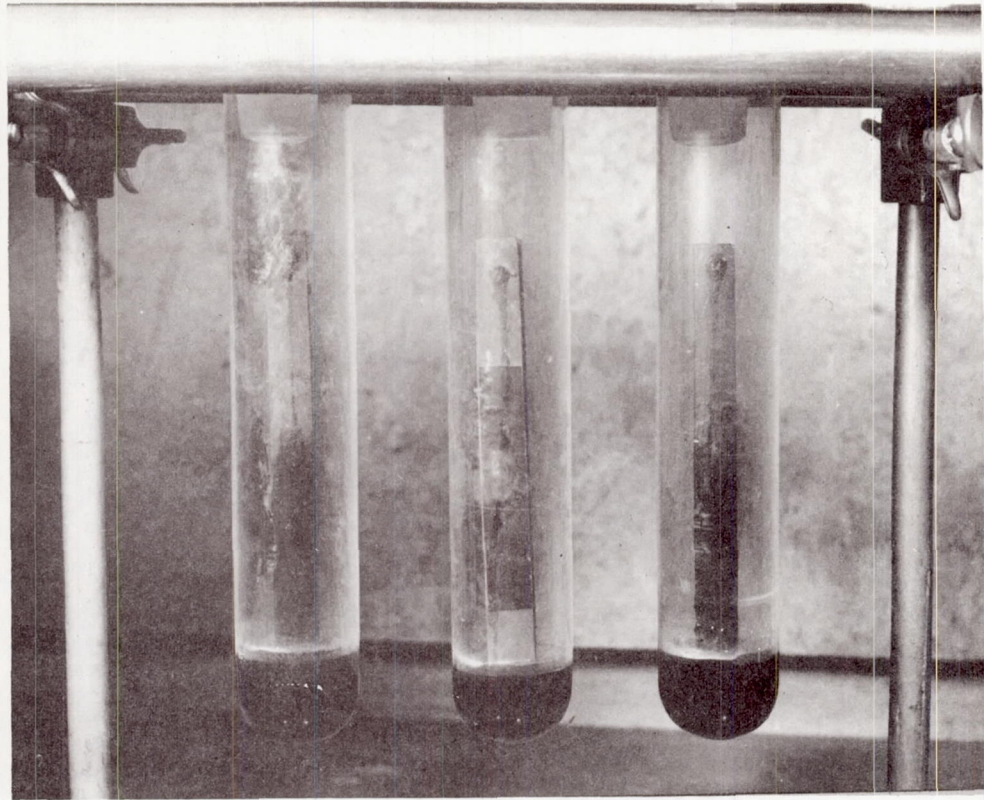


fig. IV-10 Oxidizer Test Specimens

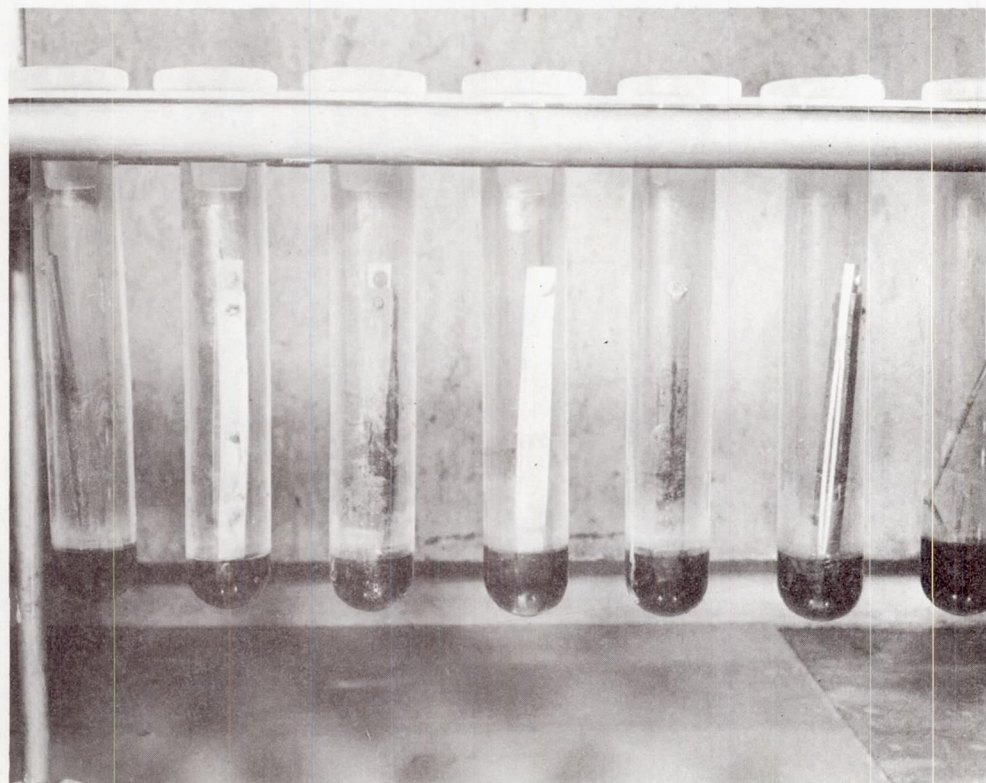


Fig. IV-11 Oxidizer Test Specimens



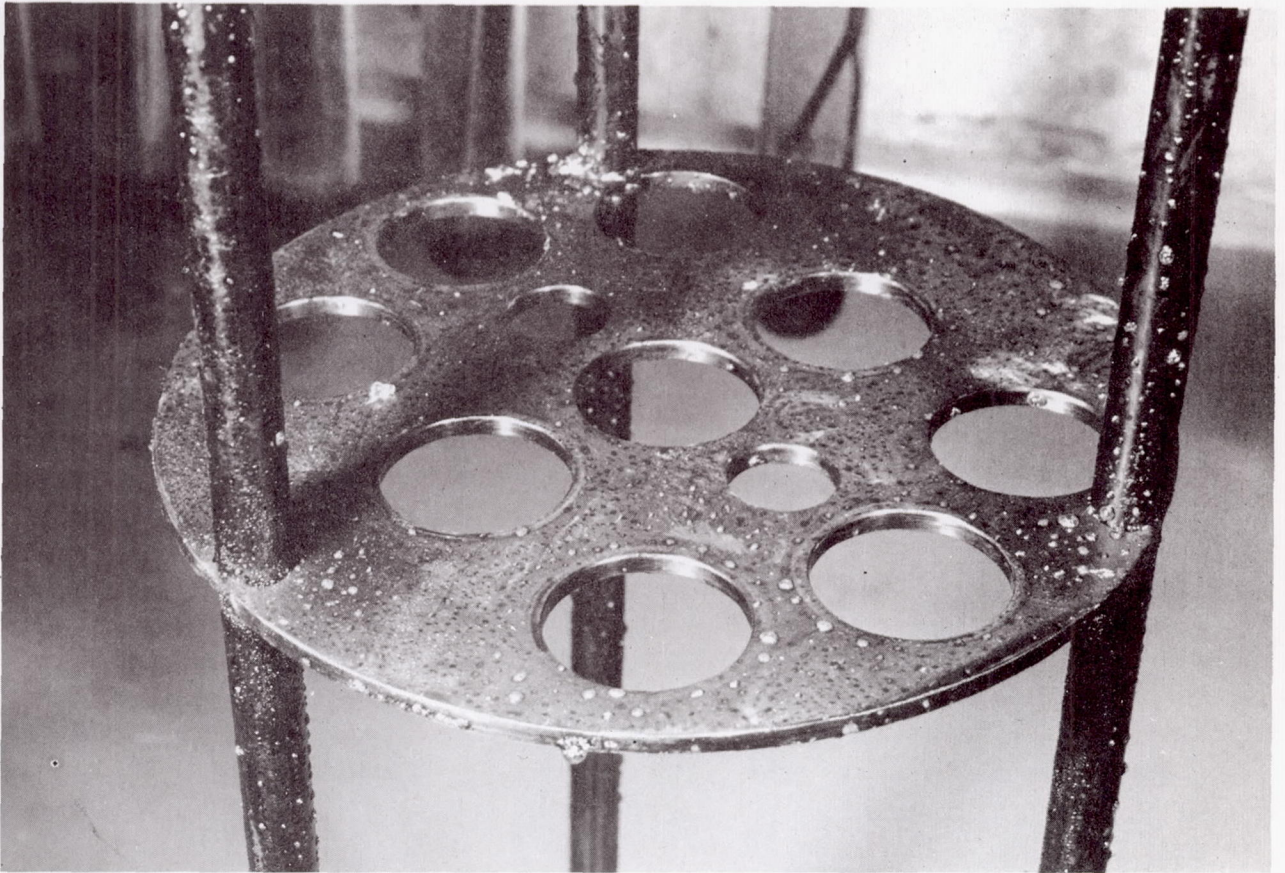


Fig. IV-12 Oxidizer Test Specimen Rack

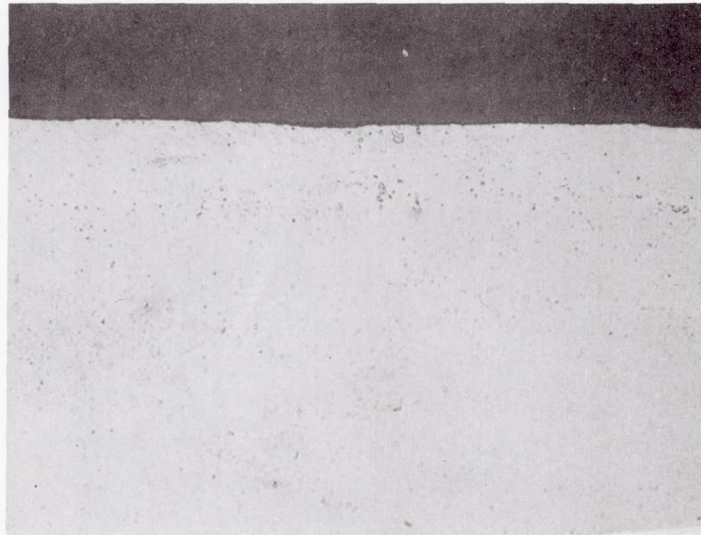
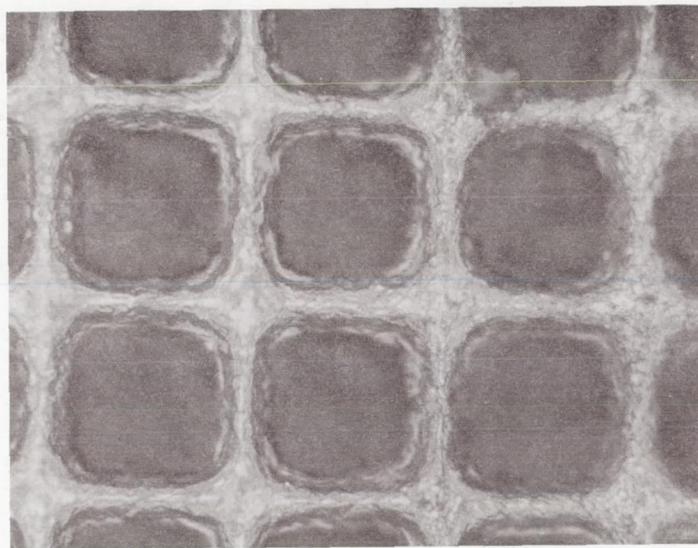
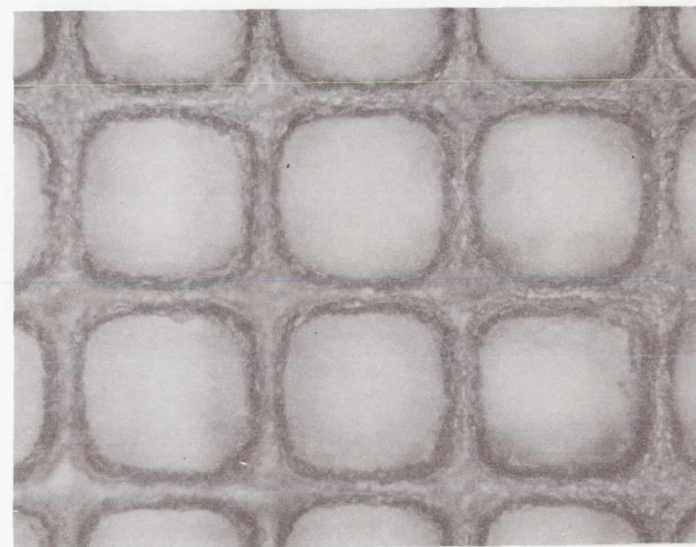


Fig. IV-13 Titanium (6Al-4V) after Exposure to  $N_2O_4$  for 600 hr (200X)





(a) Before Exposure to  $N_2O_4$



(b) After 600 hr at 275°F (200X)

Fig. IV-14 Etched Titanium Foil after Exposure to  $N_2O_4$  for 600 hr at 275°F

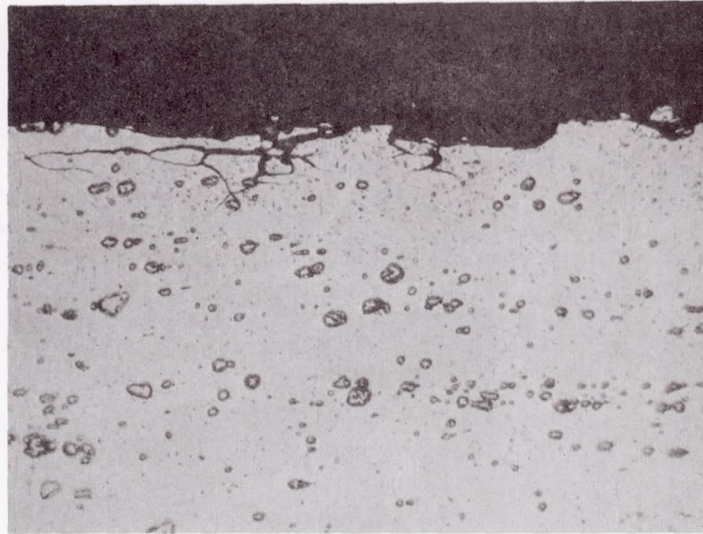


Fig. IV-15 Aluminum (6061-T6) after Exposure to N<sub>2</sub>O<sub>4</sub> for 600 hr at 275°F (200X)

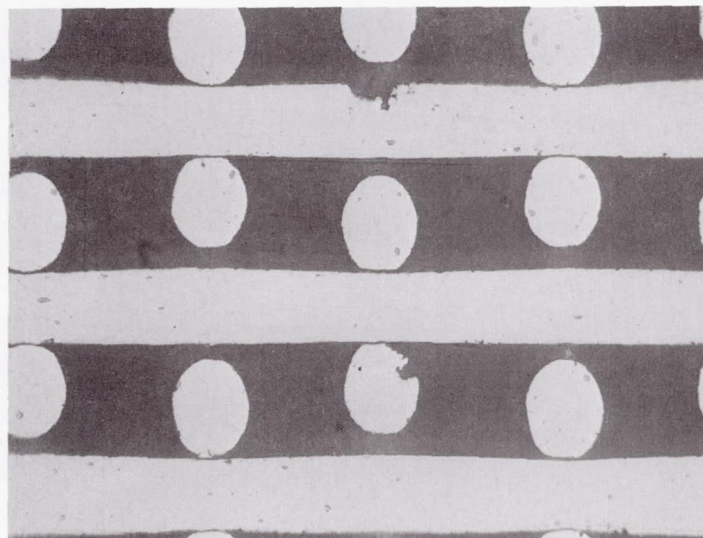


Fig. IV-16 Aluminum Screens (5056) after Exposure to N<sub>2</sub>O<sub>4</sub> at 275°F



Stainless Steels - Alloys of 304, 321, 347, 17-4pH, 17-7pH, and A-286 were exposed to  $N_2O_4$ . All alloys were attacked by the propellant, resulting in intergranular corrosion and pitting. In all instances a residual corrosion product was formed. The product was extremely viscous, amorphous on drying, and accelerated corrosion of dissimilar metals, except titanium. Spectrographic analysis of a typical corrosion product indicated that elements present were the same as those contained in the alloy. Figure IV-17 shows the attack on the 347 alloy which was representative of this group of alloys.

Maraging Steel - This material was severely attacked. All specimens showed evidence of pitting, intergranular corrosion, and stress corrosion. Maraging steel specimens were the only specimens tested that fractured. Figure IV-18 shows the severe attack.

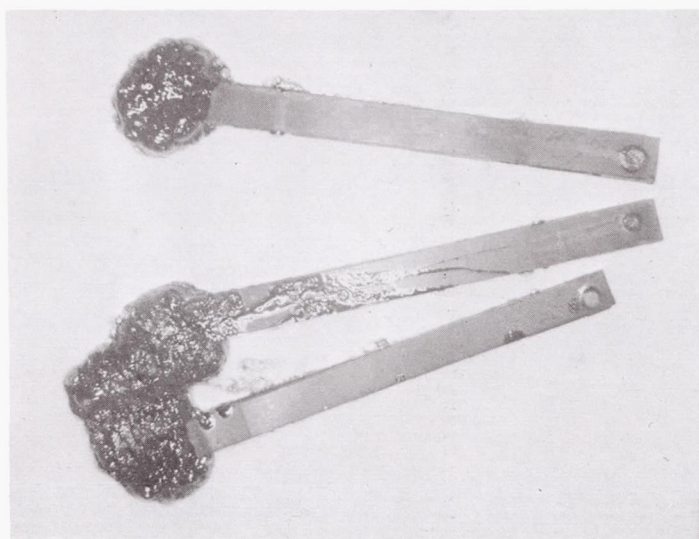
Carpenter 20 Cb and Hastelloy C - Both of these materials were attacked to a minor degree. Figure IV-19 shows photomicrograph of the specimens.

Bimetallics - Specimens of bimetallic beams were tested to determine the cathodic effect if any. Aluminum was tested as combined specimens with either 321 steel and titanium 6Al-4V. The results indicate no deleterious effect of the bimetallic specimens. The results of the bimetallics were the same as the individual specimens. Figure IV-20 shows the results of the bimetallic test from a titanium-6061 aluminum specimen. The viscous adduct resulted from attack on the monel rivet.

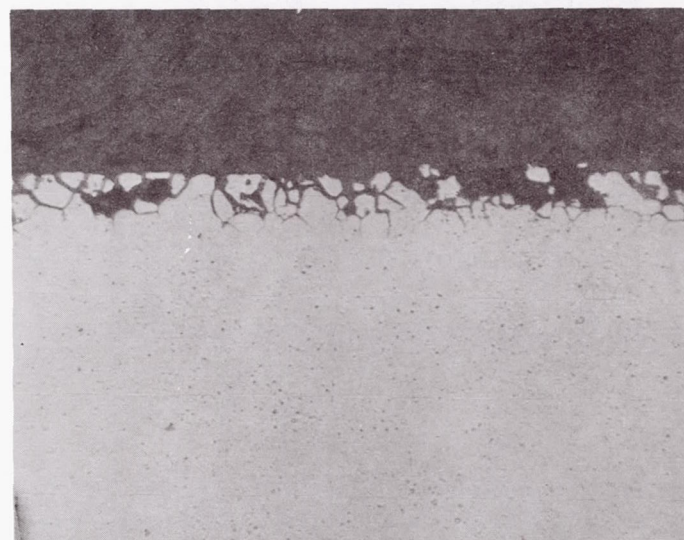
Nickel - Nickel screen material was exposed to  $N_2O_4$  and was severely attacked with a resultant heavy deposit of nickel nitrate (Fig. IV-21).

Long-Term Storage Tests - The long-term tests described previously completed the sterilization exposure to propellants on June 6, 1967. Ambient storage began June 6, 1967 without cleaning the propellants. Fuel and oxidizer tank specimens were opened at 4-month intervals. After 12 months the fuel tank showed no degradation of the materials or propellant.





(a) As Removed from Test



(b) Specimen Section (200X)

Fig. IV-17 Stainless Steel (Type 347) after Exposure to  $N_2O_4$  for 600 hr at 275°F

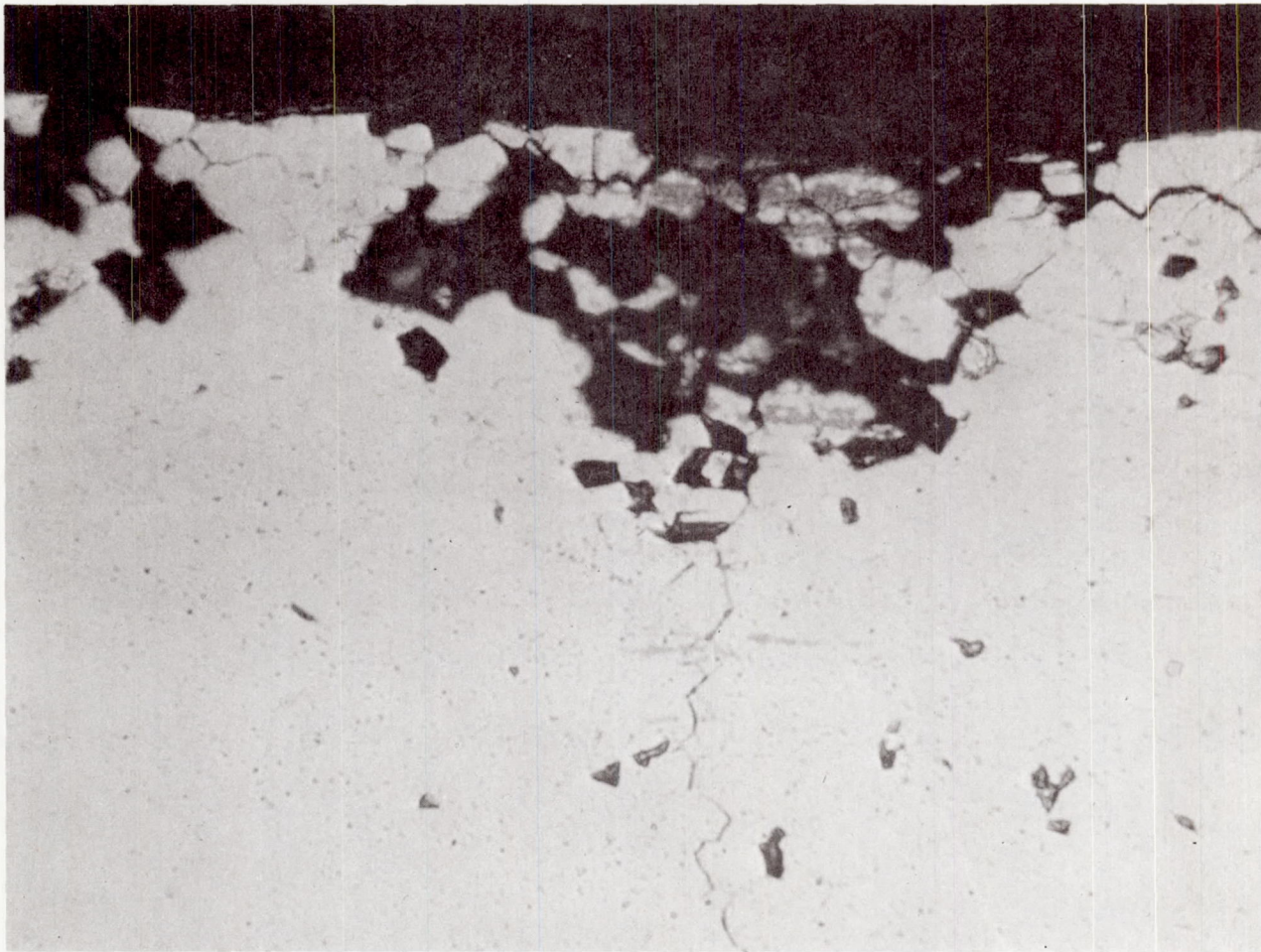
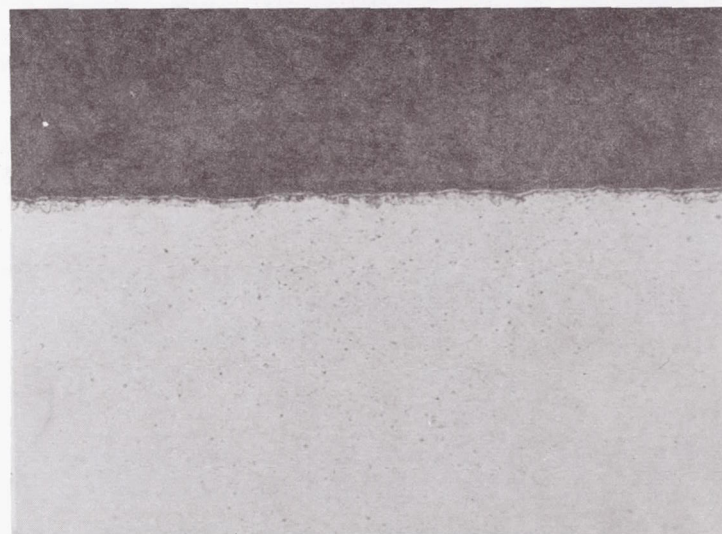


Fig. IV-18 Steel (Maraging) after Exposure to  $N_2O_4$  for 600 hr at 275°F



(a) Carpenter 20 Cb



(b) Hastelloy C

Fig. IV-19 Materials after Exposure to  $N_2O_4$  for 600 hr at 275°F (200X)



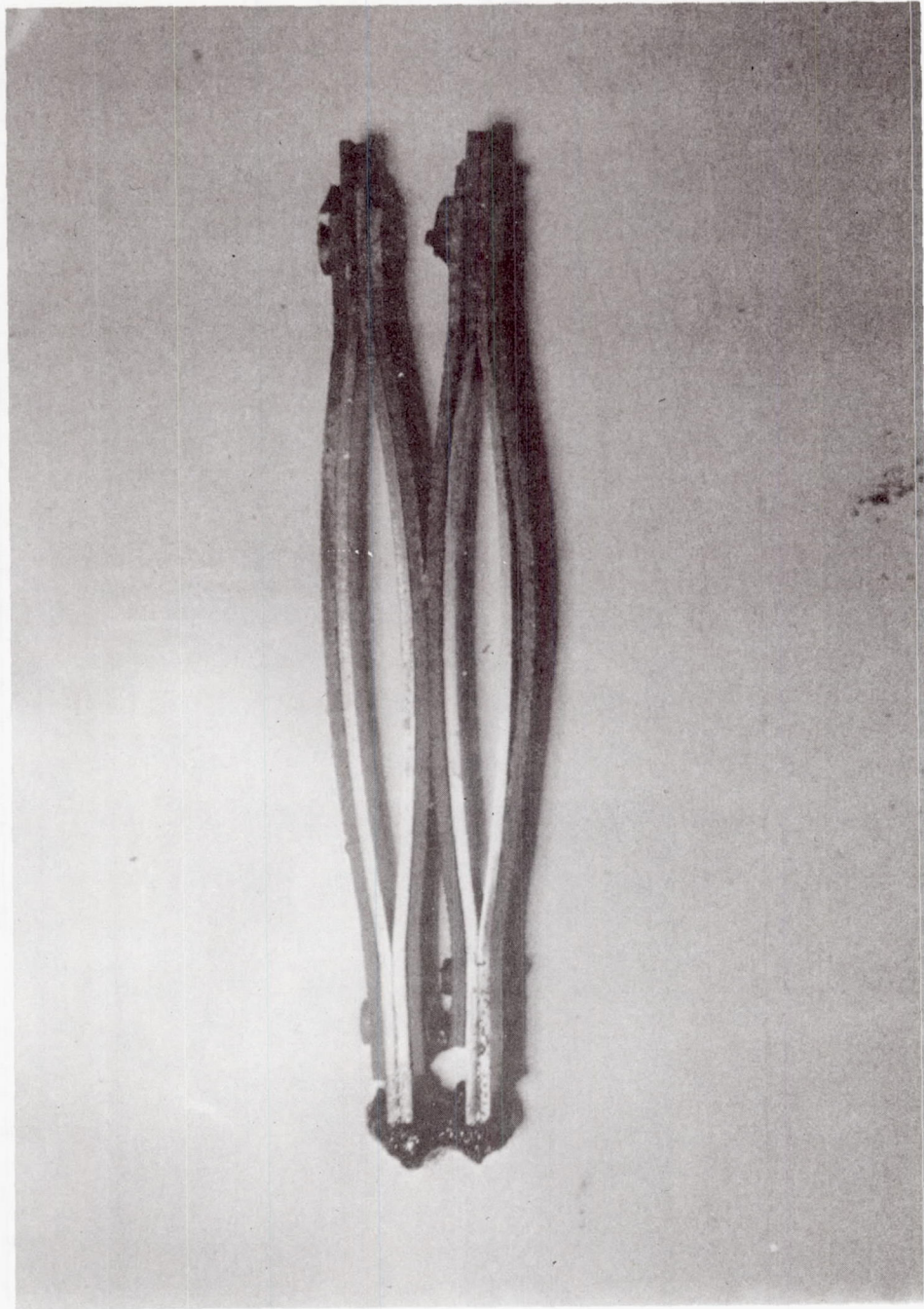
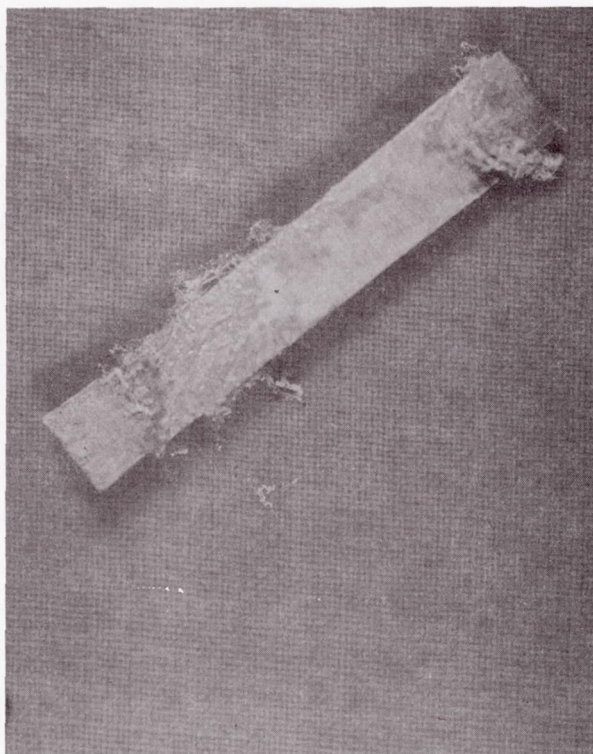


Fig. IV-20 Bimetallic Couples Titanium 6Al-4V and 6061-T6 Aluminum after Exposure to  $N_2O_4$  for 600 hr at 275°F



**Fig. IV-21** Pure Nickel Screen after Exposure to  $N_2O_4$  for 600 hr at 275°F

The oxidizer tank showed no degradation of the Teflon. The stress welded specimen of titanium showed some discoloration. Figures IV-22 and IV-23, show the welded specimen. Detailed examination revealed no cracks had formed. Magnification up to 2000X showed the discoloration to be a surface phenomenon. It was concluded that the deterioration resulted from the formation of oxides, that the oxide was only Angstroms thick, and that the presence of the discoloration of the specimen has no detrimental effect on the properties of titanium.

## 2) Nonmetals Tested in Propellants

Teflon and Kynar were tested in both fuel and oxidizer. Teflon showed no attack by the MMH fuel, however, some white flocking was visible in the  $N_2O_4$  vials. The weight loss was less than 0.1 mg. No other attack was experienced in the  $N_2O_4$ .

Kynar was severely attacked by both the MMH and  $N_2O_4$ . It has no value in this application.



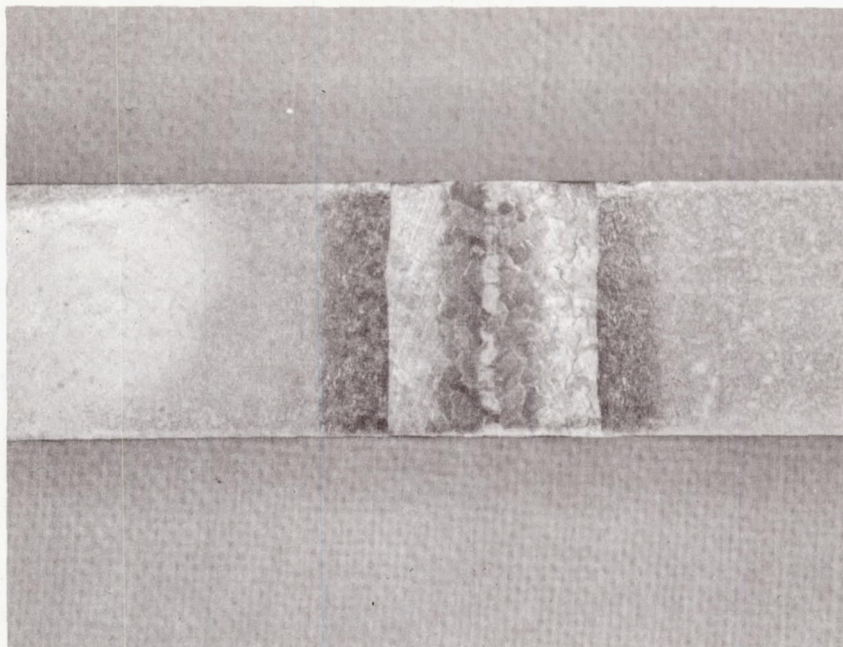


Fig. IV-22 Face of Stressed Titanium Specimen

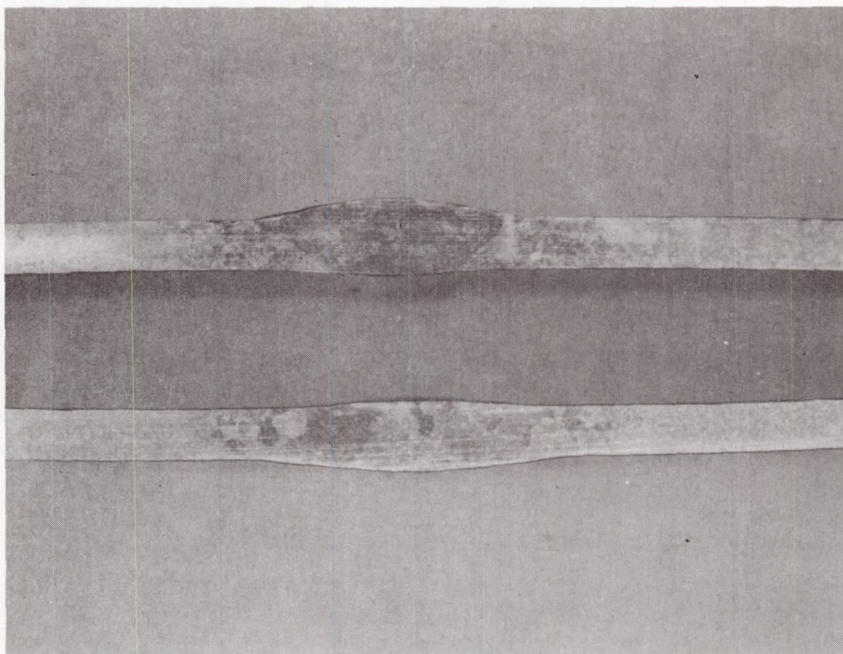


Fig. IV-23 Edge of Stressed Titanium Specimen



## 2. Materials Tested in Dry Heat

All the materials in the following discussion were exposed to 275°F for 600 hr in a gaseous nitrogen atmosphere. Table IV-7 presents the results of the testing performed on adhesives. A significant increase in shear strength is shown for each adhesive after exposure to 275°F. This is a result of further cross linking of molecules, which is attendant with postcures for these types of materials. Along with the increase in shear strength, a decrease in flexibility occurs that causes the adhesive to become brittle and lose its ability to resist failure under vibrational loading.

Table IV-7 Properties of adhesives after Exposure to 275°F

Material	Tensile Shear Adhesion (avg psia)			Mode of Failure
	Control	300 hr	600 hr	
Dow-Corning 93-046	160	130	227	80% adhesive; 20% cohesive
Hysol 1-C Epoxy	1000	2280	2440	85% adhesive; 15% cohesive
Armstrong A-6 Epoxy	780	3090	2376	10% adhesive; 90% cohesive
Devcon F Epoxy	530	2360	3910	2% adhesive; 98% cohesive

Table IV-8 presents the results of the testing performed on plastics and rubber filmw. The aluminized Mylar, S-9711 rubber, EPR-1 rubber, and SR634 butyl rubber, were degraded by the heat exposure. The major effect appears to be an increase in hardness and hence, reduction of elongation.

Table IV-9 presents the results of testing of potting compounds and sealing resins. Only PR-1527 compound of polymethane degraded to an unacceptable level. This is evident by the reduction in hardness.

Table IV-10 presents the results of testing on coatings and finishes.

## 3. Special Tests

During the course of the program several unplanned special tests were performed to answer specific questions of materials compatibility. The majority of these tests were concerned with the compatibility of various materials in the ethylene oxide (ETO) atmosphere. The tests and results are described in the following paragraphs.

Table IV-8 Properties of Plastic and Rubber Sheet and Film after Exposure at 275°F

Material	Average Tensile Strength (psi)			Percent Elongation (avg)		Durometer Hardness	
	Control	300 hr	600 hr	Control	600 hr	Control	600 hr
Kynar	7,460	7230	7044	---	30%	D78	D81
Aluminized Mylar	19,700	---	16300	89%	51%	NA	NA
Teflon (TFE)	2,200	2060	2210	---	167%	D60	D64
Teflon (FEP)	2,960	2920	2545	---	326%	D64	D72
EPR-1	1,773	---	1960	180%	71%	A72	A71
SR634 Butyl	1,872	---	1874	301%	180%	A77	A78
Silicone Rubber 60	638	667	681	---	150%	A60	A68
S-9711 Silicone Rubber	1,083	---	842	528%	240%	A54	A63

MCR-68-119

Table IV-9 Properties of Potting, Encapsulating, and Sealing Resins after Exposure at 275°F

Material	Volume Resistivity*		Dielectric Constant†		Durometer Hardness‡	
	Control	600 hr	Control	600 hr	Control	600 hr
Epon 828 - Mica filled (amine cure)	$6.0 \times 10^{14}$	$4.7 \times 10^{15}$	3.68	3.70	D90	D90
PR-1527 Polyurethane Casting Resin	$1.0 \times 10^{13}$	$1.0 \times 10^{12}$	5.30	5.92	A38	A15
TRV-20 Silicone Potting Resin	$4.6 \times 10^{13}$	$1.0 \times 10^{15}$	3.04	3.08	A52	A57
LTV-602 Silicone Potting Resin	$1.1 \times 10^{14}$	$8.6 \times 10^{14}$	2.82	2.82	A26	A23
Epon 828/Versamid 140 Potting Silicone Resin	$1.6 \times 10^{16}$	$6.2 \times 10^{15}$	3.32	3.28	D84	D87
Dow-Corning 0-9-0031	$2.4 \times 10^{14}$	$4.9 \times 10^{14}$	3.74	3.81	A58	A57
*Measured at 250 vdc, values in ohm-cm. †Measured at 100 KC. ‡Durometer hardness is not consistent with those in the 300-hr report.						
<u>Note:</u> 1. The MIL-S-8516 polysulfide rubber potting compound was not tested in the 600-hr test. It had lost all significant physical properties after 300 hr. 2. Only PR-1527 polyurethane was degraded to an unacceptable level. The hardness is especially reduced.						



Table IV-10 Testing of Coatings and Finishes after 600 hr  
Exposure at 275°F

Material	Remarks
White Acrylic Lacquer MMS K227	Embrittled, adhesion fair. Flakes away with checkerboard cut. Loses adhesion in the bend area after 180-deg bend around a 1/4-in. mandrel. Specimen yellowed significantly.
Ablative Coating MMS K456	Excellent adhesion. Tougher and darker than control specimens. Failed 90-deg bend over 1-in. mandrels.
High Emissivity Silicone Coating MMS K474	Good adhesion. Coating somewhat stronger than control sample. No flaking. The coating yellowed somewhat. Absorption increased from 0.14 to 0.16. Emissivity decreased from 0.86 to 0.85.

a. Reactivity of Propellants with ETO

The purpose of this test was to determine if propellants leaking from a pressurized container would react with the ETO mixture. The ETO mixture was 12% ethylene oxide/88% Freon 12 maintained at 600 mg of ETO per liter of atmosphere and at 122°F with 50% relative humidity as defined by JPL Specification VOL 50503-ETS.

Monomethylhydrazine was injected into the chamber in a sufficient quantity to produce a concentration of  $5 \times 10^5$  ppm. A 6-psi pressure rise resulted with a temperature increase of less than 5°F.

Nitrogen tetroxide was injected into a similar atmosphere at a concentration of  $5 \times 10^5$  ppm resulting in a 26-psi pressure rise and a temperature increase of 22°F. This level of reaction would have been sufficient to rupture the sterilization chamber. Vapor detectors and automatic purge systems were added to the design of the chamber to protect the chamber.

b. Capability of Vapor Detectors to Operate in an ETO Atmosphere

Fixed vapor detectors manufactured by Teledyne Systems, Inc. P/N AS1 110621, Model 4075M, with solution formulated to detect nitrogen tetroxide or Aerozine-50 were exposed to ETO. The ETO was in a mixture of 12% ETO and 88% Freon 12. The concentration of ETO was 325 mg per liter of atmosphere. Ambient temperature was used and no humidity control was provided.

The fuel detector responded with spurious signals and the signal levels increased with time. When exposed to a calibrated fuel vapor, the detector responded to the stimulus. However, the detector could not be depended on for continuous unattended use.

The oxidizer vapor detector performed normally and was satisfactory for use. Later experience in the controlled ETO atmosphere of 600 mg per liter at 122°F and 50% relative humidity for 180 hr has shown the detector to perform normally.

c. Compatibility of Copper with ETO

Two copper tube fittings were exposed to the ETO environment as specified by VOL 50503-ETS for TA approval of piece parts. The results of the test are indicated in Fig. IV-24. Only superficial staining was found on the test specimen. Copper is considered compatible on the basis of this test.



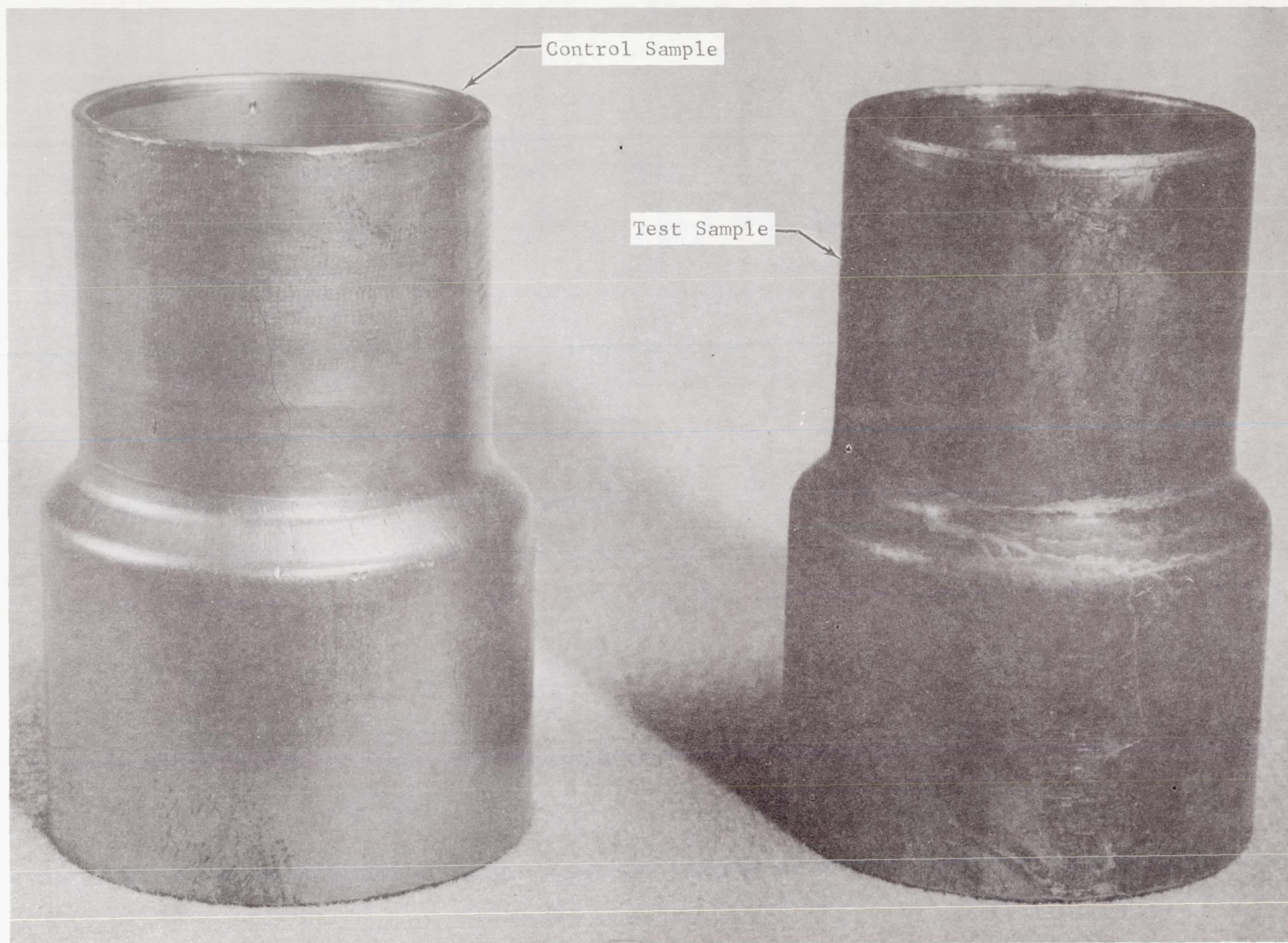
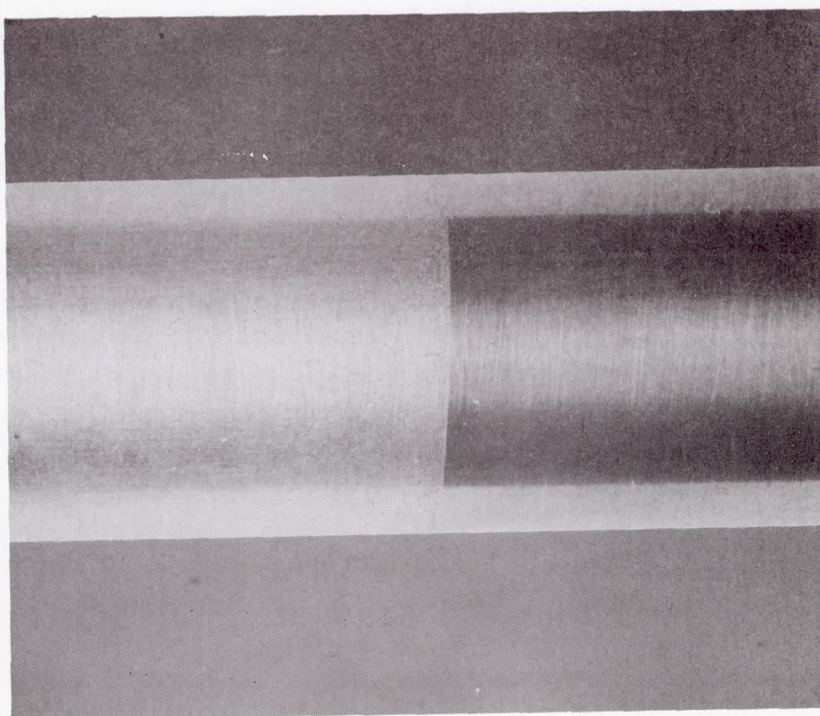


Fig. IV-24 Copper Tube Fittings from ETO Test



d. Compatibility of Transition Joints with Propellants

The object of this test was to expose a cold welded extruded transition joint to propellants under the sterilization environment. A  $\frac{1}{4}$ -in. joint of 6Al-4V titanium and 6061-T6 aluminum was exposed to  $N_2O_4$  at 275°F for 600 hr. Figure IV-25 shows the joint after test. The joint was examined visually under high magnification. There was no evidence of degradation of the bonded joint. A fine coat of aluminum oxide was found on the aluminum portion of the tube joint.



**Fig. IV-25** Transition Joint, Titanium 6Al-4V and 6061-T6 Aluminum Alloy

A second transition joint of 304L stainless steel and titanium 6Al-4V alloy was exposed to monomethylhydrazine at 275°F for 600 hr. No attack was noted on the specimen and no fuel decomposition occurred.

e. Compatibility of Grease with ETO

A general purpose high temperature grease was tested for compatibility with ETO. The grease was Martin Marietta Specification MMS-N312, which is a synthetic base lubricant containing 10% tungsten disulfide suitable for -65 to +400°F application. There was no breakdown of the grease when tested for 26 hr in ETO according to specification VOL 50503-ETS. Subsequent usage in the sterilization chamber for a blower bearing lubricant showed completely satisfactory performance.

f. Freon/Titanium Compatibility Test

Data developed by other investigators, namely NASA-MSD, Boeing, duPont, and Aerospace Corporation, have shown that titanium 6Al-4V alloy was not compatible with Freon MF, but that it was compatible with Freon TF/Oxyfume 12 material. The decontamination agent in sterilization exposure contains Freon 12, which is equivalent to a DF or "difluoro" designation between MF-"monofluoro" and TF-"trifluoro" formulations. Therefore, it was decided to perform tests to ascertain the compatibility of the materials.

The problem involved the availability of chlorine in the Freon 12 and its effect on titanium. Specifically, it was desired to know if the decontamination atmosphere would initiate stress cracking or whether an existing structural flaw would propagate. Four specimens were tested. Each was a Langley sample stressed to 125,000 psi. Two specimens were notched in the area of maximum stress and two were not. The test was run for 168 hr under the following conditions:

- 1) The decontamination mixture was 12% ethylene oxide and 88% Freon 12 at a concentration of 600 mg per liter of chamber volume;
- 2) Relative humidity was maintained at  $45 \pm 10\%$ ;
- 3) The temperature was  $122 \pm 1^\circ\text{F}$  at all times. The decontamination gas was preheated to  $122^\circ\text{F}$  before introduction into the test chamber.

The photomicrographs of the specimens shown in Fig. IV-26 show no detrimental effects resulting from the tests.



(a) Unnotched Specimen, Titanium  
6Al-4V (200X)



(b) Notched Specimen, Titanium  
6Al-4V (200X)

Fig. IV-26 Titanium 6Al-4V Alloy Exposed to ET0/Freon 12



g. Ardeform 301 Stainless Steel Compatibility with  $N_2O_4$

A specimen of 301 stainless steel formed by the Ardeform process and supplied by Arde Incorporated, was exposed to  $N_2O_4$  at 275°F for 600 hr. The degree of attack was substantially less than any other 300 series steel alloy. Although the amount of viscous adduct was substantially less, the material was not considered suitable for propulsion system construction when sterilization is a requirement.

h. Compatibility of Fluorosint with  $N_2O_4$

A sample of fluorosint valve seat material, supplied by JPL, was exposed to  $N_2O_4$  at 275°F for 600 hr. No change in weight or dimensions was noted.

i. Passivation of Monomethylhydrazine Systems

Considerable interest was shown in whether or not MMH would violently decompose when heated to 275°F. During the materials testing program decomposition of MMH was often evidenced by extreme discoloration and elevated pressures in the test vessels. It soon became apparent that the decomposition of MMH at 275°F was associated with system cleanliness. When any alloy tested was exposed to heated MMH without proper cleaning, decomposition was observed.

A program to develop and verify cleaning and passivation procedures was initiated. The chemical cleaning consisted of hydrochloric acid baths. This was followed by a solution of nitric acid fortified with 17% hydrofluoric acid in extreme cases. The passivation procedure consisted of exposing the materials to a 25% MMH solution in water at 275°F for 76 hr.

The procedure was verified by testing a bimetallic specimen of 2014 aluminum and 304 stainless steel joined with monel rivets. This combination of materials was selected because these materials were considered the most potentially reactive, based on previous test experience of nonpassivated specimens. The specimen was cleaned and passivated according to the above procedures. The metal specimen was immersed in a vial of MMH and exposed to 275°F for 600 hr. A control vial of MMH containing no specimen was also exposed.

The propellant decomposition is listed in the following tabulation as obtained by gas chromatography techniques.

	Standard MMH	Control Sample	MMH with Bimetallic Specimen
MMH	99.49%	98.06%	97.61%
Water	0.46	1.48	1.94
Hydrazine	0.00	0.22	0.20
Ammonia	0.04	0.23	0.24
Air	0.01	0.01	0.01

These results indicate very little difference between the control and test specimen. From these results it was concluded the cleaning passivation procedures was verified.

j. Determination of the Vapor Pressure of MMH at Elevated Temperatures

A test was conducted to verify the vapor pressure and stability characteristics of MMH fuel at the temperature levels associated with the decontamination and sterilization processes.

The schematic of the test fixture is shown in Fig. IV-27. The glass test vessel had a capacity of 185 ml, and contained an integral thermometer well. The glass outlet tube of the test vessel was connected to the stainless steel fixture piping by a Swagelok connector with a Teflon seal. A relief valve and appropriate hand valves were provided in the system.

The test vessel was supported and completely immersed in an ethylene glycol bath. The bath container was equipped with wall heaters and an agitator to control the heating of the bath.

A vacuum pump was provided to evacuate the test vessel and connecting piping before filling with MMH. A 300-series stainless steel Hoke bottle (300 ml capacity) was provided to hold the fuel sample for introduction into the test vessel.

The instrumentation locations are shown in the schematic of the test fixture (Fig. IV-27). Vapor pressure was measured with a strain gage-type transducer and a potentiometric voltmeter. Accuracy of this system was  $\pm 0.1$  psia for pressures up to 50 psia and  $\pm 0.5$  psia for pressures above 50 psia. Temperature of the MMH was determined with a mercury-in-glass thermometer having a range of 0°F to 300°F and an accuracy of  $\pm 1^\circ\text{F}$ . Bath temperature was read with a copper-constantan pyrometer having an accuracy of  $\pm 3^\circ\text{F}$  in the range of interest.



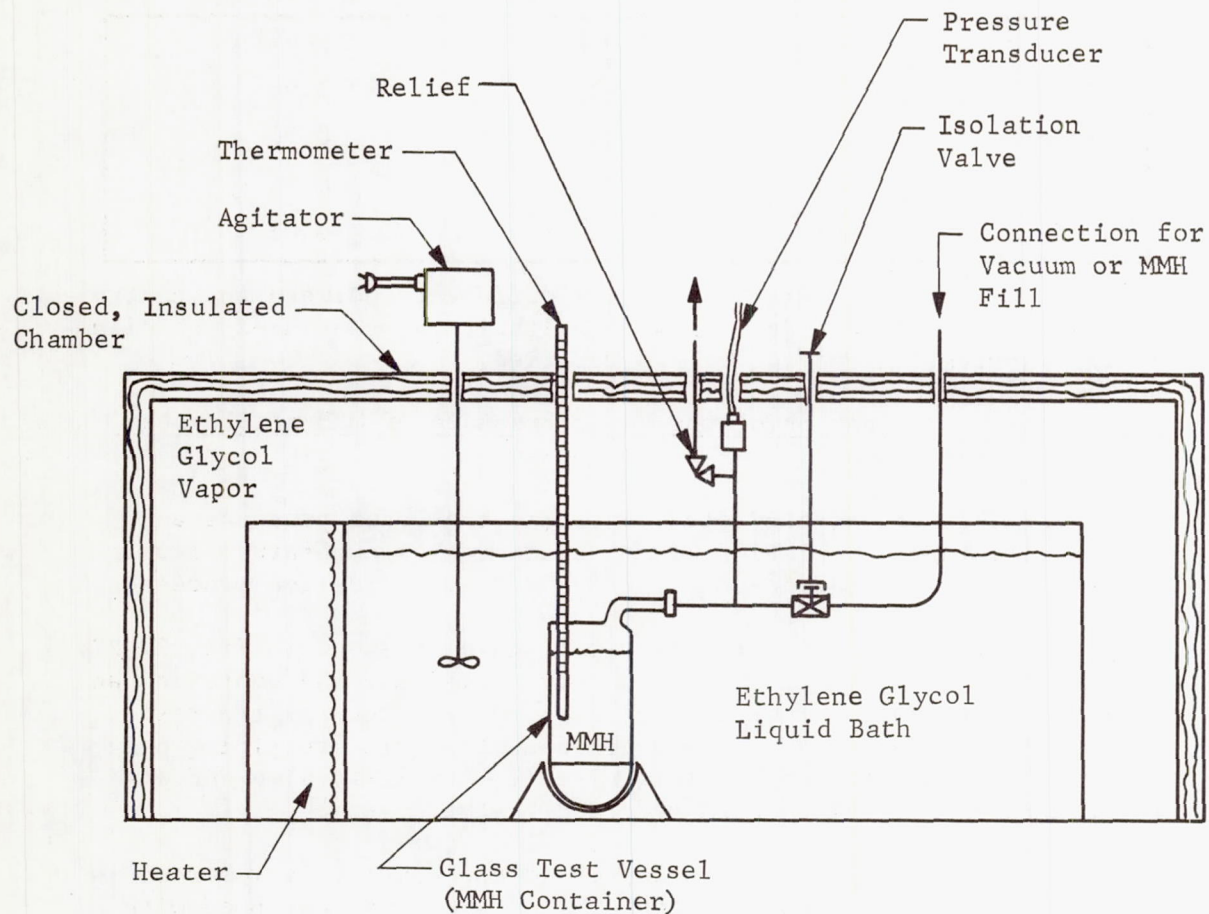


Fig. IV-27 Monomethylhydrazine Vapor Pressure Test Fixture



The test system was thoroughly cleaned before assembly, and proof-pressure tested after assembly. The system was then leak-checked at 285°F with helium, using a mass spectrometer leak detector.

The 300 ml supply bottle was filled from the storage drum by  $\text{GN}_2$  pressure transfer and then connected to the test fixture fill port with the bottle stop valves closed. The test system up to the bottle stop valve was then evacuated to approximately 150- $\mu$  Hg. The vacuum system was then isolated and the stop valves on the supply bottle opened to admit approximately 120 ml of MMH into the test vessel (MMH level about 2 in. above the bottom of the thermometer well). The fill valve was then closed and the supply bottle was disconnected.

The test runs were made by heating the bath to obtain MMH temperatures of 150°F, 200°F, 250°F, 275°F, and 285°F. In some cases, the temperatures was first brought to 285°F and the set-points were run in descending order. One test run included a hold period of 30 minutes at 285°F as a stability test.

The results of the test are shown in Fig. IV-28. The experimental results indicate a vapor pressure of 63 psia at 275°F, which is 11% higher than the previously published data.

#### k. Compatibility of Humidity Sensor with ETO

The primary relative humidity sensor was an Alnor dew-pointer. Since the Alnor is not a continuous device and provides no output signal for recording and control, a secondary system was installed. The secondary system is an electrical hygrometer manufactured by Hygro Dynamics Inc. and consists of a lithium chloride cell, the resistance of which responds to temperature and water vapor content, and an electrical control box that provides an output to be used to drive a strip chart recorder.

The object of this test was to determine whether or not the device was affected by the presence of ETO. Testing was conducted at 122°F in a 100% sterilant gas mixture with humidities ranging from 30 to 70%.

The results of these tests indicated the sensor was affected by the presence of ETO but the effect was not commulative and it was repeatable. The sensitivity of the device was greatly affected because the resistance of the sensor changed from approximately 2 megohms to approximately 20,000 ohms. For this reason a broadband sensor gave meaningless information. With narrowband sensor, 40 to 60% relative humidity was successfully correlated with the Alnor dewpointer and was incorporated into the control system.

There was evidence the electrical sensor was affected by ETO concentration, however, this was not pursued since the chamber was operated at a constant concentration of ETO.

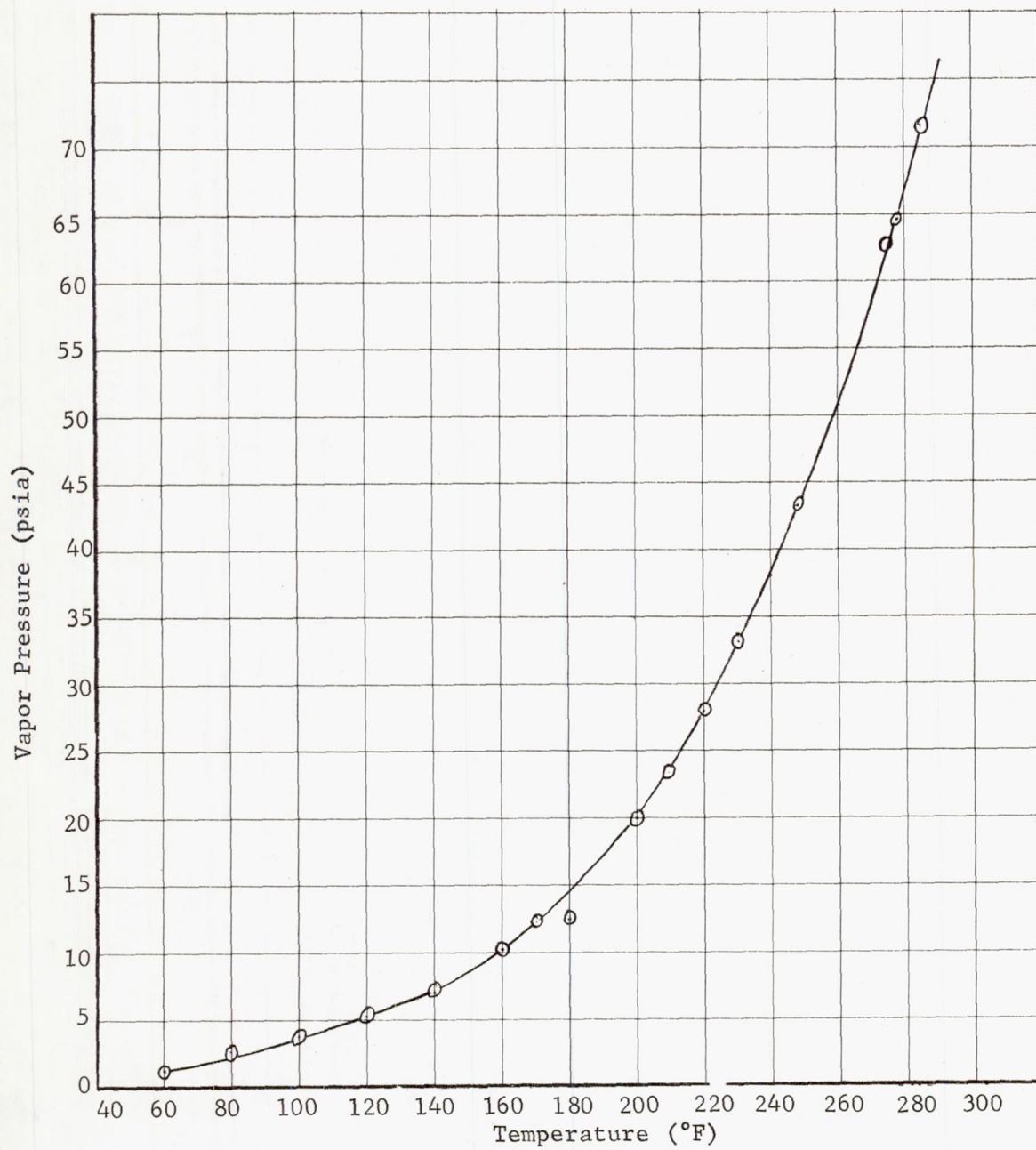


Fig. IV-28 Monomethylhydrazine Vapor Pressure



## V. COMPONENT DEVELOPMENT AND TEST

### A. COMPONENT PROCUREMENT AND ACCEPTANCE

To assure compliance with the specifications set forth under Component Selection, Chapter III.D, each of the component acceptance tests was witnessed by a Martin Marietta engineer or representative. During these tests it became apparent that further development was necessary on some components to achieve the required objectives. These problems were attacked as soon as they were defined and changes were made to produce an acceptable component. The component procurement acceptance tests and problem areas are discussed in this section.

#### 1. Propellant Tanks

##### a. Oxidizer Tank with Diaphragm

The diaphragms for the oxidizer tanks were manufactured and tested at the Dilectrix Company. All units passed the acceptance test and were then shipped to Pressure Systems, Inc, for assembly into the oxidizer tanks.

The first oxidizer tank was tested for acceptance at the Wyle Laboratories on July 17, 1967. Following visual examination and recording the outside diameter in three diametral planes, the unit was subjected to a gaseous proof pressure of 2050 psig for three minutes. The unit was then vented to room ambient pressure and allowed to stabilize to room temperature. A recheck of the three recorded diameters showed no change. Internal leakage through the Teflon bladder was then checked with gaseous helium at 1.0 psig. After stabilization, the leakage was constant at 0.56 cc/min or 33.6 cc/hr. The acceptance level for the bladder alone is zero bubbles of gaseous nitrogen in 5 minutes. Since the bladders had all passed this preliminary test, it was assumed that the indicated leakage was a result of the assembly of the tank hemispheres and Teflon bladder. This could be accounted for as increased diffusion rate through the bladder because of the use of helium instead of nitrogen and/or a leak at the rim seal. Because the leak was not enough to cause any great discrepancy during expulsion, this discrepancy was accepted and a change in the rim seal design on the next unit was planned.



The final test was the external leakage check using helium gas at 2045 psig over a period of three minutes. No leakage was detected with a mass spectrometer. The unit was accepted for component test. This was the first attempt by the tank manufacturer to install a hemispherical Teflon laminate bladder in a propellant tank. His previous experience history involved only elastic rubber bladders that do not cold flow or creep under relatively low loads.

Sealing of a rubber diaphragm involves clamping of the rubber lip at the tank girth in a cavity made up of flat machined surfaces. Due to the elasticity of the rubber, enough squeeze can be built in to provide a good seal. In the case of Teflon the preload resulting from squeeze is soon relieved by cold flow of the material and must, in some manner, be restricted to maintain a seal. Restriction may be accomplished by minimizing the flow area. A joint design shown in Fig. V-1 was used for the first tank. The serrations penetrate the Teflon and act as multiple series orifices to limit the Teflon flow. For this joint to work properly, it must be preloaded adequately to allow proper penetration of the serrations. In the first tank, several conditions were present that were not conducive to making a proper seal: (1) the diaphragm lip seal area was rough and irregular; (2) tank hemisphere preload was not measured and was probably too low to cause proper penetration; and (3) the height of the serrations was not sufficient to bridge across measured irregularities in lip seal thickness. It was decided that a revised seal design, Fig. V-2 would be used for the module tank.

Since the surface between the gas side hemisphere and the diaphragm lip is the primary seal area across the diaphragm, only this area was modified. This serration configuration was designed to provide several advantages over the previous configuration of Fig. V-1. With a hemisphere loading of 50 lb per linear inch of seal, the two large serrations will fully penetrate the Teflon skin of the seal surface. The displaced Teflon will fill the cavity between the serrations. With the two larger serrations fully penetrated, the two shorter serrations will penetrate approximately half way through the Teflon. This will provide a grip in the Teflon if the larger serrations have separated the seal completely. Therefore, a fully trapped Teflon seal is provided (between the large serrations) with gripping action by the smaller serrations to assure diaphragm retention.

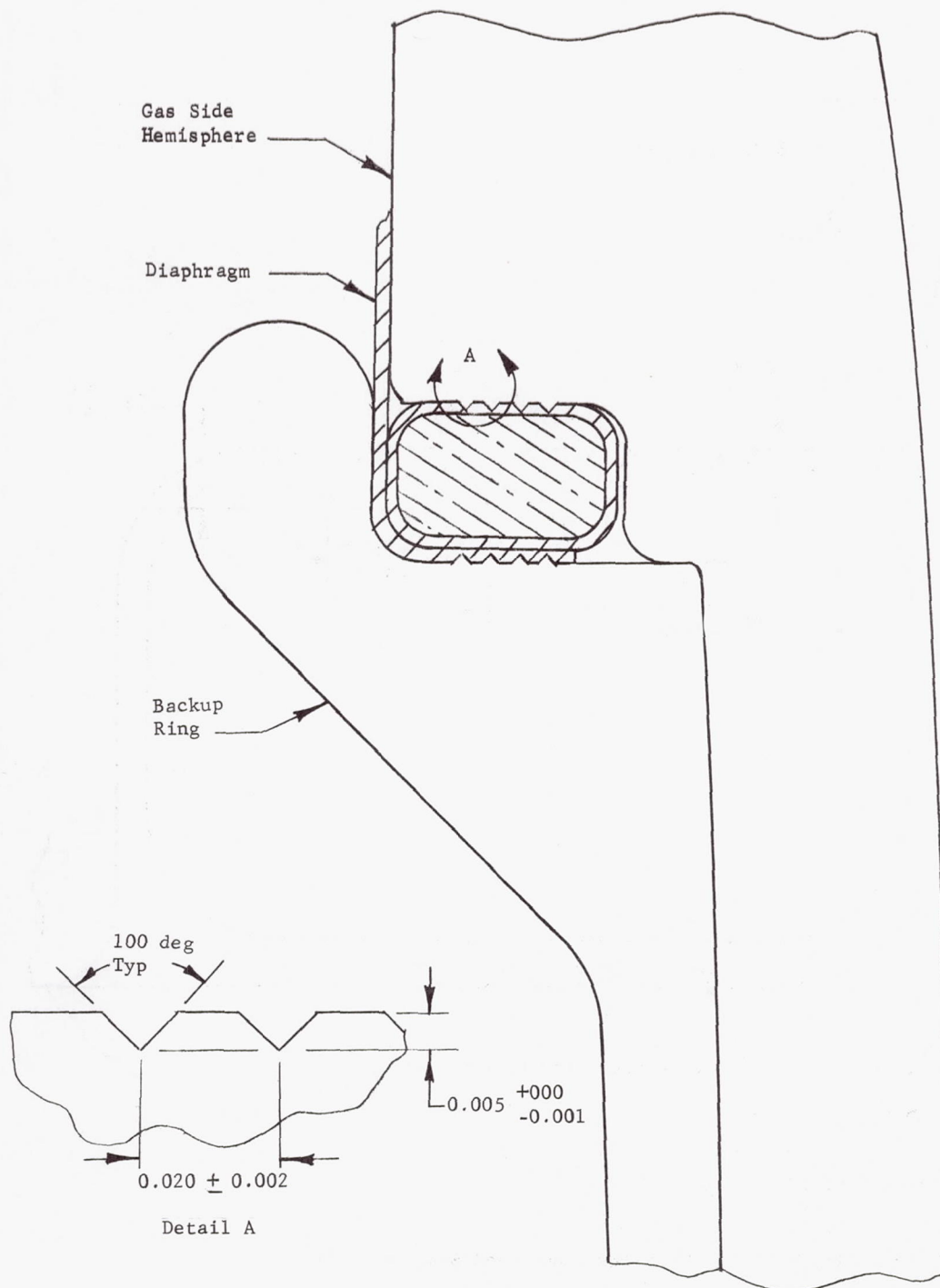


Fig. V-1 Oxidizer Tank, Seal Joint Design

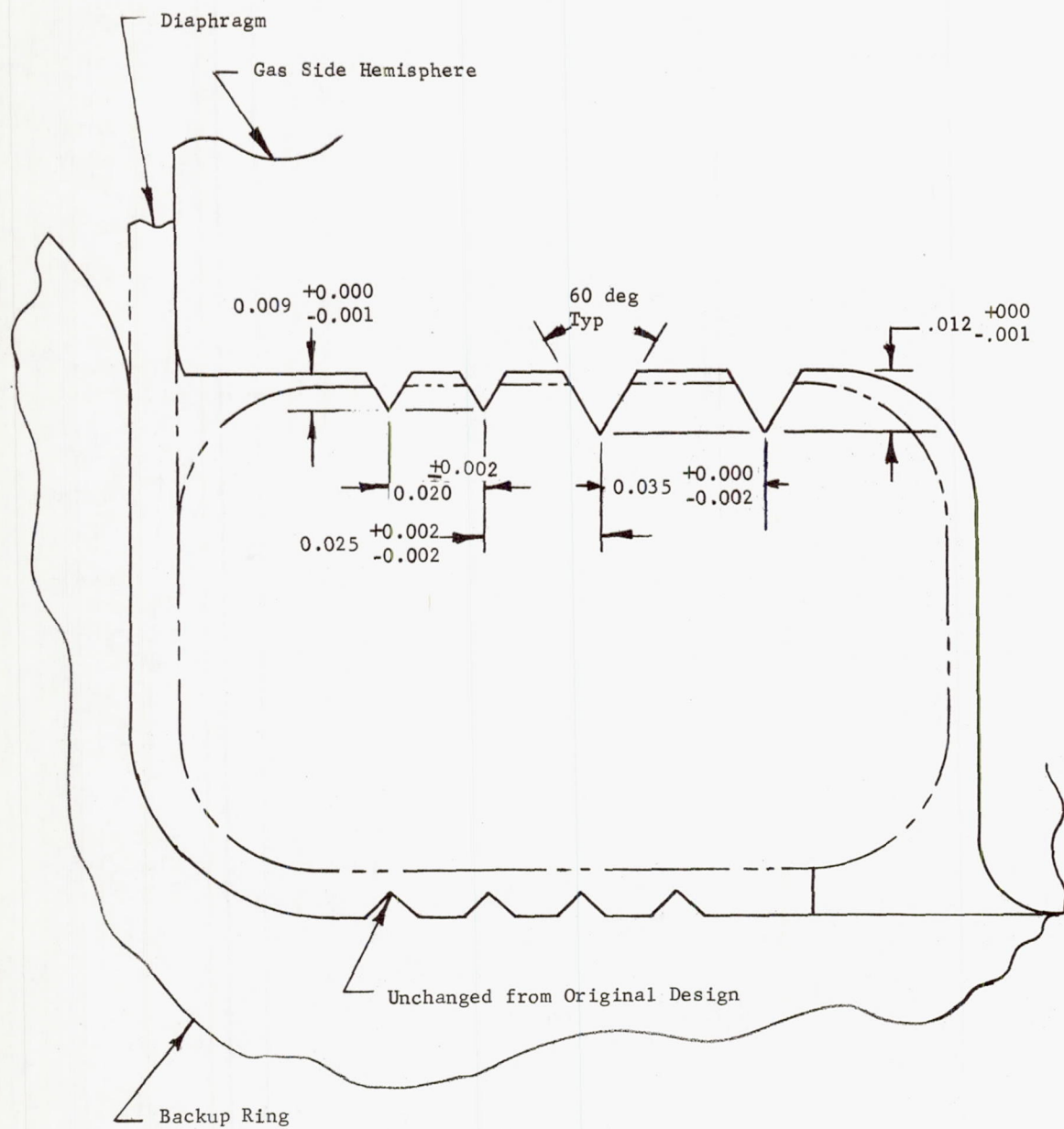


Fig. V-2 Oxidizer Tank, Improved Seal Joint Design



For this assembly 50 lb/in. of seal preload was used. It was a requirement that the preload be measured by a torque calibration of the threaded rods used to load the hemispheres during welding.

As one additional step to ensure a leaktight system, the diaphragm seal area was hand worked to provide a better finish and tighter tolerance on the seal thickness. The initial seal thickness was 0.1170 to 0.1238 in. After rework by hand sanding, the thickness was 0.1170 to 0.1190 in.

Following the above changes, the module unit was assembled and submitted for acceptance test. A diaphragm leak check was performed using 1 psig helium gas on the tank liquid side. A tube was connected to the gas side port and submerged in water to collect leakage gas. No leak was noted over a 5-minute period. At the completion of this check the tank was vented and then pressurized at both ports to 2060 psig for shell proof pressure. On venting to ambient another diaphragm leak check was performed with an indicated leakage of 9 scc/minute of helium. The tank was held at 1 psig for a considerable time with no reduction in leak rate. Pressure was increased on the liquid side port in 100 psi increments to 700 psig. The leak rate was considerably higher at the higher pressure level. The tank pressure was then reduced to 1 psig. At about 15 psig a large quantity of gas was suddenly expelled, indicating a gas bubble had existed on the gas side of the diaphragm. At this time, leakage began to decrease and after one hour the rate was at 3.8 cc/minute with 1 psig on the tank liquid port.

After considering various courses of action, including cutting the tank open with possible loss of hemispheres or diaphragm, it was decided that the tank would be accepted with the indicated leakage. Enough firing margin exists to allow for a 3.8 cc/minute oxidizer leakage over the 5-minute firing time. In addition, it is not anticipated that this leakage rate can occur during firing since a  $\Delta P$  of much less than 1 psi is sufficient to move the diaphragm during expulsion.

A final check of diametral dimensions showed no change before and after the proof pressure.

b. Fuel Tank and Screen Trap

The screen trap assembly design was revised during the latter stage of trap fabrication. Welding of the cone section at its large diameter end to the flat sheet portion did result in a problem. The acute angle (approximately 23 deg) weld resulted in the formation of metal oxides within the angle. Since the oxides generally cause fuel decomposition, they must be removed before fuel exposure. The procedures available for removal included such mechanical cleaning as wire brushing and grinding or pickling using a mixture of nitric acid and hydrogen fluoride. The weld area is inaccessible to effective wire brush or grind cleaning. In addition, pickling results in chemical attack of the metal, which is insignificant on the sheet stock, but is quite significant on the wire screen.

The pickling approach was used with care so that the solution did not contact the screen. Subsequent exposure to MMH indicated the cleaning was adequate.

Welding of the cap on the small diameter end of the cone resulted in a similar problem with the weld surface on the inside of the assembly. To allow mechanical cleaning a 1-in.-diameter hole was cut in the center of the cap and was later covered with a riveted patch. A single rivet hole was left in the center of the patch for final bubble point check (Fig. IV-3).

The bubble points obtained for the complete assemblies were 2 and 2.5 in. of water, respectively.

The two units were then shipped to Pressure Systems, Inc, for assembly into the fuel tanks.

The first fuel tank, for use in the component test, was tested for acceptance at the Wyle Laboratories on July 12, 1967. After passing visual examination, the outside diameter was measured in three diametral planes. The unit was then subjected to gaseous proof pressure of 2050 psig for 3 minutes and then returned to room pressure. The outside diameter was again checked at the same points and showed no change within the limits of the micrometer (0.001 in.). The unit was then subjected to the outside leak test. After pressurizing to 950 psig for 3 minutes with He, the maximum indicated leakage was  $1.0 \times 10^{-9}$  scc/sec. The maximum allowable is  $1.0 \times 10^{-8}$  scc/sec. Therefore, the unit passed all tests satisfactorily.



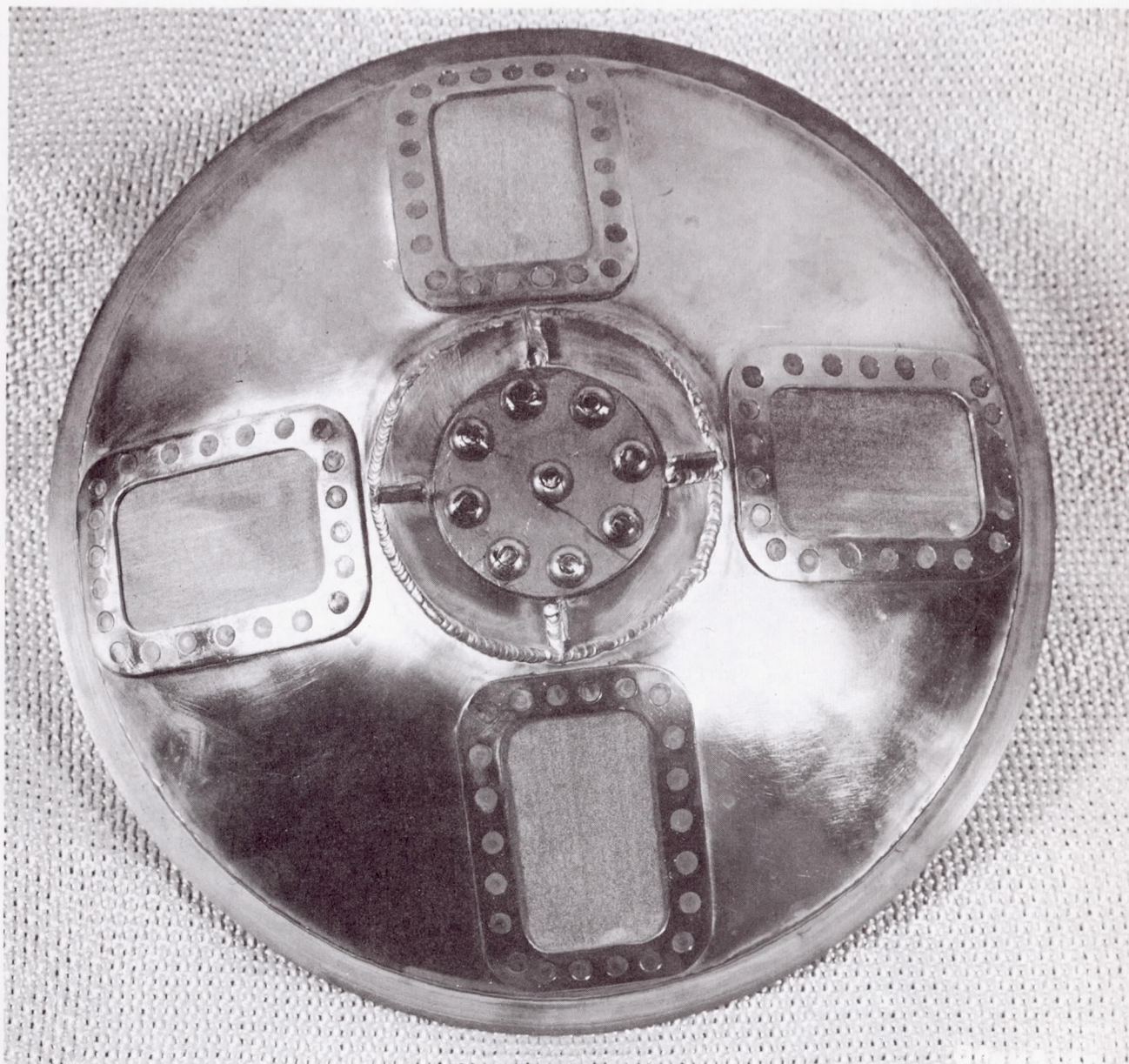


Fig. V-3 Fuel Tank Screen Trap Assembly



The second fuel tank, for use on the module, passed all acceptance tests. The only difference from the first unit was in the leakage rate, which was  $5.8 \times 10^{-9}$  scc/sec He. This is still below the allowable rate and therefore acceptable.

## 2. Gas Pressurant Tank

The gas pressurant tank was purchased as an off-the-shelf item. It had been proof and leak tested by the vendor. The only addition to this tank was the welding of special fittings furnished by Martin Marietta Corporation. The welded joints were X-rayed and showed no excessive porosity, therefore, the unit was accepted for inclusion in the module.

## 3. Gas Pressure Regulator

The first of two regulators was passed through the acceptance test on July 10, 1967, and the second on July 13, 1967. Results of the tests are tabulated below.

	<u>S/N 1</u>	<u>S/N 2</u>
<u>Examination of Product</u>	Accepted	Accepted
<u>Proof Pressure</u>		
Inlet Pressure (psig)	2400	2400
Outlet Pressure (psig)	380	380
Time Applied (min)	2.0	2.0
<u>Internal Leakage</u>		
Inlet Pressure (psig)	1600	1600
Leakage (10.0 max)	4.2 scc/hr (GN <sub>2</sub> )	6.4 scc/hr (GN <sub>2</sub> )
<u>External Leakage</u>		
Inlet Pressure (psig)	1600	1600
Leakage (0.1 max)	0.04 scc/hr (GN <sub>2</sub> )	0.02 scc/hr (GN <sub>2</sub> )
Time Applied (min)	15	15
<u>Overshoot Pressure</u>		
Inlet Pressure (psig)	1600	1600
Lockup Pressure (psig) (278 max)	264	259.0

	<u>S/N 1</u>	<u>S/N 2</u>
<u>Regulation</u>		
Inlet Pressure (psig)	1600	1600
Final Pressure (psig)	350	350
Flow Rate (lb/sec)	0.015	0.015
Outlet Pressure (psig)	Max 248	Max 248
(248 $\pm$ 5)	Min 249	Min 244
<u>Lockup Pressure</u>		
Inlet Pressure (psig)	1600	1600
Flow Rate (lb/sec)	0.015	0.015
Lockup Pressure (270 max)	264 psig	261 psig

Both units passed satisfactorily and were accepted.

Later in the program, when the S/N 2 unit was assembled into the module, a functional test disclosed that the internal leakage was excessive and the regulation pressure had shifted downward. The leakage value was 68 scc/hr of GN<sub>2</sub> compared to the allowable value of 10 scc/hr. The regulation pressure was 241 to 245 psig compared to the allowable 248  $\pm$  5 psig. The regulator was returned to the supplier for repair and adjustment so that the sterilization exposure would be initiated with the regulation band in the required limits.

The supplier's investigation revealed a scratch mark in the regulator valve seat, presumably the result of passage of a foreign particle. The regulator seat was repaired, and the regulation spring was heat treated at 325°F for 24 hr at its working stress level to obviate the set-point degradation that had been exhibited by the component test regulator. On receipt of the repaired regulator, it was found that the inlet tube had been indexed incorrectly; therefore, the inlet flange and tube assembly was removed in the Class 100 clean room and reinstalled in the correct position. The results of the acceptance test, conducted at the supplier's facility, is listed in the following tabulation.



	<u>S/N 2 (after rework)</u>
<u>Examination of Product</u>	Accepted
<u>Proof Pressure</u>	
Inlet Pressure (psig)	2400
Outlet Pressure (psig)	380
Time Applied (min)	2.0
<u>Internal Leakage</u>	
Inlet Pressure (psig)	1600
Leakage (10.0 max)	3.0 scc/hr
<u>External Leakage</u>	
Inlet Pressure (psig)	1600
Leakage (0.1 max)	0 scc/hr (GN <sub>2</sub> )
Time Applied (min)	15
<u>Overshoot Pressure</u>	
Inlet Pressure (psig)	1600
Lockup Pressure (psig) (278 max)	269
<u>Regulation</u>	
Initial Pressure (psig)	1600
Final Pressure (psig)	350
Flow Rate (lb/sec)	0.015
Outlet Pressure (psig) (248 ± 5)	Max 251, Min 244
<u>Lockup Pressure</u>	
Inlet Pressure (psig)	1600
Flow Rate (lb/sec)	0.015
Lockup Pressure (psig) (270 Max)	264

Following installation in the module, the prefiring functional tests were conducted. The tests confirmed that all parameters were within specification except the internal leakage. This was measured at 14.5 scc/hr compared to the allowable 10 scc/hr. Because time did not permit another return to the supplier, and the excessive leakage was not in a range that would be harmful during the firing stage, it was decided to accept the unit for test.

4. Solenoid Valve

The solenoid valves were tested at the vendor's facility and were accepted. Results of the tests are listed below.

	<u>S/N 1</u>	<u>S/N 2</u>
<u>Examination of Product</u>	Accepted	Accepted
<u>Proof Pressure</u>		
Inlet/Outlet Pressure (psig)	3750	3750
Time Applied (min)	1	1
<u>Dielectric</u>		
Voltage Applied (500 ± 50 vac)		
Application time (min/ap- plication)	1	1
Arcing or Flashover		
Pin A to Body	None	None
Pin B to C	None	None
Fault Indicator Light		
Pin A to Body	No	No
Pin B to C	No	No
<u>Insulation Resistance</u>		
Applied Voltage (500 ± 50 vdc)		
Pin A to C Resistance (50 megohms min)	500+	500+
<u>Coil Resistance</u>		
Resistance Pin A to B (20 ohms min)	22	22
<u>Performance Test</u>		
<u>Flow Test</u>		
Inlet Pressure Drop while Flowing (1550 psig and 12.5 scfm, GN <sub>2</sub> )		
Pressure Drop (50 psi min)	27	27
<u>Internal Leakage (Deenergized)</u>		
Inlet Pressure (psig)	1550	1550
Stabilization Period (min)	5	5
Internal Leakage (50 scc/hr He, max)	0.22	0.52



	<u>S/N 1</u>	<u>S/N 2</u>
<u>External Leakage (Energized)</u>		
Inlet Pressure (psig)	2250	2250
Stabilization Period (min)	5	5
External Leakage ( $1 \times 10^{-8}$ scc/sec He, max)	0	0
<u>Opening and Closing Response</u>		
Initial Inlet Pressure (psig)	1550	1550
Step Input Signal (vdc)	25	25
Opening Response (0.050 sec, max)	27	26
Closing Response (0.050 sec, max)	12	13
<u>Contamination Check</u>		
Cleanliness Verified per SPS 881	Accepted	Accepted

#### 5. Filter

Acceptance testing of the four filter units was conducted at the Garwood Laboratories Inc. Each unit was subjected to visual examination, proof pressure, and an external leakage check, per LAB 6002513, and passed satisfactorily.

The units were then subjected to the bubble point check while submersed in alcohol and indicated 22, 23.25, 24.0, and 24.2 in. of  $H_2O$  pressure, respectively. The minimum acceptable is 15.9 in. of  $H_2O$  pressure, therefore, all units passed satisfactorily.

#### 6. Hand Shutoff Valve

The first of nine hand valves was passed through the acceptance test on June 8, 1967. Results are shown in the following tabulation.

	<u>S/N 1</u>
<u>Examination of Product</u>	Accepted
<u>Proof Pressure</u>	
Pressure (psig)	1500
Time (min)	2
<u>External Leakage</u>	
Inlet Pressure (psig)	1000
Leakage ( $1 \times 10^{-8}$ scc/sec He, max)	$2 \times 10^{-8}$
<u>Internal Leakage</u>	
Inlet Pressure (psig)	1000
Leakage (zero bubbles in 5 minutes)	Zero

The only parameter in question was the external leakage. Since there was some doubt about the heavy helium background being responsible for this out of specification reading, the unit was accepted.

The final eight units were inspected and all met the specifications listed above.

During the assembly of components on the chamber cover for the component test series, difficulty was experienced with the hand valve. The tank-side port is 0.020-in. wall aluminum tube welded into the valve body. Connecting tubing is butt-welded to this port. This process anneals the tube in the area of the weld and makes the unit quite fragile. In two cases the joint was broken adjacent to the weld on the valve body side. Since stresses would be induced into this joint in the module through thermal effects during sterilization, it was decided that all valves would be modified in-house to improve the strength in this area. The tube port was machined out of one of the valve bodies and a 1/4-in. AN male fitting was welded into the body. A short test series consisting of proof pressure, and internal and external leaks was conducted at Martin Marietta to prove this change. The valve passed all tests satisfactorily and the other valves were also converted to provide units for the module assembly.



## B. TEST FIXTURE DESIGN AND FABRICATION

### 1. Component Functional Test Fixtures

Test fixtures were designed and developed for the functional test of each component. A typical schematic and actual test setup for the regulator valve are shown in Fig. V-4 and V-5.

To ensure that the test was performed correctly and uniformly each time, the same instrumentation and piping was maintained throughout, and where possible, the same personnel were used for each test. The test units were supplied with spool connections for easy insertion and removal from the test fixture. Also where necessary, as in the case of the regulator, Fig. V-6, a holding fixture was used to maintain the integrity of the connecting points and to prevent inadvertent handling damage.

The cleanliness of all gases used for test was assured by periodic sampling and certification and by including filters within the test fixture

### 2. Decontamination and Sterilization Chamber

Assembly of the decontamination/sterilization chamber was completed, and checkout tests were conducted, culminating in qualification of the chamber in both the decontamination and the sterilization configurations.

Figure V-7 is a schematic of the chamber and accessories. Figure V-8 shows the open chamber with the shroud removed. The electrical heaters (heat source for sterilization tests) are located on the lower flange of the shroud. Figure V-9 is a view into the chamber showing the blower assembly and the hot water heat exchanger. The hot water heat exchanger is the heat source for ETO decontamination tests. The locations of the distribution temperature thermocouples are shown schematically in Fig. V-10.

Following a preliminary adjustment of the cam controlling the ascent portion of the heat sterilization cycle, the checkout tests resulted in qualification of the chamber. Temperatures were maintained within the limits specified in JPL Specification VOL 50503-ETS.

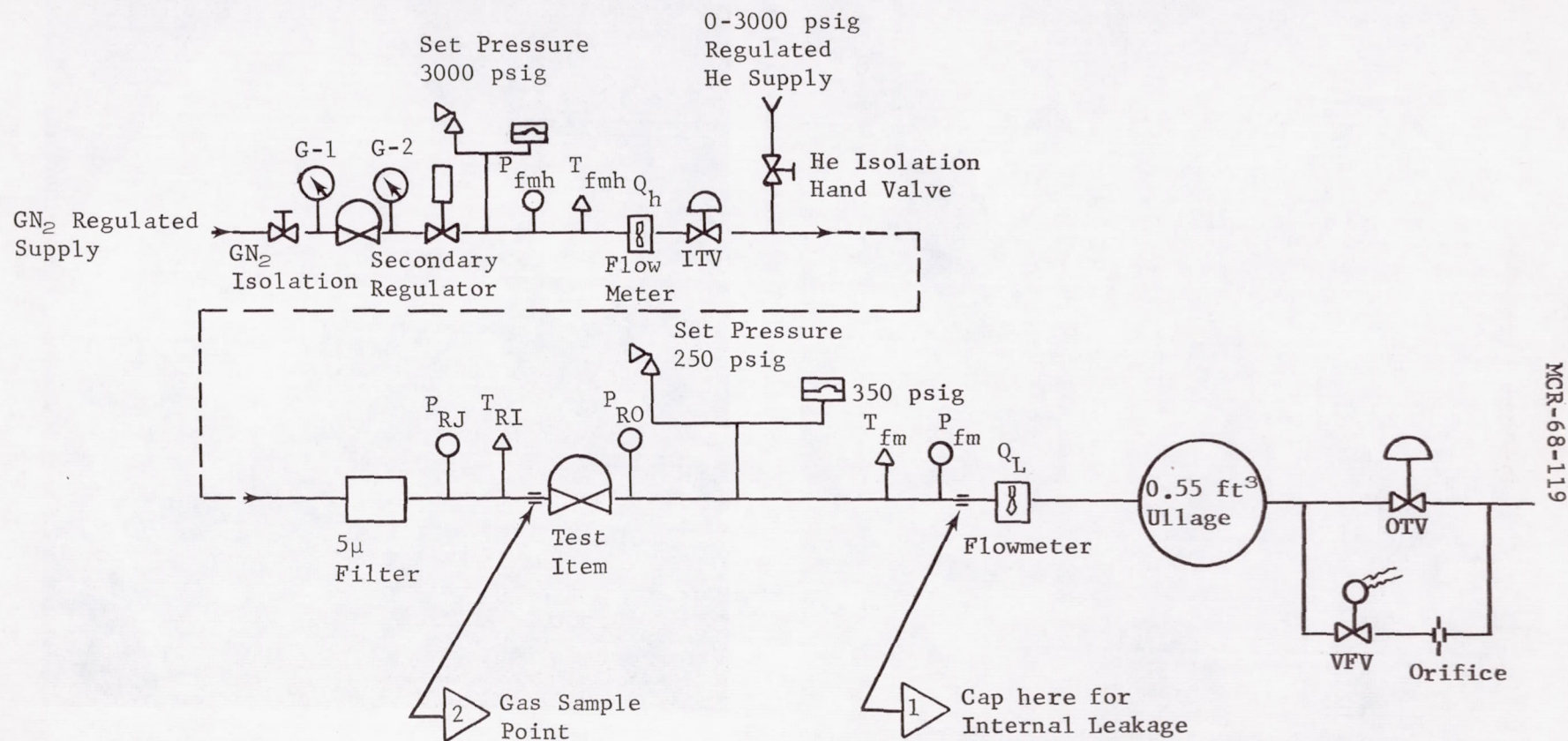


Fig. V-4 Test Fixture Schematic, Regulator Valve Functional Test



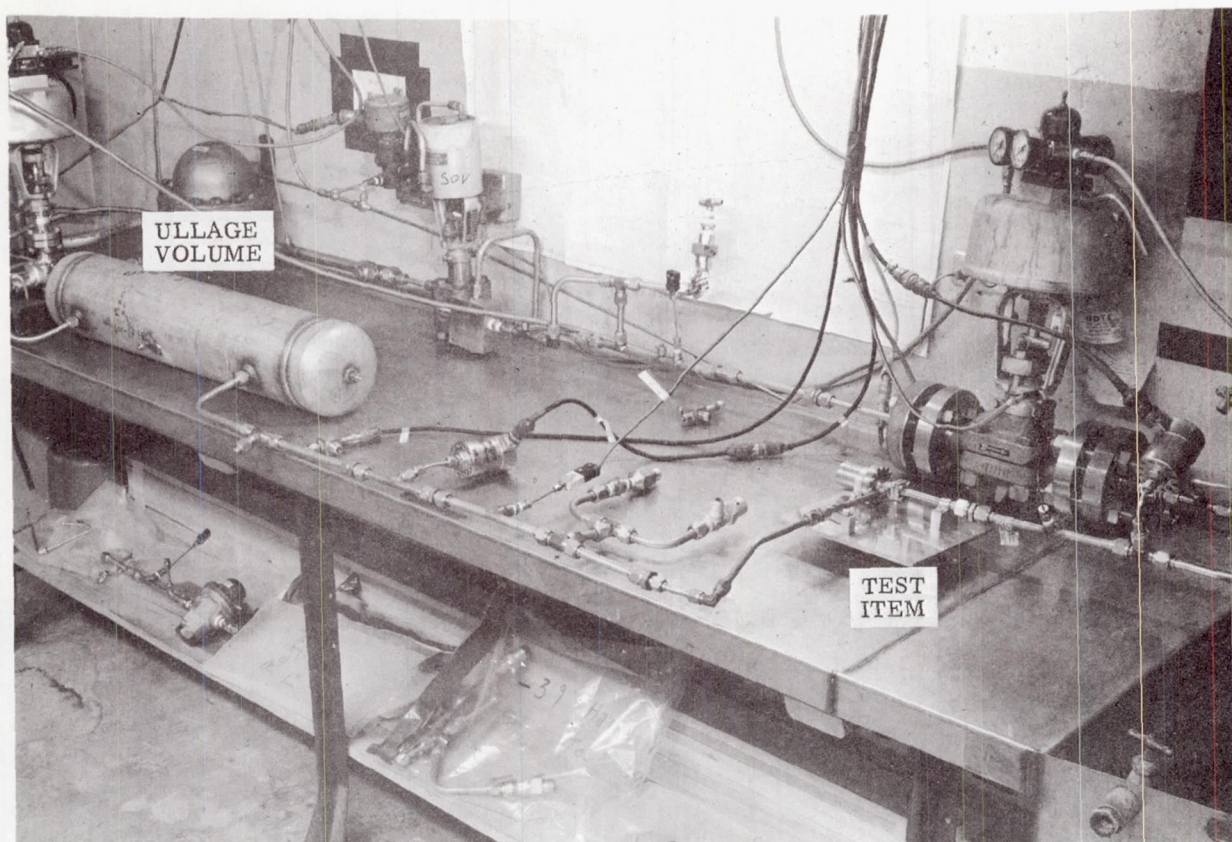


Fig. V-5 Functional Test Setup, Regulator

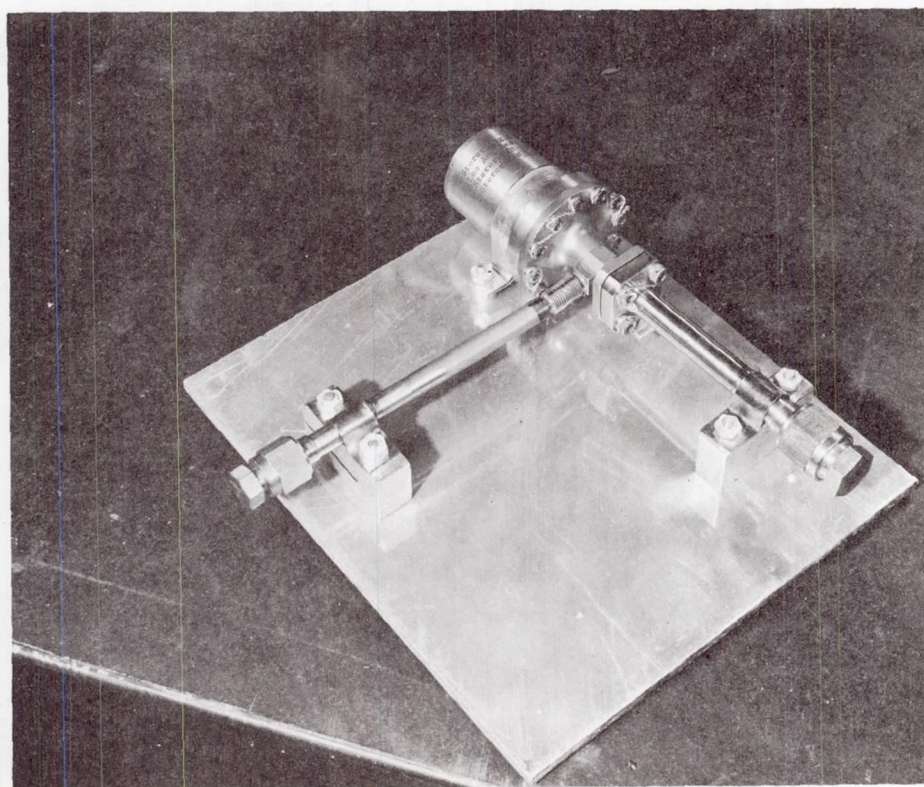


Fig. V-6 Regulator Holding Fixture



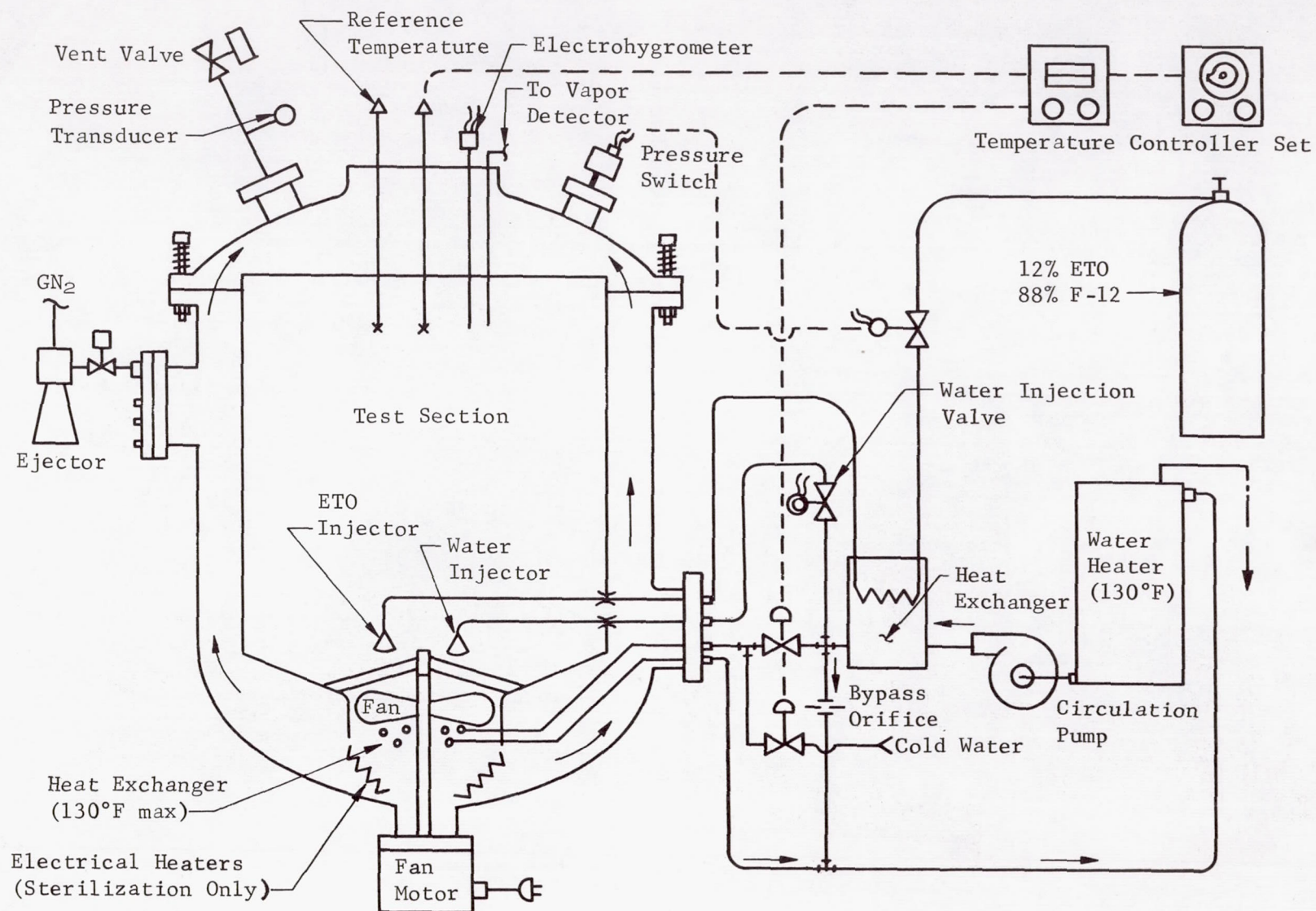


Fig. V-7 Sterilization and Decontamination Test Fixture



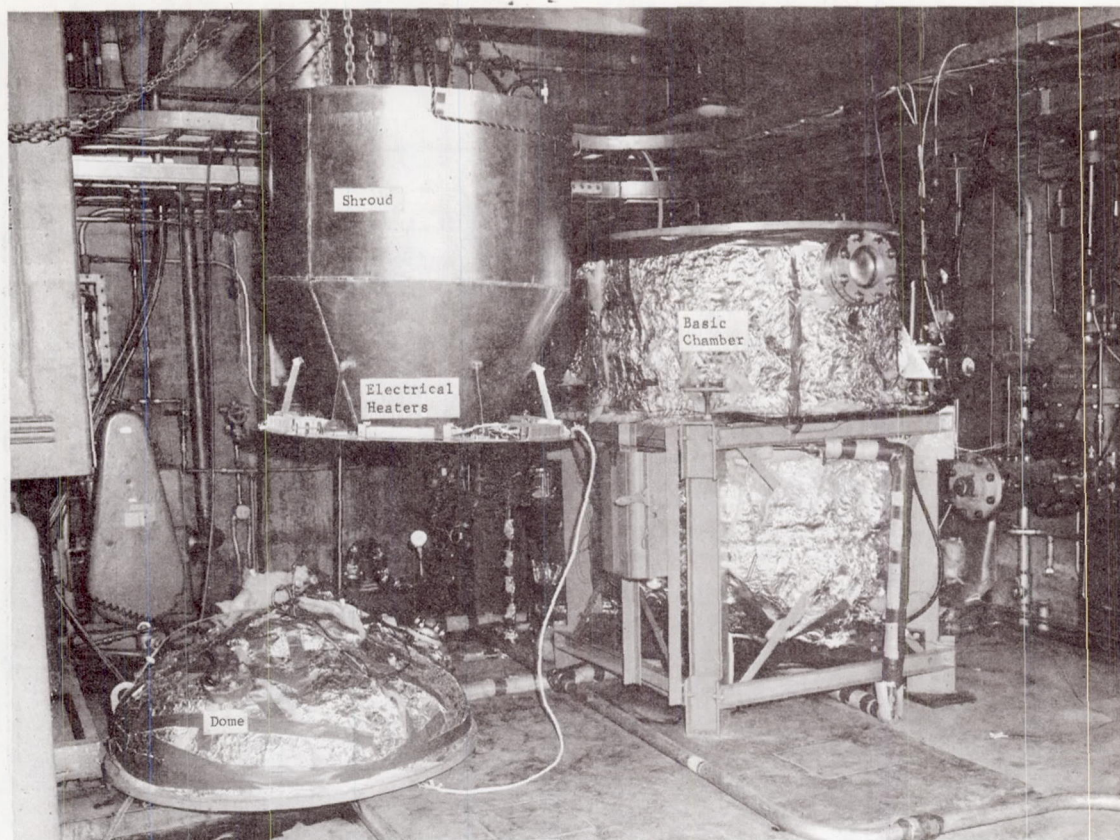


Fig. V-8 Sterilization Chamber, Shroud and Dome Removed

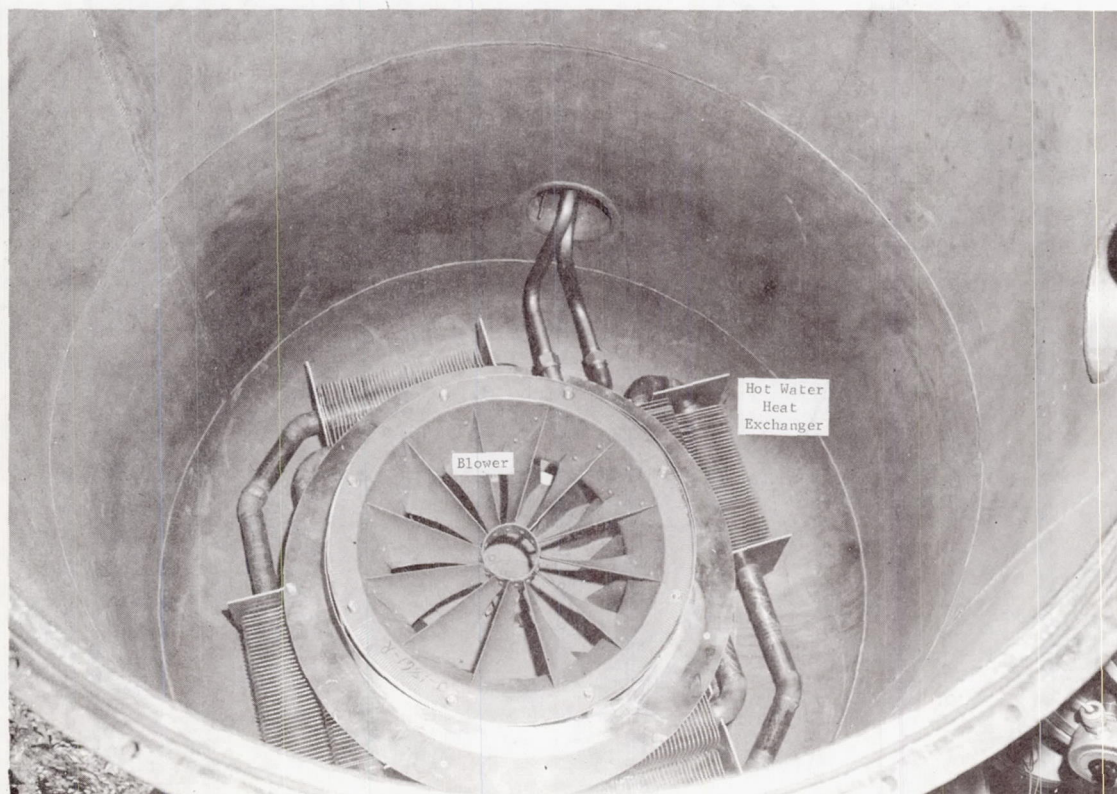


Fig. V-9 Sterilization Chamber, Internal View

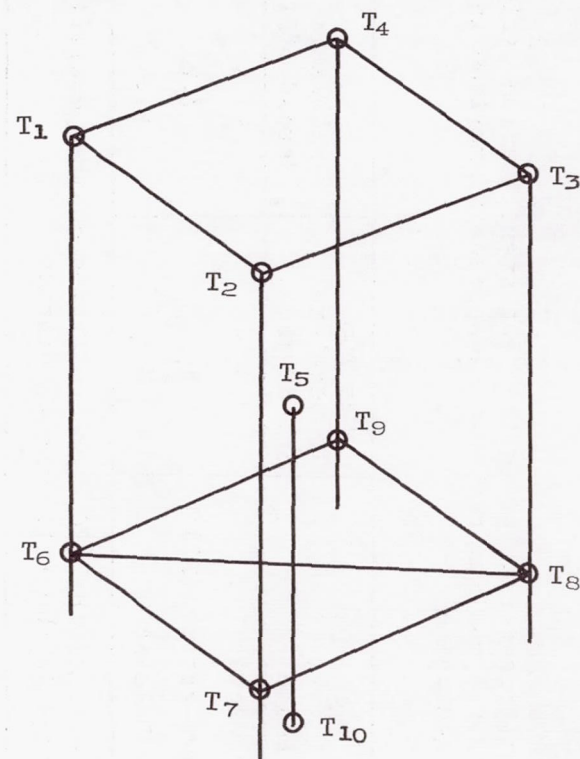
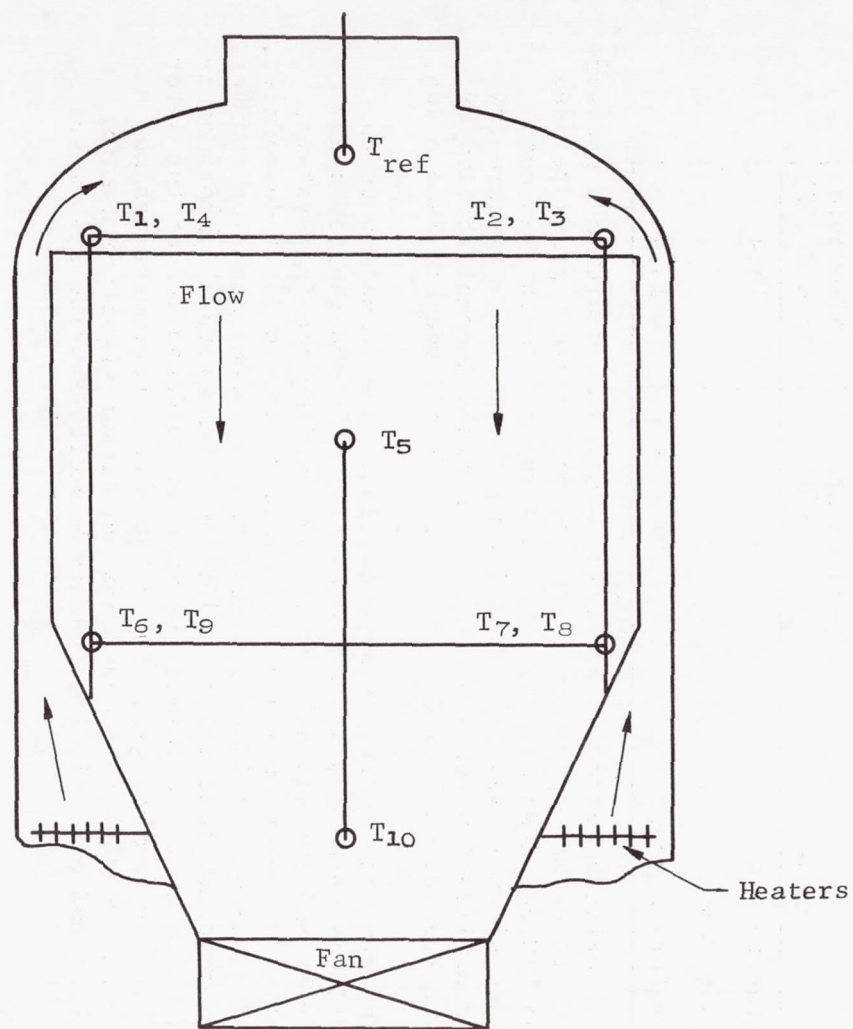


Fig. V-10 Sterilization Chamber Qualification Distribution Thermocouple Array



The significant results in the heat sterilization cycle are indicated by the maximum temperature spreads summarized in the following tabulation.

Phase	Maximum Temperature Spread (F°)	Allowable Spread (°F)
Temperature Ascent	5	14.4
Constant Temperature (275°F)	5	7.2
Temperature Descent	3	14.4

The results of the ETO decontamination chamber qualification are summarized in the following tabulation.

Phase	Maximum Temperature Spread (°F)	Allowable Spread (°F)
Temperature Ascent	5	14.4
Constant Temperature (122°F)	2	7.2
Temperature Descent	1	14.4

The oxidizer vapor detector was encapsulated within a pressure chamber to permit operation at the 22 psia chamber pressure used during ETO decontamination. The fuel vapor detector was not enclosed since it was only used during the ambient-pressure dry heat sterilization tests because of chemical incompatibility of the wet reagent cell used in the detector and the ethylene oxide.

The humidity control system initially was conceived as an essentially open-loop system consisting of a superheated steam generator and two visually monitored humidity sensing systems. The prime measurement system for humidity was an Alnor dewpointer. This instrument was installed next to the decontamination chamber in an enclosure that maintained it at a temperature approximately equal to that of the chamber to prevent condensation of the water vapor in the chamber gas. Since the Alnor instrument was not a continuous readout device and has no output signal to use for recording and control, a secondary humidity sensing system was

installed in the chamber. The secondary system was an electrical hygrometer manufactured by Hygro-dynamics, Inc. The hygrometer consisted of a lithium chloride cell, the resistance of which responds to temperature and water vapor content, and an electrical control box that has an output used to drive a strip-chart recorder.

The feasibility of using the electrohygrometer for easier monitoring of relative humidity was established earlier in the program by pilot tests. The test results showed that, although the output of the hygrometer cell was affected by the presence of sterilant gas, the output could be correlated with the true relative humidity as determined with the Alnor dewpointer. Furthermore, the test results indicated that the effect of sterilant gas on the sensing cell was not cumulative, i.e., there was no change with exposure time. It was, therefore, concluded that the electrohygrometer could be used as a relative measure of humidity conditions in the chamber after establishing the required conditions on the basis of Alnor dewpoint data.

Installation and checkout of the fuel vapor detector and oxidizer vapor detector was completed, placing the sterilization chamber in a ready condition for Task II sterilization.

Instrument Accuracy - A test program to verify the instrumentation accuracy of the Cold Flow Laboratory was completed.

Typical empirical  $2\sigma$  accuracies for pressure measurements using the nominal 2% full-scale system accuracy technique were better than 1%. An in-system stimulus calibration was performed on the same transducers to demonstrate the nominal 1% full-scale accuracy capability and the typical  $2\sigma$  accuracies were better than 0.32% full-scale on all recorders. A 4-hr drift evaluation of the same parameters indicated a slight degrading effect of system accuracies. Accuracy varied with the type of recorder used. Typical end-to-end system accuracies over a 4-hr period were better than 0.26% full scale using the CEC recorder, 0.32% full scale using Bristol recorder, and 0.68% full scale using a Sanborn recorder.

A simulated dynamic stimulus was used to demonstrate the merit of electronically filtering dynamic signals that have frequency components beyond the recorder response. This filtering was performed at the data amplifier. Typical data showed no significant change in the accuracy of the CEC and Bristol recording. A 250 Hz



input to the Sanborn recorder produced an error of 9.58% full scale. Electronic filtering to 10 Hz reduced this error to 0.57% full scale.

Typical 2 $\sigma$  accuracies for thrust measurements were better than 0.37% full scale over a 4-hr period.

Temperature data acquisition and recording indicated a better than 0.80% full scale accuracy over a 4-hr period for thermocouples subjected to a temperature range of -100°F to +250°F. The platinum temperature probe demonstrated a 0.12% accuracy over the same period.

### C. TEST METHOD

The test methods for each component are defined by the Component and System Test Plan, MCR-67-20. In addition to this document, detailed procedures were written for each component. Each procedure is complete in itself providing step-by-step direction, and lists of necessary equipment and instrumentation. A schedule for the component functional tests is shown in Table V-1.

Detailed procedures were also prepared for component installation and removal and for the heat sterilization test.

Table V-1 Component Functional Test Schedule

Component	Before and After Each Sterilization Test		Before Final Disassembly	
	Test Type	No. Runs	Test Type	No. Runs
Oxidizer Tank with Diaphragm	Leakage	1	Expulsion Demonstration	1
Fuel Tank with Screen Trap	Leakage	1	Expulsion Demonstration	1
Regulator	Leakage	1		
	Cracking Pressure	1		
	Regulation Band	1		
	Lockup Pressure	1		
	Response	1		
	Flow Capacity	1		
Solenoid Valve	Leakage	1		
	Response	3		
	Flow Capacity	1		
	Dielectric Resistance	1		
Filter	Flow Capacity	1		
Hand Shutoff Valve	Leakage	1		
	Flow Capacity	1		
	Operating Torque	1		
Ordnance Valve	Leakage	1	Opening Response	1
	Bridge Wire	1	Opening Flow Capacity	1
	Resistance		Leakage (Cartridge Pins)	1
Throttling Valve	(JPL to Perform Functionals)			
Thrust Chamber Valve (1 ea)	Flow Characteristics	5		
	Response Time	3		
	Leakage	1		
	Dielectric Test	1		
	Voltage, Pull In	3		



## D. COMPONENT STERILIZATION

### 1. Presterilization Functional Testing

A presterilization check of the critical parameters was run on all the components to establish a baseline for comparison. Some of the parameters may not agree exactly with those determined during acceptance testing and reported in Section A of this chapter. This can be explained by the difference in test setup and instruments used. Nevertheless these figures are valid for a comparison test. The one notable difference is in the leak test on the oxidizer propellant tank. The oxidizer tank as received from the supplier was reported to have a leak through the diaphragm. Leakage rate was indicated to be 0.56 cc/minute of helium with a pressure across the diaphragm of 1 psi. When the same leak check was performed at Martin Marietta using nitrogen, no leakage could be detected. The pressure was raised in increments from 1 psi to 250 psi across the diaphragm with no indicated leakage. The applied pressure was from the tank liquid outlet side, which pressed the diaphragm against the tank gas side hemisphere. The conclusion reached was that the leak was originally in the lip seal area rather than through the skin of the diaphragm. In addition, cold flow of the Teflon in the seal area finally closed the leak originally detected at the supplier test facility. The results of these tests are shown under Subsection 4, following.

### 2. First Sterilization Series

Following the completion of all required presterilization functional tests, the test components were loaded with propellants as required and were mounted in the sterilization chamber lid as shown in Fig. V-11. X-ray photographs were taken of the oxidizer tank in an effort to determine the position of the diaphragm. The diaphragm could not be detected in the pictures because if it were properly placed against the inlet side of the tank it would not be detectable.

Analysis of the loaded oxidizer showed that the NO content was 0.47%, which was within the 0.4 to 0.8% specified by the MSC-PPD-2 specification.

Sterilization testing of the components was started on August 1, 1967, and continued through six cycles of heat sterilization. Testing was completed on August 29, 1967. The sterilization was per JPL Specification VOL-50503-ETS.



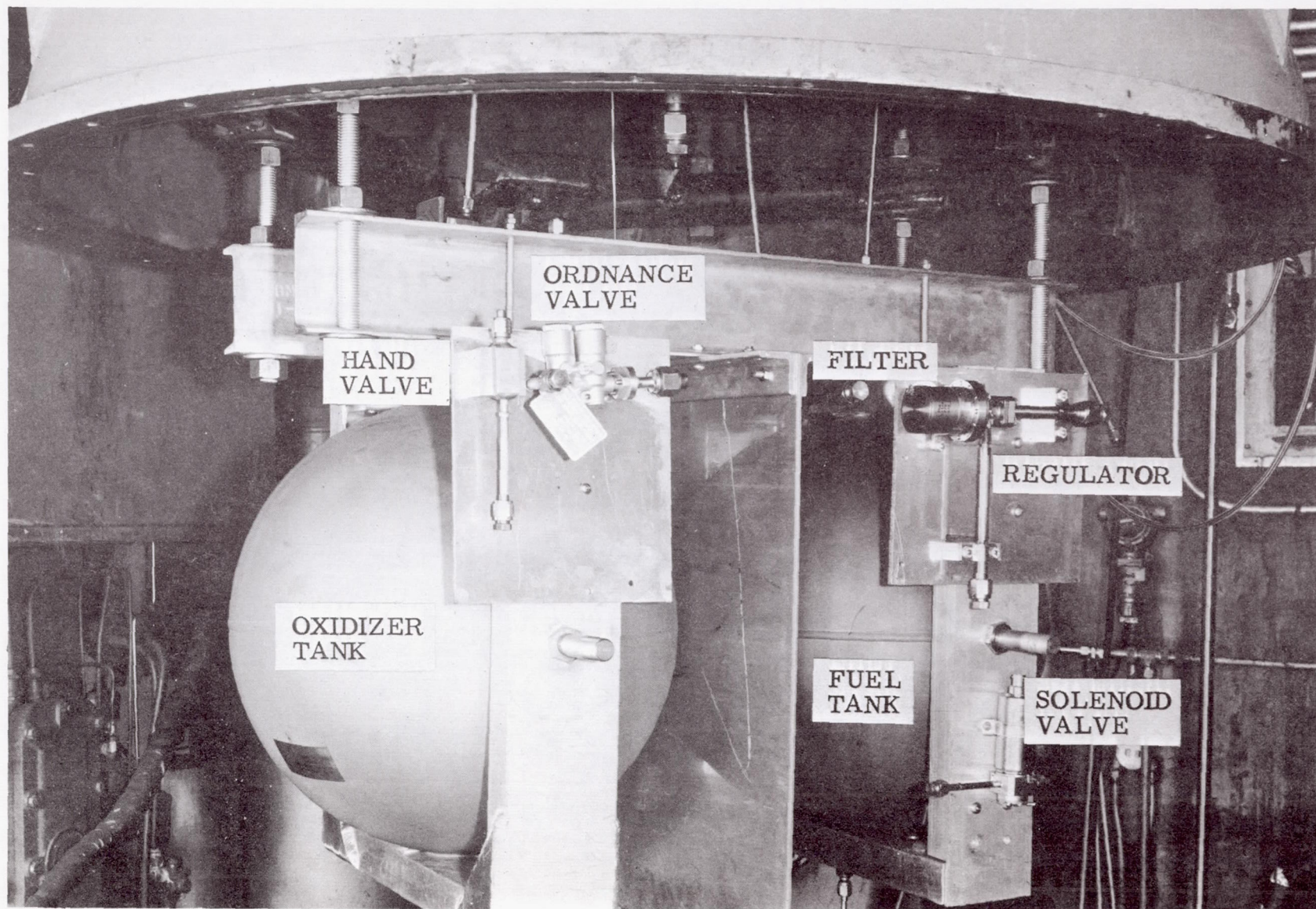


Fig. V-11 Component Installation in Sterilization Chamber



Components exposed to the first series of heat sterilization cycles and the fluids contained during the series are listed in the following tabulation.

<u>Component</u>	<u>Fluid Contained</u>
Oxidizer Tank* with Teflon Diaphragm	N <sub>2</sub> O <sub>4</sub>
Fuel Tank with Screen Trap	MMH
Regulator	Air
Solenoid Valve	Air
Filter	Air
Hand Shutoff Valve	N <sub>2</sub> O <sub>4</sub>
Ordinance Valve	N <sub>2</sub> O <sub>4</sub>

\*The oxidizer tank failed during the sixth cycle and was removed before completion of the sixth cycle.

The results of each cycle of sterilization are summarized in the following paragraphs.

Cycle 1 was completed without incident with respect to the chamber. The oxidizer tank pressure history, however, indicated that the chamber temperature was approximately 3°F low during most of the constant temperature portion of the cycle, while the fuel tank was at equilibrium pressure for the indicated temperature. It was believed at this time that the chamber temperature was actually low, therefore the temperature was raised at the third cycle to compensate for this disparity. However, following the failure of the platinum resistance probe used for chamber temperature control during the sixth cycle, a test was run to determine the actual vapor pressure versus temperature for the MMH. This is reported in Chapter IV.D.3, "Special Tests." The results of these tests proved that the oxidizer vapor pressure was correct for the intended chamber temperature. The fault was in the temperature readout and the fuel vapor pressure versus temperature data were not correct. Therefore, for most of the first six cycles, the chamber temperature was actually above the intended sterilization temperature.

Cycle 2 was interrupted at 31 hr and 50 minutes into the run by a failure of the facility power system. On restart, a blower drive bearing failed, causing additional down time. After repairs

the test was restarted with cycle time starting when propellant vapor pressures were stable at 275°F. This occurred 16 hours after the start of heating and at an agreed on cycle time of 30 hr into the run. Therefore, the cycle was penalized 1 hr and 50 minutes plus the reheat time of 16 hr because of the down time.

Cycle 3 was completed without a problem.

During Cycle 4, the chamber temperature ran low at 273°F due to a malfunction in the temperature recorder/controller. In addition, the oxidizer tank pressure appeared to be unduly low during the run and a leak in this tank system was suspected. After the cycle was completed, the oxidizer tank and connecting lines were pressurized to 750 psig with  $\text{GN}_2$ . No leaks were found as a result of this check. To avoid introducing a correction in oxidizer tank pressure in later cycles, the  $\text{GN}_2$  was removed by evacuating the system and allowing the oxidizer to boil for approximately 20 minutes. Detailed evaluation of the data at the low chamber temperature indicated that the oxidizer tank pressure was consistent with previous cycle test data.

The chamber temperature recorder/controller was repaired and Cycle 5 was run at a chamber set temperature of 277°F. The cycle was completed without incident except for the continuing suspected low oxidizer pressures. This is explained in Chapter IV.D.3, "Special Tests."

Cycle 6 was marked by periodic malfunction of the chamber reference temperature (Trc) recording system, because of heat-induced degradation of the electrical lead to the sensor in the chamber. Since the Trc recorder is also the controller, the spurious signals from the sensor caused the chamber temperature to drop below the required operating band during certain periods of the test. To compensate for the test time at under-temperature conditions, the normal 76-hr test period was extended on an hour-for-hour basis.

Toward the end of the extended test run (within 4 hr of the scheduled initiation of cooling), the chamber oxidizer vapor detector sensed a leak from the oxidizer tank test item and caused an automatic shutdown of the chamber. The oxidizer tank test item was removed for inspection and failure analysis. Cycle 6 was continued with all the remaining components by reheating the chamber at the prescribed rate, allowing a stabilization period of 8 hr at 275°F chamber temperature, and then completing the remaining 4 hr of scheduled time at 275°F plus the normal 6-hr cool-down.



### 3. Second Sterilization Series

The second series of heat sterilization cycles on the system components was completed on October 13, 1967. Cycles 7 thru 12 are summarized in the following paragraphs.

Cycle 7 was started after all components had been subjected to the midsterilization functional tests. The oxidizer tank was not installed, having been removed from sterilization testing for failure analysis during the previous cycle. The throttling valve furnished by JPL was installed in the chamber to undergo the first six cycles of sterilization testing. The fuel and oxidizer passages in the throttling valve were half-filled with MMH and  $N_2O_4$ , respectively. The remaining components were installed in the sterilization chamber as they had been installed during the first six sterilization cycles. This cycle was uneventful with the exception of a chamber shutdown at  $T + 17$  hr caused by spurious signals from the fuel vapor detector. Chamber temperature was restored in approximately 2 hr. Equilibrium fuel vapor pressure (fuel temperature) was reestablished 8 hr after shutdown, at which time testing was resumed at the  $T + 17$  hr mark.

Cycle 8 was marked by an unusually wide excursion in chamber reference temperature during the first half of the run. This was caused by slippage of a shim under the cam follower of the temperature controller. During the latter half of the cycle, the temperature set-point was increased to compensate for the lower temperature experienced during the earlier part of the cycle. The controller problem was rectified at the conclusion of the cycle.

Cycle 9 was interrupted at  $T + 48:50$  hr by loss of facility  $GN_2$  pressure in the test area, which caused the chamber temperature controller to shut off the chamber heaters. This condition occurred during unattended chamber operation on Sunday, October 1. The shutdown could not activate the chamber kill alarm system, therefore, it was not detected until the following morning, at which time the chamber had been at under-temperature conditions for approximately 18 hr. Equilibrium chamber temperature and fuel vapor pressure (fuel temperature) were reestablished at 16:50 on October 2, at which time the cycle timing was resumed at  $T + 48:50$  hr elapsed time. The cycle was concluded without further incident.

Cycles 10, 11, and 12 were completed without incident.

#### 4. Sterilization (Pre, Mid, and Post) Functional Tests

Results of the pre, mid, and poststerilization functional tests on each of the components are presented in the summary data sheets (Tables V-2 thru V-8). The performance of the thrust chamber valves is shown for the functional tests run before sterilization and after completion of the 12 sterilization cycles. The response data from the midsterilization functional test was adversely affected by interaction between the valve solenoid coils caused by the data acquisition system loading the direct coil. Loading of the direct (data pickoff) coil caused the response time of the valves to increase by approximately a factor of three. Inasmuch as the interaction phenomenon was not discovered until after the second series of sterilization cycles was underway, accurate retrieval of the true response characteristics of the valves was not feasible. In addition, since the operating characteristics of the valves was not significantly changed after 12 sterilization cycles, it was assumed that there was no significant change in valve performance at the midsterilization point.



Table V-2 Performance Data, Propellant Tanks

Component Name:	Propellant Tank
Part Numbers:	
Oxidizer -	Martin Marietta LAB 6002514-009
	Pressure Systems, Inc 80092
Fuel -	Martin Marietta LAB 6002514-019
	Pressure Systems, Inc 80092
Serial Numbers:	
Oxidizer -	S/N 0001
Fuel -	S/N 0001

Item	Presterilization	Midsterilization	Poststerilization
<u>Fuel Tank</u>			
<u>External Leakage</u>			
Helium at 400 psig (scc/sec)	Zero	--	Zero
Hydrion Paper Indica- tion (pH)	--	No basic indica- tion	--
<u>Expulsion, -1 g</u>			
Quantity Loaded (1b)	50.5	--	--
Quantity Expelled (1b)	--	--	0.96
<u>Oxidizer Tank</u>			
<u>External Leakage</u>			
Helium at 930 psig (scc/sec)	Zero	--	
Hydrion Paper Indica- tion (pH)	--	Leakage at test fitting	Not Tested
<u>Internal Leakage</u>			
GN <sub>2</sub> , 1 psid (cc/hr)	Zero	210 cc/min (He)	
<u>Expulsion, -1 g</u>			
Quantity Loaded (1b)	80.7	--	--
Quantity Expelled (1b)	--	--	

Table V-3 Performance Data, Pressure Regulator

Component Name: Pressure Regulator  
 Part Number: Sterer P/N 35540  
 Martin Marietta P/N LAB 6002515-009  
 Serial Number: 1

Item	Presterilization	Midsterilization		Poststerilization
		Initial	Final	
<u>Leakage Rate</u>				
External (Bubbles GN <sub>2</sub> )	Zero	Zero	Zero	*
Internal (GN <sub>2</sub> scc/hr)	4.2	56,000	1200	4900
<u>Hysteresis</u>				
Initial Outlet Lockup Pressure (psig)	269	250	264	256
Minimum Outlet Pressure (psig)	259	243	248	246
Maximum Outlet Pressure (psig)	263	247	253	254
<u>Regulation</u>				
Inlet Pressure, Initial (psig)	1560	1,513	1500	1519
Inlet Pressure, Final (psig)	408	320	342	351
Average Flow Rate (lb/sec)	0.015	0.014	0.015	0.015
Outlet Pressure (psig)				
Minimum	247	231	234	231
Maximum	250	235	234	235
<u>Response</u>				
Inlet Pressure, Average (psig)	1650	1,500	--	1599
Outlet Pressure, Lockup (psig)	260	252	--	244
Overshoot (psig)	0	0	--	0
*One 1/4-in.-diameter bubble every 5 minutes.				



Table V-4 Performance Data, Solenoid Valve

Component Name:	Solenoid Valve
Part Number:	Sterer P/N 35580
	Martin Marietta P/N 6002516-001
Serial Number:	2

Item	Presterilization	Midsterilization	Poststerilization
<u>Leakage Rate</u>			
Internal Leakage (Helium)			
Inlet Pressure (psig)	1560	1530	1544
Leakage (scc/hr)	3.3	2.0	0
External Leakage (Helium)			
Inlet/Outlet Pressure (psig)	2200	2200	2200
Leakage Rate (scc/hr)	Zero	Zero	Zero
<u>Flow Capacity (GN<sub>2</sub>)</u>			
Corrected Inlet Pressure (psia)	1550	1550	1550
Corrected Inlet Temperature (°F)	70	50	70
Corrected Flow Rate (lb/sec)	0.070	0.072	0.071
<u>Response</u>			
Average Inlet Pressure (psig)	1545	1543	1533
Opening Time (sec)			
Minimum	0.102	0.102	0.104
Maximum	0.102	0.108	0.104
Closing Time (sec)			
Minimum	0.082	0.081	0.084
Maximum	0.089	0.092	0.084
<u>Dielectric Strength</u>			
Pin A to Case, 500 vac (microamps)	4	0	500
Pin B to Case, 500 vac (microamps)	4	0	500

Table V-5 Performance Data, Filter

Component Name: Filter, 5 Micron Nominal  
Part Number: Western Filter Company P/N 20477-5  
Serial Number: Martin Marietta P/N LAB 6002513-009  
None

Item	Presterilization	Midsterilization	Poststerilization
<u>Pressure Drop (GN<sub>2</sub>)</u>			
<u>High Pressure</u>			
Inlet Pressure (psig)	1550	1537	1552
Flow Rate (lb/sec)	0.015	0.015	0.016
Pressure Drop (psi)	0	0	0
<u>Low Pressure</u>			
Inlet Pressure (psig)	375	248	280
Flow Rate (lb/sec)	0.014	0.016	0.014
Pressure Drop (psi)	0	0	0



Table V-6 Performance Data, Hand Shutoff Valve

Component Name: Hand Shutoff Valve  
 Part Number: VACCO NVB 32181  
 Martin Marietta LAB 6002512-009  
 Serial Number: 21385-1

Item	Presterilization	Midsterilization	Poststerilization
<u>Operating Torque (Helium 248 psig)</u>			
Shutoff Torque (in./lb)	10*	10*	10*
Leakage at Shutoff (cc/min)	1.9 to 3.8	41.0 to 44.5	16.0 to 20.0
<u>Leakage (Helium, 935 psig)</u>			
Internal (cc/min)	19	720	Zero (16 in.-lb)
External (scc/sec)	Zero	$1.12 \times 10^{-5}$	$1.35 \times 10^{-5}$
<u>Flow Capacity (GN<sub>2</sub>)</u>	250	250	250
Inlet Pressure (psig)	250	250	250
Outlet Pressure (psig)	0	0	0
Flow Rate (lb/sec)	0.0765	0.0720	0.0725
Capacity Factor (C <sub>v</sub> )	0.45	0.42	0.43
*Maximum allowable torque. Complete shutoff was not obtained, as indicated by leakage rate noted. Complete shutoff occurred at 17 in.-lb.			

Table V-7 Performance Data, Ordnance Valve

Component Name:	Ordnance Valve
Part Number:	JPL No. D4700696
Serial No:	015
Squib:	P/N J4700697

Item	Presterilization	Midsterilization	Poststerilization	
			Pre-firing	Post-firing
<u>Leakage Rate, Helium</u> @ 2250 $\pm$ 50 psig (scc/sec)				
Internal:	Zero	Zero	Zero	Zero
External:	Zero	Zero	Zero	$7.3 \times 10^{-7}$
<u>Response</u>				
$dP_c/dt$ , psi/sec	N/A	N/A	N/A	42,500
<u>Pressure Drop, Design <math>GN_2</math></u> <u>Flow @ 260 psia (psi)</u>	N/A	N/A	N/A	1.4



Table V-8 Performance Data, Thrust Chamber Valves

Item	Presterilization	Poststerilization
<u>Oxidizer Valve, S/N 575</u>		
Pull-in Voltage (vdc)		
Maximum	14.0	13.2
Minimum	14.0	13.0
Opening Response (sec)		
Maximum	0.0118	0.0125
Minimum	0.0112	0.0123
Closing Response (sec)		
Maximum	0.0084	0.0090
Minimum	0.0079	0.0090
Leakage: External (bubbles GN <sub>2</sub> )	Zero	Zero
Internal (cc GN <sub>2</sub> / hr)	Zero	Zero
Pressure Drop, Design Flow (psi)	27.5	29.2
Insulation Resistance (megohms)	500+	500+
<u>Fuel Valve, S/N 576</u>		
Pull-in Voltage (vdc)		
Maximum	11.5	11.3
Minimum	11.5	11.3
Opening Response (sec)		
Maximum	0.0089	0.0118
Minimum	0.0087	0.0120
Closing Response (sec)		
Maximum	0.0094	0.0096
Minimum	0.0091	0.0087
Leakage:		
External (bubbles GN <sub>2</sub> )	Zero	Zero
Internal (cc GN <sub>2</sub> /hr)	Zero	Zero
Pressure Drop, Design Flow (psi)	13.8	14.2
Insulation Resistance (megohms)	500+	500+

## E. COMPONENT DISASSEMBLY, INSPECTION, AND PERFORMANCE

### 1. Propellant Tanks

#### a. Oxidizer Tank

A major problem occurred during the final cycle of first sterilization series. With approximately 4 hr remaining in the constant temperature portion of the cycle, an oxidizer leak caused an automatic chamber shutdown. When the chamber cover was removed, an oxidizer vapor leak was detected on the lower fitting of the oxidizer tank. Since the tank was sterilized in the inverted position, the leak was coming from the gas side port.

The tank was removed from the chamber and the leak rate was measured without changing the tank's orientation. This was accomplished by removing the hand valve and cap from the gas side port and attaching a piece of tubing. The tubing was routed to a graduated cylinder. Tank liquid side pressure (top port) was increased to 60 psig using gaseous nitrogen as a pressurant. Liquid leakage from the gas side port was measured at 58 cc/minute. This indicated that liquid was passing through the diaphragm or around the diaphragm seal at the tank girth. X-ray pictures were taken of the tank to determine diaphragm position and liquid level. There appeared to be gas pockets near the girth seal on the gas side of the diaphragm and the tank liquid surface was just at the girth weld. To establish the leakage point, the tank was plumbed to a receiver vessel as shown by Fig. V-12 and the receiver tank scale reading was taken. The two tank hand valves were opened and the liquid side was pressurized to 60 psig. An increasing scale reading indicated the liquid leak was still present. To determine the leakage point the leak was allowed to continue until liquid stopped flowing and either gas was expelled or no further flow of gas or liquid was noted. A stopping of liquid flow followed by no gas flow could indicate a quantity of liquid on the gas side of the diaphragm. This could result from permeation of the Teflon diaphragm during temperature cycles and would not represent a leak in the normal sense. A continuation of gas flow after termination of liquid flow would indicate an uncovering of the leak point, Fig. V-13.



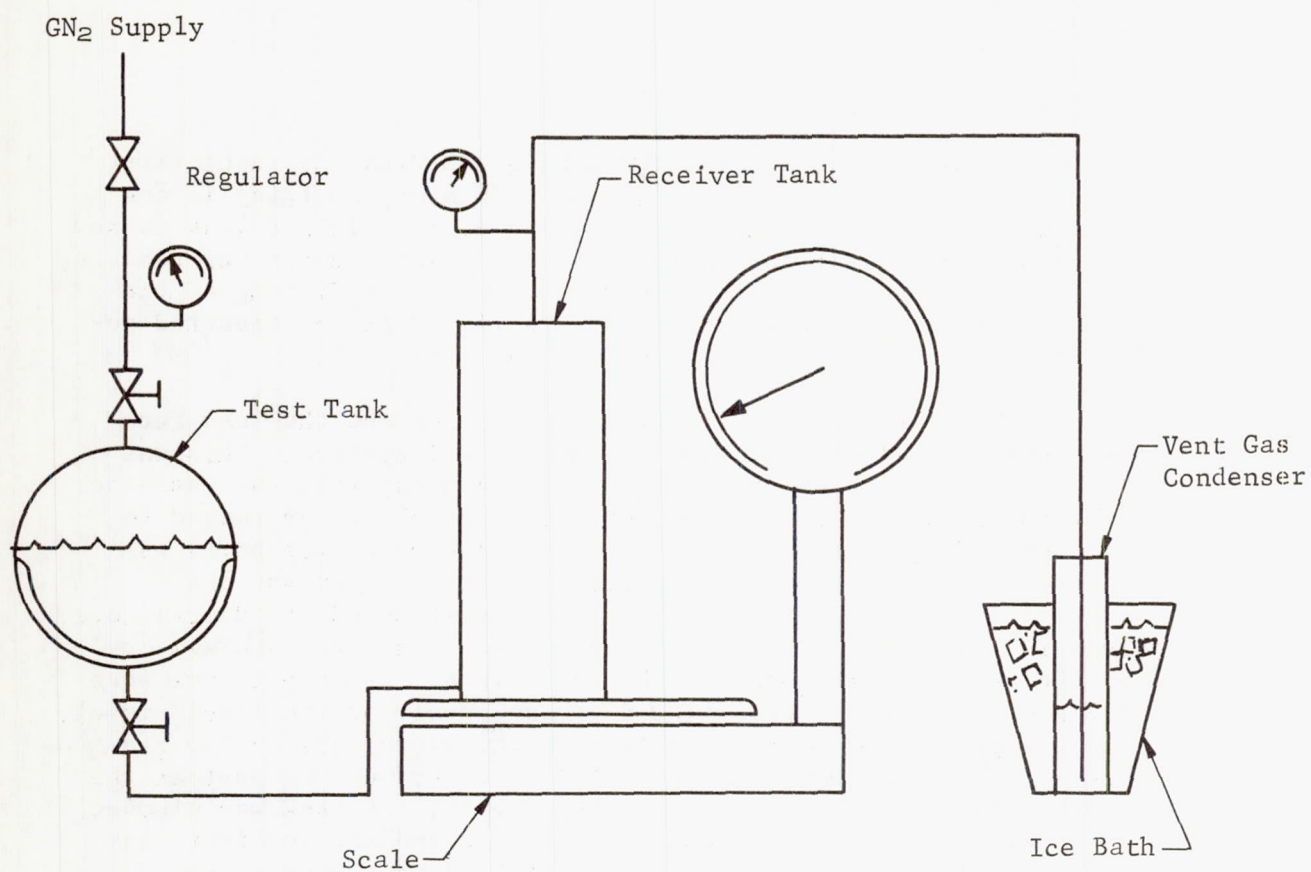


Fig. V-12 Oxidizer Tank Leak Measurement Schematic

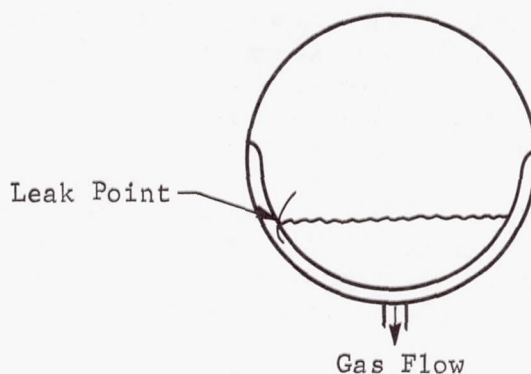


Fig. V-13 Determination of Leak Point during Drain

At the completion of liquid flow, a scale reading was taken and gas flow continued. Tipping the tank did not reestablish the liquid flow and all indications were that the tank was empty. Since all liquid drained through the leak, the indication was that the leak was in the gas inlet port area.

A decontamination process was initiated that consisted of placing the tank in an oven at 200°F. A gas ejector was connected to the tank gas port to hold the diaphragm in place and a tube was inserted approximately 6 in. into the liquid side port and a gaseous nitrogen purge was maintained. After two days of baking and purging, the contamination level was at 11 ppm and no further decrease could be noted. At this time decontamination was terminated.

Additional X-ray pictures were then taken and a borescope inspection was attempted. A clear picture of the diaphragm was obtained indicating that the diaphragm was not in contact with the dome in the area of the diaphragm seal. The borescope inspection was unsuccessful because the light was inadequate to get a clear image and the instrument could not be placed close enough to the inside surface to obtain any detail.

The oxidizer tank was sectioned through the weld joining the tank hemispheres so the diaphragm could be removed in one piece. The diaphragm retainer ring did not separate from the sectioned tank as expected, and as a result some diaphragm damage was incurred near the seal when removing it.



A leak test of the diaphragm after removal disclosed a leak at the apex of the hemisphere and another near the seal. The leak near the seal may have been incurred when the diaphragm was removed from the tank. The leak at the apex, shown in Fig. V-14, was identified before the tank was sectioned. The failure of the diaphragm at the apex is attributed to a high stress concentration imposed at the failure point because of the sudden change in cross-section area at that point (Fig. V-15). The original design called for a gentle taper over the cross section area change, however, it was not provided in the finished part.

Creases in the removed diaphragm shown in Fig. V-14, V-16, and V-17, while not desirable did not disclose any leakage. The creases resulted from a slightly oversized hemispherical diaphragm with respect to the hemispherical tank internal dimensions. In addition to providing potential leakage points in the diaphragm, these creases also create voids between the diaphragm and tank wall that provide additional gas side volume for propellant permeation. Future diaphragms of this type should be designed so that a small amount of stretch is required to prevent accumulation of material and subsequent creases. TFE-FEP diaphragms may be stretched up to 2% before the material begins to yield. The diaphragm design stretch must be considered for the worst case during sterilization and the tank wall growth must also be considered.

This failure resulted in further investigation of the diaphragm permeation mechanism and the affect of diaphragm leakage on other sterilization program objectives.

The main concern presented by diaphragm leakage is insufficient oxidizer to complete the planned 280-sec hot fire demonstration. Oxidizer depletion could cause engine shutdown in a fuel-rich condition. This would not be detrimental to the engine but would cut the hot fire demonstration short.

The diaphragm was to be positioned at the bottom of the tank with the propellant hydrostatic head maintaining it in intimate contact with the tank wall. This would prevent diaphragm flexing during system sterilization, thereby extending its useful life. If the diaphragm leaks, this positioning would be unsatisfactory because the propellant transferred to the gas side would not provide the expulsion efficiency required for successful system operation. The problem is trapping of usable propellant on the gas side during expulsion.

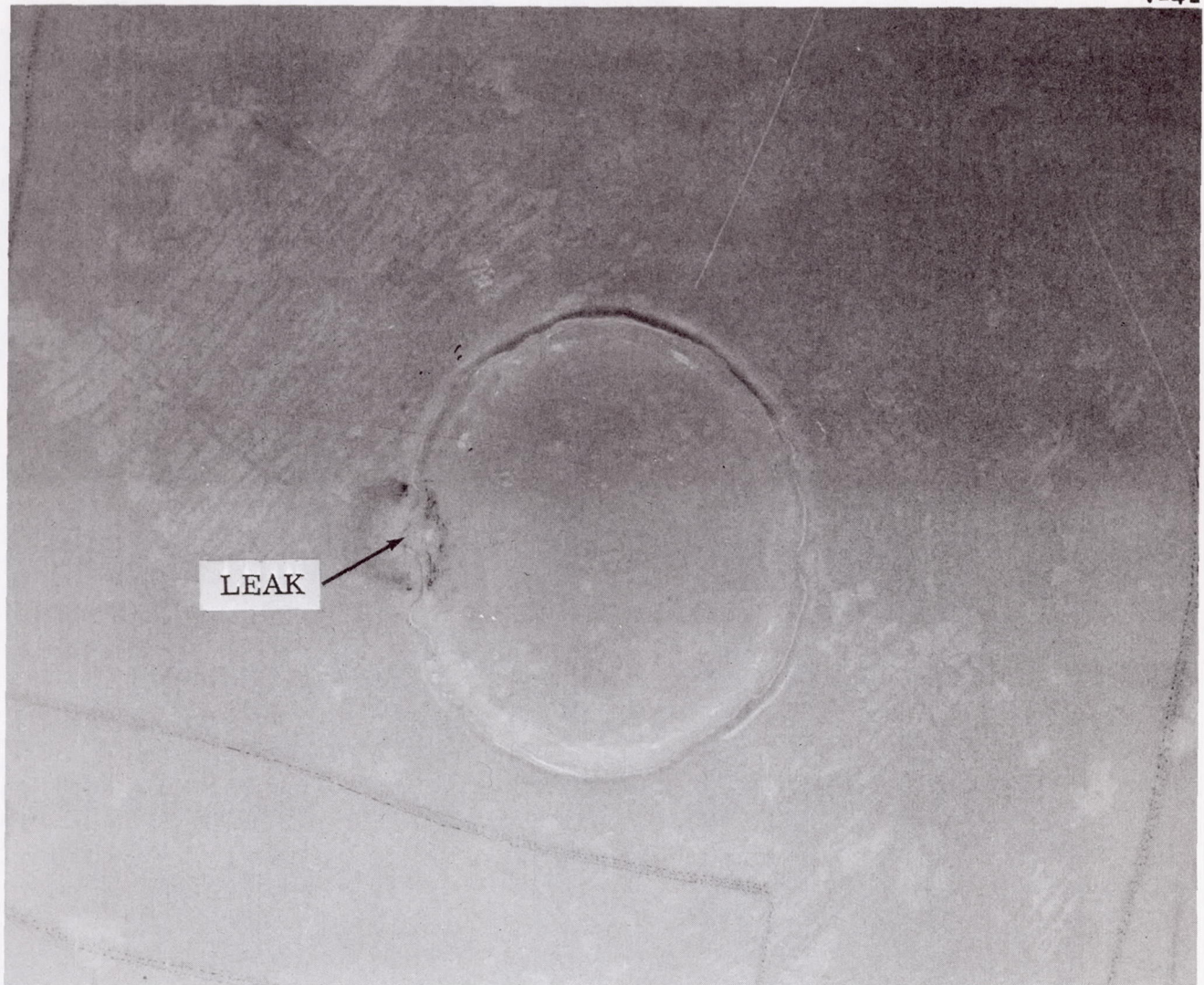


Fig. V-14 Diaphragm Apex Patch

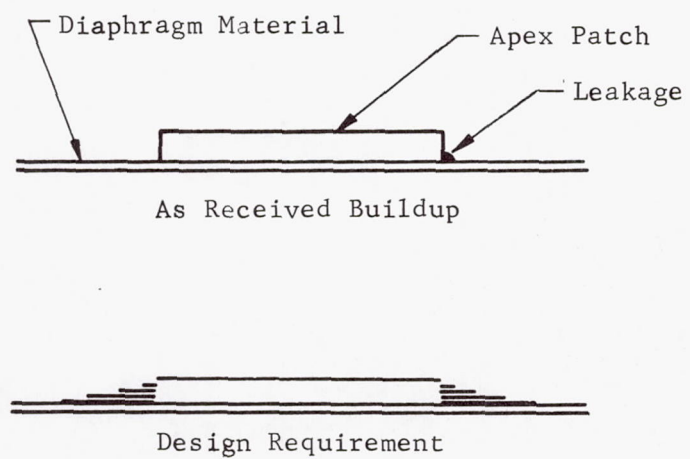


Fig. V-15 Diaphragm Apex Patch



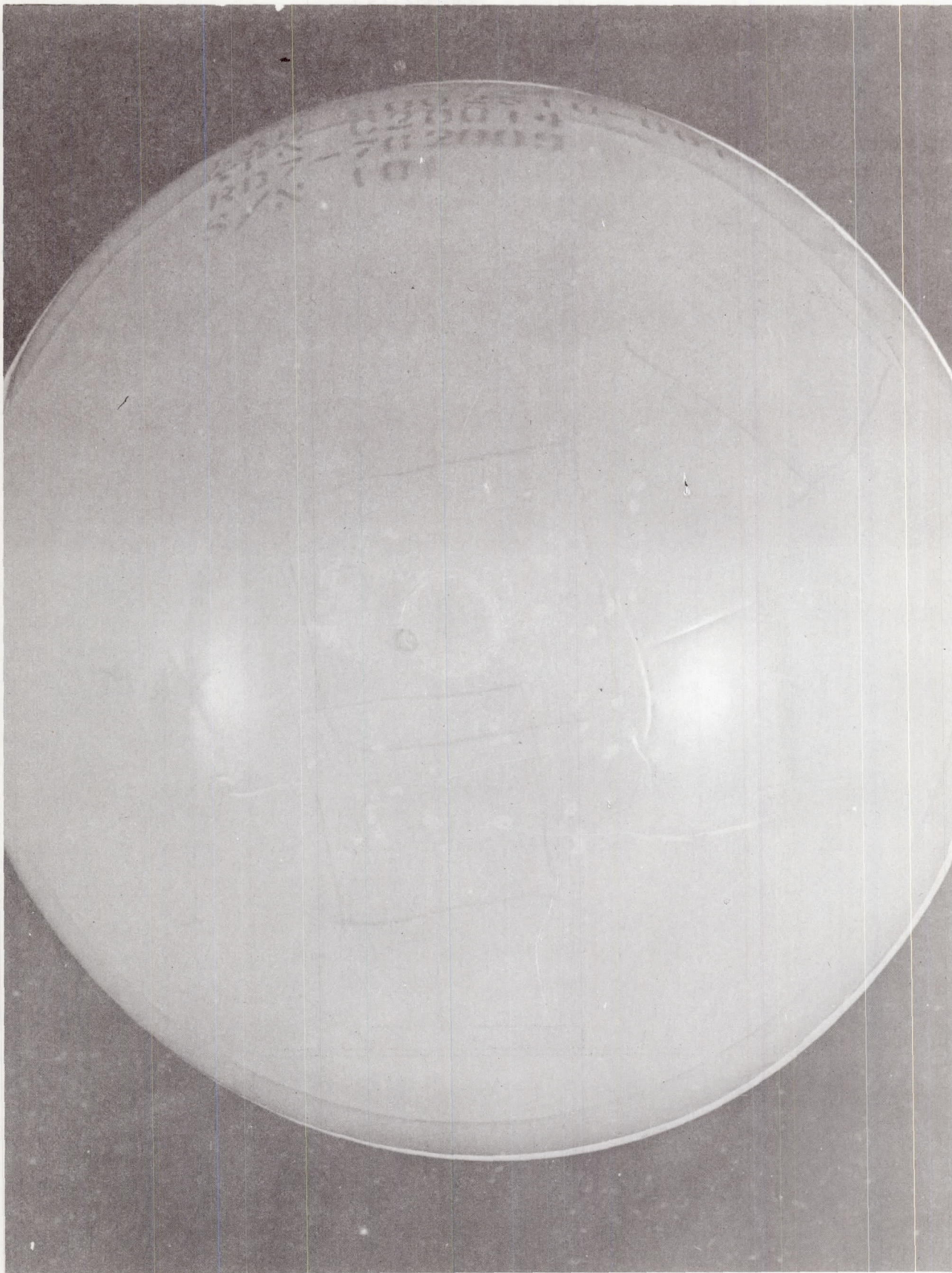
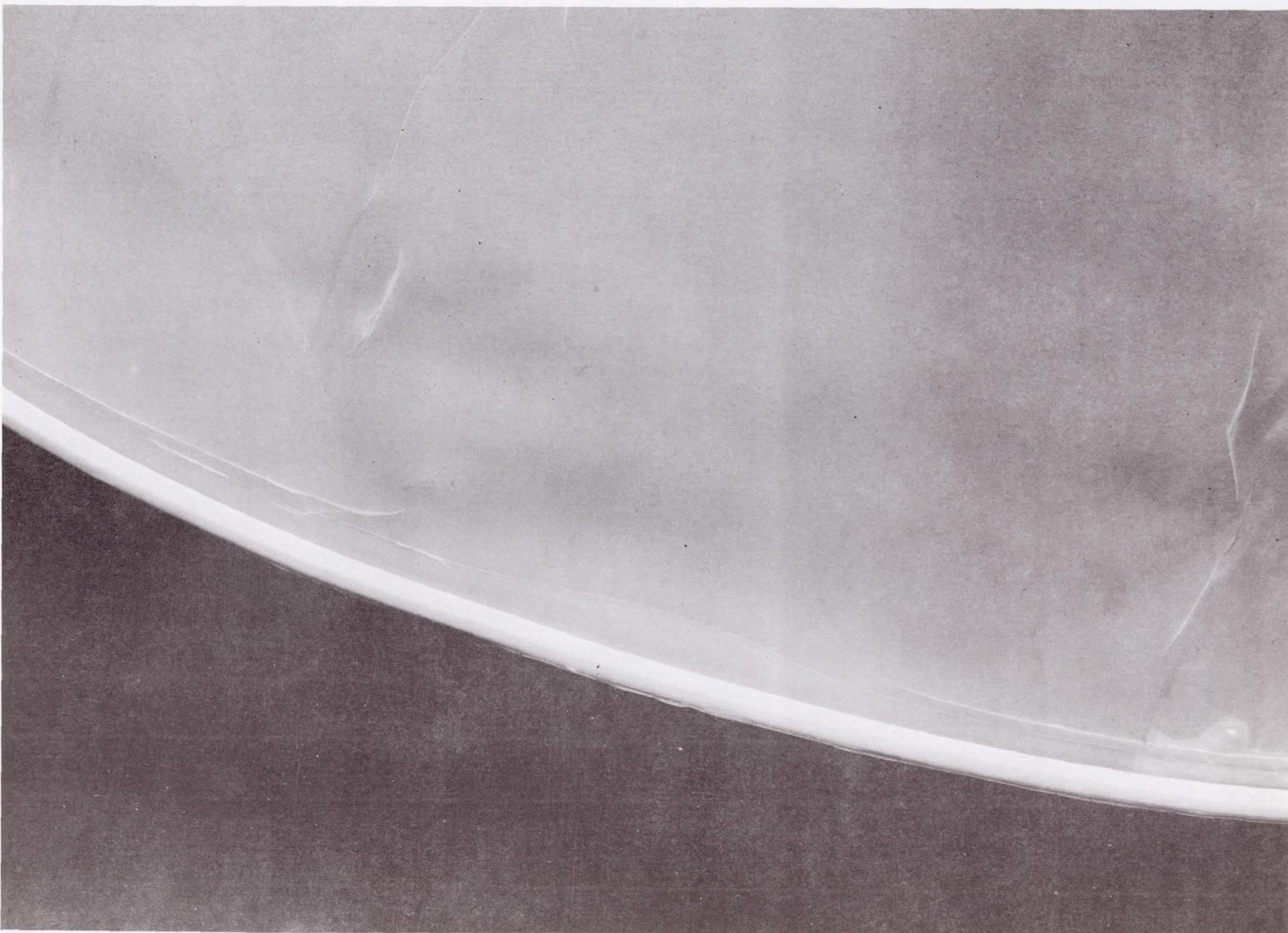


Fig. V-16 Oxidizer Tank Diaphragm





MCR-68-119

V-43

Fig. V-17 Oxidizer Tank Diaphragm Seal Area



Teflon permeation to  $N_2O_4$  liquid and vapor was reviewed to assure complete understanding of the permeation mechanism and the effect of permeation on the containment of the liquid propellant during the sterilization cycle.

In a crack-free diaphragm that has no pin holes, the mechanism of permeation occurs in three distinct steps:

- 1) Solution of permeant into diaphragm - The permeant dissolves into the permeable Teflon membrane on the side of its higher concentration. High absorption of  $N_2O_4$  into the Teflon is evidenced by swelling of the membrane;
- 2) Diffusion of permeant through the membrane - The permeant diffuses through the membrane to the side of lower concentration. (The process depends on the formation of "holes" in the plastic network due to thermal agitation of the chain segments.);
- 3) Evaporation on the low concentration side of the membrane - The permeant emerges as vapor due to evaporation on the low concentration side of the membrane.

Generalization of permeation by activated diffusion is governed as follows:

- 1) Permeation rate increases exponentially with temperature;
- 2) Permeation is essentially independent of hydrostatic pressure;
- 3) Materials of the same molecular size that wet the membrane permeate at a higher rate;
- 4) Once nitrogen tetroxide is absorbed in the Teflon membrane, the diffusion through the lattice is molecular in nature;
- 5) The driving force required for permeation to occur is the differential partial pressure, gas pressure, or vapor pressure (different mole concentration) between the two environments separated by the membrane.

In contrast to permeation by activated diffusion, the mechanism of permeation through porous materials does not cause the permeating molecule to change from undissolved to dissolved and does not form transient holes in its passage. Further, small pin holes or cracks in the membrane result in liquid leakage, which is completely unacceptable.

Because of the diaphragm leak, its position during sterilization as affected by leakage and the risk to program completion were reevaluated. The analysis indicates that the tank diaphragm with potential leakage points should be sterilized in an upward position to prevent an unacceptable amount of propellant from transferring to the tank pressurant side. Further, with a diaphragm sterilized in the upward position, the amount of flexing due to thermal cycling can be a maximum of approximately 6.5 in. in amplitude, which would be an acceptable condition for a 8.25-in.-radius hemispherical diaphragm.

The positioning of the diaphragm in the propellant tank during sterilization becomes critical under certain conditions. To evaluate the most desirable position, the effect of various pertinent conditions were investigated. These conditions are presented in Table V-9. The items noted by 1 and 2 are desirable; 3, 4, and 5 are undesirable; and 6 and 7 are unacceptable for diaphragm positioning during sterilizations.

The tank assembly for the system demonstration test contains a leaking diaphragm and has a small tank outlet volume. For these conditions, Table V-9 shows that sterilization with the diaphragm in the bottom of the tank would be unacceptable. If the diaphragm were positioned in the top of the tank, the result of the sterilization would be acceptable.

Calculations for the existing oxidizer tank assembly having a small tank outlet volume of approximately 1.548 cu in. supporting the above evaluation are presented in Appendix B. In addition, Appendix C presents calculations of propellant level and ullage during sterilization.



Table V-9 Diaphragm Positions

Diaphragm Position	Conditions (tank outlet volume includes voids between diaphragm and tank wall)	Expected Result
Top of Tank	Leak in diaphragm	
	Large tank outlet volume	3 5
	Small tank outlet volume	3 5
	Zero tank outlet volume	2
	No leak in diaphragm	
	Large tank outlet volume	3 4
	Small tank outlet volume	1
	Zero tank outlet volume	2
Bottom of Tank	Leak in diaphragm	
	Large tank outlet volume	6 7
	Small tank outlet volume	6 7
	Zero tank outlet volume	2
	No leak in diaphragm	
	Large tank outlet volume	7
	Small tank outlet volume	2 4
	Zero tank outlet volume	2
<u>Code:</u> <ol style="list-style-type: none"> <li>1 Minimum (maximum of 2 in.) amplitude diaphragm flex for each heat cycle.</li> <li>2 Negligible diaphragm movement.</li> <li>3 Large (maximum of 6.5 in.) amplitude diaphragm flex for each heat cycle.</li> <li>4 Overall tank heat rate sensitive.</li> <li>5 Uncertainty in position of leak and amount of propellant transfer to pressurant side.</li> <li>6 Excessive propellant on gas side after sterilization.</li> <li>7 Flex of diaphragm and entrapment of vapor bubble below seal.</li> </ol>		

Diaphragm flexing will occur depending on the tank heat input rate and distribution. Considering a diaphragm leaking at the apex of the hemisphere with the diaphragm positioned in the tank bottom, propellant will leak under the hydrostatic head of approximately 1 psi filling the pressure side tank outlet volume. The tank outlet volume is approximately 1.548 cu in. If the heat input is assumed to reach the propellant in the outlet (a worst-case condition during the sterilization heat cycle) before the propellant side is affected the propellant on the pressurant side will heat to 275°F with a resulting vapor pressure of ~800 psia. Under these conditions, the liquid previously at 70°F equivalent to 0.08 lb<sub>m</sub> [see Fig. V-18(a)] would expand and vaporize resulting a large gas bubble that would separate the diaphragm from the wall.

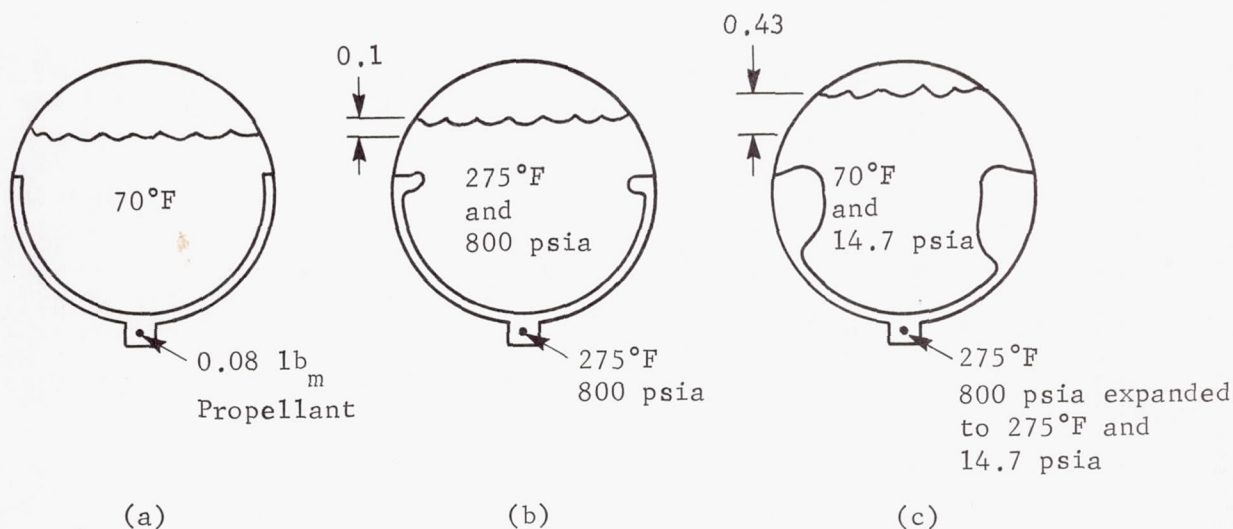


Fig. V-18 Oxidizer Tank Diaphragm Configurations and Propellant Heights during Sterilization

Figure V-18(b) shows 0.08 lb<sub>m</sub> of N<sub>2</sub>O<sub>4</sub> at 275°F and 800 psia would occupy  $\frac{0.08 \text{ lb}}{9.3 \text{ lb/cu ft}} = 0.008 \text{ ft}^3$  of space or 13.8 cu in., thereby raising the liquid level approximately 0.1 in. This amount of gas, if it occupied an annulus below the seal at the tank O.D. having a height of 1.0 in. would be approximately 0.8 in. wide or would separate the diaphragm 0.8 in. from the tank wall just below the seal. If the bulk temperature of the propellant remains at 70°F and 14.7 psia while the propellant in the pressurant side outlet volume is heated to 275°F, the 13.8 cu in.



of vapor at 800 psia would expand to 75 cu in. if the final vapor pressure were 14.7 psia. Expansion to 14.7 psia would cause the liquid level to rise approximately 0.43 in. [see Fig. V-18(c)].

Further, as the gas rises from the pressurant side outlet volume, more propellant will leak into this cavity continually increasing the propellant quantity on the pressurant side until an equilibrium condition is reached.

If the tank were sterilized in the upright configuration, i.e., the diaphragm in the top of the tank, the vapor that would leak through or permeate the diaphragm during equilibrium conditions at 275°F would amount to approximately 0.0083 lb<sub>m</sub>. If this quantity were expanded to 275°F and 800 psia, a condition would exist in which the diaphragm would be pushed away from the top of the tank wall by less than 1 in.

Various conditions of volume due to permeation and leakage as a function of diaphragm position are presented in Table V-10.

Table V-10 Volume due to Permeation and Leakage as a Function of Diaphragm Position

Diaphragm Position	Propellant			Volume @ 800 psia and 275°F (cu in.)	Volume Expanded to 14.7 psia and 70°F (cu in.)	Volume Expanded to 14.7 psia and 275°F (cu in.)
	Propellant State	Weight (lb <sub>m</sub> )	Temperature (°F)			
Top of Tank	Permeated or leaked vapor	0.008	275	1.548 Vapor	21.6 Vapor	84.5 Vapor
Bottom of Tank	Propellant Leak Liquid	0.080	70	1.548 Liquid	13.8 Liquid	75.0 Vapor
Nonleak Diaphragm Bottom	Permeated Vapor	0.008	275	1.548 Vapor	21.6 Vapor	84.5 Vapor

b. Fuel Tank

The fuel tank poststerilization functional test consisted of an expulsion test at -1 g conditions and an external leakage test. Inasmuch as the fuel tank had been subjected to sterilization testing in the inverted position, a partial expulsion was first made in the +1 g orientation to fill the propellant trap. Subsequent attempts to perform -1 g expulsions resulted in expulsion of only a portion of the capacity of the trap. Furthermore, the effluent was a mixture of gas and liquid throughout the expulsion sequence. The quantity of fuel expelled during the various expulsion attempts responded to the method used to fill the trap. Since the intent of the poststerilization functional test was to assess heat-induced degradation, the results shown in Table V-2 represent the expulsions associated with the most effective trap filling technique. The 0.96-lb quantity expelled at -1 g conditions was demonstrated after the tank had been in the -1 g attitude for about 16 hr. Completely gas-free flow was not attained in any of the several -1 g expulsion tests.

A sample of the MMH fuel was taken from the fuel tank test item after about half of the 50-lb load had been expelled. The laboratory analysis, shown in Table V-11 indicated that no significant degradation of the fuel had taken place. The fuel was still water-white at the end of the Phase II sterilization testing, indicating that no oxidation had taken place and the slight increase in vapor pressure observed during sterilization was minor.

Table V-11 MMH Gas Chromatograph Analysis Results

Component	Volume Fraction (%)
Monomethyl Hydrazine	98.95
Nitrogen	0.12
Ammonia	0.09
Water	0.70
Unknown	0.14
<u>Note:</u> MMH from the Task II fuel tank after sterilization, LAB Report 67B2123.	



After the initial attempts to obtain single-phase liquid flow under -1 g conditions, a short test program was initiated to accomplish two objectives. The first objective was to establish a tank fill technique which would assure filling of the trap so that -1 g operation of the trap could be determined exclusive of sterilization effects. The second objective was to demonstrate initiation of positive 1 g outflow without gas entrainment to assure proper engine operation during the module firing.

The tank had been filled initially by evacuating the tank in the upright position and allowing fuel to fill through the outlet port. This resulted in some fuel vapor caused by fuel flashing into the vacuum. Load was determined by checking the weight of the source vessel during tank fill. At the completion of fill only propellant liquid and vapor were in the tank, resulting in a tank pressure of approximately 2 psia under ambient conditions. This technique could result in fuel vapor being held in the trap with consequent trap performance degradation. The second technique used for filling involved overfill of the tank and subsequent drain back to the proper load. This sequence was accomplished by filling the tank under a 1 atmosphere blanket of nitrogen in the upright position until the tank was completely filled, i.e., liquid fuel flowed from the gas inlet port. At this time the tank was inverted and liquid was flowed into the gas inlet port until all bubbles from the liquid outlet port were removed. The tank was then rotated to the upright position and nitrogen was introduced at the gas inlet port to drain back to the correct load. The quantity drained was collected in a receiver vessel on a scale to determine proper drain back. As a check, the propellant tank was weighed when empty and again after fill. The desired load was 51.03 lb and the amount loaded was 50.70 lb which is well within the loading accuracy required.

Under this load condition the tank was outflowed in the upright position and flow was observed in a sight glass. No gas flow was noted and after a flow of approximately 10 lb of fuel the tank was inverted and -1 g outflow was attempted. Again a two-phase mixture was expelled with almost the same total liquid weight that had been expelled using the vacuum loading technique.

As a result of the special testing accomplished on the fuel tank during the completion of Phase II, it was decided that the overfill loading technique would be used on the module fuel tank. In this way single phase liquid outflow to the engine will be assured even though -1 g outflow will not be attempted as a part of the firing sequence.

Upon completion of the expulsion tests, the fuel tank was decontaminated and then cut in two at the girth weld. After cleaning, the lower half containing the screen trap (Fig. V-19), was subjected to a leak and bubble test. The weld joint proved to be intact and the first leak appeared at the outer row of rivets, where the titanium is riveted to the stainless steel trap (see arrows, Fig. V-20). This leak started at 5 in. of  $H_2O$  pressure. The screen started bubbling at 8 in. of  $H_2O$  pressure at the sand-wich connection edge and through the screen.

The screen trap was then separated from the tank half and a hole drilled in the upper plate to permit gas pressure injection. The trap unit was then subjected to a bubble check. Leaks started at the closure plate riveted connection (Fig. V-3) at  $1\frac{1}{2}$  in. of  $H_2O$  pressure.

The above test indicates that the screen trap was functioning properly although the bubble point was lower than when installed; therefore, some other factor was responsible for the two-phase flow indicated earlier.

An examination of the trap and tank assembly indicated that there was a suspect area, namely, the flow area between the smaller diameter base of the cone frustum and the tank wall. It appears that on fabrication, this area was smaller than had been anticipated due to shop tolerances. If this area should provide a restriction in excess of the bubble point of the trap closure plate rivets ( $1\frac{1}{2}$  in. of  $H_2O$ ) then the two-phase flow would indeed occur.

To test this theory, accurate measurements were made of the tank and trap (see Appendix A) and calculation showed that the pressure drop at rated flow was equivalent to 2.663 in. of  $H_2O$  pressure. Therefore, two-phase flow would occur due to a breakdown of the trap at the closure plate rivets.

## 2. Pressure Regulator

The results of the poststerilization tests on the pressure regulator showed that the regulation characteristics were substantially the same as those exhibited at the midsterilization point, i.e., the regulation band was approximately 15 psig below the specification value. This indicated that the shift in regulation band that occurred during the first set of six sterilization cycles did not progress measurably during the second six cycles. The internal leakage of the regulator had increased by a factor of four over the results obtained during the midsterilization functional test. The leakage rate did not change after exercising the regulator.



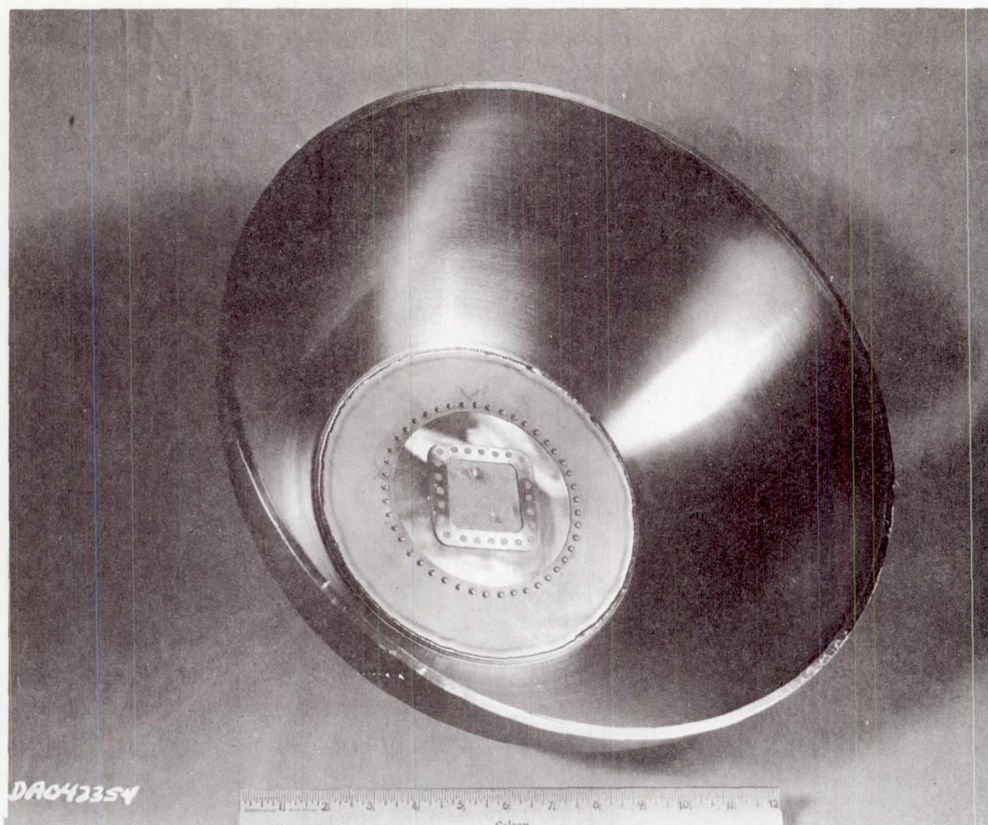


Fig. V-19 Fuel Tank Screen Trap Assembly

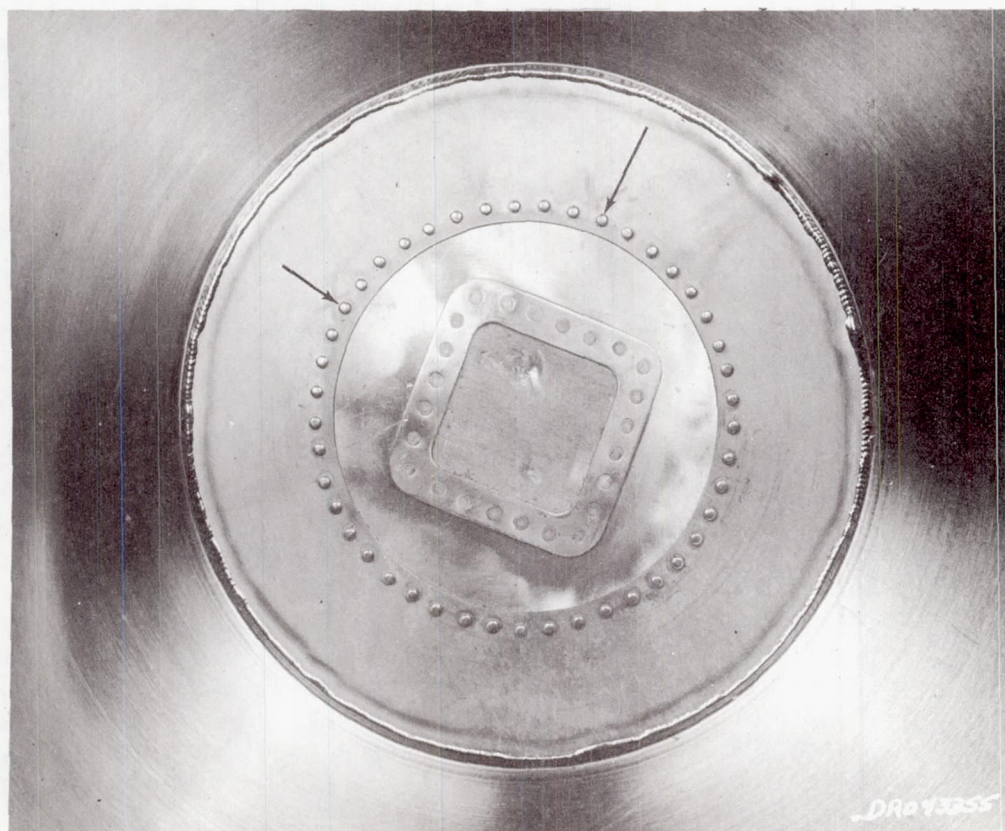


Fig. V-20 Fuel Tank Screen Trap Leakage Points

Tear down of the unit started at the square flange holding the inlet tube and filter to the main body. The four screws required very low torque to loosen (approximately 5-in.-lb).

The filter, Fig. V-21, showed some accumulation of dirt on the upstream side, but this was not excessive.

The area inside the unit in the vicinity of the poppet was heavily coated with moisture.

The tungsten carbide ball poppet, Fig. V-22, was coated with oxide. The contact area of the stainless steel poppet seat was bright as were the sliding areas along the poppet guide. Several other bright areas (see arrows) around the seat contact indicated a probable contaminant rubbing of the oxide coat. No contaminants could be seen in the seat area at this time.

The low torque required to loosen the square flange holding screws indicates a relaxation of the holding force during sterilization cycling. This was probably the cause of the external leak at this point in the poststerilization testing. It is recommended that future designs incorporate an increased number of holding screws to six or eight, and/or change the hard seat cone seal to a flat flange with a spring-loaded metallic seal (K-type seal).

The presence of moisture inside the unit and the bright spots along the poppet seat contact indicates that contaminants could have damaged the body seat and are responsible for the higher internal leak. Future designs may consider a downstream filter to trap back flow contaminants and/or exercise care in system blow-down procedure to assure complete pressure relief on the downstream side.

A corrective action for the shift in pressure band is discussed in Section A of this chapter.



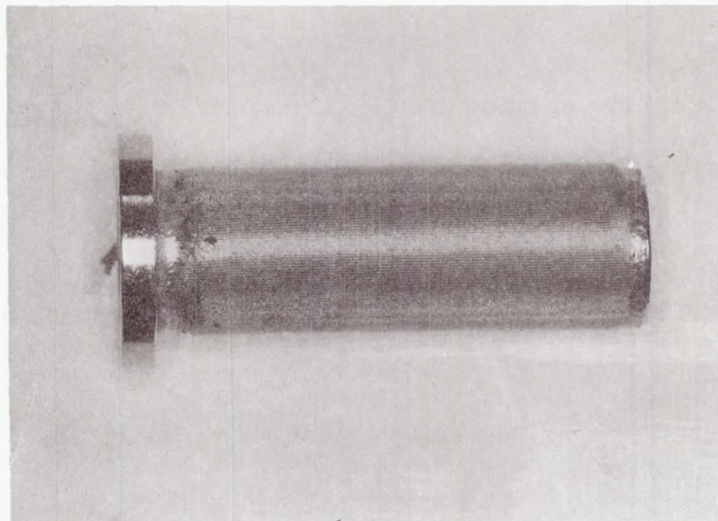


Fig. V-21 Regulator Internal Filter

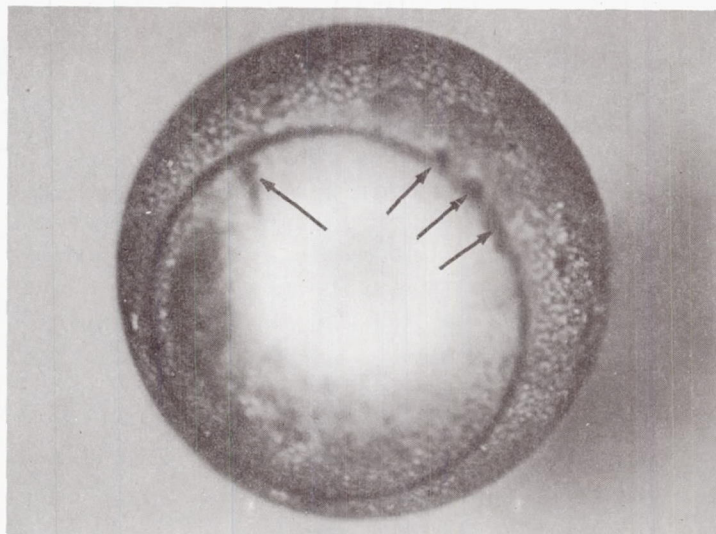


Fig. V-22 Regulator Poppet Ball

### 3. Solenoid Valve

There was no measurable change in the performance of the solenoid valve; however, the dielectric strength of the solenoid coil showed degradation during the last six heat sterilization cycles. Moisture may have had condensed inside the potted area since the valve is not hermetically sealed. To check this theory the unit was placed in a vacuum oven at a pressure of 24 in. of Hg below local ambient and a temperature of 250°F for a total period of 32 hr. After cooling down to room temperature, the unit still indicated about 22 microamps to 500 vac. It was then discovered that the measuring instrument was in error. A small circuit breaker in the instrument was opening at 22 microamps and the instrument could not read above this point. The unit was then retested on a hi-pot-type instrument. This test shows approximately 500 microamps leakage current at 500 vac, as shown in Table V-4. This increase in leakage current indicates a very definite degradation in dielectric strength.

The unit was sent to the vendor for disassembly and failure analysis. When tested by the vendor with 500 vdc applied from Pin A or Pin B to case, the insulation resistance was less than 1 megohm. The resistance from Pin A to Pin B (through the coil) was 22 ohms, which is the nominal requirement.

The unit was then disassembled, while measuring the insulation resistance at each step; namely, after connector plate screws were removed, after connector was removed, after potting compound was removed, and after the shell was removed. The insulation resistance and coil resistance remained relatively constant throughout the disassembly process.

The insulation on the outside of the coil winding was charred black (Fig. V-23). The magnet wire used for the coil was No. 27 single Formvar. According to the Bridgeport Insulated Wire Company's catalog, the rated temperature limit for Formvar insulation is 221°F. The varnish used in wet winding the coil, Tri Var No. 116, is also rated at 221°F.

Any future design should be specific in calling out a Teflon-coated wire insulation or some other high temperature-type insulation that is definitely suitable for extended exposure to sterilization temperatures. Coil impregnation, coil wrappings, and potting compounds must also be included in this high temperature category.





Fig. V-23 Solenoid Valve Coil

#### 4. Filter

There was no measurable change in the flow characteristics of the filter, as shown in Table V-5. Pressure drop through the filter at design flow rate remained at zero (no measurable pressure drop using a differential pressure transducer having a range of 0 to 5 psi).

Following the flow capacity tests, the unit was subjected to a bubble point check. With  $\text{GN}_2$  pressure applied at the inlet side and the outlet wetted and covered with methanol, the bubble point was between 17.25 and 17.5 in. of  $\text{H}_2\text{O}$ . This shows a degradation from the acceptance test figures that were between 22 and 24.2 in. of  $\text{H}_2\text{O}$ . However, this is still within the acceptable range since the minimum specification bubble point for this filter weave is 15.9 in. of  $\text{H}_2\text{O}$ . Future designs should incorporate an allowance in the acceptance test to allow for some degradation.

The unit was cut open (Fig. V-24) and examined. No dirt was evident on the inlet side and no separation was visible along the welded joints or on the screen surface.

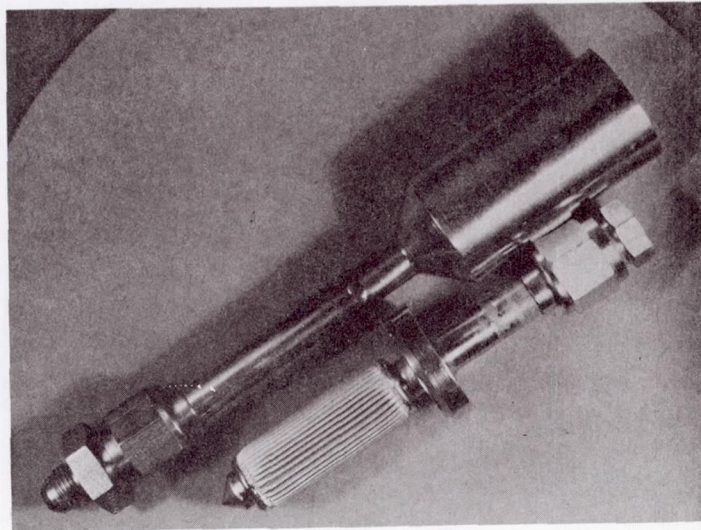


Fig. V-24 Component Test Filter Disassembly

#### 5. Hand Shutoff Valve

The hand shutoff valve continued to leak internally at the limiting torque value of 10 in.-lb used throughout the test. However, at the conclusion of all sterilization testing, the valve exhibited zero internal leakage (zero cc in 15 minutes) when the stem was torqued closed to 16 to 17 in.-lb. The valve should therefore be judged satisfactory from the standpoint of shutoff capability.

The external leakage at the conclusion of the sterilization test was substantially unchanged from that observed at the mid-sterilization point, being in the neighborhood of  $1 \times 10^{-5}$  scc/sec of helium. The leakage was noted at the bonnet cap, indicating that both the stem packing and the bonnet cap seal were leaking. Maximum allowable leakage is specified at  $1 \times 10^{-8}$  scc/sec of helium at 935 psig.

Disassembly of the valve, Fig. V-25 disclosed a very heavy coating of white, powdery, aluminum oxide on the exposed portion of the poppet. This was most severe on the 1100-0 poppet nose (Fig. V-26). The oxidation of the anodized body was very slight.



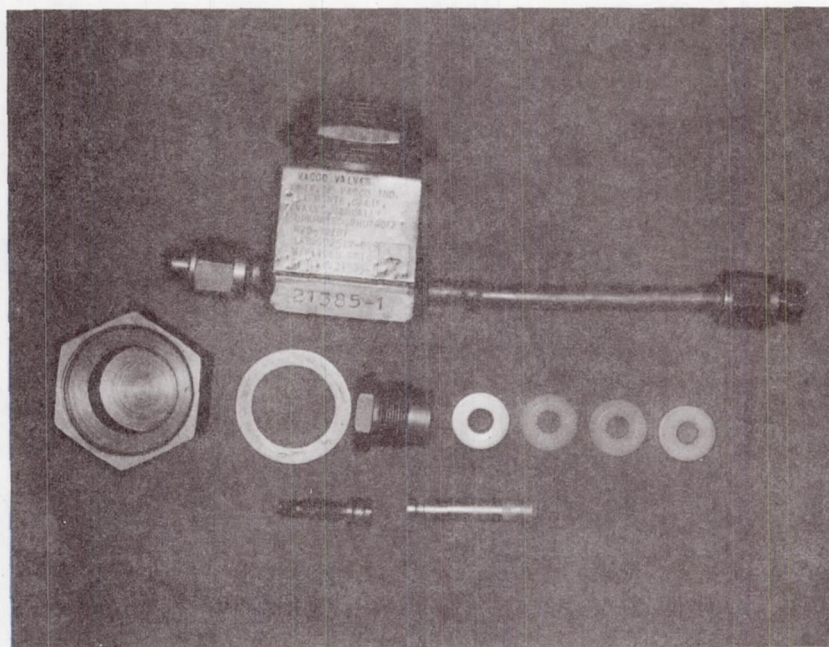


Fig. V-25 Hand Valve Disassembly

The stem chevron Teflon packing showed considerable extrusion between the stem and the backup washer (Fig. V-27). The stem measured 0.2476 in. in diameter in the region covered by the chevron packing, and the backup washer was 0.2815 in. at the inner diameter. This left a diameter clearance of 0.0339 in.

The heavy oxide coating was anticipated because material tests did show reaction between aluminum alloys and the oxidizer at sterilization temperatures. Future designs should consider all-titanium construction with a bellows-type stem seal.

The Teflon packing extrusion could have caused the external leakage reported in the poststerilization test results by permitting a relaxation of the sealing force. The diametral clearance between stem and washer is excessive and future tests could determine maximum clearance versus gland nut torque over extended periods at sterilization temperatures.

A program was initiated to improve the stem cap seal [Fig. V-28(a)], since some leakage of the Teflon stem packing must be expected with operation. As a first step the 1100 aluminum alloy gaskets were annealed to the soft condition (1100-0) and maximum allowable torque was applied to the cap. The test unit still leaked under these conditions. Examination of the unit indicated a combination of effects were probably preventing the use of a metallic seal. Surface finish on the valve body and inside the cap along with out-of-parallel seal surfaces were the main contributors.

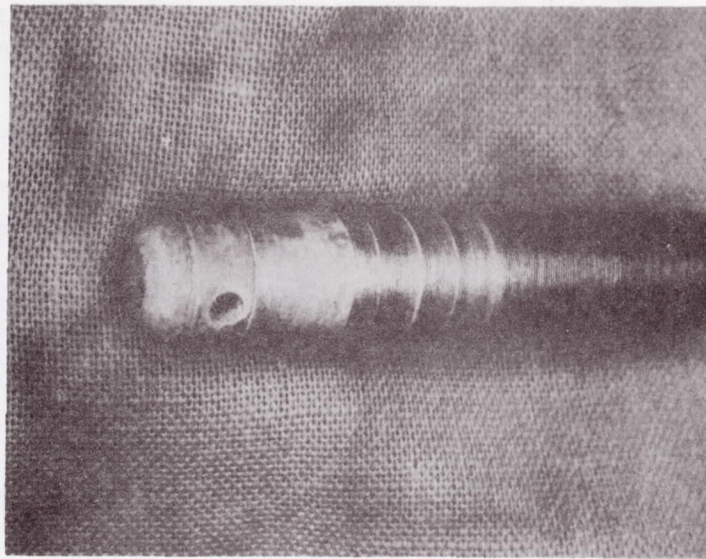


Fig. V-26 Hand Valve Poppet

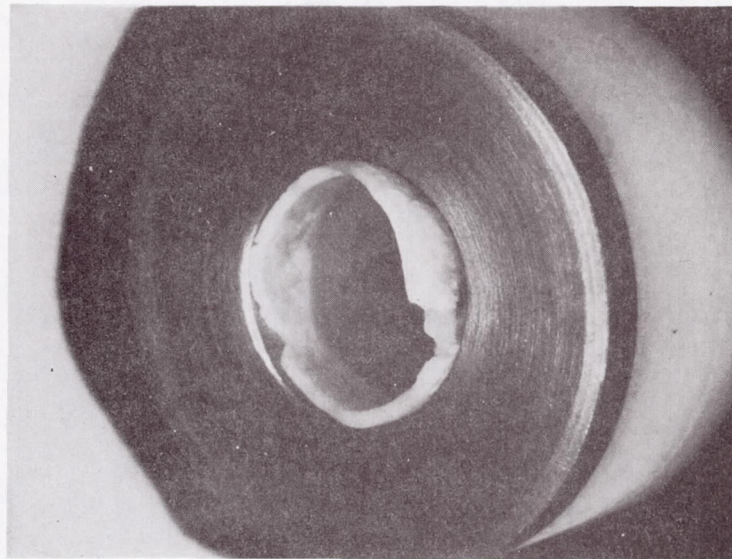
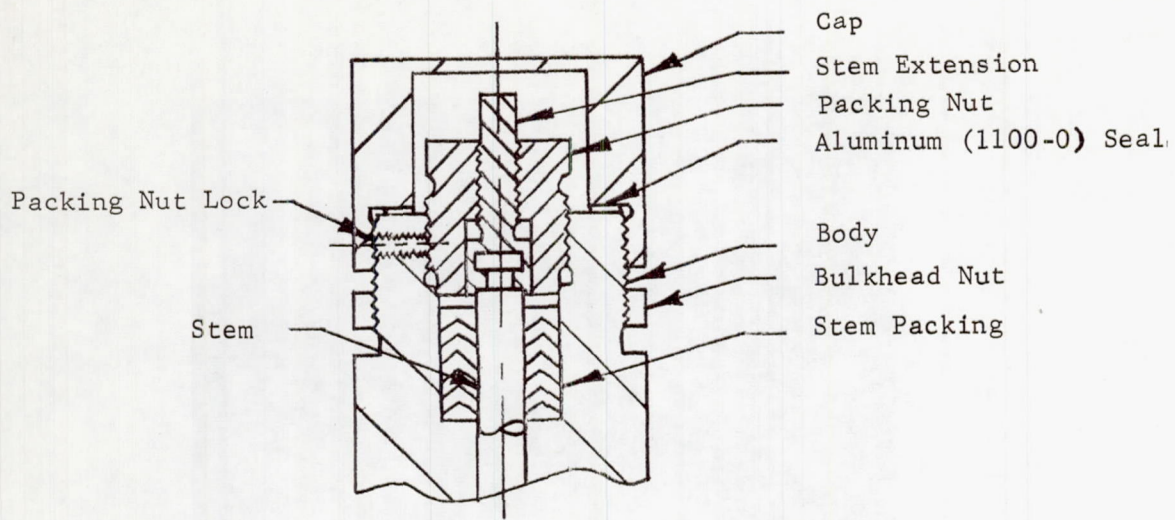
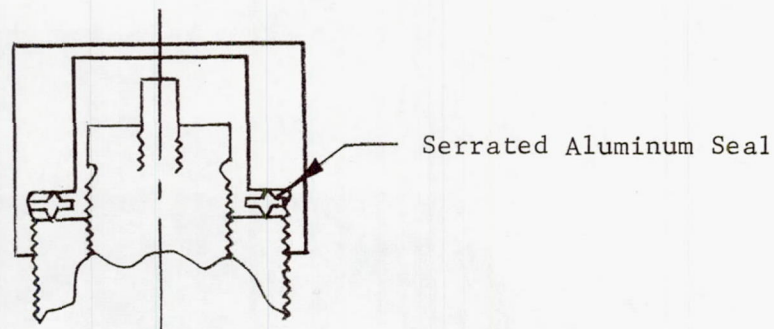


Fig. V-27 Hand Valve Stem Seal Chevrons

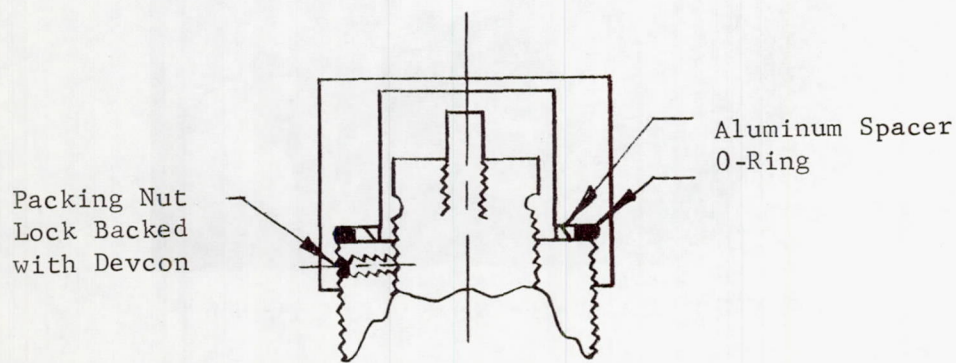




(a)



(b)



(c)

Fig. V-28 Hand Valve Stem Cap Seal Configurations

The valve was reassembled using thin (0.010 in.) Teflon gaskets on each surface of the soft aluminum gasket. Although leakage was decreased considerably, it was not eliminated. In addition the Teflon sheet was extruded from between the aluminum washer and the valve body and the valve cap. This extrusion process would probably continue until virtually no Teflon remained between the metal surfaces. At that time the seal loading would be equal to the compressive yield strength of the Teflon. With heating and cooling, this seal load would be reduced until the seal would be ineffective.

Two other approaches were tried as shown in Fig. V-28(b) and (c). Soft aluminum seals with single and double serrations and a combination O-ring and aluminum spacer ring were used. The aluminum seals with serrations did not solve the problem because of the surface finishes involved. The combination O-ring and spacer ring, however, proved to be tight under hand torques. Several installations were tried in two different test units with no leakage detected in either case. The valves were soaked in an oven at approximately 250°F for 24 hr, followed by a mass spectrometer leak check using helium at 950 psig. There was no indication of leakage. The Viton rubber O-rings were good for operating temperatures up to 400°F. This material, while not completely compatible with the propellants, resists attack of both oxidizer and fuel. It was decided that the module units would be modified to use the O-ring seal because the stem cap seal is a secondary seal and at worst would see dilute propellant vapors.

An additional problem involved leakage from the stem packing nut lock device, Fig. V-28(c). This locking device consists of a nylon plug backed up by a set screw. During the stem cap seal tests this lock frequently leaked. As a repair for the two valves in test, a Teflon plug was cut and installed with the set screw. The screw was torqued into the body until it was well below the external body threads. The cavity behind (on the outside of) the set screw was packed with Devcon WR. Devcon WR is a suspension of metal particles in an epoxy resin and is generally used as metal patching compound. Although the epoxy resin is probably not compatible with either the fuel or oxidizer, it was used because of this particular application. The area of possible contact is the clearance area between the set screw threads and the valve body. In addition only a dilute mixture of propellant vapor and air trapped in the cap volume would contact the material. Although some degradation might take place at the surface, complete breakdown is not anticipated. This modification proved adequate for the test units and was also added to the module valves.



## 6. Ordnance Valve

There was no change in the performance (i.e., leakage characteristics) of the ordnance valve after exposure to the 12 sterilization cycles. The valve exhibited zero internal and external leakage when checked with the helium mass spectrometer leak detector. Following the leakage tests, the normally-closed portion of the valve was fired open with the same squib which had been exposed to all sterilization tests in the valve. The pressure drop of the valve was then measured at the design conditions for the propulsion module pressurant gas supply at the propellant tanks. Following the flow capacity test, the normally-open section of the valve was fired closed for the final leakage test. Internal leakage was again zero; however, external leakage of helium at the inlet flange mechanical seal had increased from zero to  $7.3 \times 10^{-7}$  scc/sec.

The flanged joint of the unit was disassembled. The three holding screws required considerable torque to loosen. The aluminum gasket showed a good imprint of the circular ridges and was spread out tightly against the body section.

The external leakage indicated at the flange joint during postfiring tests can only be attributed to closing forces of the squib actuator. Future design or application should incorporate a welded tube design as this is the only truly hermetic seal. Attempts to design a hermetic bolted seal always poses problems of differential expansion between dissimilar flanges and seals. In this case an aluminum flange was bolted to a titanium flange with stainless steel machine screws and the seal was aluminum of a different alloy from that of the aluminum flange. Even when similar materials are used, there is a problem of heat sink, and when transient temperatures are involved, there can still be a differential movement unless the masses and exposed areas are exactly alike.

## 7. Thrust Chamber Valves

In general, the performance of the thrust chamber valves was not adversely affected by the sterilization series. A minor deviation was noted in the response time, which increased by 1 to 2 msec, although there was a slight decrease in the pull-in voltage. This would indicate that internal friction had not increased.

## F. RELIABILITY EVALUATION

A reliability estimate was performed on the system. The generic failure rates were based on Martin Marietta data. The calculations were divided into two major phases, launch and cruise, and burn (Table V-12).

The launch and cruise phase has a duration of 6500 hr. Two modes are considered during this phase and are weighed differently. Tanks and associated hardware are considered semi-operational for the entire duration, while the remainder of the system is in a completely dormant mode. A factor of  $0.1 \times G_{FR}$  is applied to the first category, and  $0.01 \times G_{FR}$  for the second.

The burn lasts approximately 300 sec and the standard factor of  $1000 \times G_{FR}$  is applied for this phase.

Review of hardware problems experienced during the component sterilization and test procedures revealed no evidence that any significant degradation of system performance should be assessed to sterilization. The sample size prohibits definite conclusions concerning the dynamic effect of heat sterilization on the system. Instances of material changes were identified and further testing would be required to establish the limits of shift ranges. Additional testing would also be required to validate pertinent fixes prescribed. It appears that solution of the problems documented would exclude these as reliability risks in future operation.



Table V-12 Sterilizable Liquid Propulsion System Reliability Estimate

Components (Quantity)	$G_{FR}/10^6$	Launch and Cruise Phase, 6500 hr	Burn Phase (0.083 hr)	Total Mission	Reliability
Propellant Diaphragm Tank (2)	1.5	.001950	.000246	.002196	.997804
N <sub>2</sub> Storage Tank	0.18	.000117	.000015	.000132	.999868
Press Regulator	0.7	.000046	.000058	.000105	.999895
Filter (3)	0.04	.000008	.000009	.000017	.999983
Ordnance Valve N.C. (5)	1000	--	--	.0050	.995000
Ordnance Valve N.O. (5)	10	--	--	.000050	.999950
Thrust Chamber Valves (2)	2.27	.000295	.000374	.000669	.999331
Orifice Assembly (2)	0.01	.000001	.000002	.000003	.999997
Test Point (7)	0.01	.000046	.000006	.000052	.999948
Lines and Fittings	0.1	.000065	.000008	.000073	.999927
Structure	0.001	--	--	--	.999999
Total System					.991581

## VI. SYSTEM ASSEMBLY AND TEST

### A. SYSTEM FABRICATION AND ASSEMBLY

This phase of the program involved the fabrication, assembly, checkout, and test of the complete propulsion system. Fabrication and assembly were separate steps. Fabrication consisted of building the structural truss (Fig. III-3), component mounting brackets, and other structural pieces. Assembly consisted of the mounting of supplier components on the truss, tubing development, and welding and checkout of the completed system. The assembled module is shown in Fig. VI-1.

During assembly, numerous leak checks were made to avoid any significant disassembly for repair. The leak check criterion was severe for the hermitically sealed portions of the system. The fuel storage system, the oxidizer storage system, and the pressurant gas storage system were leak checked using a helium mass spectrometer. No leak should be greater than  $1 \times 10^{-3}$  scc/sec of helium at each system maximum operating pressure. The leakage criterion for the remainder of the system, which included the propellant feed systems, the engine, and the pressurant gas feed system was less severe. In this case, bubble tightness at maximum operating pressure using gaseous nitrogen was the requirement.

There was no difficulty in making the system leak tight. The functional tests were completed before module sterilization. The baseline functional tests were performed on the module solenoid ( $\text{GN}_2$  loading) valve, the two thrust chamber valves, and the pressure regulator as stipulated in the test plan. The results indicated that the solenoid valve and the thrust chamber valves were performing satisfactorily. The pressure regulator exhibited excessive internal leakage and low pressure regulation. The leakage value was 68 sec/hr of  $\text{GN}_2$  compared to the allowable value of 10 sec/hr. Further, the regulation pressure was 241 to 245 psig compared to the allowable of  $248 \pm 5$  psig. The regulator was returned to the supplier for repair and adjustment so the sterilization exposure would be initiated with the regulation band in the required limits. The supplier's investigation revealed a scratch mark in the regulator valve seat, presumably the result of passage of a foreign particle. The regulator seat was repaired, and the regulation spring was heat-treated at 325°F for 24 hr at its working stress level to obviate the set-point degradation exhibited by the component test regulator.



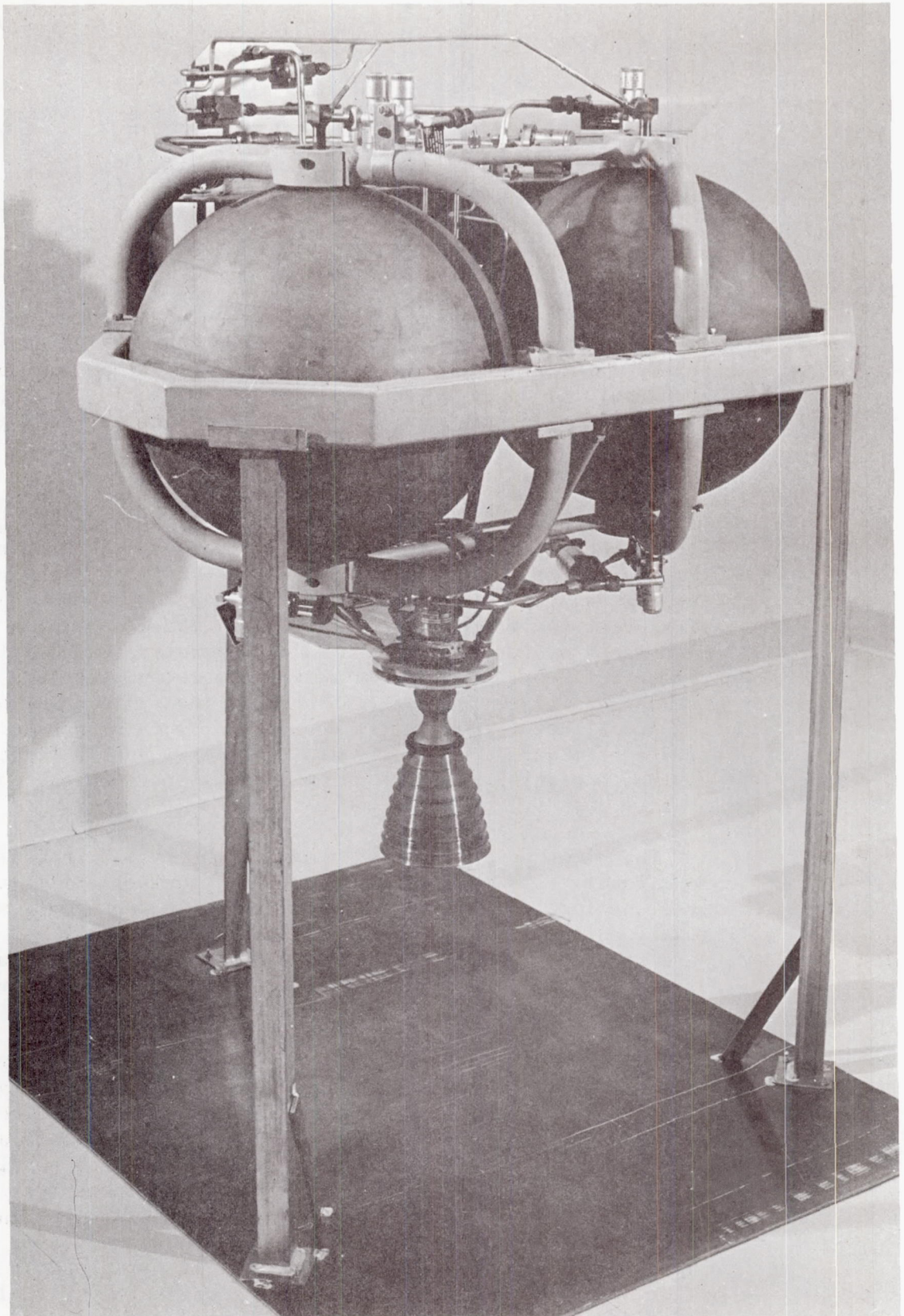


Fig. VI-1 Assembled Propulsion Module

The inlet tube of the repaired regulator was indexed incorrectly. Therefore, the inlet flange and tube assembly were removed in the Class 100 clean room and reinstalled in the correct position. Following installation in the module, the presterilization functional tests were conducted. The results of the functional test showed that the regulation band was within specification limits; however, the internal leakage was again in excess of the allowable leakage (14.5 scc/hr, compared to the allowable 10 scc/hr).

Before the installation and functional test, the facility  $\text{GN}_2$  supply and exhaust interfaces at the module service panel were equipped with 5-micron nominal filters to protect the regulator from contaminant particles in the supply gas and also from possible backflow of effluent  $\text{GN}_2$ .

The performance of the pressure regulator was judged adequate for the desired performance of the module; therefore, no further testing was done.

#### B. SYSTEM TEST FIXTURES

The final proof of success of module sterilization was a system hot firing. In the case of an actual spacecraft, system checkout or functional testing would probably not be possible after sterilization and before system usage. In the case of the test system, assurance was required that critical components were functional before the firing. To accomplish this, special test fixtures were required. Critical components were considered to be the module regulator, the solenoid valve, and the engine thrust chamber valves. Although the system ordnance valves were considered to be critical components, they could not be functionally checked because of their single usage capability.

The test fixture used for the regulator functional test is shown schematically in Fig. VI-2. This system provides an ullage for the regulator to operate on along with all pertinent instrumentation necessary for performance measurement. Gas is introduced upstream of the module line filter, passes through the filter and regulator and exists to the test fixture just downstream of the regulator.



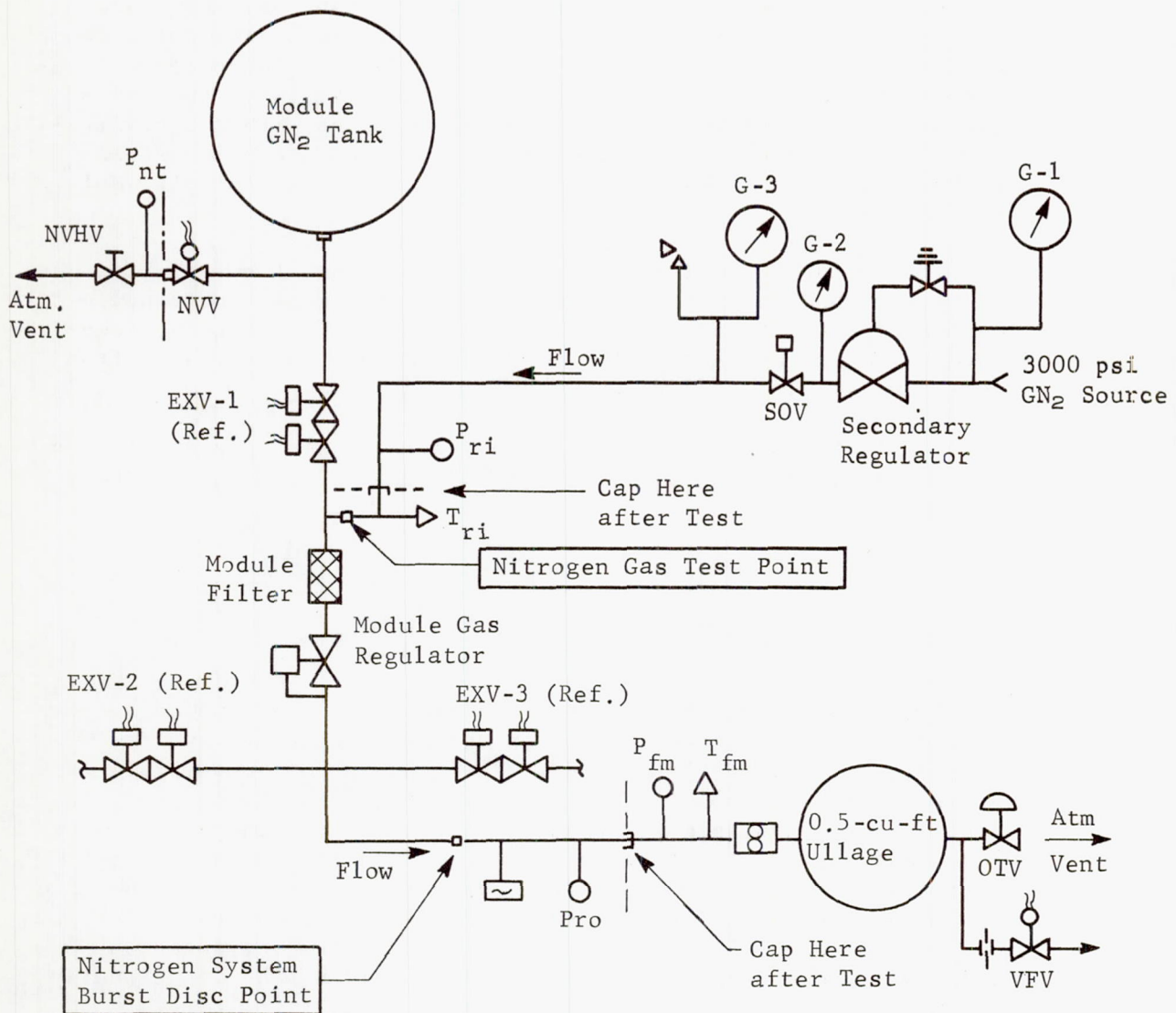


Fig. VI-2 Schematic of Regulator Functional Test

For the solenoid valve the functional test consisted of opening and closing the valve. The solenoid valve is indicated as NVV in Fig. VI-2. With the line hand valve (NVHV) closed the opening of NVV results in nitrogen tank pressure showing on  $P_{nt}$ . NVV was then closed and NVHV opened with  $P_{nt}$  returning to zero.

Functional testing of the thrust chamber valves (Fig. VI-3) involved a response and internal and external leakage test. Nitrogen gas was introduced at 250 psig upstream of each valve and three valve actuations were made. The engine throat plug was then installed, and internal and external leak tests were conducted. External leakage involved bubble checking all joints in the feed systems and thrust chamber valves. Internal leakage consisted of attaching a tube to the engine throat plug and conducting a water displacement test.

After completion of the functional tests, the test fixtures were disconnected from the module ports and the ports were capped. The system was then ready for the firing sequence.



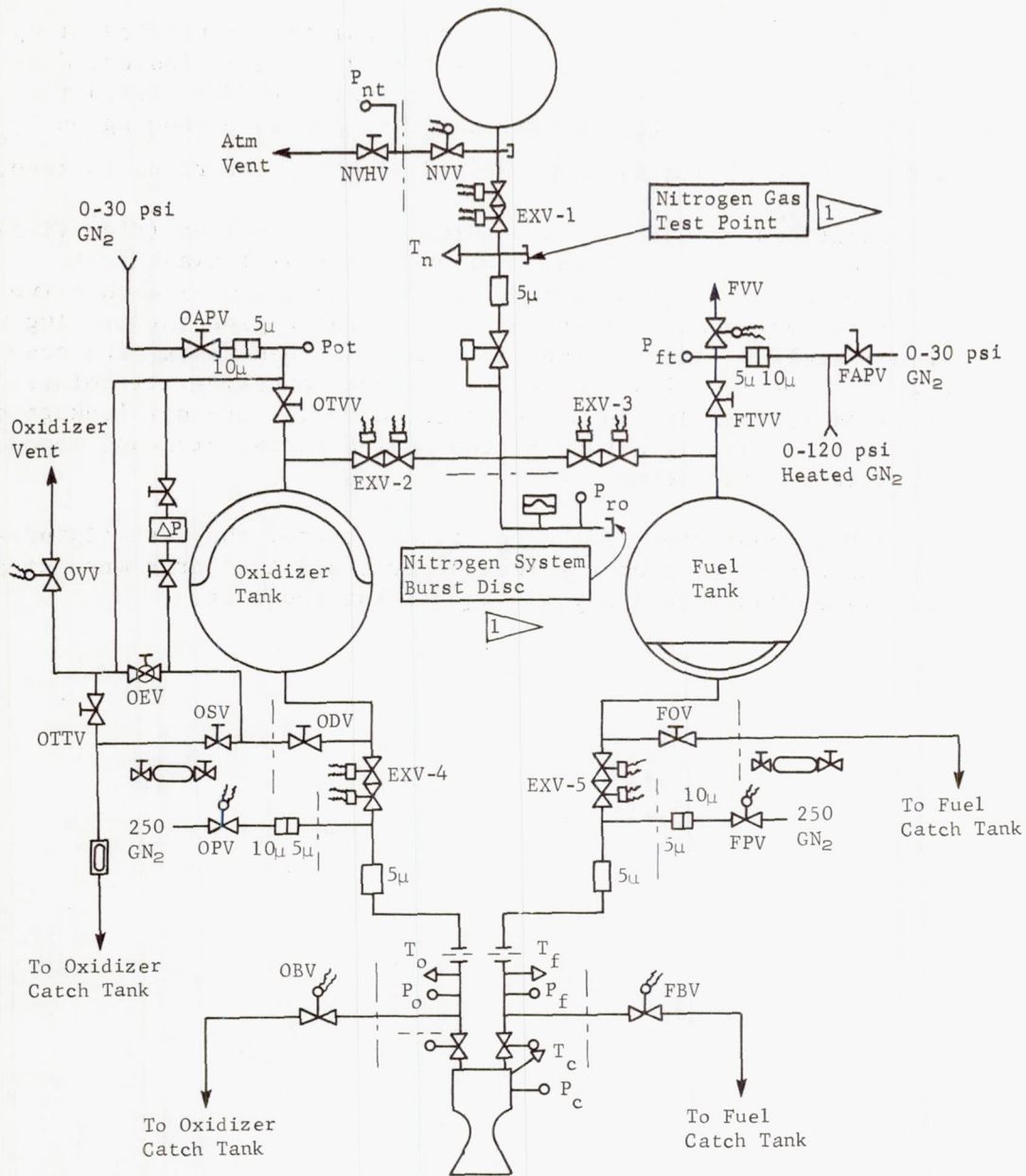


Fig. VI-3 Firing Test Schematic

### C. TEST METHOD

The propulsion module test method was basically defined by the Component and System Test Plan, MCR-67-20. In addition to the plan, detailed procedures were written to cover each sequence of module usage or test. Procedures written specifically for the module are:

- 1) Propulsion module assembly;
- 2) Propulsion module installation and removal;
- 3) Firing test;
- 4) Module propellant loading.

Each procedure is complete and provides step-by-step direction. Lists of necessary equipment and instrumentation are provided along with a blank for signoff of each step by the technician. Decontamination and heat sterilization was covered by a procedure written to cover general operation of the chamber and was applicable to both the components and the assembled module.

### D. DECONTAMINATION AND STERILIZATION

After module assembly and checkout, propellants were loaded. Propellant quantities were measured by weighing the source containers before and after loading. The amount of fuel and oxidizer loaded was 51.9 lb<sub>m</sub> and 84.5 lb<sub>m</sub>, respectively. The fuel tank was loaded by an overfill technique to eliminate entrapment of a bubble in the fuel tank trap. This consisted of loading the fuel tank in the upright position through the liquid port until liquid fuel was expelled from the gas port. The module was then inverted and liquid filling was resumed through the gas port until all gas bubbles were expelled from the liquid port. The module was then returned to the upright position and nitrogen gas was introduced into the gas port to drain back to the correct load.

The oxidizer tank was then loaded with the module in the upright position using a vacuum load technique. The gas inlet port was evacuated, followed by evacuation of the liquid outlet port. While holding the vacuum on the gas inlet port, oxidizer was introduced at the liquid outlet port until the proper quantity was loaded.



After loading, the module was installed on the sterilization chamber lid and the instrumentation and safety packages were connected. A final leak check of the systems was conducted and a leak was found at the oxidizer tank outlet ordnance valve. A vapor leak was noted at the valve crush gasket flange. Recommended torque of the screws on this flange was 40 in.-lb although 30 in.-lb had been used because of the heat sterilization environment. At 275°F the strength of the aluminum flange drops to the point where the tapped holes for the flange screws were near the yield point under the load created by the 800 psia oxidizer vapor pressure. At this time it was decided to use longer screws with nuts at the prescribed 40 in.-lb of torque. The screws were replaced in all five ordnance valve flanges one at a time without flange disassembly or replacement of the gaskets. For this operation, propellants were not unloaded although the gas vessel nitrogen pressure was reduced to 1 atmosphere. While the new screws and nuts were torqued, the flanges bottomed out (this was not the case at 30 in.-lb). A final leak check indicated no further leakage.

As the final item of preparation of the module for decontamination and sterilization testing, the module hand shutoff valves were equipped with stem cap seals. The stem lockscrew holes were filled on the outside of the lockscrew with the Devcon WR epoxy resin. After opening the required valves to admit the propellant tank pressure to the pressure transducers and safety package, the stem caps were installed and torqued to the 90 in.-lb specification value.

The installation of the propulsion module in the decontamination/sterilization chamber is shown schematically in Fig. VI-4. The module fuel tank was connected so that the tank could be pressure drained if uncontrolled decomposition of the MMH occurred by operating remotely controlled valves.

The first cycle of the required six ethylene oxide decontamination cycles was started, but was aborted shortly after the 26-hr exposure period started. This abort was caused by an inability to control chamber temperature. After a series of check runs, the problem of uncontrolled heating of the chamber was traced to Joule heating of the sterilant gas by the blower. In addition, problems were encountered in the relative humidity control and monitoring systems.

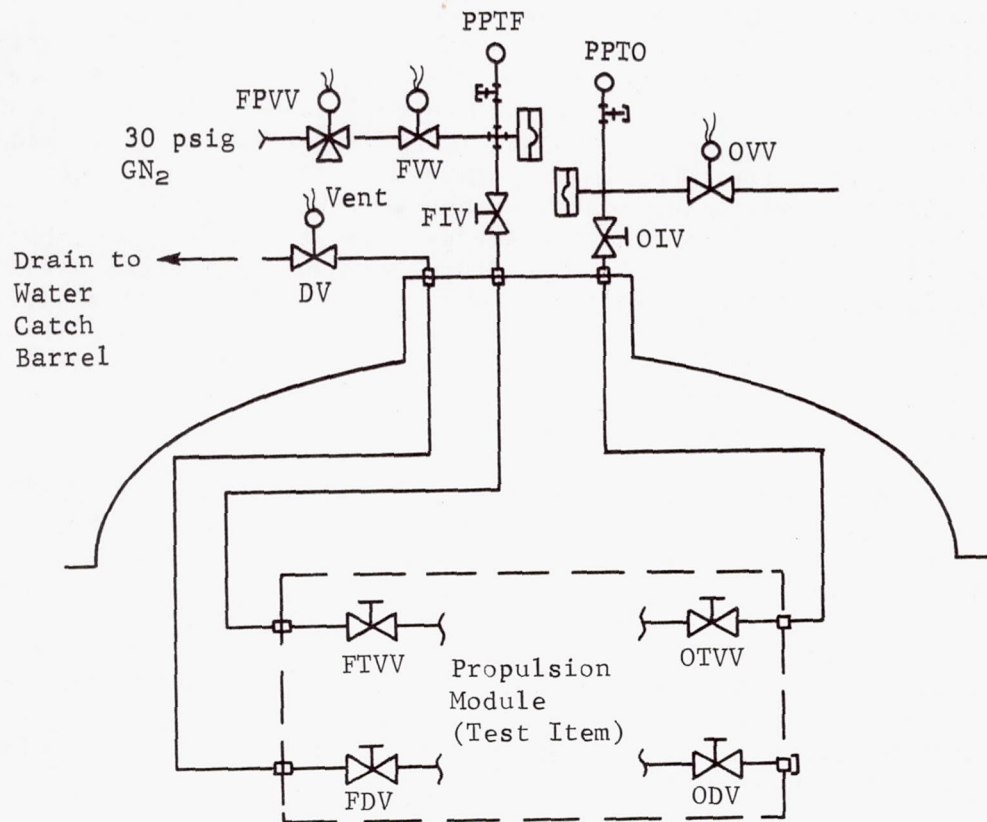


Fig. VI-4 Decontamination and Sterilization Chamber Schematic



During the initial heating phase of the several attempts at the first cycle, it became apparent that the 132°F water supply temperature to the chamber heat exchanger was not hot enough to maintain the required temperature ascent schedule. This was attributed to the thermal load created by the propulsion module, because the chamber heating system had performed satisfactorily with 132°F water during the qualification tests (no test item in chamber). To accommodate the thermal load of the module, the operating procedure was changed to permit operation of the chamber water supply system at 150°F during the initial 1.5-hr heating and humidity conditioning phase. Since that phase of the test does not involve the use of sterilant gas, the specification constraint of 132°F maximum heater temperature for heating a sterilant gas environment was not violated. With this change the first cycle was completed without incident. Some initial adjustment of the humidity control system was required to maintain the desired range of relative humidity (Alnor dewpoint). A data history of the first ETO cycle is shown in Fig. VI-5.

The second cycle was started approximately 3 hr after the first cycle was completed. Due to a procedural oversight, the heating water temperature was maintained at 132°F instead of 150°F; therefore, the ascent to the desired chamber temperature of 122°F required 2.3 hr. The balance of the test was completed without significant incident. Figure VI-6 shows the chamber temperature rose slowly to a maximum temperature of 130°F during the latter part of the test. This temperature rise was caused by setting the cold water bleed flow at too low a rate just before the period of unattended chamber operation.

Sterilant gas consumption due to chamber leakage remained in the range of 4 to 5 lb/hr. Automatic control of humidity was maintained throughout the test, although the control set point was slightly higher than desired, as from the relative humidity history. A chamber gas sample was taken during the test; however, the sample container capacity was inadequate for effective purging of the Orsat analyzer. A larger container was acquired after the second cycle had been completed.

The third through sixth cycles were completed without incident. A sample of chamber gas was taken during the third cycle. The sample assayed at only 18% by volume ethylene oxide (ETO) compared to the specification value of 27.3%. Investigation showed that the sample temperature was such that the vapor pressure of ETO was very close to the 22 psia pressure of the sample. To obtain assurance that the ETO fraction was in the vapor state, it was decided to heat subsequent samples to 120°F before conduction the Orsat analysis. During the fourth cycle a chamber gas sample was taken and assayed at 26.5% ETO content by volume.

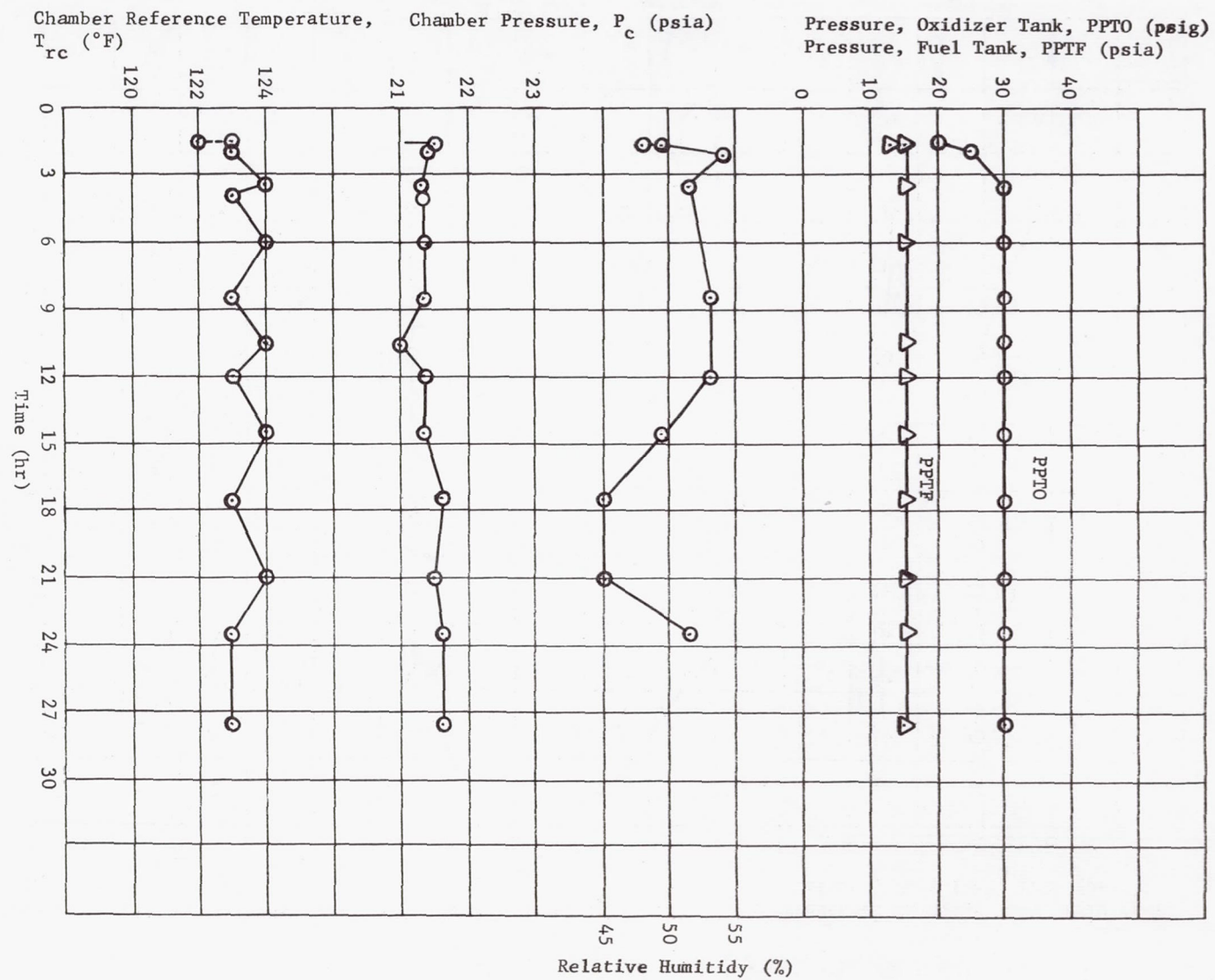


Fig. VI-5 ETO Cycle No. 1 Test History



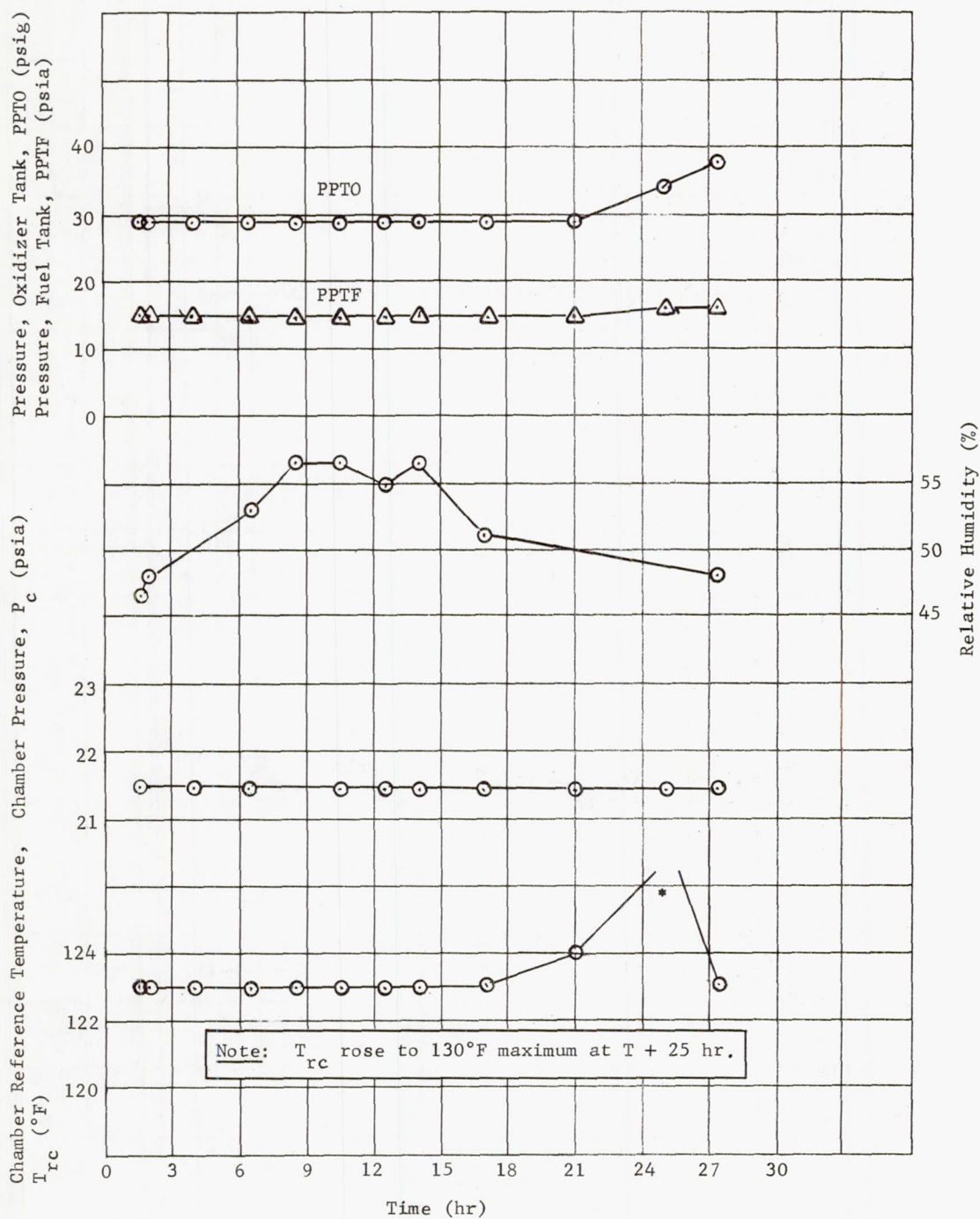


Fig. VI-6 ETO Cycle No. 2 Test History

The chamber heating problem was a slow increase in chamber temperature at a time when no heating water was being admitted to the chamber. The possible causes were thought to be an exothermic reaction of the ETO with the water vapor, a reaction between the ETO and possible undetected propellant vapor leaking from the module, the heat load introduced with the 132°F sterilant gas makeup, or the Joule heating by the chamber blower.

A systematic series of tests was made to obtain an explanation of the uncontrolled temperature increase. The series culminated in a test in which all chamber conditions were representative of a decontamination test, except the blower was turned off for an extended period. The chamber temperature decayed slowly during this test, indicating that the dissipation of the blower energy was responsible for the temperature increase.

Although this phenomenon has not been rigorously analyzed, the explanation is credited to the significant increase in blower horsepower required when circulating the relatively dense sterilant gas and the relatively low heat capacity of the sterilant gas. The phenomenon was not observed when operating with nitrogen gas in the chamber.

The problem was resolved by providing a continuous low flow rate of tap water (approximately 60°F temperature) into the chamber heat exchanger. This water extracted heat at a slightly greater rate than that added by the blower and provides positive cooling in that the hot water control valve would be required to open periodically. This system had the adverse characteristic of cooling a fraction of the chamber heat exchanger below the dewpoint causing cyclic condensation and reevaporation of water. This cyclic phenomenon was detected by an abrupt increase in the output of the sensitive electrohygrometer cell when the hot water admission valve was opened. Alnor dewpoint readings taken during this phenomenon proved that the relative humidity excursions did not exceed the desired bandwidth of 45 to 55%.

Future control systems for the water supply system to the heat exchanger should incorporate a mixing control valve. This valve would provide water temperatures at the heat exchanger ranging between the maximum of 132°F (55°C) and a minimum, which is a safe margin above the dewpoint of the chamber gas.



Difficulties encountered during the first decontamination test demonstrated that, due to normal chamber leakage and possible hydrolysis of the ethylene oxide, frequent water vapor injection was required. It became apparent that the open-loop system was feasible only if an operator was constantly monitoring the hygrometer output since attempts at steady-state injection of water vapor were unsuccessful. During these attempts, however, sufficient correlation between the recorded output of the electrohygrometer and the Alnor dewpoint readings was obtained to permit installation of a control microswitch on the hygrometer output recorder. The function of the microswitch was to open the superheated steam injection valve whenever the hygrometer output dropped to midscale on the recorder and to reclose the valve as soon as the hygrometer output signal responded with an increase in signal on the recorder. A metering valve was installed in the steam injection line to control the time constant of the system to prevent excessive excursions in relative humidity.

The automatic control of relative humidity which evolved in the above manner proved to be entirely satisfactory through Tests 2 thru 6. Humidity control was completely automatic; however, Alnor dewpoint readings were taken at 1- to 2-hr intervals during the day and evening work shifts. Alnor checks made on the mornings following unattended night operation verified that the hygrometer recorder/controller was effective in maintaining the relative humidity within specification limits with no operator attention.

When the decontamination test series was completed, the propulsion module was removed from the chamber to change the chamber to the heat sterilization configuration. The module remained mounted in the chamber lid and all connections from the module to the pressure transducers and safety packages remained undisturbed.

Before starting the required series of six heat sterilization tests, the pressure in the module  $\text{GN}_2$  storage tank was checked since the pressure was not monitored during decontamination or sterilization testing. The pressure in the  $\text{GN}_2$  tank decayed from the original 1550 psig to 1120 psig over the 23-day decontamination test period. The  $\text{GN}_2$  leakage was traced to internal leakage through the transducer isolation valve (test equipment). This valve permitted installation of a pressure transducer for the firing test after the decontamination and sterilization tests. It was decided that the module  $\text{GN}_2$  loading (solenoid) valve inlet port would be a suitable point to use for pressure measurement

during the firing test; therefore, the transducer isolation valve and its connecting flared tubing were removed from the module. The module  $\text{GN}_2$  tank was recharged to 1500 psig with  $\text{GN}_2$ , then topped off to 1550 psig with helium as an aid in locating the source of any future leakage.

Six heat sterilization cycles on the propulsion module were completed. Histories of the chamber temperature and propellant tank pressures for sterilization Cycles 1 and 6 are shown in Fig. VI-7 and VI-8 for the constant-temperature exposure period. All cycles were completed without significant incident with the exception of an automatic chamber shutdown during the latter part of Cycle 2. Shutdown was caused by a spurious signal from the chamber fuel vapor detector. Cycle time was resumed at  $T + 67.5$  hr after reheating the chamber and permitting the propellant vapor pressures to attain preshutdown values.

Pressure in the module  $\text{GN}_2$  tank was checked at 1540 psig after completion of sterilization Cycle 3 with the tank at room temperature, thus indicating that the  $\text{GN}_2$  system was leak free.

Pressure in the module fuel tank increased approximately 11 psi during the six sterilization cycles, indicating very little fuel decomposition. Oxidizer tank pressures were as expected, averaging slightly over 800 psia during sterilization.



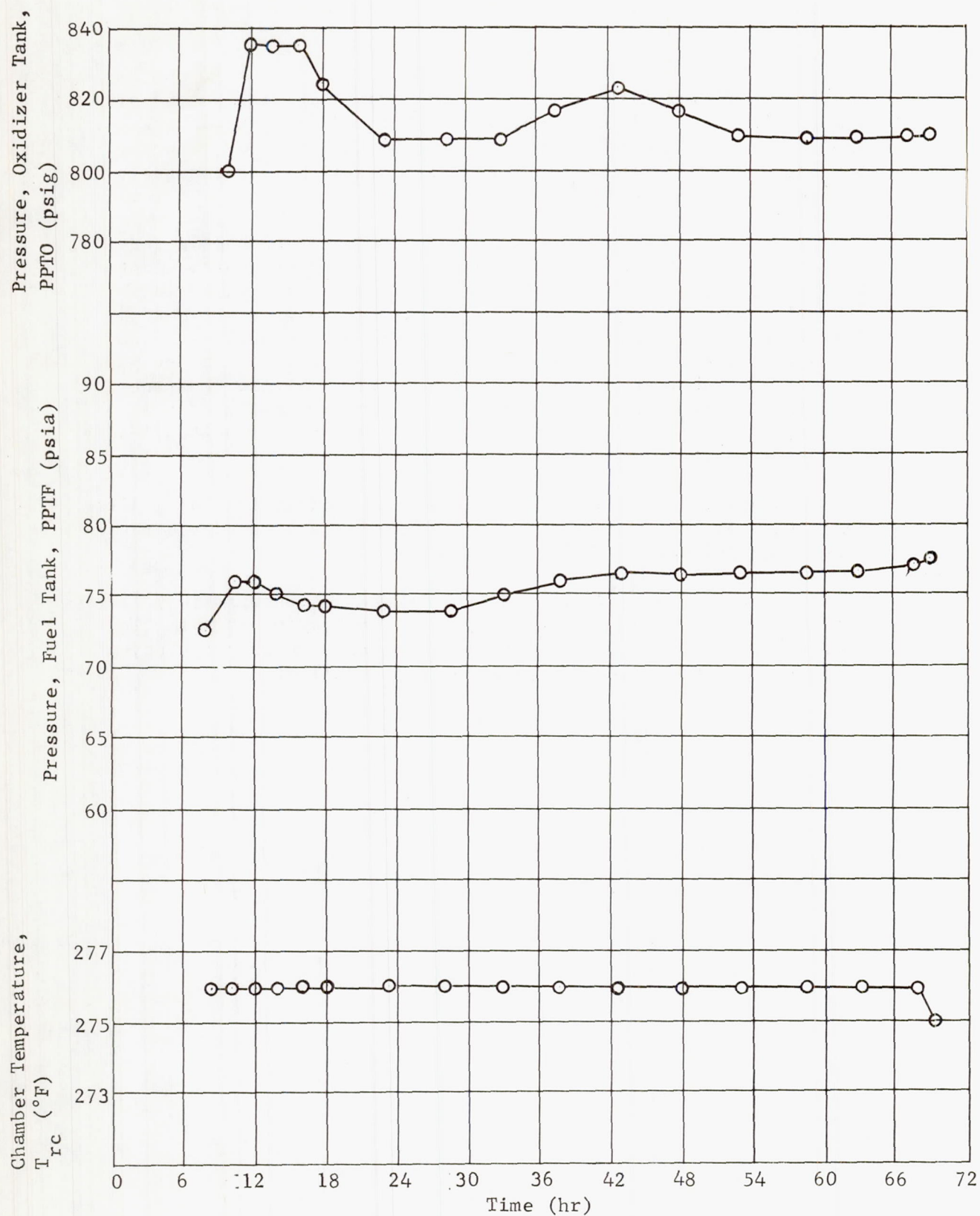


Fig. VI-7 Dry Heat Sterilization, Cycle 1

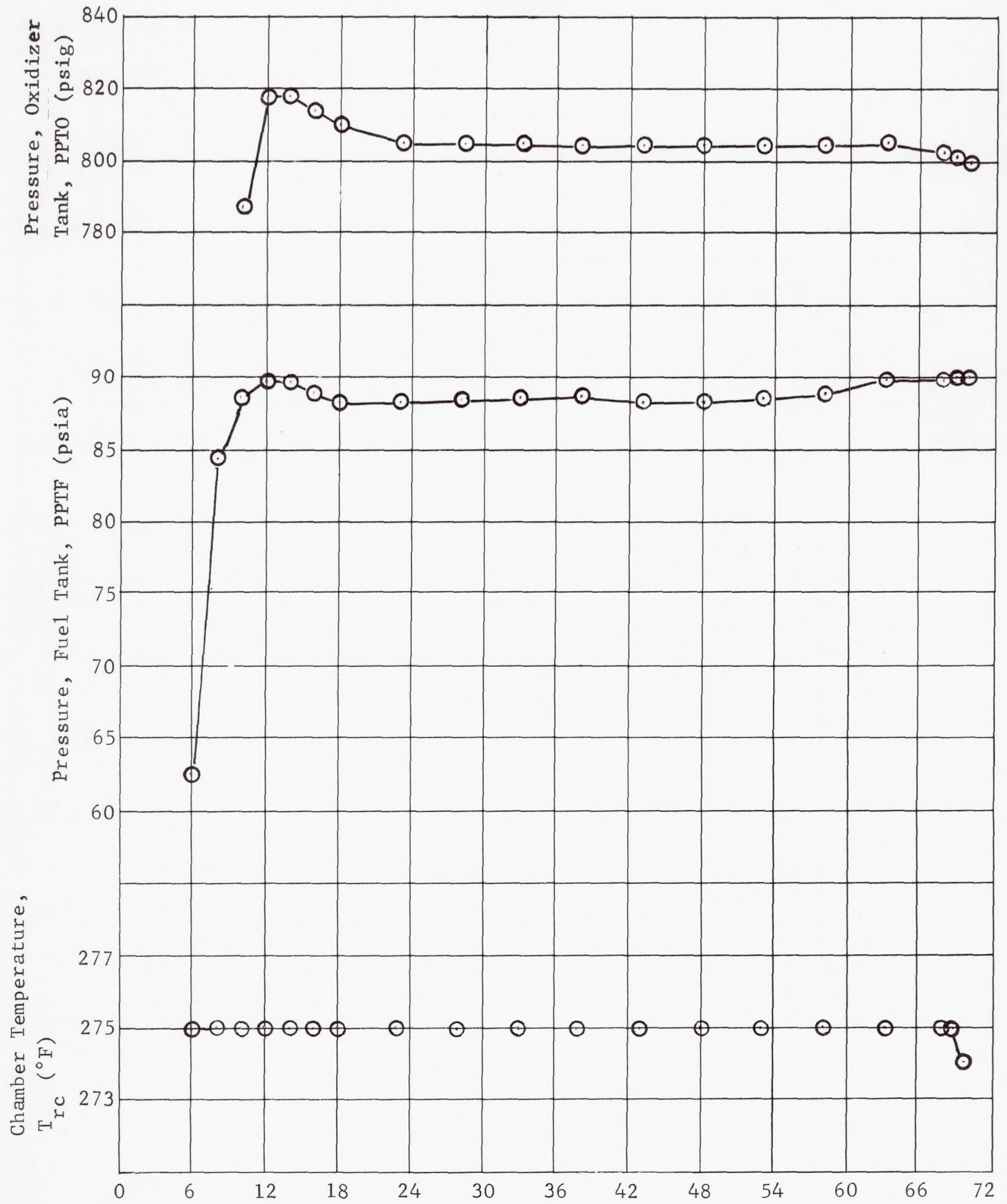


Fig. VI-8 Dry Heat Sterilization, Cycle 6



## E. SYSTEM TEST FIRING

After completion of ETO decontamination and heat sterilization, the module was ready to be moved to the firing stand. The preparations for removing it from the chamber required that the hand valve positions be changed so the safety relief valve capability could be transferred from the chamber to the transportation fixture. The removal of the hand valve caps, to facilitate turning the stem, was extremely difficult, requiring several hundred foot-pounds of torque. Examination of the stem cap seal indicated a deterioration of the Viton O-ring caused by vapors from either propellant. The stem packing gland of Teflon had apparently again exhibited cold flow, as seen in the component tests, allowing leakage from the open valve through the stem area into the cap seal area.

After the module was installed in the test stand, system and component functional tests were completed. Performance tests of the thrust chamber valves, the solenoid valve (GN<sub>2</sub> loading valve) and the GN<sub>2</sub> pressure regulator were completed. During these tests all systems control wiring and instrumentation circuits were validated. Further, it was ascertained that the poststerilization pressure in the nitrogen storage sphere was 1560 psig, indicating no system leakage resulting from the sterilization exposure.

The performance of the components before and after decontamination and dry heat sterilization is presented in Table VI-1. The thrust chamber valves and the pressure regulator showed no significant change in performance. Note that the regulator internal leakage decreased from 14.5 scc/hr GN<sub>2</sub> to no measurable amount. The solenoid valve exhibited a degradation of the dielectric strength of the solenoid coil similar to that experienced with the Task II component test unit. A comparison of the results of testing of the component unit and the module unit is presented in the following tabulation (the solenoid dielectric strength is given in microamps at 500 vac):

<u>Unit</u>	<u>Pretest</u>	<u>Posttest</u>
Task II Component	4	500
Module Assembly	6	278

Table VI-1 Performance of Propulsion Module Components before and after Decontamination and Sterilization

Component	Preexposure	Postexposure
<u>Thrust Chamber Valves</u>		
Oxidizer Valve		
Opening Response, max/min (sec)	0.0092/0.0089	0.0098/0.0095
Closing Response, max/min (sec)	0.0062/0.0060	0.0068/0.0061
Leakage - External (bubbles GN <sub>2</sub> )	zero	zero
Internal (cc GN <sub>2</sub> /hr)	zero	zero
Fuel Valve		
Opening Response, max/min (sec)	0.0073/0.0070	0.0078/0.0068
Closing Response, max/min (sec)	0.0070/0.0062	0.0078/0.0075
Leakage at 250 psig:		
External (bubbles GN <sub>2</sub> )	zero	zero
Internal (cc GN <sub>2</sub> /hr)	12	zero
<u>GN<sub>2</sub> Loading Solenoid Valve</u>		
Leakage, External (scc/sec helium)	zero	zero
Dielectric Strength ( $\mu$ amp @ 500 vac)	6	278
<u>Regulator</u>		
Internal Leakage (scc/hour GN <sub>2</sub> )	14.5	zero
External Leakage (bubbles GN <sub>2</sub> )	zero	zero
Regulation:		
Inlet Pressure, Initial (psig)	1498	1528
Inlet Pressure, Final (psig)	350	350
Average Flow Rate, GN <sub>2</sub> (lb/sec)	0.015	0.014
Outlet Pressure Variation, max/min (psig)	250/247	248/244
Hysteresis:		
Initial Outlet Lockup Pressure (psig)	263	259
Outlet Pressure Range (psig)	250/247	258/252
Response:		
Inlet Pressure, Average (psig)	1520	1517
Outlet Pressure, Lockup (psig)	261	257
Overshoot (psig)	0	0



As part of the prefire preparations, the propulsion module propellant tanks were X-rayed and propellant samples were removed for analysis. From the X-ray photos, it was determined that the oxidizer tank diaphragm was in the proper position against the upper tank wall with no apparent tears in the membrane. Also, the fuel level indicated that no measurable fuel loss had been incurred. The liquid level in the oxidizer tank could not be determined because of inadequate definition in the photos. Optimum positioning of the X-ray source and the film holder was not attained because of access limitations imposed by the transport fixture, module truss, and hardware.

The results of the chemical analyses of the propellant samples are shown below:

<u>Oxidizer (% volume)</u>		<u>Fuel (% volume)</u>	
$N_2O_4$	99.88	MMH	99.15
NO	0.31	$NH_3$	0.34
$H_2O$	0.033	$H_2O$	0.51

These results indicated propellant decomposition had not taken place and the propellants were satisfactory for use.

At this time all firing prerequisites for the module had been met and on 16 January 1968 the firing was completed without incident. Although the original plan had been to fire for 300 sec, a duration of 280 sec was used to allow sufficient margin on oxidizer usage. This reduction was necessary due to the inability to see the liquid level in the X-rays and to the oversizing of the flow control orifice in the oxidizer feed system.

The predicted and actual system performance is shown in Table VI-2 and Fig. VI-9, which show that performance was quite close to predicted values. The mixture ratio was approximately 3% low. This was attributed to the higher than expected fuel flow. The high fuel flow was caused by improper fuel orifice sizing resulting from drilling the orifice with the nearest standard twist drill. Figure VI-9 shows the chamber pressure to be very close to prediction or slightly above. The thrust washers were indicating low. Further, it is known the load washers are temperature sensitive. The computed (from  $P_c$ ) specific impulse obtained was 188 sec. This corresponds to a specific impulse under vacuum conditions of 294 sec at an expansion ratio of 40:1.

Table VI-2 Propulsion Module Firing Test Quick-Look Data

Parameter	Predicted Value	T + 0 sec	T + 5 sec*	T + 140 sec	T + 275 sec	T + 280 sec
Burn Time (sec)	280	--	--	--	--	280
GN <sub>2</sub> Tank Pressure, P <sub>nt</sub> (psia)	1560	1630/1210	1200	910	670	660
Pressure, Regulator Outlet, P <sub>ro</sub> (psia)	260	270	264	264	265	266
Pressure, Oxidizer Tank, P <sub>ot</sub> (psia)	260	271	263	264	265	265
Pressure, Fuel Tank, P <sub>ft</sub> (psia)	260	271	263	264	265	265
Pressure, Oxidizer Feed Line, P <sub>o</sub> (psia)	217	272	216	217	217	219
Pressure, Fuel Feed Line, P <sub>f</sub> (psia)	217	272	223	227	225	225
Chamber Pressure, P <sub>c</sub> (psia)	103	0	105	105	105	105
Flow Rate, Oxidizer, $\dot{w}_o$ (lb <sub>m</sub> /sec)	0.227	0	0.225	0.226	0.226	0.227
Flow Rate, Fuel, $\dot{w}_f$ (lb <sub>m</sub> /sec)	0.143	0	0.146	0.148	0.146	0.146
Mixture Ratio, MR (oxid/fuel)	1.59	--	1.54	1.53	1.55	1.56
Thrust, F (lb <sub>f</sub> ) <sup>†</sup>	69.5	--	67.4	--	--	67.5

\*Values read at stabilized conditions between T + 5 sec and T + 30 sec.

†Data from two of three load washers, obtained by:  $\left[ \frac{F_1 + F_2}{2} \right] \times 3$ .

TVC Response: Opening oxid = 0.0128 sec, fuel = 0.0091 sec,  
Closing oxid = 0.0083 sec, fuel = 0.0078 sec.

Ignition 0.0128 sec after oxid TCV opening.

Thrust Termination: Started 0.0022 sec, complete 0.0066 sec after oxid TCV closure.



MCR-68-119

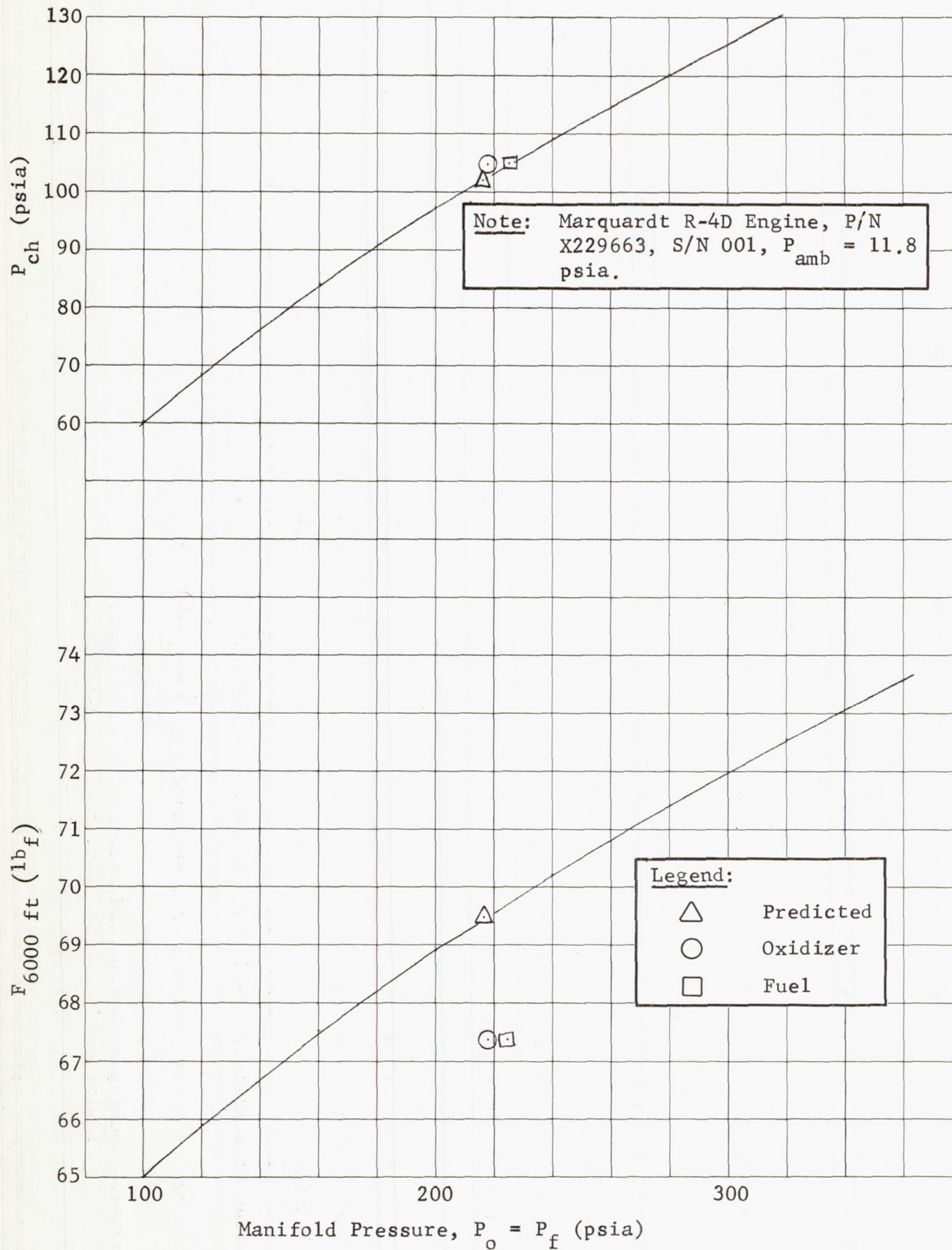


Fig. VI-9 Engine Performance

The high initial pressure in the nitrogen sphere was attributed to the heat flux caused by the sun lamps in position to give adequate lighting for 1000 fps motion pictures. It was concluded that the system performance was satisfactory and there was no significant degradation caused by the exposure to the sterilization environment.

A visual inspection of the propulsion module after the firing test revealed two leaks in the oxidizer system, neither of which was seen on the TV monitor. One was a vapor leak at the interface between the oxidizer tank outlet and the ordnance valve (EXV-4) and a liquid leak at the oxidizer drain valve (ODV) outlet tube connection (Fig. VI-3).

#### F. DISASSEMBLY AND EXAMINATION

Following the postfiring inspection, the residual fuel and oxidizer were drained into catch tanks for inventory. The fuel residual was 9.9 lb, compared to the calculated residual of 9.2 lb predicted on the expected fuel flow rate and burn time of 280 sec. The oxidizer residual, however, was only 11.7 lb as opposed to an expected residual of 20.4 lb. No conclusive cause was found to account for the loss of the 8.4 lb of oxidizer.

In the process of draining the propellant tanks, an internal leakage through the oxidizer diaphragm of 14,000 cc/min of  $\text{GN}_2$  was determined at a differential pressure of 1 psid. The diaphragm was recycled to the initial position, at the tank top, at which time the leakage was again determined to be 14,000 cc/min of  $\text{GN}_2$ . It was concluded that the diaphragm was ruptured.

The oxidizer tank was removed from the module and decontaminated by baking at 150°F with a 1 psig  $\text{GN}_2$  purge to remove all oxidizer vapors. The decontamination procedure was discontinued when the vapor detector indicated a vapor concentration of 2 ppm. The tank halves were separated and the inspection revealed the diaphragm in the propellant expelled position with a 16-in. tear across the dome.

The Marquardt R-4D engine assembly was removed from the propulsion module, visually inspected, and decontaminated according to Marquardt Corporation procedures.



When the hand valve stem caps were removed, several hundred foot-pounds of breakaway torque was required. The Viton O-ring was highly deteriorated. Normal cap torque was 90 in.-lb. While the seal was highly effective with no evidence of leakage throughout the test, the O-ring lost all elasticity and some evidence of plastic flow into the threads was found. Figure VI-10 shows the condition of the seal that was typical of both the fuel and oxidizer hand valves.

The Viton material was chosen with knowledge of marginal compatibility. If a bellows stem is incorporated into future valves, the compatibility of the stem seal will not be a problem.

The dielectric strength of both the component and module solenoid valves showed degradation. Failure analysis of the component test unit revealed the coil winding badly charred and black in color, as shown in Fig. V-23. The coil wire was No. 27 Formvar wire from the Bridgeport Insulated Wire Company. The coil was coated with Tri-Var No. 116, both of which were rated at 221°F. Consequently, exposure to 275°F lead to a breakdown in the coil winding.

The corrective action would be to use a Teflon-coated wire in the coil winding, coated with a high temperature material rated at 400°F or above.

As indicated earlier, the module assembly began leaking at the oxidizer tank outlet flange after loading. Further, the motion pictures of the firing showed the same flange was leaking after the ordnance valves were actuated. The flange in question is shown in Fig. VI-11. Microscopic examination of the flange serrations showed no positive cause of leakage, such as a double imprint or improper seating of the seal.

The leakage immediately following the firing of the squib on the module duplicated the component test unit. That unit also began leaking immediately after firing of the squib. While this flange was previously an aluminum structure throughout, this was the first time the flange was used with an aluminum/titanium interface at sterilization temperatures in the presence of  $N_2O_4$ .



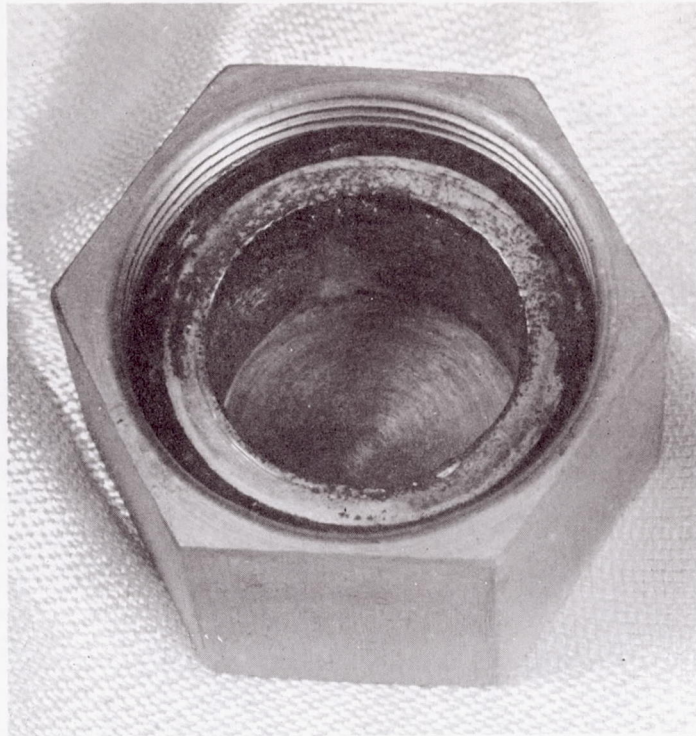


Fig. VI-10 Hand Valve Stem Cap and Seal

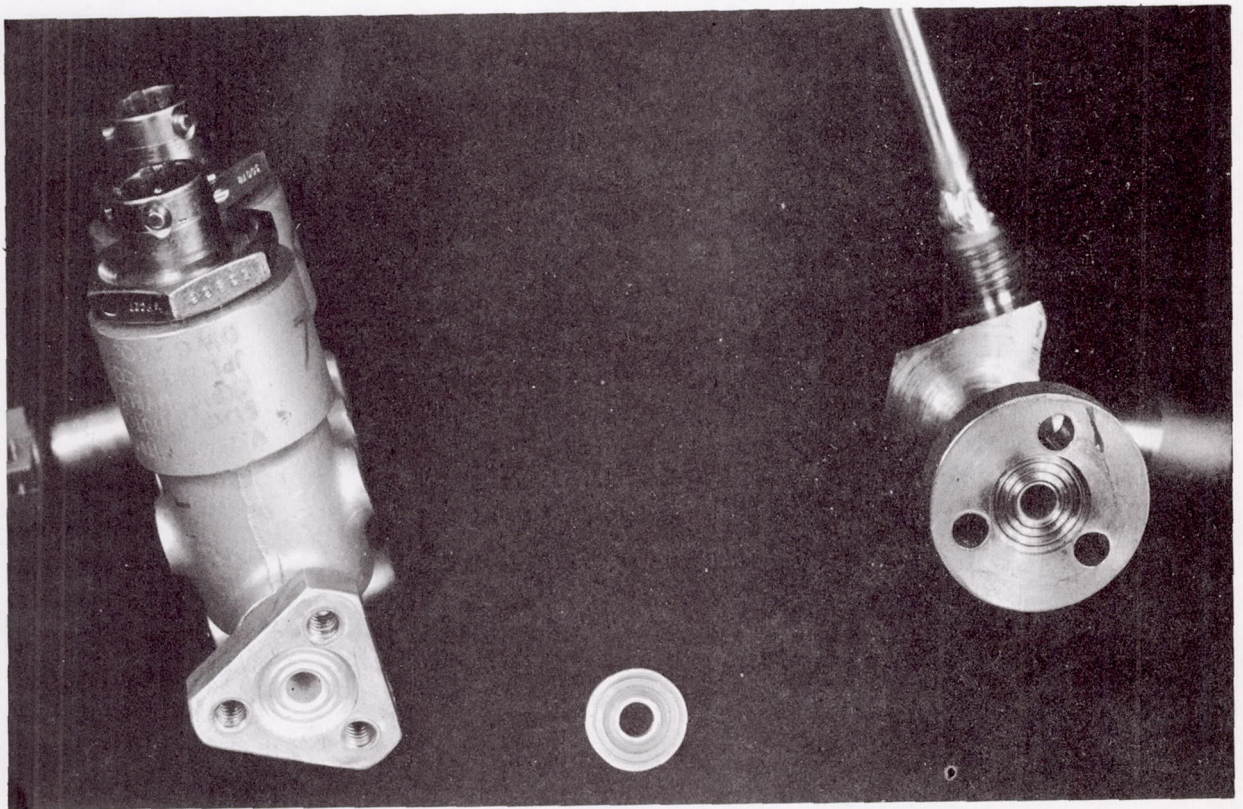


Fig. VI-11 Ordnance Valve Flange and Gasket



The flange differential growth caused by the titanium/aluminum interface contributed to a condition that leaks when shock loaded by the firing of the squib. The corrective action should be to provide a welded joint at every position inside the hermetically sealed area and to provide heavier mounting brackets for the ordnance valve.

Figure VI-12 shows an overall view of the tube shape, and Fig. VI-13 and VI-14 show a closeup of the failure. The failure was typical of high tensile loads caused by very short bend radii. No corrosion of the tube is evident. The tube material was aluminum alloy 6061-T6. A bend radius of 1/2 in. was allowed by Martin Marietta standards for pressures below 1500 psi; however, it is not recommended in sterilizable systems. A rebuild of this tube on subsequent firings would limit the bend radius to 4D or 1 in.

Figures VI-15 and VI-16 show two views of the diaphragm after separation of the tank halves. The diaphragm was in the expelled position and, because of the size of the tear, was not cycled back by the postfiring activities. Figure VI-17 shows a close-up of the apex doubler. It should be pointed out that the doubler was round and symmetrical before the Teflon laminate cure.

The basic Teflon laminate was 0.004 in. of TFE and 0.004 in. FEP. Inspection reveals no degradation of the membrane, indicating complete compatibility. Mud cracking was very minimal although the diaphragm was slightly oversized as seen by the discoloration of the tank hemisphere shown in Fig. VI-18.

A complete review of the system loading calculations and the facility loading fixture tare weights was made. Further, additional leak checks were made to explain the 8.4-lb loss of oxidizer. The results of the review indicated two areas of concern. First, an error was made in the loading statement, resulting in a residual weight of 10.9 lb rather than 20.4 lb. Second, a small leak was found in the tubing run from the module oxidizer tank drain valve to the facility safety package on the outside of the chamber. While the leak as measured would not account for the full leakage, it was measured at ambient temperature rather than the 275°F working temperature. While the tank capacity would accommodate either incident separately, it could not accommodate the combined effect.



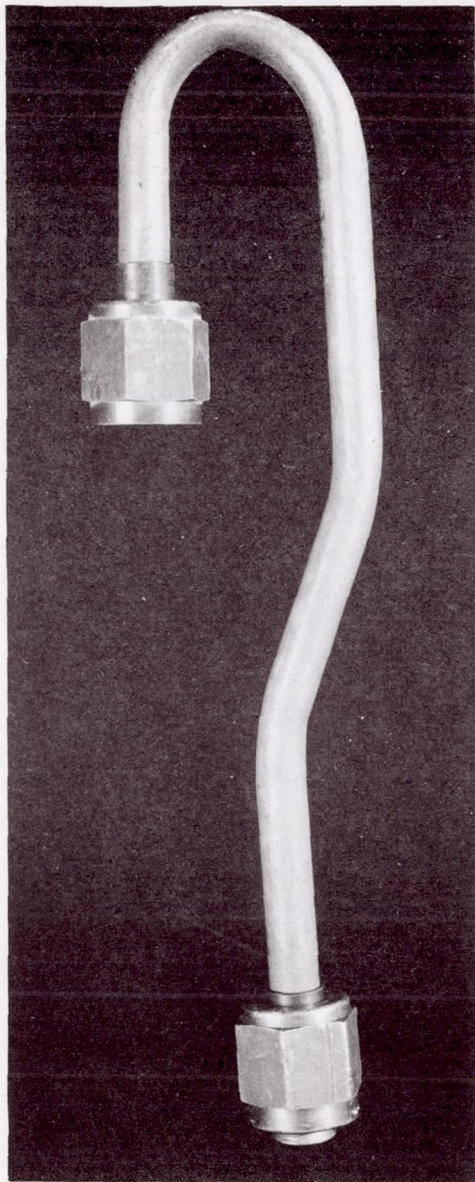


Fig. VI-12 Oxidizer Fill and Drain Tube

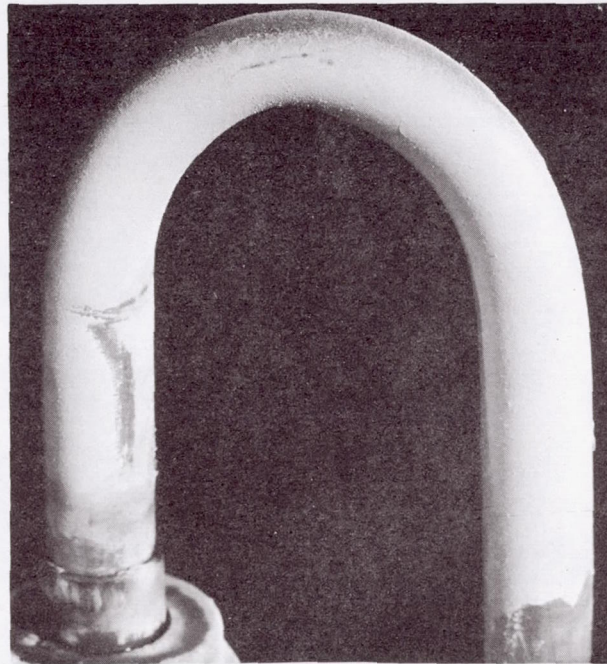


Fig. VI-13 Oxidizer Fill and Drain Tube Crack, External View

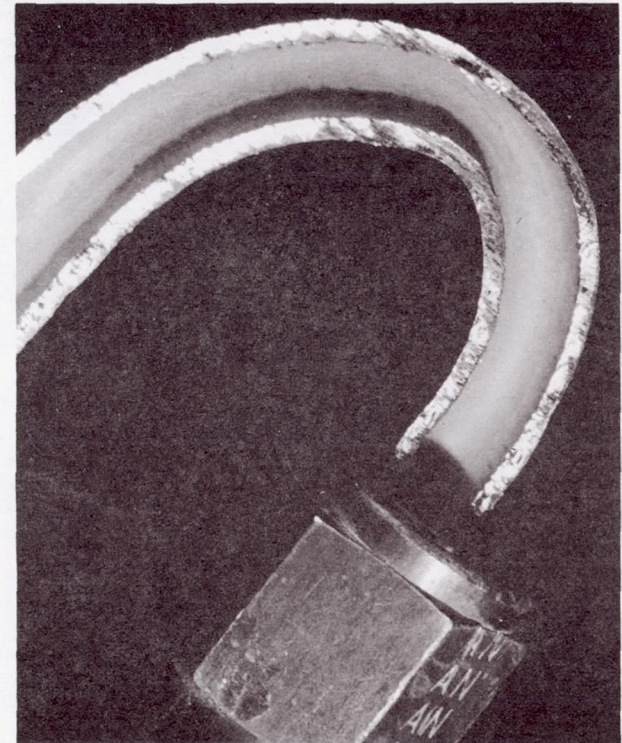


Fig. VI-14 Oxidizer Fill and Drain Tube Crack, Internal View

MCR-68-119

VI-27



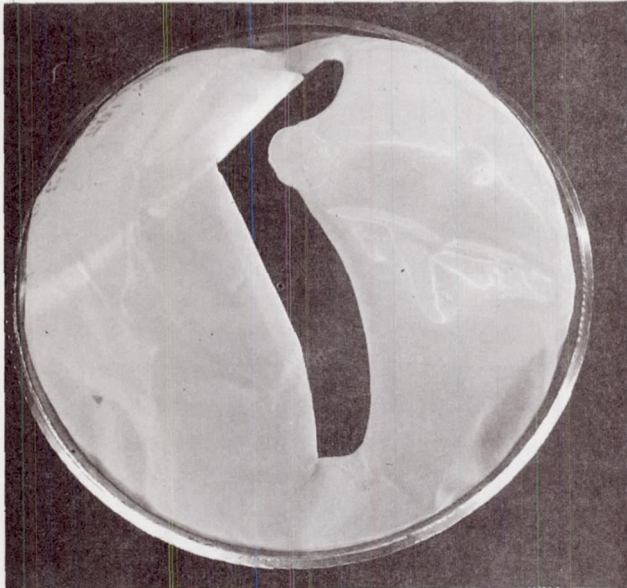


Fig. VI-15 Module Oxidizer Tank  
Diaphragm Failure,  
Side View

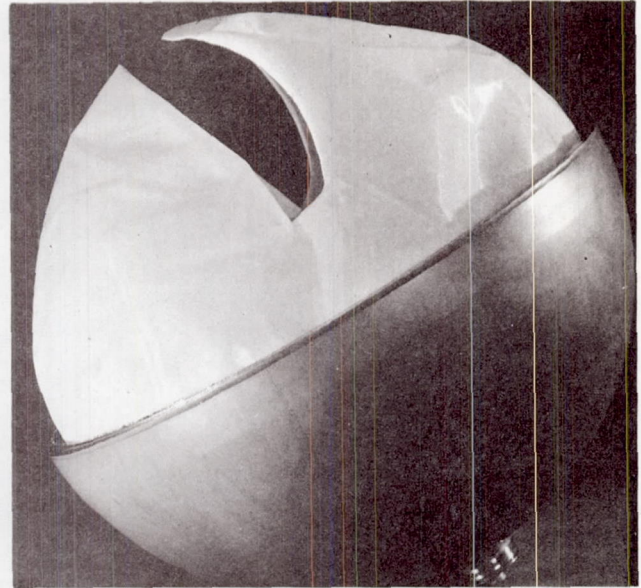


Fig. VI-16 Module Oxidizer Tank  
Diaphragm Failure,  
Top View



Fig. VI-17 Diaphragm Apex Doubler

It was concluded the diaphragm ruptured because of propellant depletion. Performance calculations indicated the diaphragm would have been required to stretch 0.022 in. This represents a surface stretch of only 0.3%. Biaxial loading of a Teflon membrane should result in stretch of up to at least 2%. Therefore, the evidence seems to point to the initial failure at the stress riser at the apex doubler, as shown in Fig. VI-17.

Further analysis shows the apex doubler, when in the prefire position against the gas inlet side of the tank, shifted during the repeated sterilization cycles as seen in Fig. VI-19. Some permeation was evident and a small amount of diaphragm leakage, 4 scc/hr, was present at the initiation of the testing. It is significant, however, that the diaphragm membrane showed no tendency to extrude through the shower head holes when the doubler was off center.

It was concluded that had the run time been reduced to 250 sec, the diaphragm would have successfully survived the system firing. Further, the failure was not a compatibility problem associated with the sterilization requirements.



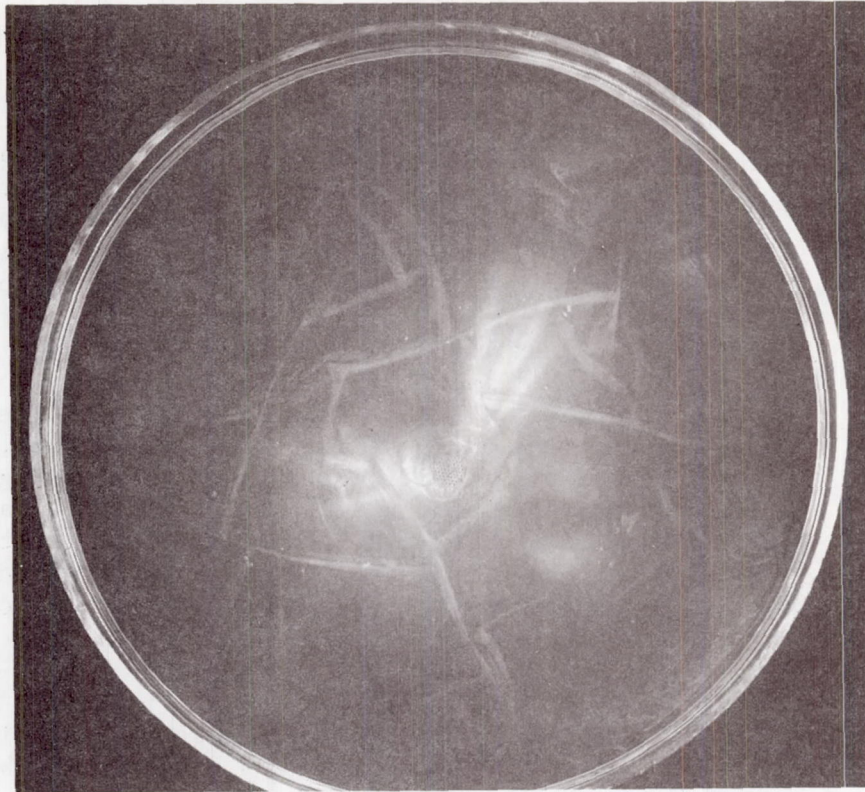


Fig. VI-18 Module Oxidizer Inlet Hemisphere

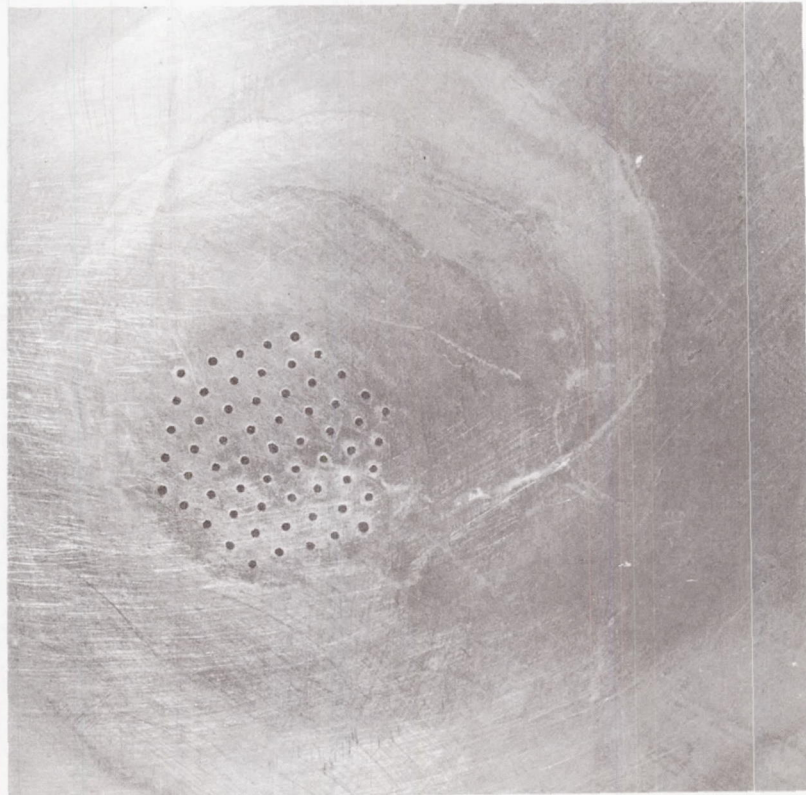


Fig. VI-19 Module Oxidizer Tank Gas Inlet Fitting

## VII. CONCLUSIONS

The conclusions are categorized into four separate areas: system, components, piece parts and materials, and facilities.

### A. SYSTEM

Successful survival of exposure to the sterilization environment by a propulsion module loaded with propellants as demonstrated by a full duration firing was achieved. Performance of the module was within specifications. Operation of the module was smooth and normal.

A mechanical seal or joint within the hermetically sealed portions of the system is an unnecessary risk. All joints within the hermetically sealed areas should be welded.

Generous allowance should be made for tube bends, line runs, and component mounting to withstand thermal expansion.

### B. COMPONENTS

Only the thrust chamber valves, the standard cartridges and the storage tank shells showed no degradation due to the sterilization exposure. The remaining components indicated some degradation during the Task II testing as shown below.

Pressure Regulator - Regulated pressure shifted downward 16 psi. Corrective action was taken to age the spring for the module unit. The action was successful.

Hand Shutoff Valve - Stem leakage was evident after six of the 12 cycles of exposure. Corrective action would be to add a bellows-type seal, which was not implemented for this program.



Solenoid Valve - Dielectric strength increased. Operation was satisfactory but examination revealed a breakdown in the coil insulation. Corrective action would be to use a high-temperature Teflon insulation, which was not implemented for this program.

Filter and Fuel Tank Screen Trap - Both units showed degradation of bubble point. Allowance could be made for this degradation.

Ordinance Valve - External leakage increased after actuation. This was a mechanical joint that should be redesigned to provide a welded tube attachment.

Oxidizer Tank Diaphragm - Both the component and system unit failed at the doubler located at the apex of the hemisphere that acted as a stress riser. The failure in the system unit indicated the diaphragm had successfully folded through before failure, therefore, the objective of positive expulsion was achieved. It was further concluded the failure at the doubler occurred because of overexpulsion. The component unit was never outflowed. New design criteria of the doubler are needed to improve the diaphragm design. This was the only failure that requires new technology or improved state of the art to fix.

It was concluded that with the exception of the diaphragm, all of the components may be corrected with new technology.

#### C. PIECE PARTS AND MATERIALS

Titanium 6Al-4V alloy was the only material found to be completely compatible with  $N_2O_4$  during exposure to the sterilization environment.

Aluminum alloys 1100, 2014, 2219, 5056, and 6061 all showed intergranular attack after 600 hr. No attack was found at 300 hr. Fine wire sizes for wire cloth disintegrated in less than 100 hr.

Teflon, while exhibiting a fine flocking in the propellant, was the only nonmetal acceptable for use in both MMH and  $N_2O_4$ .

Nonmetals such as butyl, silicon, and ethylene propylene rubbers and Kynar were not compatible in either the  $N_2O_4$  or MMH.

System cleanliness and materials passivation must be assured to successfully sterilize a fuel system.

Normal steel welding practices that allow formulation of metal oxides are unsatisfactory for use in sterilizable hydrazine base fuel systems.

For the same reason as above seam welding of fraying surfaces is not satisfactory in sterilizable hydrazine base fuel systems.

#### D. FACILITIES

Both MMH and  $N_2O_4$  react to some degree with ETO decontamination agent at 500,000 ppm.  $N_2O_4$  caused an increase in pressure to 22 psia, which may rupture environmental chambers.

Vapor detectors are satisfactory to determine  $N_2O_4$  in the ETO atmosphere but give unreliable results when sampling MMH and ETO.

Vapor detectors to determine relative humidity in the ETO atmosphere may be successfully calibrated to provide automatic control of the relative humidity.



### VIII. RECOMMENDATIONS

#### A. SYSTEM

Additional experience should be accumulated on the module to improve the credibility of the test results. This should include additional sterilization cycles and an additional system firing. Although this will provide an improvement in the confidence of the results, it will not allow improvement of the component reliability predictions.

#### B. COMPONENTS

Components containing heat sterilized springs with the springs in a stressed condition should receive pretest heat treatment. The complete component or the stressed spring should undergo heat soak at a temperature in excess of the sterilization temperature for a period of time sufficient to allow stabilization of the spring. Heat soaking should be done with the spring under stress, preferably at minimum working height, and at a temperature of not less than 15% more than the sterilizing temperature.

A problem was identified during the sterilization of the oxidizer ( $N_2O_4$ ) tank which contained a hemispherical Teflon laminate diaphragm. No proved sterilizable positive expulsion device now exists for a spacecraft oxidizer tank using  $N_2O_4$  as the propellant. A program should be initiated to solve the problems uncovered using the present system, or other expulsion devices should be designed and built for exposure to the sterilization environment. Because the problems are known and solvable, the primary approach should be to continue with a Teflon diaphragm. Other workable approaches include the design and build of a screen trap assembly made of titanium woven screen or etched titanium foil.

Teflon bladders have historically demonstrated a high permeability of propellants. Recent Teflon bladder material tests in  $N_2O_4$  at 275°F have shown a tendency to slough off Teflon particles

that may cause filters to clog or pulsing valves to leak. It is recommended that a development program be set up to deposit tantalum, columbium, and/or gold on Teflon laminate coupons, and perform such propellant compatibility tests and mechanical properties tests as abrasion, permeation, and adhesion.

#### C. PIECE PARTS AND MATERIALS

If  $N_2O_4$  is used as the oxidizer for a sterilizable system, all portions of the system in contact with the oxidizer during sterilization should be constructed of titanium alloy, 6Al-4V.

Although MMH is compatible with all metals tested, the use of titanium 6Al-4V is recommended, based upon high strength-to-weight ratio.

If an elastic material is required to perform the seat or seal, Teflon is recommended for both  $N_2O_4$  or MMH use during sterilization. Provision to prevent cold flow of Teflon must be provided.

#### D. FACILITIES AND PROCESSES

If  $N_2O_4$  is used as the oxidizer for a sterilizable system, it should be required to meet the minimum nitric oxide (NO) content specified by NASA Specification MSC-PPD-2A, dated June 1, 1966.

Current testing at sterilization temperatures indicates that inadequate cleaning and passivation of materials in contact with amine fuels such as MMH, UDMH, or hydrazine can result in decomposition. The decomposition can lead to very high pressures resulting in tank rupture, formation of corrosive compounds, or degradation of normal performance. It is recommended that such systems be thoroughly cleaned, followed by passivation of the system in accordance with Martin Marietta Materials Engineering Report 67-1R.

Welding of steel or titanium parts that will see hydrazine fuels at sterilization temperatures should be done in an inert atmosphere, preferably in an inert-gas purged glove box.



A welding development program should be implemented so that steel screens may be attached to other basic metals. A welded leaktight system is preferred over the riveted joint chosen in this program.

An exhaustive test program should be initiated to determine the mechanics of fuel decomposition caused by metal oxides. The program should determine whether all metal oxides cause fuel decomposition or whether the process is caused by only a few of the metal oxides used in the material of construction.

The feasibility of presterilization of both propulsion system components before loading should be determined to eliminate the many penalties involved in designing tankage for exposure to propellants at 275°F.

Possible methods of nonthermal sterilization of propellants during load should be explored. Potential methods include ultraviolet radiation, ultrasonic vibration, and filtration.

IX. NEW TECHNOLOGY

The following new technology disclosures have been submitted in accordance with the general provision of this contract.

<u>Number</u>	<u>Title</u>	<u>Type</u>
2	Use of Vapor Detectors in Decontamination Atmosphere	Development
3	Materials of Construction for Nitrogen Tetroxide Tankage in Sterilizable Systems	Production
4	Sterilization of Fully Submerged Teflon Bladders in Nitrogen Tetroxide.	Concept
15	Vapor Pressure of Monomethylhydrazine.	Production

One additional disclosure is in process at the present time entitled, "Sterilization of Cold Welded Transition Tubes in Propellants."

A fixed vapor detector manufactured by Teledyne Systems, Inc, was successfully used to detect nitrogen tetroxide,  $N_2O_4$ , vapors at concentration of 5 ppm in the presence of an ethylene oxide/Freon decontamination atmosphere (ETO). Conversely an attempt to employ a similar detector to warn of monomethylhydrazine vapors in the ETO was unsuccessful. The detector produced spurious and unreliable signals.

The only construction materials tested in this program that were compatible with  $N_2O_4$  were commercially pure titanium and its alloys. Steel suffered severe degradation in short duration tests, of the order of 24 hr. Not only were the steels affected, but the  $N_2O_4$  formed iron adduct that was undesirable in propulsion systems. Aluminum and its alloys showed no attack at 300 hr, but intergranular attack was evident at 600 hr.

The concept of sterilization of fully submerged Teflon diaphragms was an effort to prevent the development of high pressures across the membranes. This concept was found to be unnecessary in actual use.



The vapor pressure determination of monomethylhydrazine presents new data showing the vapor pressure to be 13.3% higher at 275°F than previously published. The Martin Marietta determination at 275°F was 63.0 psia as opposed to previously published values of 55.6 psia. These data showed that mild decomposition was, in fact, not taking place every time the fuel was heated. Rather it conformed to the vapor pressure curve presented in Fig. IV-28.

The module design used cold welded transition joints that allowed the coupling of dissimilar metals not possible with normal fusion welding techniques. Materials testing and production usage have proved the joints to be compatible at 275°F in a propellant environment.

The items mentioned above are the only items of new technology that have been identified. No subcontracts over \$50,000 and containing the new technology clause were awarded during this program.

X. REFERENCES AND BIBLIOGRAPHY

## A. REFERENCES

1. C. Grelecki: Private Communications. Reaction Motors Division, Thiokol, October 1966.
2. "Materials and Propellant Compatibility." NAA Letter No. 66RC14027. Rocketdyne, Canago Park, California, 17 October 1966.
3. A Study of the Effects of Gas Evolution in a Hydrazine-Base Heterogeneous Suspension. M-65-77. Martin Company, Denver, Colorado.
4. Monomethyl Hydrazine Product Data. Olin Chemical Division, Olin Mathieson Chemical Corporation.
5. Hydrazine Solution - Storage and Handling. Olin Mathieson Chemical Corporation.
6. A. Schaeffle: Propellants Compatibility Report. CR-64-88. Martin Marietta Corporation, 1964.
7. R. W. Lawrence: Handbook of Properties of Unsymmetrical-Dimethyl Hydrazine and Monomethyl Hydrazine. Report 1292. Aerojet-General Corporation.
8. Design Criteria Manual for Hydrazine. R-3130. North American Aviation, Rocketdyne Division, 1963.
9. Compatibilities of Materials with Rocket Propellants and Oxidizers. Memo 201. Defense Metals Information Center, Battelle Memorial Institute, 1956.
10. Alley, Hayford, and Scott: "Effects of Nitrogen Tetroxide on Metals and Plastics." 17th Annual Conference, National Association of Corrosion Engineers, 1961.
11. Ralph R. Liberto: Storable Propellant Data for the Titan II Program, 8182-933001 (AFBMD-TR-61-55). Bell Aerosystems Company, 1961.



12. Ralph R. Liberto: Storable Propellants Handbook. 8182--933004 (AFBSD TR 62-2). Bell Aerosystems Company, 1962.
13. Hydrazine Handling Properties. R3134. North American Aviation, Rocketdyne Division, 1963.
14. Research and Development on the Basic Design of Storable High Energy Propellant Systems and Components. AFFTC-TR-60-61. Bell Aerosystems, May 19, 1961.
15. Design Criteria for Typical Planetary Spacecraft to be Sterilized by Heating. 655D4518. General Electric Company.

#### B. BIBLIOGRAPHY

Addison, Boorman, and Logan: "Adducts of Iron Nitrate with Oxides of Nitrogen." Article 917, Journal of Chemical Society, London 1965.

Compatibility of Studies of Metals for Titan II Engines. Report MM 155-5. Aerojet-General Corporation, 1961.

Kit, B. and Evered, D. S.: Rocket Propellant Handbook. 1960.

Liberto, Ralph R.: Research and Development on Basic Design of Storable High-Energy Propellant System. Quarterly Progress Report 8086-933002.

Masteller, R.: Stress Corrosion of Titanium in  $N_2O_4$ . ME 66/IP. Martin Marietta Corporation, 1966.

Monomethyl Hydrazine Manual. Olin Mathieson Chemical Corporation, 1961.

Spakowski, A.: Thermal Stability of Unsymmetrical Dimethylhydrazine. TM12-13-58E. Lewis Research Center, National Aeronautics and Space Administration.

Storable Liquid Propellants. Report CRP 198. Aerojet-General Corporation, 1962.

Thomas, D. D.: Thermal Decomposition of Hydrazine. Report 9-14. Jet Propulsion Laboratory, 1947.

York, H.: Compatibility of Materials of Construction with Nitrogen Tetroxide. Report RM-13. Aerojet-General Corporation, 1958.

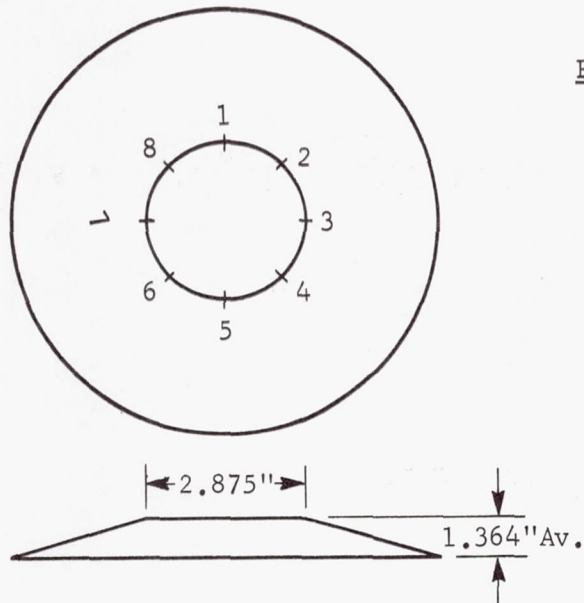
York, H.: Compatibility of Various Materials of Construction with UDMH. Report RM 6-1. Aerojet-General Corporation, 1958.



MCR-68-119

APPENDIX A

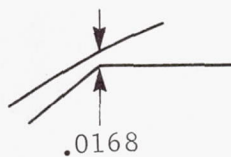
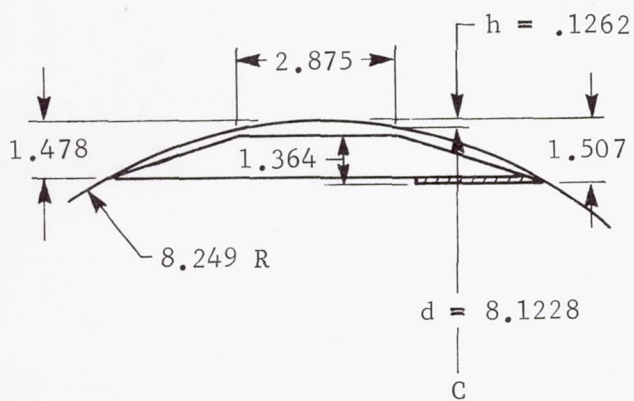
CALCULATION OF FLOW ANNULUS



<u>Position</u>	<u>Height</u>	<u>- Base</u>	<u>Actual Height</u>
1	2.553	1.200	1.353
2	2.565	1.200	1.365
3	2.568	1.200	1.368
4	2.573	1.200	1.373
5	2.571	1.200	1.371
6	2.553	1.200	1.353
7	2.571	1.200	1.371
8	2.558	1.200	<u>1.358</u>

Average 1.364

From Burington Handbook - page 12



$$\begin{array}{r}
 1.478'' \\
 \underline{.029} \\
 1.507 \\
 \underline{-1.364} \\
 .1430 \\
 \underline{-.1262} \\
 \underline{.0168}
 \end{array}$$

Annulus

$$2.875\pi \times .0168 = A \quad A = .152 \text{ in}^2$$

$$l = 2 \sqrt{R^2 - d^2}$$

$$2.875 = 2 \sqrt{(8.249)^2 - d^2}$$

$$8.2656 = 4(68.046 - d^2)$$

$$8.2656 = 272.184 - 4d^2$$

$$4d^2 = 263.9184$$

$$d^2 = 65.9796$$

$$d = 8.1228$$

$$h = R - d$$

$$h = 8.249 - 8.1228$$

$$h = 0.1262 \text{ in}$$



$$\text{Annulus} = 0.152 \text{ in}^2$$

$$\text{Equivalent orifice diameter} \quad d_{eo} = \sqrt{\frac{A}{0.7854}} = \sqrt{\frac{0.152}{0.7854}} = \sqrt{0.19353}$$

$$\underline{d_{eo} = 0.4399 \text{ in.}}$$

$$W = 0.525 C_f d_{eo}^2 \rho \Delta P$$

$$0.14 = 0.525 (0.6) (0.19353) \sqrt{54.86 \Delta P}$$

$$2.2965 = \sqrt{54.86 \Delta P}$$

$$5.2739 = 54.86 \Delta P$$

$$\underline{\Delta P = 0.09613 \text{ psi}}$$

$$1 \text{ psi} = 2717 \text{ in. H}_2\text{O}$$

$$\text{then } 0.09613 \times 27.7 = 2.663 \text{ in. H}_2\text{O } (\Delta P)$$

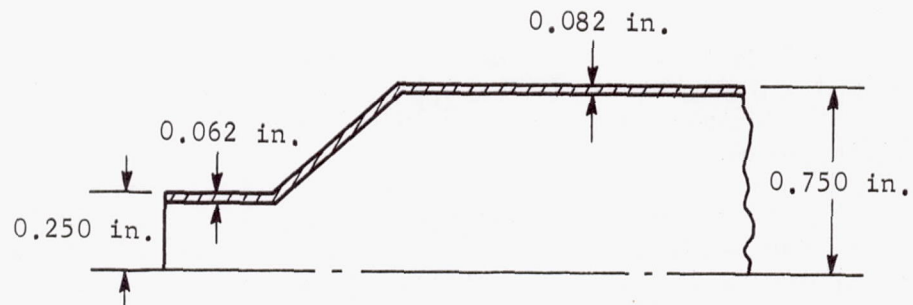
MCR-68-119

APPENDIX B

STERILIZABLE LIQUID PROPULSION SYSTEM  
COMPONENT DESIGN ANALYSIS



## A. FILTER, LAB 6002513

1. Stress Analysis

Hoop stress at the larger diameter at burst pressure of 4000 psi

$$S_2 = \frac{P R}{t} \quad (\text{Ref B-1})$$

where

$$R = 0.750 - 0.041 = 0.709$$

$$S_2 = \frac{4000 \times 0.709}{0.082}$$

$$S_2 = 34,600 \text{ psi}$$

Hoop stress at the smaller diameter at burst pressure of 4000 psi

$$S_{2_1} = \frac{P R_1}{t_1} \quad (\text{Ref B-1})$$

where

$$R = 0.250 - 0.031 = 0.219$$

$$S_{2_1} = \frac{4000 \times 0.219}{0.062}$$

$$S_{2_1} = 14,150 \text{ psi}$$

The highest static stress is at the larger median diameter, even though the wall thickness is less at the welding neck. This stress is on the safe side, since the yield stress for 304 stainless steel is 35,000 psi and the ultimate in tension is 75,000 psi.

An investigation of the static stress on the end plate at 4000 psi using Roark's (Ref B-1) case 17 equation for flat plates indicates a maximum stress of 19,800 psi. This is well below the yield point.

In reference to any dynamic loading on the screen filter, due to sudden opening of the ordnance valve, a pressure wave generated at the nominal 0.174-in. internal diameter of the valve passes through a 90-deg bend and then into a 3/8-in. tube; and after one more bend into a 1/2-in. tube, and finally is expanded within the filter to an equivalent diameter of 1.06 in. Even discounting the line losses, it is not possible for the initial  $\text{GN}_2$  loading of 1600 psia maximum to exceed the design differential pressure of 3000 psi for the filter screen. Since the gas loading is at the highest pressure within the system, this would be the worst case.

## 2. Tolerance Analysis over Natural and Induced Temperature Range

All of the parts making up the filter are of 304 stainless steel. Therefore, there is no basis for a tolerance analysis over the natural and induced temperature ranges.

## 3. Failure Mode Analysis

An inspection of the filter design, combined with failure mode analyses conducted on the Titan systems, indicates that the principal failure mode would be nonfiltration. This could be caused by an internal rupture of the screen or by a structural failure of the screen.

A secondary mode of failure would be a structural failure of the outside seal weld, causing external leakage.



## B. GAS PRESSURE REGULATOR, LAB 6002515

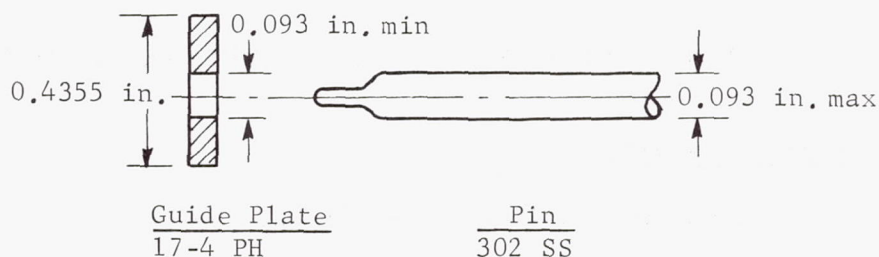
1. Stress Analysis

By inspection, the weakest section in the unit is the bellows outlet under a possible fail open mode. However, during sterilization, the unit is isolated from the pressurant tank by an ordnance valve, and during the actual firing setup, a burst disc is installed downstream. The burst disc is set at 350 psig and the bellows is proof-rated at 380 psig and has a burst design of not less than 633 psig. Therefore, no part of the regulator would be affected or destroyed if this failure mode occurred.

During the early phases of this component design, the vendor decided, because of the repeated heat cycling, that it would be best to employ a loading spring with a higher spring rate. This was done within the same envelope by using a rectangular wire spring. This permits the proper loading within a smaller percentage of the total spring capacity, thereby minimizing the possibility of further set or relaxation that would cause the pressure-set band to move downward.

2. Tolerance Analysis over Natural and Induced Temperature Range

The induced temperature range is most critical from 68 to 285°F. The expansion coefficient for 17-4 PH is  $6.0 \times 10^{-6}$  in./in./°F and  $9.6 \times 10^{-6}$  in./in./°F for 302 stainless steel.



$$\Delta d_1 = 0.093 \times 217 \times 6.0 \times 10^{-6}$$

$$\Delta d_1 = 121 \times 10^{-6}$$

$$\Delta d_2 = 0.093 \times 217 \times 9.6 \times 10^{-6}$$

$$\Delta d_2 = 194 \times 10^{-6} \text{ in.}$$

Then, the decrease in clearance between pin and guide plate is:

$$\begin{array}{r} 194 \times 10^{-6} \\ -121 \times 10^{-6} \\ \hline 73 \times 10^{-6} \text{ or } 0.000073 \text{ in. on the diameter} \end{array}$$

Therefore, an initial clearance of 0.0001 in. on the diameter would be sufficient to prevent binding with possible galling at the sterilizing temperature. Since these parts are hand fitted to a smooth sliding fit, the clearance on the diameter is not less than 0.0001 in. This has been verified by the vendor.

### 3. Failure Mode Analysis

Failure to Regulate - This could be caused by a jamming or sticking of the push pin that positions the ball poppet.

Shifting of the Regulation Band - This could be caused by an improperly-designed load spring undergoing a relaxation under compression and repeated temperature changes.

Excessive Internal Leakage Causing Overloading of the Propellant Tanks - This could be caused by contaminants on the ball seat and/or a hangup of the ball poppet.

Excessive External Leakage due to Gasket Leak -

## C. VALVE, MANUALLY OPERATED, SHUTOFF, LAB 6002512

### 1. Stress Analysis

#### a. Maximum Permissible Torque on Valve Stem

$$\text{Max } S_s = \frac{2T}{\pi r^3} \text{ (Ref B-1)}$$

where

$$T = \frac{30,000 \pi (0.093)^3}{2}$$

$$T = 37.9 \text{ in.-lb.}$$



## b. Hoop Stress at Outlet Tube

$$\text{Tube O.D.} = 0.250 \text{ in.}$$

$$\text{I.D.} = \underline{0.187 \text{ in.}}$$

$$2t = 0.063 \text{ in.}$$

$$S_2 = \frac{PR}{t} = \frac{2500 \times 0.110}{0.031} \text{ (Ref B-1)}$$

$$S_2 = 8870 \text{ psi (allowable - 34,900 psi at 280°F)}$$

## c. Gland Nut Thread Shear

$$F_1 = PA = 2500 \times \pi \times (0.375)^2$$

$$F_1 = 1103 \text{ lb}$$

$$\text{Pitch diameter} = 0.7094 \text{ in.}$$

Assuming 1/4-in. thread engagement and 75% efficiency, then shear area:

$$A_s = P.D. \times \pi \times L \times e$$

$$= 0.7094\pi \times 0.250 \times 0.75$$

$$A_s = 0.4175 \text{ in.}^2$$

$$S_s = \frac{F_1}{A_s} = \frac{1103}{0.4175}$$

$$S_s = 2645 \text{ psi (allowable - 24,300 psi at 280°F)}$$

## d. Seat Design

The present seat design depends on yield or plastic flow of a sharp-edged seat against a conical surface on the poppet to effect a seal. The material of the poppet is aluminum 1100-0 and the seat is aluminum 6061-T6. A better valve design would place the softer material (1100-0) in the seat by means of a pressed-in ring. This would have retained the geometric integrity of the poppet design. However, because of the limited use of the valve, the vendor would not accept this suggestion since it would involve higher manufacturing costs. Also, in this application, the poppet is raised from the seat and the inlet capped off during sterilization, thereby reducing probability of excessive deformation. It is recommended that future designs consider the soft-seat, hard poppet approach.

## 2. Tolerance Analysis over Natural and Induced Temperature Range

All of the metal parts of the valve that would be affected by relative movement during the sterilization cycle are made of aluminum or aluminum alloy, and there should be no adverse binding or relaxation between metal parts. The poppet is made of 1100-O aluminum and the seat and body of 6061-T6 aluminum. The relative motion between these two parts would be  $1 \times 10^{-7}$  in./in./°F and would amount to approximately  $4 \times 10^{-6}$  in. The strain imposed by closure of the valve would be greater than this amount. At the worst condition, this would result in some relaxation of the initial closure torque during the sterilization cycle, but could be compensated for by increasing the initial torque if leakage is detected during the cycle. It is probable that this will not be necessary.

## 3. Failure Mode Analysis

External Leakage - In this application, the hand valves are being used as fill and drain valves, and the outboard port is capped after filling; therefore, external leakage is of prime importance.

Failure to Open for the Drain Operation - This could be caused by torsional shear of the actuating stem.

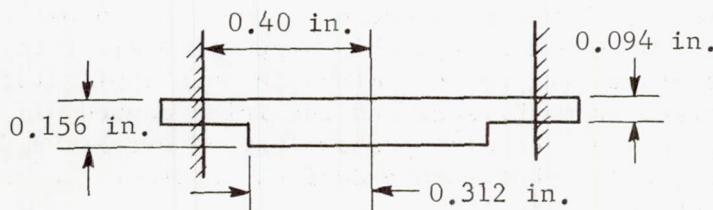
Brinelling or Indenting of the Poppet Face from Repeated Use of the Valve - Extended use is not a requirement of this application.

D. 1/4-IN. SOLENOID VALVE, N.C., LAB 6002516

## 1. Stress Analysis

### a. Stop

Sterer Detail 16 at burst pressure of 6250 psia. Material, Titanium 6Al-4V:





At edge (Roark's flat plate, case 6, Ref B-1):

$$\text{Max } S_r = \frac{3W}{4\pi t^2}; \quad S_t = \frac{3W}{4\pi mt^2}; \quad W = w\pi a^2$$

$$W = 6250 \times \pi \times 0.40^2$$

$$W' = 3140 \text{ lb.}$$

$$S_r = \frac{3 \times 3140}{4\pi \times 0.094^2} = \frac{9420}{0.1111}$$

$$S_r = 84,750$$

$$S_t = \frac{3 \times 3140}{4\pi \left(\frac{1}{0.33}\right) 0.094^2} = \frac{9420}{0.337}$$

$$S_t = 27,950$$

$$S^2 = S_r^2 + S_t^2$$

$$S^2 = 0.718 \times 10^{10} + 0.0781 \times 10^{10}$$

$$S^2 = 0.7961 \times 10^{10}$$

$$S = 0.893 \times 10^5$$

$$S = 89,300 \text{ psi (yield point at } 285^\circ\text{F} - 98,500 \text{ psi guaranteed minimum)}$$

Since the above calculation shows maximum possible stress and minimum possible yield point, it can be concluded that the design is satisfactory.

#### b. Seat Design

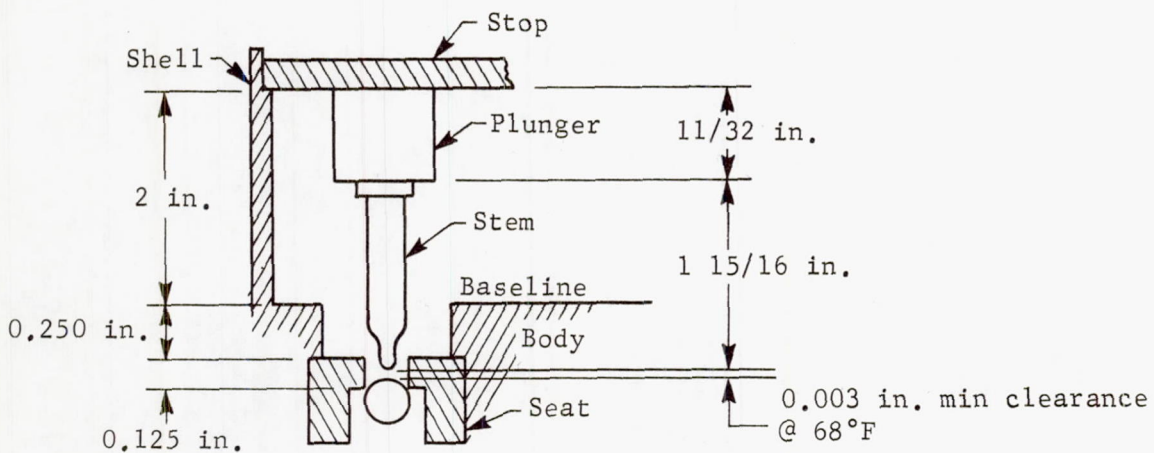
The seat and poppet design are of the hard poppet (tungsten carbide), softer seat (17-7 PH stainless steel) combination. A very fine line of contact is first established, but final sealage depends on the yield and plastic flow of the seat; therefore, seat stresses can be assumed to be at or near the yield point for the metal.

## 2. Tolerance Analysis over Natural and Induced Temperature Range

Stem and Body - 17-4 PH stainless steel. Coefficient of thermal expansion is  $6.0 \times 10^{-6}$  in./in./°F.

Seat - 17-7 PH stainless steel. Coefficient of thermal expansion is  $5.6 \times 10^{-6}$  in./in./°F.

Plunger and Shell - Low carbon iron. Coefficient of thermal expansion is  $8.4 \times 10^{-6}$  in./in./°F.



Differential movement between shell and plunger.

Shell and Plunger -

$$\Delta l = 2 \times 217 \times 8.4 \times 10^{-6} - \frac{11}{32} \times 217 \times 8.4 \times 10^{-6}$$

$$\Delta l = 3645 \times 10^{-6} - 626 \times 10^{-6}$$

$$\Delta l = 3019 \times 10^{-6} \text{ (this is movement away from stem)}$$

Stem -

$$\Delta l_1 = -1.9375 \times 217 \times 6 \times 10^{-6}$$

$$\Delta l_1 = -2520 \times 10^{-6} \text{ (this is lengthening of the stem; therefore, is negative to indicate closure of the gap)}$$



Body and Seat -

$$\begin{aligned}\Delta l_2 &= 0.25 \times 217 \times 6 \times 10^{-6} + 0.125 \times 217 \times 5.6 \times 10^{-6} \\ &= 325.5 \times 10^{-6} + 152 \times 10^{-6}\end{aligned}$$

$$\Delta l_2 = 477.5 \times 10^{-6} \text{ (movement away from stem tip)}$$

$$\text{Total} = 3019 \times 10^{-6} + 477.5 \times 10^{-6} - 2520 \times 10^{-6}$$

$$\Delta l_T = 976.5 \times 10^{-6} \text{ in.}$$

Therefore, heating causes a movement of the stem tip away from the ball, and unseating of the ball poppet could not occur. Actual specified clearance is 0.003 to 0.005 in.

The solenoid separation band will increase clearance with the plunger with increase in temperature. Therefore, there would be no binding from room temperature to the sterilization temperature of 285°F maximum.

An investigation of the ball poppet and guide shows a coefficient of expansion for the poppet of  $4.3 \times 10^{-6}$  in./in./°F and for the seat of  $5.6 \times 10^{-6}$  in./in./°F. Therefore, the seat would expand at a faster rate with increase in temperature and binding could not occur.

3. Failure Mode Analysis

## a. External Leakage

In this particular application, external leakage is the most critical failure mode. In the sequence of operation, the inlet port is capped after filling the pressurant tank; therefore, internal leakage is not a primary failure mode.

## b. Failure to Open for Initial Fill

This could be caused by electrical failure and/or excessive internal contamination. However, this is of a secondary nature because the valve is a pressure assist opening, from the fill port, design.

## E. PROPELLANT TANKS

1. Stress Analysis

## a. Fuel Tank, LAB 6002514-019

Minimum wall thickness:  $t = 0.120$  in.

Internal radius:  $8.250 \pm 0.005$  in.

I.R. = 8.255 in. max

Mean radius:  $R = 8.315$  in.

$P = 3750$  psi (burst pressure)

$$S = \frac{PR}{2t} = \frac{3750 \times 8.315}{2 \times 0.120} \quad (\text{Ref B-1})$$

$S = 130,000$  psi (Yield point at  $285^\circ\text{F} = 143,000$  psi or  $155,000$  psi at room temperature.)

The above wall section is heat treated. An investigation of the girth area, which is annealed by the welding process, shows:

$$S_1 = \frac{PR_1}{2t_1} = \frac{3750 \times 8.335}{2 \times 0.160}$$

$S_1 = 97,500$  psi (Yield point at  $285^\circ\text{F} = 98,500$  psi or  $120,000$  psi at room temperature.)

Since the tanks are not actually tested for burst pressure (3750 psi) at the higher temperature, there is an appreciable margin of safety.

An investigation was made of the screen area (the top screen is approximately 4 sq in.).

Required flow is  $0.14 \text{ lb}_m/\text{sec}$  maximum or

$$0.00258 \text{ cu ft/sec} = 0.1555 \text{ cu ft/min} = 1.162 \text{ gpm}$$

or

$$0.2905 \text{ gpm/in.}^2$$

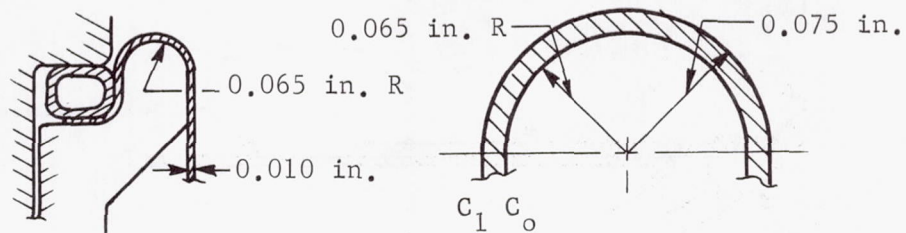


Tests made at the Martin Marietta Corporation, Denver Division, indicate that flow with Aerozine 50, with the same screen used in the fuel tank, shows no appreciable pressure drop ( $<0.25$  psi) at the required flow rate. It can be assumed that the pressure drop with MMH would not be significant.

b. Oxidizer Tank, LAB 6002514-009

The oxidizer tank wall thickness is the same as the fuel tank; therefore, the same calculation for hoop stress, as shown above, would apply.

The diaphragm does present several possible modes of flexure during expulsion; however, these are entirely random in nature, and therefore not subject to an exact stress analysis. At the end of expulsion, the diaphragm is bent around the lip of one diaphragm retainer. An investigation of this area follows.



$$C_0 = \frac{\pi D_0}{2} = \frac{\pi \times 0.130}{2}$$

$$C_0 = 0.204204 \text{ in.}$$

$$C_1 = \frac{\pi D_1}{2} = \frac{\pi \times 0.150}{2}$$

$$C_1 = 0.23562 \text{ in.}$$

$$\Delta C = C_1 - C_0 = 0.2356 - 0.2042 = 0.0314$$

then,

$$\frac{\Delta C}{C_0} = \frac{0.0314}{0.2042} \times 100$$

$$\frac{\Delta C}{C_0} = 15.38\%$$

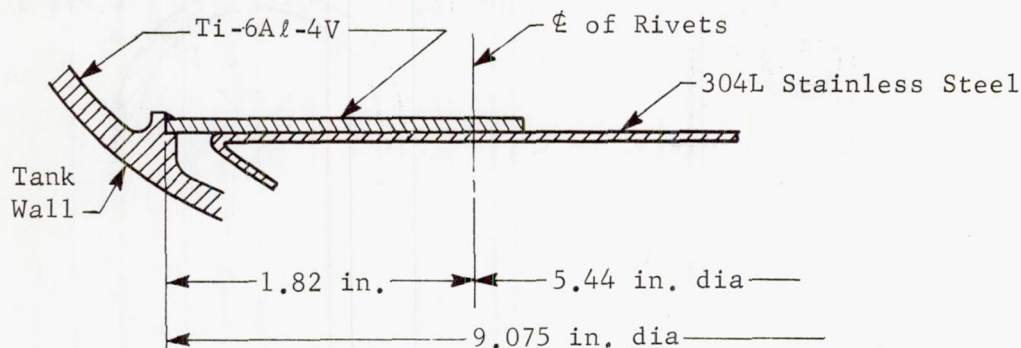
DuPont (Ref B-2) indicates a 15% strain of FEP at 73°F results in approximately 2080 psi stress. This is above the yield or permanent set point; therefore, it can be assumed that eventually, continued flexing would result in failure at this point. However, this is not anticipated within the three-cycle limit now imposed by the bladder specification limit.

To the above loading, there would be added the amount of tensile load caused by the differential pressure (1 psi) at the end of expulsion. This amounts to only 490 psi on the membrane, and is small compared to the bending load.

## 2. Tolerance Analysis over Natural and Induced Temperature Range

### a. Fuel Tank

#### Screen Assembly



From  $T_0 = 68^\circ\text{F}$  to  $T_1 = 285^\circ\text{F}$

$$\Delta T = 217^\circ\text{F}$$

$$\begin{aligned}\Delta l_{Ti} &= 5.44 \text{ in.} \times 217 \times 5.8 \times 10^{-6} \\ &= 68.4 \times 10^{-4}\end{aligned}$$

$$\Delta l_{Ti} = 0.00684 \text{ in.}$$

$$\begin{aligned}\Delta l_{SS} &= 5.44 \text{ in.} \times 217 \times 9.6 \times 10^{-6} \\ &= 113.3 \times 10^{-4}\end{aligned}$$

$$\Delta l_{SS} = 0.01133 \text{ in.}$$



The above calculation indicates that the center section of stainless steel is expanding faster than the titanium; therefore, there would be a buckling of the stainless steel section. However, this difference is only a little more than 0.004 in. over the 5.44 in. diameter, and any growth of the tank due to higher pressure at the high temperature would tend to decrease this difference.

b. Oxidizer Tank

The oxidizer tank presents no serious problem at the higher temperature/pressure range except that it is expected that the Teflon bladder may flow into all crevices that are present. To overcome this tendency, a thicker section was included at the bladder apex to prevent extrusion into the "shower head." Also, the cylindrical section near the equator is 25% thicker than the main portion of the bladder. This will resist extrusion into the small crevice formed by the radius on the inner section of the bladder rim and the connecting radius on the upper tank hemisphere.

3. Failure Mode Analysis

a. Fuel Tank

Failure of screen assembly to provide sufficient fuel for engine start under zero-g condition, caused by screen blowout or leakage through the screen, reduces the amount of fuel available. Clogging of screen pores prevents sufficient flow.

b. Oxidizer Tank

Failure to flow oxidizer under zero-g condition, due to catastrophic failure of the bladder, is caused by complete separation at the rim or excessively large cracks.

## F. PRESSURANT TANK

1. Stress Analysis

Hoop stress at the burst pressure of 6000 psig uses a derivation of the Lamé' formula as used by the Menasco Company,

$$S_1 = \frac{r_i^2}{t \times 2 (r_i + t)} \text{ (Ref B-3)}$$

$$= \frac{6000 \times 6.773^2}{0.122 \times 2(6.773 + 0.122)}$$

$$S_1 = 164,000 \text{ psi}$$

The minimum ultimate tensile strength specified by Menasco is 165,000 psi.

2. Tolerance Analysis over Natural and Induced Temperature Range

The tank is made of one material (Ti-6Al-4V), and should offer no problems over the temperature range encountered.

3. Failure Mode Analysis

Leakage at the fill-drain connecting port.

## G. REFERENCES

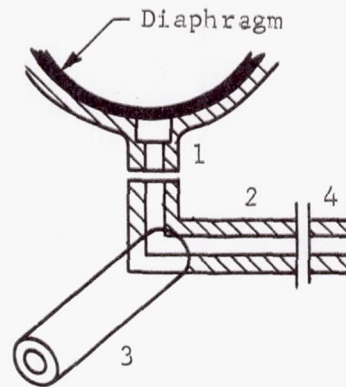
- B-1. R. J. Roark: Formulas for Stress and Strain. McGraw-Hill, New York, New York, 1954.
- B-2. Mechanical Design Data for Teflon. E. I. duPont deNemours and Company, Wilmington, Delaware.
- B-3. Lamé' Formula. Derivation by Menasco Manufacturing Company, Burbank, California.



MCR-68-119

APPENDIX C

PRESSURANT SIDE TANK OUTLET VOLUME CALCULATION



**Note:** Calculations of tank outlet volume assuming the diaphragm is in intimate contact with the tank wall.

$V_O$  = tank outlet volume, (cu in.)

$$V_O = V_1 + V_2 + V_3 + V_4$$

$$V_1 = \frac{\pi}{4} [(0.375)^2 (1.5) + (0.9)^2 (0.040)] = 0.419 \text{ cu in.}$$

$$V_2 = \frac{\pi}{4} [(0.375)^2 (1.320) + (0.177)^2 (1.75) + (0.177)^2 (1.0)] \\ = 0.214 \text{ cu in.}$$

$$V_3 = A_{\frac{1}{4}} \text{ tube I.D. (24)} = (0.0373) (24) = 0.89 \text{ cu in.}$$

$$V_4 = \frac{\pi}{4} [(0.177)^2 (1.0)] = 0.0245 \text{ cu in.}$$

$$V_O = 0.419 + 0.214 + 0.89 + 0.0245 = 1.548 \text{ cu in.}$$



MCR-68-119

APPENDIX D

PROPELLANT LOADING, LEVEL, AND  
ULLAGE CALCULATION

Propellant load, 82.47 lb<sub>m</sub> of N<sub>2</sub>O<sub>4</sub>;

Vacuum loaded into ~ 2332 cu in. loadable volume at 70°F;

Volume increase of tank expansion from 70°F to 275°F.

$$V_{\text{tank sphere @ 70°F}} = \frac{4}{3} \pi r_{70}^3$$

where

$$r_{70} = 8.25 \text{ in.}$$

$$r_{70}^3 = 561.5 \text{ cu in.}$$

$$V_{70} = \frac{4}{3} \pi (561.5) = 2352 \text{ cu in.}$$

$$\alpha_{Ti} = 4.22 \times 10^{-6} \text{ in./in./°F}$$

$$\begin{aligned} \Delta r_{70-275} &= r_{70} \alpha_{Ti} \Delta T (70-275) \\ &= (8.25)(4.22 \times 10^{-6})(205) \\ &= 7.137 \times 10^{-3} \approx 0.008 \end{aligned}$$

$$r_{275} = 8.25 + 0.008 = 8.258 \text{ in.}$$

$$r_{275}^3 = 563.15 \text{ cu in.}$$

$$V_{\text{tank sphere @ 275°F}} = \frac{4}{3} \pi r_{275}^3 = \frac{4}{3} \pi (563.15) = 2358.9$$

$$V_{\text{actual tank including backup ring}_{70°F}} = 2335 \text{ cu in.}$$

$$\begin{aligned} V_{\text{actual tank including backup ring}_{275°F}} &= 2335 \left( \frac{2358.9}{2352} \right) = \\ &= 2342 \text{ cu in.} \end{aligned}$$

$$V_{\text{diap. @ 70°F}} = 2.5 \text{ cu in.}$$



Volume increase 70 to 95°F =  $\left(\frac{25}{36}\right) (1.36)(2.5) = 0.0236$   
 (ref duPont teflon expansion data)

Volume increase 95 to 275°F =  $(1.7 \times 10^{-4})(2.52)$   
 $= 0.000425$

Volume @ 275°F =  $2.5 + 0.0236 + 0.0004 \approx 2.524$

$V_{\text{diap. @ 275°F}} = 2.52 \text{ cu in.}$

$V_{\text{usable propellant inside tank @ 70°F}} = 2335 - 2.5 =$   
 $= 2332.5 \text{ cu in.}$

$V_{\text{usable propellant inside tank @ 275°F}} = 2342 - 2.52 =$   
 $= 2339.48 \text{ cu in.}$

$\text{N}_2\text{O}_4 \rightleftharpoons \text{NO}_2$  Equilibrium Data (Ref Allied Product Bulletin)

$v_{\text{N}_2\text{O}_4} \text{ liq @ 70°F} = 0.01113 \text{ cu ft/lb}$

$\rho_{\text{N}_2\text{O}_4} \text{ liq @ 70°F} = 89.85 \text{ lb/cu ft}$

$v_{\text{NO}_2} \text{ gas @ 70°F} = 4.712 \text{ cu ft/lb}$

$\rho_{\text{NO}_2} \text{ gas @ 70°F} = 0.212 \text{ lb/cu ft}$

$\rho_{\text{N}_2\text{O}_4} \text{ gas @ 275°F} = 64.3 \text{ lb/cu ft}$

$\rho_{\text{NO}_2} \text{ gas @ 275°F} = 9.3 \text{ lb/cu ft}$

82.47 lb<sub>m</sub> loaded into 2332.5 cu in. (1.349 cu ft) @ 70°F

$\rho_{m70} = \frac{82.47}{1.349} = 61.13$

Vol @ 275°F is 2339.5 cu in. (1.354)

$$\rho_{m_{275}} = \frac{82.47}{1.354} = 60.91$$

$$\rho_m = a \rho_{N_2O_4} + b \rho_{NO_2}$$

$$b = \frac{\rho_m - a \rho_{N_2O_4}}{\rho_{NO_2}}$$

$$\text{let } a+b = 1; \text{ then, } a = 1-b$$

$$= 1 - \frac{\rho_m}{\rho_{NO_2}} + \frac{a \rho_{N_2O_4}}{\rho_{NO_2}}$$

$$a \left( \frac{\rho_{N_2O_4}}{\rho_{NO_2}} - 1 \right) = \frac{\rho_m}{\rho_{NO_2}} - 1$$

$$a (\rho_{N_2O_4} - \rho_{NO_2}) = \rho_m - \rho_{NO_2}$$

$$a = \frac{\rho_m - \rho_{NO_2}}{\rho_{N_2O_4} - \rho_{NO_2}}$$

where

$a$  = volume % of  $N_2O_4$  (sat.)

$b$  = volume % of  $NO_2$  (sat.)

$$\begin{aligned} \text{At } 70^\circ\text{F, } a_{70} &= \frac{\rho_m(70) - \rho_{NO_2}(70)}{\rho_{N_2O_4}( ) - \rho_{NO_2}(70)} \\ &= \frac{61.13 - 0.212}{89.85 - 0.212} = \frac{60.918}{89.638} = 0.680 \end{aligned}$$

$$b_{70} = 1 - a_{70} = 1 - 0.680 = 0.32$$



$$\begin{aligned} \text{At } 275^{\circ}\text{F}, a_{275} &= \frac{\rho_{m275} - \rho_{NO_2 275}}{\rho_{N_2O_4 275} - \rho_{NO_2 275}} \\ &= \frac{60.91 - 9.3}{64.3 - 9.3} = \frac{51.59}{55.00} = 0.938 \end{aligned}$$

$$b_{275} = 1 - a_{275} = 1 - 0.938 = 0.062$$

Then, volume of vapor @ 70°F and 275°F

$$V_{P_{70}} = b_{70} V_{\text{loadable } 70} = (0.32)(1.349) = 0.432 \text{ cu ft}$$

$$V_{\text{ullage } 70} = 32\%$$

$$V_{P_{275}} = b_{275} V_{\text{loadable } 275} = (0.062)(1.354) = 0.084 \text{ cu ft}$$

$$V_{\text{ullage}} = 6.2\%$$

The height of the liquid level below the tank top is equal to the height,  $H$ , of the volume of a spherical segment, which is equal to the ullage volume at the temperature of interest.

$$V = \frac{\pi H^2}{3} (3R - H) = \pi H^2 \left( R - \frac{H}{3} \right)$$

for a spherical segment as shown in Fig. D-1.

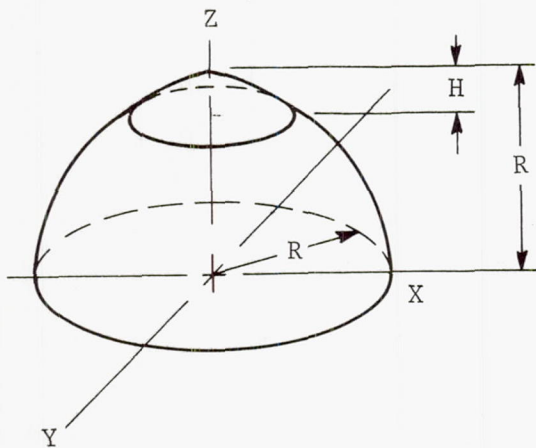


Fig. D-1 Liquid Height

A plot of the spherical volume as a function of the height is presented in Fig. D-2 from which the liquid height in the tank can be determined. The spherical volume is identical to the propellant ullage volume.

The ullage volume at 70°F,  $V_{u_{70}}$ , is 0.45 ft<sup>3</sup>, and the corresponding liquid height,  $H_{70}$  is approximately 6.4 in. from the tank top; and the ullage volume at 270°F,  $V_{u_{275}}$ , is 0.083 ft<sup>3</sup> and the corresponding liquid height,  $H_{275}$ , is approximately 2.5 in. from the tank top as illustrated in Fig. D-2.

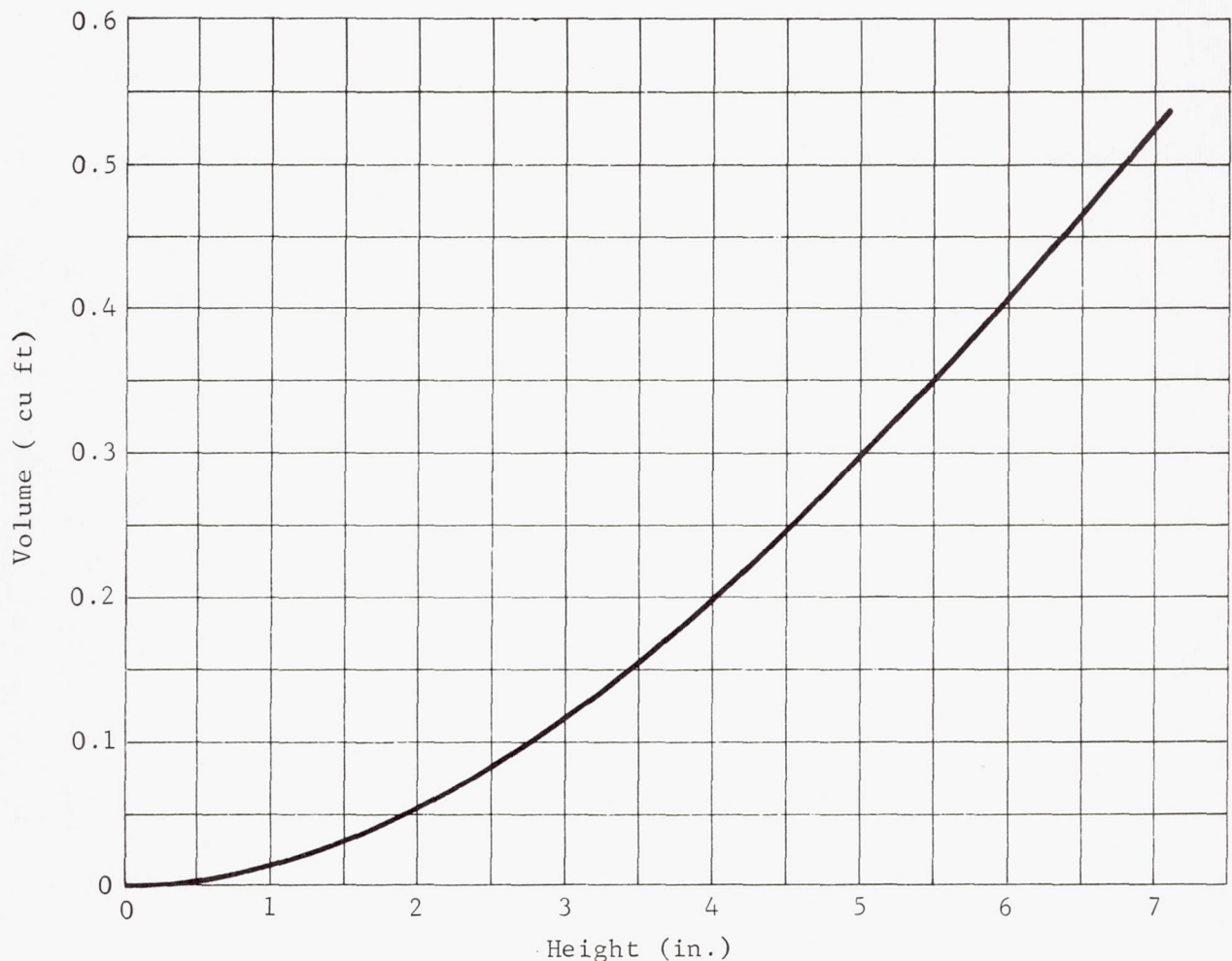


Fig. D-2 Spherical Volume vs Height